0039060

WHC-EP-0823

UC-601

Synthetic Waste Chemical Mechanism Studies

E. C. Ashby
A. Annis
E. K. Barefield
D. Boatright
F. Doctorovich
C. L. Liotta
H. M. Neumann
A. Konda
C. F. Yao
K. Zhang
Georgia Institute of Technology

N. G. McDuffie
Westinghouse Hanford Company

Date Published
October 1994

Prepared for the U.S. Department of Energy
Environmental Restoration and
Waste Management

Westinghouse Hanford Company P.O Box 1970 Richland, Washington

Hanford Operations and Engineering Contractor for the
U.S. Department of Energy under Contract DE-AC06-87RL10930

NOV 1994
RECEIVED
EDMC

Approved for Public Release

LEGAL DISCLAIMER

This report was prepared as an account of work sponsored by an agency of the United States Government. Neither the United States Government nor any agency thereof, nor any of their employees, nor any of their contractors, subcontractors or their employees, makes any warranty, express or implied, or assumes any legal liability or responsibility for the accuracy, completeness, or any third party's use or the results of such use of any information, apparatus, product, or process disclosed, or represents that its use would not infringe privately owned rights. Reference herein to any specific commercial product, process, or service by trade name, trademark, manufacturer, or otherwise, does not necessarily constitute or imply its endorsement, recommendation, or favoring by the United States Government or any agency thereof or its contractors or subcontractors. The views and opinions of authors expressed herein do not necessarily state or reflect those of the United States Government or any agency thereof.

This report has been reproduced from the best available copy.
Available in paper copy and microfiche.

Available to the U.S. Department of Energy
and its contractors from
Office of Scientific and Technical Information
P.O. Box 62
Oak Ridge, TN 37831
(615) 576-8401

Available to the public from the U.S. Department of Commerce
National Technical Information Service
5285 Port Royal Road
Springfield, VA 22161
(703) 487-4650

Printed in the United States of America

DISCLM-1.CHP (1-91)

NOV 1994
RECEIVED
EDMC

RELEASE AUTHORIZATION

Document Number:	WHC-EP-0823
Document Title:	Synthetic Waste Chemical Mechanism Studies
Release Date:	September 29, 1994

* * * * * * * * * * * * * *

This document was reviewed following the procedures described in WHC-CM-3-4 and is:

APPROVED FOR PUBLIC RELEASE

* * * * * * * * * * * * * *

WHC Information Release Administration Specialist:

Kara Broz

Kara Broz
(Signature)

September 29, 1994
(Date)

A-6001-400 (07/94) WEF256

WHC-EP-0823

SYNTHETIC WASTE CHEMICAL MECHANISM STUDIES

E. C. Ashby
Allen Annis
E. Kent Barefield
David Boatright
Fabio Doctorovich
Charles L. Liotta
H. M. Neumann
A. Konda
C.-F. Yao
K. Zhang

Final Report for Fiscal Year 1992-93
Prepared for the Westinghouse Hanford Company
under contract MJL-SVV-672084
(U.S. Department of Energy DE-AC06-87RL10930)

School of Chemistry and Biochemistry
Georgia Institute of Technology
Atlanta, GA 30332-0400

Table of Contents

Table of Contents ii
Acknowledgement iv
Acronyms and Abbreviations v
Summary vii
List of Tables xi
List of Figures. xiv
TASK 1: KINETIC STUDIES 1
1.A Reactions of HEDTA in simulated waste at different temperatures 1
1.B Determination of the activation energies for gas formation in HEDTA decomposition under argon 3
1.C Kinetics and mechanism of thermal degradation of glycolate in simulated waste7
1.C.1 Series I experiments 8
1.C.2 Series II experiments 8
1.C.3 The effect of temperature on the rate of gas formation 8
1.C.3.a Activation energy for total gas formation 9
1.C.3.b Activation energies for formation of hydrogen and nitrous oxide 11
1.D A possible explanation for the temperature dependence of gaseous product ratios for reactions of HEDTA and glycolate 14
1.E Stoichiometry and kinetics of decomposition of nitrosamines 15
1.E.1 Decomposition of N-nitrosoiminodiacetic acid, NNIDA 16
1.E.2 Decomposition of N-nitroso-N-ethylglycine, NNEG. 16
1.F Factors affecting the reactions of HEDTA, EDTA and related compounds in simulated waste. 17
1.F.1 Effect of glass 18
1.F.2 Effect of sodium silicate 18
1.F.3 Effect of sodium chloride. 19
1.F.4 Effect of aging 21
1.F.5 Effect of light 21
1.F.6 Effect of oxygen on the reactivity of metal complexants 23
1.F.6.a Sodium glycolate 24
1.F.6.b HEDTA 26
1.F.6.c EDTA and dimethylglycine (DMG). 27
1.G References. 28

TASK 2: PRODUCT IDENTIFICATION. 29
2.A Identification of HEDTA degradation products using ^{13}C NMR spectroscopy 29
2.B Identification of irradiated HEDTA degradation products using ^{13}C NMR spectroscopy 34
2.C Degradation of model systems in simulated waste 40
2.C.1 Decomposition of HEG in simulated waste 41
2.C.2 Effect of oxygen on HEG decomposition. 43
2.C.3 Other model systems; HIDA 44
2.D Role of aluminum in degradation of organic complexants: Does aluminum(III) promote the reaction of NO_2^- with nucleophiles? . . . 45

2.D.1 Nitrosation of secondary amines by sodium nitrite in the presence of $[Et_4N]AlCl_4$ . . . 45
2.D.2 Reaction of triethylamine with $[Et_4N]AlCl_4/NaNO_2$ in acetonitrile . . . 47
2.D.3 Cleavage of ß-hydroxyethylamines by $[Et_4N]AlCl_4/NaNO_2$ in acetonitrile . . . 47
2.E Preparation and degradation of nitroso derivatives of ethanolamines . . . 51
2.F Mechanism of the thermal degradation of HEDTA in simulated waste . . . 57
2.G Stability of carboxylic acid salts in simulated waste solution . . . 62
2.H Reaction of sodium citrate and isocitrate in simulated waste. . . . 63
2.I Analysis of solids from thermal reactions . . . 66
2.J References. . . . 69

TASK 5: SOURCE OF NITROUS OXIDE, NITROGEN AND AMMONIA . . . 71
5.A Reactions in SY1-SIM-91B mixtures utilizing N-15 labeled reagents. . . . 71
5.A.1 Source of N_2O and N_2 . . . 71
5.A.2 Source of NH_3 . . . 72
5.B Decomposition of nitrous oxide . . . 72
5.C Mechanistic pathways for formation of gases containing nitrogen from nitrite 73
5.C.1 The reaction of H_2NOH with organic compounds in basic solution . . 74
5.C.2 The Reaction of $N_2O_3^{2-}$ with H_2CO in basic solution . . . 76
5.C.3 Conclusions. . . . 82
5.D A redox analysis of HEDTA decomposition: How much NH_3 might be formed?. . . . 83
5.F References. . . . 85

EXPERIMENTAL SECTION . . . 86
Task 1 . . . 86
Task 2 . . . 139
Task 5 . . . 150
References. . . . 154

Acknowledgement

The work described in this report owes much to a number of people at Pacific Northwest Laboratory, Westinghouse Hanford Company, and Argonne National Laboratory who kept us apprised of their own related work, provided us with analytical results from tank 101-SY, and provided constructive criticism of our work as it progressed. Special thanks are due Dr. Norton McDuffie who has served as the interface between us and colleagues at Westinghouse Hanford and Pacific Northwest Laboratories.

Acronyms and Abbreviations

Acronyms

AcO^-	acetate, $CH_3CO_2^-$
DEEA	N,N-diethylethanolamine, $HOCH_2CH_2N(CH_2CH_3)_2$
DMG	N,N-dimethylglycine, $(CH_3)_2NCH_2CO_2H$
DMSO	dimethylsulfoxide, $(CH_3)_2S{=}O$
EA	ethanolamine, $H_2NCH_2CH_2OH$
EAMA	ethanolamine monoacetic acid, $HOCH_2CH_2NHCH_2CO_2H$
ED	ethylenediamine, $H_2NCH_2CH_2NH_2$
ED3A	ethylenediamine triacetic acid, $HO_2CCH_2N(H)CH_2CH_2N(CH_2CO_2H)_2$
ED3A lactam	ethylenediamine triacetic acid lactam, $HO_2CCH_2\underline{NCH_2CH_2NCH_2C(O)}(CH_2CO_2H)$
EDMA	ethylenediaminemonoacetic acid, $H_2NCH_2CH_2N(H)CH_2CO_2H$
EDTA	ethylenediaminetetraacetic acid, $(HO_2CCH_2)_2NCH_2CH_2N(CH_2CO_2H)_2$
EIDA	N-ethyl iminodiacetic acid, $CH_3CH_2N(CH_2CO_2H)_2$
Et	ethyl, CH_3CH_2-
GLY	glycolic acid, $HOCH_2CO_2H$
HED	(N-2-hydroxyethyl)ethylene diamine, $HOCH_2CH_2N(H)CH_2CH_2NH_2$
HEDTA	hydroxyethylethylenediamine triacetic acid, $HOCH_2CH_2N(CH_2CO_2H)CH_2CH_2N(CH_2CO_2H)_2$
HEG	N-hydroxyethyl-N-ethylglycine, $HOCH_2CH_2N(CH_2CO_2H)(CH_2CH_3)$
HIDA	N-hydroxyethyliminodiacetic acid, $HOCH_2CH_2N(CH_2CO_2H)_2$
IDA	iminodiacetic acid, $HN(CH_2CO_2H)_2$
Me	CH_3-
N-ME Glycine; MG	N-methylglycine, $HN(CH_3)CH_2CO_2H$
N-ME S-EDDA	N-methylethylenediamine-N,N'- diacetic acid, $HO_2CCH_2N(CH_3)CH_2CH_2NHCH_2CO_2H$
MIDA	N-methyliminodiacetic acid, $CH_3N(CH_2CO_2H)_2$
N-ME ED3A	N-methylethylenediamine triacetic acid, $HO_2CCH_2N(CH_3)CH_2CH_2N(CH_2CO_2H)_2$
N-ME ED	N-methylethylenediamine, $CH_3N(H)CH_2CH_2NH_2$
N-ME U-EDDA	N-methylethylenediamine-N',N'- diacetic acid, $CH_3N(H)CH_2CH_2N(CH_2CO_2H)_2$
NNEG	N-nitroso-N-ethylglycine, $O{=}NN(CH_2CO_2H)(CH_2CH_3)$
NNIDA	N-nitrosoiminodiacetic acid, $O{=}NN(CH_2CO_2H)_2$
NTA	nitrilotriacetic acid, $N(CH_2CO_2H)_3$
Ph	C_6H_5-
S-EDDA	ethylenediamine-N,N'-diacetic acid, $HO_2CCH_2N(H)CH_2CH_2NHCH_2CO_2H$
TMS	tetramethylsilane, $(CH_3)_4Si$
U-EDDA	ethylenediamine-N,N-diacetic acid, $H_2NCH_2CH_2N(CH_2CO_2H)_2$

Abbreviations

101-SY	waste storage tank SY-101
atm.	atmosphere
C-13	carbon, atomic mass 13
cont'd	continued
exp't	experimental
e^-	electron
FID	free induction decay
FY	fiscal year
GC	gas chromatography
IC	ion chromatography
MW	molecular weight
N-14	nitrogen, atomic mass 14
N-15	nitrogen, atomic mass 15
NMR	nuclear magnetic resonance
r.t.	room temperature
rxn.	reaction
S.M.	starting material
SY1-SIM-91B	simulated waste (see page 87)

Summary

This is the final report for work done at Georgia Tech during fiscal year 1992-1993. Five tasks were originally to be undertaken. These were 1) Kinetic studies of gas evolution and metal complexant decomposition in simulated waste media, 2) Product identification from metal complexant decomposition in simulated waste media, 3) Round robin tests of glycolate decomposition in simulated waste media involving PNL, Westinghouse, ANL and Georgia Tech, 4) Other waste tank chemistry including the effects of organics on gas generation, and 5) Determine the pathway by which N_2O, N_2, and NH_3 are formed in simulated waste media. Essentially all of the Georgia Tech effort was devoted to tasks 1, 2 and 5; therefore, the report is divided into three parts denoted Task 1, Task 2 and Task 5. Because the work during the twelve month period rested heavily upon last six months of the preceding year, this report actually summarizes and correlates results obtained during the eighteen month period April 1992 through September 1993. Some highlights of this phase of our work on elucidation of thermal mechanisms for gas formation follow. A "global" mechanism for the degradation of HEDTA has been postulated (Scheme 2.4 and 2.5) that incorporates the known dependence on nitrite and aluminum and which accounts for most of the known products.

TASK 1: KINETICS STUDIES

Long term studies (> 6 months) of HEDTA decomposition under argon and argon-oxygen atmospheres conducted at 60° C, 90° C, and 120° C indicate: 1) ED3A is much less reactive than HEDTA, 2) that the rate of production of N_2 and N_2O decreases significantly at about the time that HEDTA is completely consumed (< 2000 h at 120° C), 3) that the activation energy for hydrogen gas evolution is 17 kcal/mol (71 kJ/mol).

Kinetics studies of sodium glycolate decomposition in simulated waste indicate a first order dependence on glycolate, nitrite and aluminate. This is consistent with the hypothesis that activation of nitrite for reaction with glycolate occurs by prior coordination to aluminum. An activation energy for total gas formation from glycolate of 26 kcal/mol was determined. Activation energies for hydrogen formation from glycolate under argon and under argonoxygen atmospheres of 30 kcal/mol and 27 kcal/mol, respectively, were determined.

Large differences in the relative amounts of N_2, N_2O and H_2 formed at 90° C versus those at 120° C were observed for both HEDTA and glycolate decompositions. In both cases N_2 was the major gas at 90° C, whereas N_2O was the major product at 120° C. A possible explanation may be the effect of the viscosity of the medium on the reactivities of NO^- and CH_2O or $HC(O)CO_2^-$.

Kinetics studies of the base induced decomposition of the preformed nitrosamines, N-nitrosoiminodiacetic acid and N-nitroso-N-ethylglycine indicate half-lives for decomposition in 2 M NaOH of 250 h at 120° C for the former and 40 h at 100° C for the latter. Products of these decompositions include formate, oxalate, hydrogen and nitrous oxide. These observations support the mechanistic hypothesis that nitrosation of a secondary amine such as ED3A, IDA, etc can lead to a reactive species that produces the same gaseous and non-volatile fragments that are formed in tank 101-SY and in simulated waste media.

The possible effects of a variety of additives and reaction conditions on the rates and products of decomposition of several complexants were examined. The most dramatic differences resulted from the elimination of oxygen from the atmosphere above the reaction mixture; the amount of hydrogen produced from metal complexants is substantially greater for decompositions that are conducted under an oxygen containing atmosphere than for those conducted under an oxygen-free atmosphere. The reactivity of HEDTA and the amount of hydrogen produced are considerably increased by aging, especially for reactions conducted under an oxygen atmosphere. Nitrous oxide production was reduced under these conditions and oxygen consumption increased relative to a comparable reaction in which the solution was not aged.

TASK 2: PRODUCT IDENTIFICATION

Monitoring of thermal decompositions (120° C) of two ^{13}C-labeled forms of HEDTA by ^{13}C NMR spectroscopy provided significant information concerning the temporal formation of degradation products. Decomposition of a form of HEDTA in which both carbon atoms of the hydroxyethyl group were labeled indicated that formate, carbon dioxide, oxalate and glycine were derived from the hydroxyethyl group. Unlabeled glycine, which must be derived from the carboxymethyl groups, was also detected late in the reaction; the ratio of labeled to unlabeled was estimated as about 1:6.

Similar monitoring by ^{13}C NMR spectroscopy of the decomposition of HEDTA in which both carbons of all three carboxymethyl groups were ^{13}C-labeled was particularly informative. ED3A, U-EDDA, S-EDDA and IDA were detected as products and the decay of ED3A to S-EDDA was evident from the time dependent spectra. Some of the ED3A was found in the cyclized lactam form.

Comparison of the ^{13}C NMR spectra of samples of both of the above ^{13}C-labeled derivatives after irradiation at Argonne National Laboratory (D. Meisel) with those of thermally treated samples at similar levels of conversion showed significant differences in product distributions. In particular, IDA appeared to be formed in larger amount in the irradiated samples. The amount of ED3A might be less than that present in the thermally decomposed samples.

Thermal decomposition in simulated waste of N-hydroxyethyl-N-ethylglycine (HEG), a simpler compound chosen as a model for HEDTA, showed that cleavage of the hydroxyethyl group occurred to give predominantly formate and N-ethylglycine. Small amounts of oxalate and glycine were also formed. Hydrogen, nitrogen, and nitrous oxide were also produced. The limited amount of glycine formed in these decompositions suggested that N-ethylglycine, like ED3A, was quite unreactive toward further degradation. Independent tests of the reactivity of commercially available N-methylglycine in simulated waste indicated that it produced no glycine after 1000 h at 120° C. Thus the origin of the glycine observed from HEG may be a result of nitrosation of N-ethylglycine by the nitrite ester of HEG, which competes with its thermal decomposition. Like HEDTA, HEG produces more hydrogen and less nitrogen gases under an oxygen containing atmosphere than in an oxygen free atmosphere.

Several experiments were done to explore the hypothesis that nitrite is activated for reaction with nucleophiles by coordination to aluminum. The first series involved the reaction of a mixture of $[Et_4N][AlCl_4]$ and sodium nitrite in acetonitrile with various ethanolamines. That cleavage of the hydroxyethyl group occurred when the tetrachloroaluminate was present, but no reaction occurred when it was not, is consistent with the observations made on the simulated waste mixtures. Nitrosamines were formed as the nitrogen containing products. Although not identified, nitrite esters or nitrosammonium intermediates are believed to be generated in these reactions.

In another series of experiments, the alkoxide of N,N-diethylethanolamine (DEEA) was treated with nitrosonium tetrafluoroborate in acetonitrile to generate the nitrite ester, which was found to be in equilibrium with the N-nitrosammonium tautomer. Thermolysis of the mixture for several hours at 60° C followed by quenching with aqueous sodium hydroxide, generated DEEA and diethylamine and initially a mixture of NO, N_2 and N_2O. Subsequently, nitric oxide was consumed and was replaced by a mixture of nitrogen and nitrous oxide. Production of NO could result by homolytic cleavage of the N-O bond in the nitrite ester. Nitric oxide is known to react with hydroxylamine to give N_2 and N_2O but not direct evidence for the formation of hydroxylamine in this reaction has been found.

The thermal stability of several carboxylate salts, including formate and oxalate, citrate and isocitrate, in simulated waste media were examined. No evidence of any decomposition of formate and oxalate was found. Particular attention was also given to the possible production of hydrogen from the reaction of formate under inert and oxygen atmospheres. Although minute amounts of hydrogen were detected, control experiments showed that the amount of hydrogen formed was the same when formate was absent as when it was present. Unless formate and oxalate are rapidly decomposed by radiolytic processes, or they react with intermediates produced in thermal reactions, we conclude that there should be significant quantities present in Tank 101-SY. Both citrate and isocitrate thermally decompose in simulated waste without the evolution of hydrogen or nitrous oxide. Control experiments indicate that neither nitrite or aluminum is required for the thermal decomposition.

Solids invariably deposit during thermal decompositions of metal complexants in simulated waste mixtures. Analyses of some of these solids derived from degradation of HEDTA were done in an effort to obtain a more complete mass balance for the decomposition reactions. Prior to the use of Teflon-capped vessels that eliminated exposure of glass to splashing of the caustic simulated waste mixture, these solids contained aluminosilicates. Solids formed from reactions done in Teflon-capped vessels were aluminosilicate free and appeared to be almost entirely sodium oxalate. No evidence was found on the basis of x-ray powder diffraction for any of the several known basic aluminum oxalate phases.

TASK 5: SOURCE OF NITROUS OXIDE, NITROGEN AND AMMONIA

Thermal degradation of HEDTA in simulated waste mixtures prepared using ^{15}N-labeled sodium nitrite and/or ^{15}N-labeled nitrate demonstrated that both the N_2O and N_2 formed in the decomposition are derived exclusively from nitrite. The bulk of the ammonia produced in these reactions was derived from nitrite but a small amount contained unlabeled

nitrogen derived from HEDTA. Production of ammonia from HEDTA is included in the "global" mechanism for HEDTA decomposition.

Early in our studies of the thermal decomposition of HEDTA at 120° C, the amount of nitrous oxide formed was frequently observed to reach a maximum value and then to decrease. This was determined to be a result of the decomposition of nitrous oxide to nitrogen and oxygen, which control experiments indicated could occur in glass vessels in the absence of any liquid phase.

A series of experiments was performed to test the possibility that NO^- produced by fragmentation of a nitrite ester (or $N_2O_3^{2-}$ produced by the subsequent reaction of NO^- with nitrite) might be reduced by formaldehyde first to hydroxylamine and then to ammonia. Although these experiments are incomplete, evidence was obtained that suggested that the reaction of $N_2O_3^{2-}$ with formaldehyde at 90° C produced formate, nitrogen and ammonia. Cyanide was detected by ^{15}N NMR measurements and could be the precursor of at least part of the ammonia. However, cyanide could only reasonably have formed by hydrolysis of the oxime derived from hydroxylamine and formaldehyde so that ammonia and nitrogen could also arise from disproportionation of hydroxylamine.

The importance of ammonia as a waste tank gas was not known at the time that many of the HEDTA decompositions described in this report were studied and no quantitative analyses for ammonia were done. However, it should be possible to calculate the amount of ammonia that should be produced for runs where carbon mass balances are obtained and analyses for other known reduction products (hydrogen, nitrogen and nitrous oxide) are available. A sample "redox" analysis of one HEDTA decomposition was performed where these criteria were met. Future studies of ammonia production should demonstrate the validity of this approach.

TABLES

1.1 Reaction of HEDTA in Simulated Waste at Different Temperatures 2
1.2 Rate Constants for the Thermal Degradation of Glycolate under Air in the presence of Glass 9
1.3 Rate Constants for Thermal Degradation of Glycolate under Argon in the Absence of Glass at 120° C 11
1.4 Effect of Glass on the Reaction of HEDTA in Simulated Waste (500 h, 120° C) 19
1.5 Effect of Glass on the Reaction of HEDTA in Simulated Waste in the Absence of Sodium Aluminate (500 h, Ar, 120° C) 20
1.6 Effect of Sodium Silicate on the Reaction of HEDTA in Simulated Waste (500 h, Ar, 120° C). 20
1.7 Effect of Added NaCl on the Reaction of HEDTA in Simulated Waste (500 h, 120° C) 21
1.8 Effect of Solution Aging on the Reaction of HEDTA in Simulated Waste (500 h, 120° C) 22
1.9 Effect of Light on the Reactions of HEDTA and HEG in Simulated Waste (120° C, Ar, 200 h) 22
1.10 Effect of Oxygen on the Reaction of Metal Complexants in Simulated Waste Solution (120° C, 1000 h) 24
1.11 Reaction of Sodium Glycolate in Modified Simulated Waste Solutions (120° C, 500 h). 25
1.12 Effect of Oxygen on Reactions of HEDTA in Modified Simulated Waste (120° C, 500 h) 26
1.13 Effect of Oxygen on the Reaction of EDTA and DMG in Simulated Waste (120° C, 1000 h) 27
2.1 ^{13}C Chemical Shifts (ppm) in Simulated Waste Solution 30
2.2 Reaction of HEG in Simulated Waste and in NaOH (120° C) 42
2.3 Reaction of Model Systems in SY1-SIM-91B Solution (120° C, 1000 h) . . . 44
2.4 Nitrosation of Diethylamine in Acetonitrile under Various Conditions 46
2.5 Nitrosation of Piperidine under Various Conditions 46
2.6 Cleavage and Nitrosation of 2-(N,N-Diethylamino)ethanol (I) and 2-Piperidinoethanol (II) with $[Et_4N]AlCl_4/NaNO_2$ in Acetonitrile 48
2.7 Reactivity of N-Methylenepiperidinium Ion under Various Conditions 49
2.8 Cleavage and Nitrosation of N-(2-hydroxy-1-phenylethyl)-piperidine (V) and N-(2-hydroxy-2-phenylethyl)-piperidine (VI) with $[Et_4N][AlCl_4]/NaNO_2$ . . 50
2.9 Composition of the Gas Phase After Hydrolysis of Nitroso-DEEA Derivative as a Function of Time 55
2.10 Gas Generation in the Reaction of Sodium Formate in Simulated Waste . . 62
2.11 Reaction of Citric Acid and Isocitric Acid in SY1-SIM-91B Solution (1000 h, 120° C) Comparison with Sodium Glycolate 65
2.12 Reaction of Sodium Citrate in 2 M NaOH (120° C, 1000 h) Comparison with the Reaction in Simulated Waste 65
2.13 Analysis of Solids Produced by the Reaction of Glycolate in Simulated Waste 67

2.14 Analysis of Solids Produced by the Reaction of HEDTA and Related Compounds in Simulated Waste . . . 68
2.15 Aluminum Analysis of Solids Produced by the Reactions of Glycolate and MIDA in Simulated Waste . . . 69
5.1 Gas Composition After Heating N_2O at 120° C . . . 72
5.2 Rate Constant for Nitrous Oxide Decomposition . . . 73
5.3 Results of Reactions of H_2NOH in Modified SY1-SIM-91B Mixtures . . . 75
5.4 Nitrogen-14 Chemical Shift (ppm) Referred to External CH_3NO_2 . . . 75
5.5 Results of Reactions of $N_2O_3^{2-}$ in Modified SY1-SIM-91B Mixtures . . . 79
5.6 Survey of Reactions of $N_2O_3^{2-}$ with Formaldehyde and Hydroxylamine . . . 82
E.1 Reproducibility of ion chromatographic analyses of nitrite and nitrate ion . . . 87
E.2 Reproducibility of ion chromatographic analyses of nitrate ion . . . 88
E.3 Data for Figure 1.1 (Trial: HEDTA-10B) . . . 92
E.4 Data for Figure 1.2 (Trial: HEDTA-11B) . . . 92
E.5 Data for Figure 1.3 (Trial: HEDTA-12B) . . . 93
E.6 Data for Figure 1.4 (Trial: HEDTA-19B) . . . 93
E.7 Data for Figure 1.5 (Trial: HEDTA-12B) . . . 94
E.8 Data for Figure 1.6 (Trial: HEDTA-17B) . . . 94
E.9 Data for Figure 1.7 . . . 95
E.10 Data for Figure 1.9 (Trial GLY-3) . . . 95
E.11 Data for Figure 1.10 (Trial: GLY-4B) . . . 95
E.12 Data for Figure 1.11 . . . 96
E.13 Data for Figure 1.12 . . . 96
E.14 Analysis of Nonvolatile Reaction Components of the Reaction of SY1-SIM-91B Containing 0.21 M Glycolate; 1.54 M Aluminate; 2.24 M Nitrite; 0.42 M Carbonate; 2.59 M Nitrate; 2.00 M Hydroxide in Air . . . 98
E.15 Analysis of Nonvolatile Reaction Components of the Reaction of SY1-SIM-91B Containing 0.10 M Glycolate; 1.54 M Aluminate; 2.24 M Nitrite; 0.42 M Carbonate; 2.59 M Nitrate; 2.00 M Hydroxide in Air . . . 99
E.16 Analysis of Nonvolatile Reaction Components of the Reaction of SY1-SIM-91B Containing 0.21 M Glycolate; 1.00 M Aluminate; 2.24 M Nitrite; 0.42 M Carbonate; 2.59 M Nitrate; 2.00 M Hydroxide in Air . . . 100
E.17 Analysis of Nonvolatile Reaction Components of the Reaction of SY1-SIM-91B Containing 0.21 M Glycolate; 1.54 M Aluminate; 1.12 M Nitrite; 0.42 M Carbonate; 2.59 M Nitrate; 2.00 M Hydroxide in Air . . . 101
E.18 Analysis of Nonvolatile Reaction Components of the Reaction of SY1-SIM-91B Containing 0.21 M Glycolate; 1.54 M Aluminate; 2.24 M Nitrite; 0.42 M Carbonate; 2.59 M Nitrate; 2.00 M Hydroxide under an Argon Atmosphere . . . 101
E.19 Analysis of Nonvolatile Reaction Components of the Reaction of SY1-SIM-91B Containing 0.21 M Glycolate; 1.00 M Aluminate; 2.24 M Nitrite; 0.42 M Carbonate; 2.59 M Nitrate; 2.00 M Hydroxide under an Argon Atmosphere . . . 102
E.20 Analysis of Nonvolatile Reaction Components of the Reaction of SY1-SIM-91B Containing 0.21 M Glycolate; 1.54 M Aluminate; 1.12 M Nitrite; 0.42 M Carbonate; 2.59 M Nitrate; 2.00 M Hydroxide under an Argon Atmosphere . . . 102

E.21 Total Gas Measurements for the Reaction of SY1-SIM-91B Containing 0.21 M Glycolate at 60° C in Air 104
E.22 Total Gas Measurements for the Reaction of SY1-SIM-91B Containing 0.21 M Glycolate at 90° C in Air 119
E.23 Total Gas Measurements for the Reaction of SY1-SIM-91B Containing 0.21 M Glycolate at 120° C in Air 134
E.24 ^{1}H-NMR Database for Model Systems 142
E.25 High Resolution Mass Spectral Data for New Compounds 143

FIGURES

1.1 Gas Evolution for the Reaction of HEDTA in Simulated Waste (60°C, Ar) . . . 3
1.2 Gas Evolution for the Reaction of HEDTA in Simulated Waste (90° C, Ar) . . . 4
1.3 Gas Evolution for the Reaction of HEDTA in Simulated Waste (120° C, Ar; data are for experiment 12B in Table11) . . . 4
1.4 Gas Evolution for the Reaction of HEDTA in Simulated Waste (120° C, Ar; data are for experiment 19B in Table 11). . . . 5
1.5 Evolution of Nitrogen plus Nitrous Oxide for the Reaction of HEDTA in Simulated Waste (120° C, Ar; data are for experiment 12B in Table 11) . . . 5
1.6 Gas Evolution for the Reaction of HEDTA in Simulated Waste (90° C, Ar/O_2) . . . 6
1.7 Arrhenius Plot for the Formation of Hydrogen from HEDTA in Simulated Waste (60-120° C , Ar). . . . 6
1.8 Total Gas Evolution for the Reaction of Glycolate in Simulated Waste at (a) 60° C; (b) 90° C; and (c) 120° C . . . 10
1.9 Gas Evolution for the Reaction of Glycolate in Simulated Waste (90° C , Ar) . . . 12
1.10 Gas Evolution for the Reaction of Glycolate in Simulated Waste (90° C , Ar/O_2) . . . 13
1.11 Gas Evolution for the Reaction of Glycolate in Simulated Waste (120° C, Ar) . . . 13
1.12 Gas Evolution for the Reaction of Glycolate in Simulated Waste (120° C, Ar/O_2) . . . 14
2.1 ^{13}C NMR Spectrum of HEDTA-A in Simulated Waste Mixture after Heating at 120° C for 1452 h . . . 35
2.2 ^{13}C NMR Spectrum of HEDTA-B in Simulated Waste Mixture after Heating at 120° C for 1808 h . . . 36
2.3 ^{13}C NMR Spectrum of HEDTA-B in Simulated Waste (120° C): Signals due to ED3A and s-EDDA A: 905 h; B: 1808 h; C: 2492 h . . . 37
2.4 ^{13}C NMR Spectrum of HEDTA-A in Simulated Waste Mixture after Irradiation (196 Mrad dose) . . . 38
2.5 ^{13}C NMR Spectrum of HEDTA-B in Simulated Waste Mixture after Irradiation (208 Mrad dose) . . . 39
2.6 ^{1}H NMR of the Reaction of DEEA-alkoxide with $NOBF_4$ (DEEA:$NOBF_4$ ≈1) . . . 53
2.7 ^{1}H NMR of DEEA-alkoxide . . . 53
2.8 ^{1}H NMR of the Reaction of DEEA-alkoxide with Excess $NOBF_4$ . . . 54
5.1 KHA-14. ^{14}N NMR of Reaction H_2NOH with H_2CO in Basic Solution at Room Temperature for 20 minutes . . . 77
5.2 KHA-14. ^{14}N NMR of Reaction H_2NOH with H_2CO in Basic Solution at 60° C for 2 hours . . . 77
5.3 KHA-14. ^{14}N NMR of Reaction H_2NOH with H_2CO in Basic Solution at 90° C for 25 hours. . . . 78

5.4 KHA-14. ^{14}N NMR of Reaction H_2NOH with H_2CO in Basic Solution at 90° C for 90 hours. 78
5.5 KON-17. ^{14}N NMR of Reaction $N_2O_3^{2-}$ with H_2CO in Basic Solution at Room Temperature for 50 hours 80
5.6 KON-19. ^{14}N NMR of Reaction $N_2O_3^{2-}$ with H_2CO in Basic Solution at Room Temperature for 05 hours 80
5.7 KON-19. ^{14}N NMR of Reaction $N_2O_3^{2-}$ with H_2CO in Basic Solution at 65° C for 2 hours 81
5.8 KON-19. ^{14}N NMR of Reaction $N_2O_3^{2-}$ with H_2CO in Basic Solution at 90° C for 18 hours 81
E.1 Apparatus used for Reactions in Simulated Waste ("A" Runs) 90
E.2 Apparatus used for Reactions in Simulated Waste ("B" Runs) 91
E.3 Teflon Liner with Cap 91
E.4 Reaction vessel for Series 2 Glycolate Kinetics 97
E.5 Long Term Gas Kinetics Apparatus 103
E.6 Reaction Vessel Used for the Thermal Decomposition of ^{13}C-Labeled Compounds 141
E.7 Decoupled ^{13}C NMR spectrum of A (mixture of diastereoisomers) 144
E.8 Decoupled ^{13}C NMR spectrum of A (mixture of diastereoisomers) 145
E.9 (a) Decoupled ^{13}C NMR spectrum of A' 146
(b) Off-resonance decoupled ^{13}C NMR spectrum of A'. 147
E.10 (a) Decoupled ^{13}C NMR spectrum of B' 148
(b) Off-resonance decoupled ^{13}C NMR spectrum of B'. 149
E.11 Mass spectrum of headspace gases for reaction of HEDTA in SY1-SIM-91B made with $Na^{15}NO_2$ (helium atmosphere). 152
E.12 Mass spectrum of headspace gases for reaction of HEDTA in SY1-SIM-91B made with $Na^{15}NO_3$ (helium atmosphere). 153

This page intentionally left blank.

TASK 1: KINETIC STUDIES

This section describes studies designed to elucidate the factors affecting the rate of reaction of metal complexants in simulated waste media and to determine rate constants and activation energies for reactions leading to gaseous products. Five major studies are described: 1) kinetics of individual product gases from HEDTA decomposition at three temperatures; an activation energy for hydrogen formation has been determined, 2) kinetics of decomposition of sodium glycolate as a function of constituent concentration at 120° C, 3) kinetics of both total gas, and individual gas, formation from decomposition of sodium glycolate as a function of temperature; activation energies have been determined, 4) kinetics of decomposition of nitroso derivatives of ED3A models have been determined, and 5) factors affecting the rate of decomposition of HEDTA.

1.A Reactions of HEDTA in simulated waste at different temperatures.

A series of reactions of HEDTA were conducted in SY1-SIM-91B solution at 60° C, and 90° C, under argon and oxygen containing atmospheres, and at 120° C under an argon atmosphere. An experiment at 120° C under an oxygen containing atmosphere was aborted after a few hundred hours when the reaction vessel was discovered to be leaking. Analyses of gaseous products were done as a function of time; analyses of unreacted HEDTA, and identifiable carbon fragments were performed at the time that the experiment was terminated. Table 1.1 summarizes the amounts of all products at the time that each experiment was terminated, except for experiment 12B where analyses of gaseous products obtained at a comparable time to those of experiment 19B are also shown. These two sets of data indicate the reproducibility of these types of experiments. Plots of the amounts of gaseous products as a function of time for several of these experiments are shown in Figures 1.1-1.6. These experiments may be considered as preliminaries to those to be done in FY 1994 where analyses for both gaseous and condensed phase products will be done as a function of time.

Very little reaction occurs at 60° C under either argon or oxygen/argon atmospheres, although it does appear that more HEDTA has reacted in a shorter period of time in the oxygen containing atmosphere. At 90° C the opposite is clearly the case; the reactivity is lower in the presence of oxygen and oxygen is steadily consumed in the course of the reaction (Figure 1.6). A long induction period is observed for nitrous oxide evolution under an argon atmosphere (Figure 1.2), but the amount of N_2O produced is ultimately much larger than under the oxygen atmosphere (24.5 % vs. 1.0 %). This suggests that oxygen may inhibit the formation of nitrous oxide. The induction period under the argon atmosphere could be the result of the presence of small amounts of oxygen that are ultimately consumed. Also, as was noted in the Georgia Tech memo of November 30, 1992, the amount of hydrogen produced is significantly higher (3x) under the oxygen containing atmosphere. The oxalate/formate ratio is also higher (0.5/0.1).

Two experiments were conducted under argon at 120° C. Gaseous products were monitored as a function of time to 5000 h in experiment 12B; the second experiment (19B) was carried to only 2000 h and measurements of both condensed and gaseous products were made at that time. The agreement of the analyses of the gaseous products at

comparable times for the two experiments is very good. There are several noteworthy points.

Table 1.1. Reaction of HEDTA in Simulated Waste at Different Temperatures.[1]

Exp't	10B	16B	11B	17B	19B	12B	
T/°C	60	60	90	90	120	120	
Cover Gas	Ar	Ar\O_2	Ar	Ar\O_2	Ar	Ar	
Time (h)	5036	3695	4942	3695	2038	2017	4921
HEDTA	98	93	36	88	<2		<2
$HCOO^-$	<1	13	107	25	139		152
$(COO^-)_2$	<2	<1	12	13	17		19
ED3A	<2	6	55	12	67		60
s-EDDA	<2	<2	6	~5	11		13
EDTA	<2	<2	<2	<2	~2		~2
AcO^-	<1	<1	~2	<1	3		4
H_2	0.6	0.9	3.9	11.7	6.3	6.4	11.3
O_2[2]	-	15	-	29	-	-	-
N_2	~3	~5	30	16	33	31	53
CH_4	<0.1	<0.1	0.5	<0.1	1.8	3.5	7.5
N_2O	<0.1	<0.1	24.5	1.0	36.1	31.9	27.1

[1]Unless otherwise stated, all products are indicated in moles per 100 moles of organic starting material. [2]Moles of O_2 *consumed* per 100 moles of HEDTA.

- Essentially all of the HEDTA has reacted after 2000 h at 120° C.
- The reactivity of ED3A is significantly lower than that of HEDTA; only ca. 10% of that present after 2000 h has reacted in an additional 2900 h. That s-EDDA has not increased by a comparable amount may indicate that ED3A decomposes to other products that have not been accounted for in these experiments.
- The amount of nitrous oxide goes through a maximum at about 2000 h for the reaction conducted at 120° C under argon. Its conversion to nitrogen is clearly indicated by Figure 1.3. Independent experiments that verify the instability of nitrous oxide under these reaction conditions are described under Task 5.
- The rate of hydrogen formation is not affected by the disappearance of HEDTA at 2000 h but has decreased markedly at 4900 h.
- Methane generation has also slowed but probably not to the same extent as hydrogen.

- The rate of production of nitrogen gases (nitrogen plus nitrous oxide) decreases significantly after 2000 h, which is at, or after, the time that all of the HEDTA had reacted (see Figure 1.5).

1.B Determination of the activation energies for gas formation in HEDTA decomposition under argon. The amounts of gases produced by reaction of HEDTA in simulated waste were monitored at 60° C, 90° C, and 120° C as a function of time under an argon atmosphere (Figures 1.1-1.3). Taking the initial rates of hydrogen evolution from the plots at different temperatures, the Arrhenius plot shown in Figure 1.7 may be obtained. A calculation of the activation energy from the slope of the line gives a value of 17 kcal/mol. This may be compared with the value of 24.5 kcal/mol obtained by Delegard[1] based on total gas evolution.

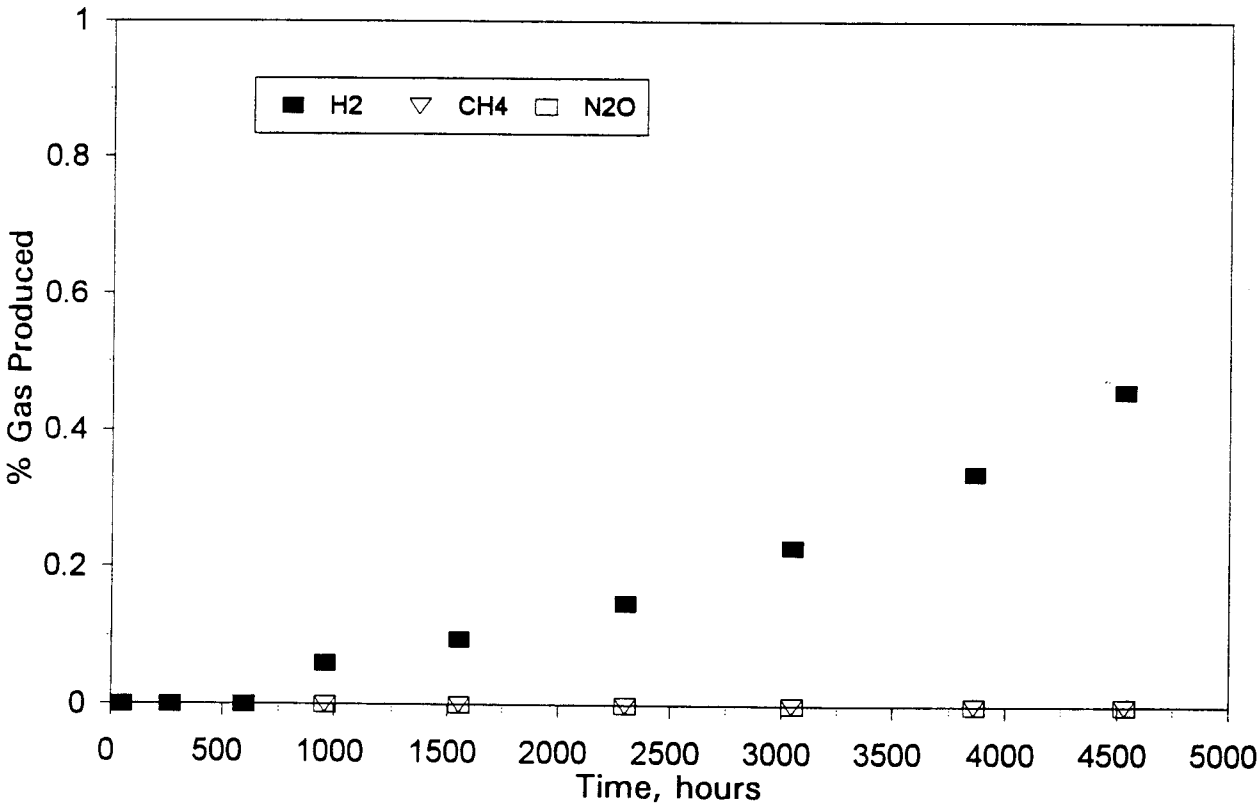

Figure 1.1. Gas Evolution for the Reaction of HEDTA in Simulated Waste (60° C, Ar).

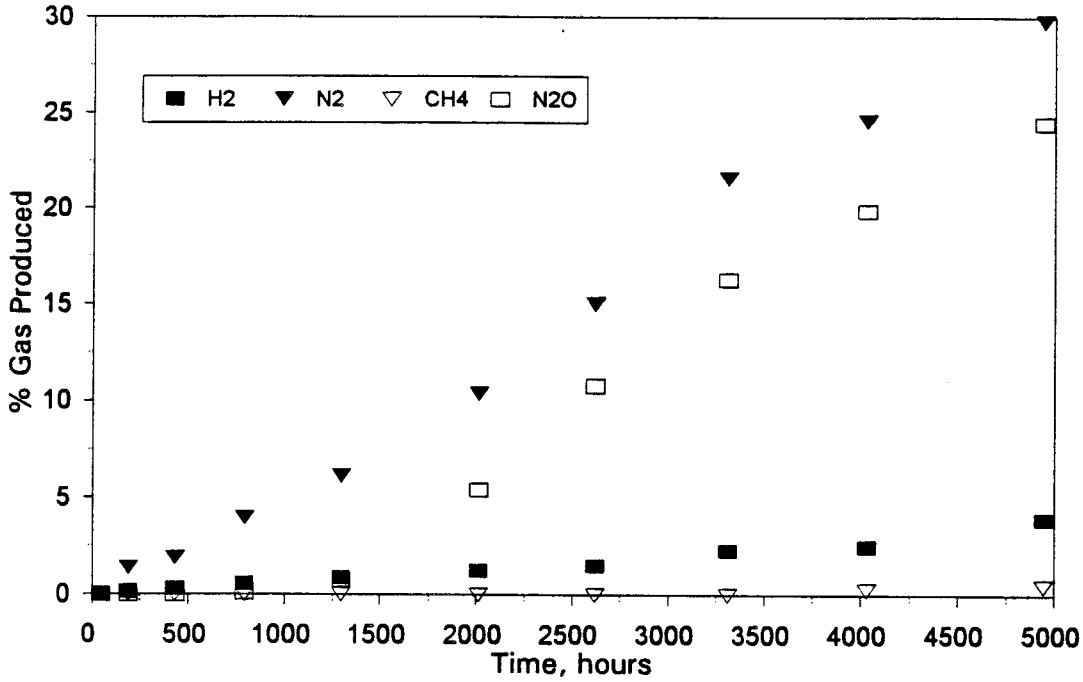

Figure 1.2. Gas Evolution for the Reaction of HEDTA in Simulated Waste (90° C, Ar).

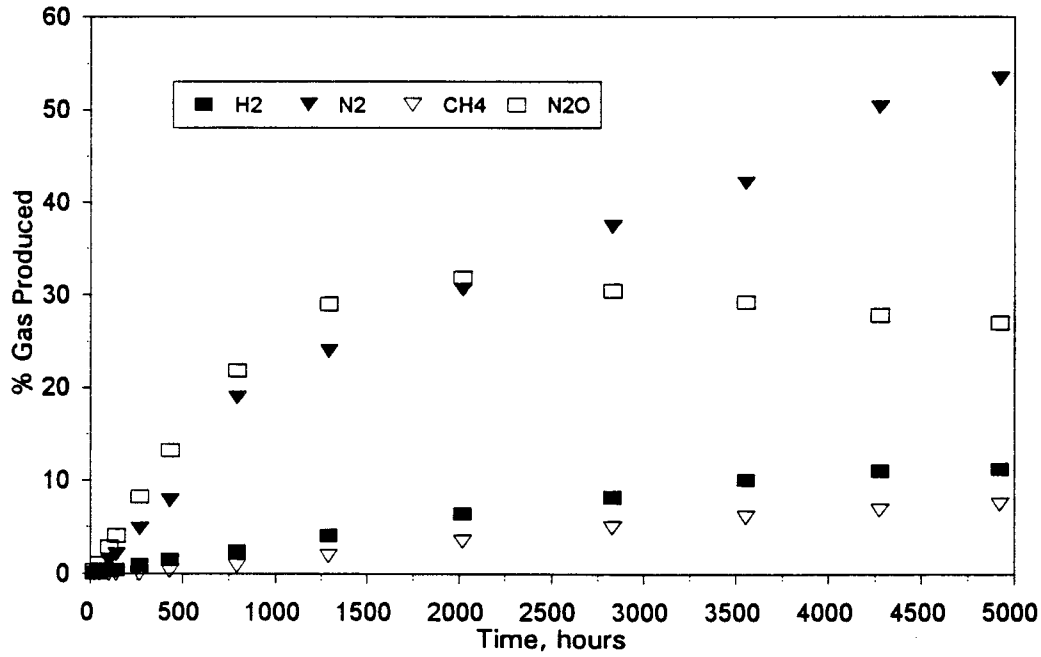

Figure 1.3. Gas Evolution for the Reaction of HEDTA in Simulated Waste (120° C, Ar; data are for experiment 12B in Table 1.1).

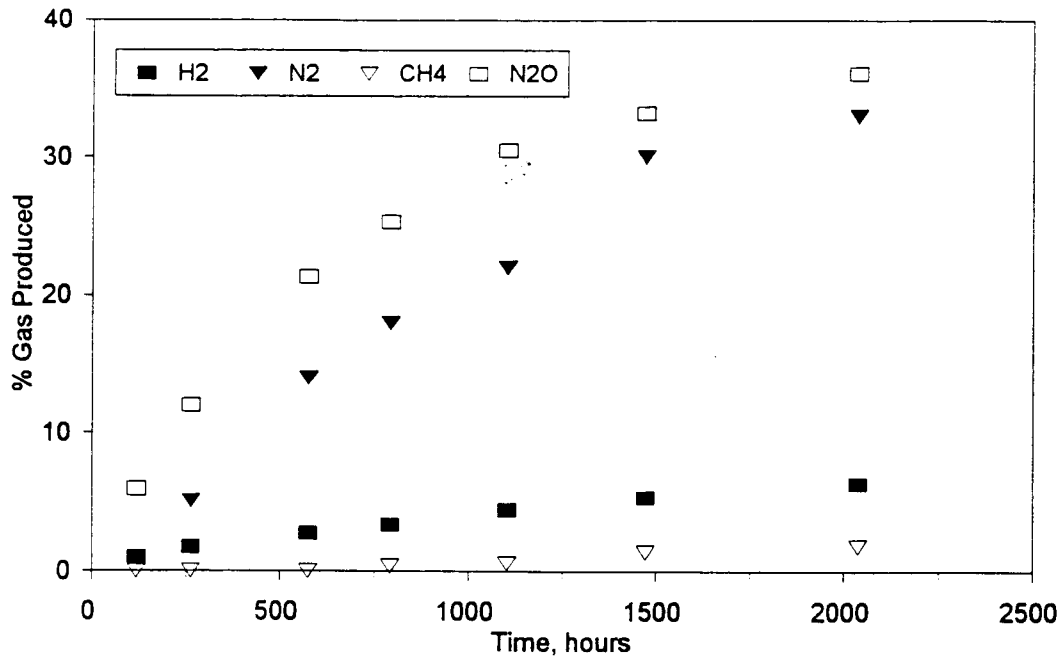

Figure 1.4. Gas Evolution for the Reaction of HEDTA in Simulated Waste (120° C, Ar; data are for experiment 19B in Table 1.1)

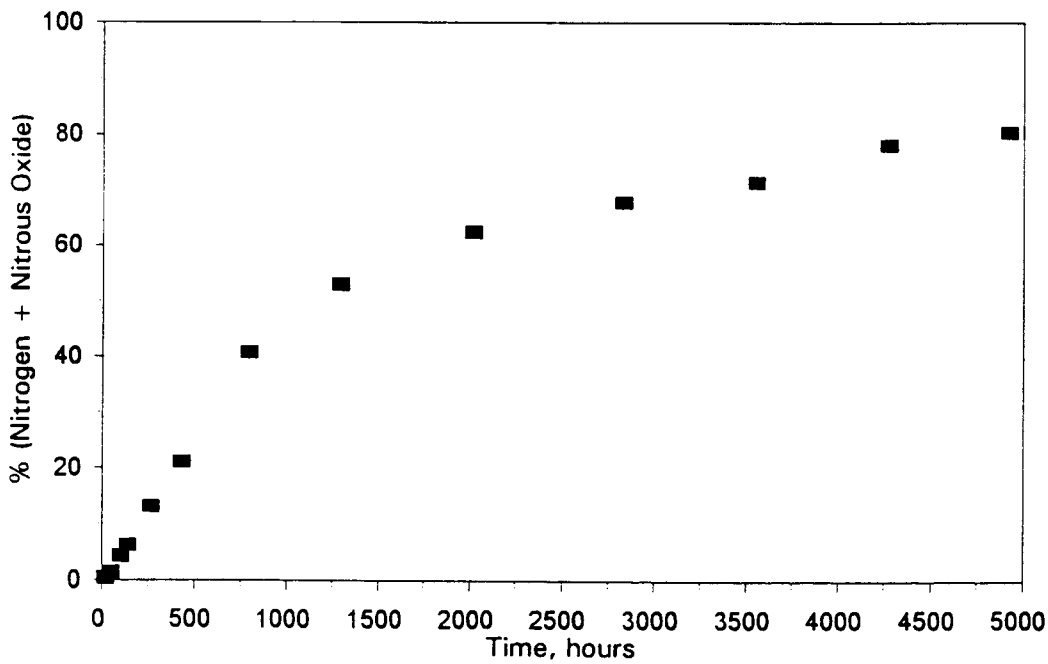

Figure 1.5. Evolution of Nitrogen plus Nitrous Oxide for the Reaction of HEDTA in Simulated Waste (120° C, Ar; data are for experiment 12B in Table 1.1)

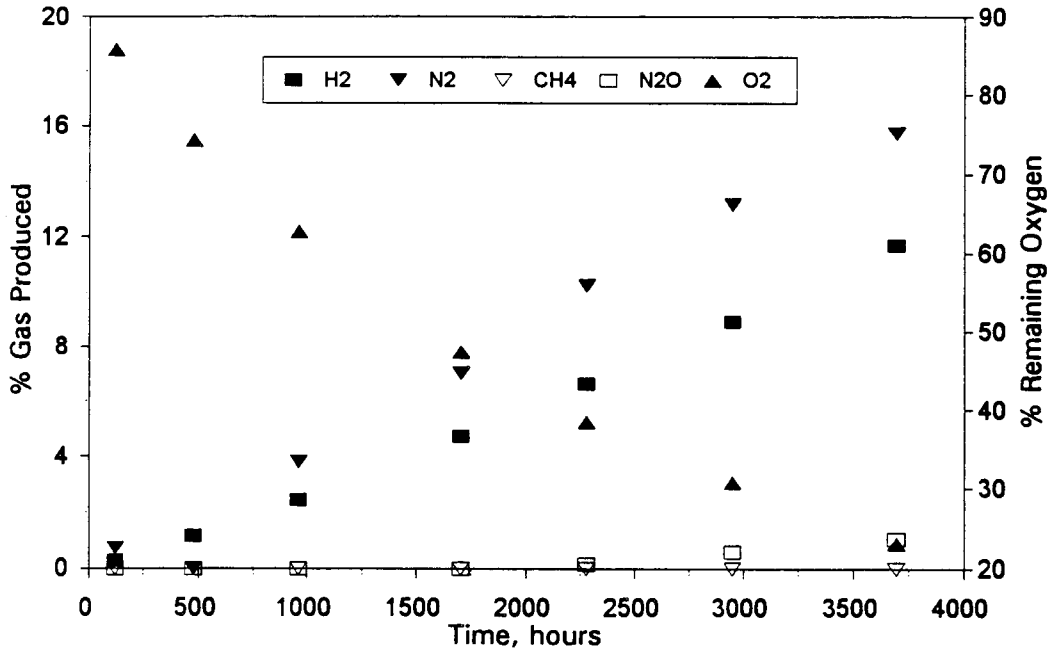

Figure 1.6. Gas Evolution for the Reaction of HEDTA in Simulated Waste (90° C, Ar/O_2).

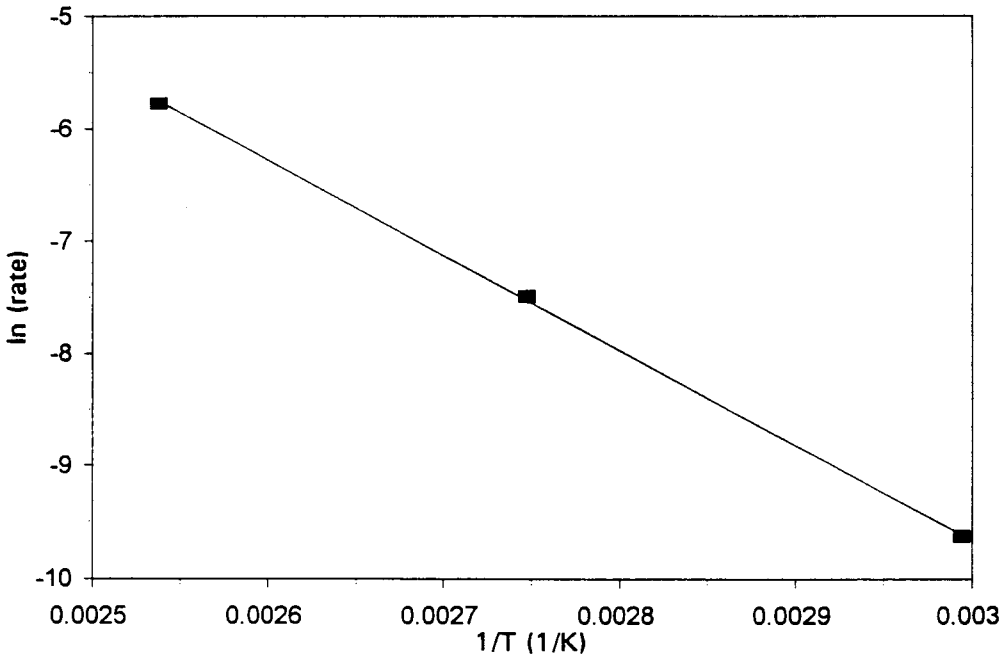

Figure 1.7. Arrhenius Plot for the Formation of Hydrogen from HEDTA in Simulated Waste (60-120° C , Ar).

1.C Kinetics and mechanism of thermal degradation of glycolate in simulated waste

The mechanism for the decomposition of glycolate in SY1-SIM-91B, based on the general notions described in more detail under Task 2, is the following:

$$Al(OH)_4^- + NO_2^- \rightleftharpoons Al(OH)_3\text{-}O\text{-}N{=}O + OH^- \quad (1.1)$$

$$Al(OH)_3\text{-}O\text{-}N{=}O + HO\text{-}CH_2\text{-}CO_2^- \rightarrow Al(OH)_4^- + O{=}N\text{-}O\text{-}CH_2\text{-}CO_2^- \quad (1.2)$$

$$O{=}N\text{-}O\text{-}CH_2\text{-}CO_2^- \rightarrow NO^- + O{=}CH_2 + CO_2 \quad (1.3)$$

$$O{=}N\text{-}O\text{-}CH_2\text{-}CO_2^- + OH^- \rightarrow NO^- + H\text{-}C(O)\text{-}CO_2^- + H_2O \quad (1.4)$$

$$NO^- + NO_2^- \rightleftharpoons N_2O_3^{2-} \quad (1.5)$$

$$2NO^- \rightleftharpoons N_2O_2^{-2} \quad (1.6)$$

$$N_2O_2^{-2} + H_2O \rightleftharpoons HN_2O_2^- + OH^- \quad (1.7)$$

$$HN_2O_2^- \rightarrow N_2O + OH^- \quad (1.8)$$

$$CH_2{=}O + OH^- \rightleftharpoons HO\text{-}CH_2\text{-}O^- \quad (1.9)$$

$$HO\text{-}CH_2\text{-}O^- + OH^- \rightleftharpoons {}^-O\text{-}CH_2\text{-}O^- + H_2O \quad (1.10)$$

$${}^-O\text{-}CH_2\text{-}O^- + H_2O \rightarrow H_2 + H\text{-}COO^- + OH^- \quad (1.11)$$

$$HC(O)\text{-}CO_2^- + OH^- \rightleftharpoons {}^-O\text{-}CH(OH)\text{-}CO_2^- \overset{OH^-}{\rightleftharpoons} ({}^-O)_2\text{-}CH\text{-}CO_2^- + H_2O \quad (1.12)$$

$$({}^-O)_2\text{-}CH\text{-}CO_2^- + H_2O \rightarrow H_2 + {}^-O_2C\text{-}CO_2^- + OH^- \quad (1.13)$$

If it is assumed that the decomposition of the nitrite ester of glycolate (Equation 1.3) is fast compared to its rate of formation (Equation 1.2), then all steps following the decomposition can be assumed to be fast and therefore can be excluded from the kinetic analysis. Based on these assumptions a rate (Equation 1.14) can be derived:

$$Rate = \frac{k[Gly]^n[Al(OH)_4^-]^m[NO_2^-]^p}{[OH^-]^q} \quad (1.14)$$

where n=1 and m, p and q are to be determined. Since glycolate is present in small quantities compared to aluminate, nitrite and hydroxide, the disappearance of glycolate should follow pseudo first-order kinetics (Equation 1.15).

$$ln[Gly]_t - ln[Gly]_{t=0} = k't \quad (1.15)$$

Thus, a plot of ln [Glycolate] vs. time should give a straight line with slope equal to k', (Equation 1.16),

$$k' = \frac{k[Al(OH)_4^-]^m[NO_2^-]^p}{[OH^-]^q} \quad (1.16)$$

where this derivation assumes m and p order dependence in $Al(OH)_4^-$ and NO_2^-, respectively. Rearranging the above expression, (Equation 1.17) produces:

$$\frac{k}{[OH^-]^q} = \frac{k'}{[Al(OH)_4^-]^m[NO_2^-]^p} \tag{1.17}$$

Two series of experiments have been conducted in an attempt to determine the effect of changes in concentration of $Al(OH)_4^-$, glycolate and NO_2^- in SY1-SIM-91B on $k/[OH^-]^q$. The first series of experiments (hereafter Series I) was done in Teflon lined glass vessels in which there was the potential for splattering of the solution onto glass above the Teflon liner. The second series (hereafter Series II) was done in Teflon lined vessels in which there was a Teflon cover over the liner that prevented any contact of the solution with glass. Series I experiments were done under air and Series II experiments were done under an argon atmosphere. Both series were done at 120° C. For each run (done in duplicate or triplicate) samples were taken at intervals and the condensed phase contents were analyzed by ion chromatography. In Series I experiments the concentrations of glycolate, formate and oxalate were determined at each time. In Series II experiments only the glycolate concentration was determined due to instrument limitations. The composition of each run and the rate constant obtained following the analysis outlined above for Series I are given in Table 1.2. The analogous data for Series II are given in Table 1.3. The data for individual runs that were used to determine the rate constants given in Tables 1.2 and 1.3 are given in the Experimental Section.

1.C.1 Series I experiments. If it is assumed that the reaction is first-order with respect to each of the reactants, then the $k/[OH^-]^q$ values for each series should be identical. The $k/[OH^-]^q$ values for Series I (Table 1.2) are very nearly the same, suggesting that the reaction is first order in glycolate, aluminate and nitrite. The ratio of oxalate to formate is approximately 3:2 (see data in Experimental Section). These products must be generated by competitive pathways, which means that the ratio of the rate constants for those pathways must also be 3:2.

1.C.2 Series II experiments. Although there is a somewhat greater spread to the $k/[OH^-]^q$ values for the Series II experiments (Table 1.3) than for those of Series I, the values also suggest that the dependence of the rate of decomposition of glycolate is first order for both aluminate and nitrite.

1.C.3 The effect of temperature on the rate of gas formation. The effect of temperature on the rate of gas formation from sodium glycolate in SY1-SIM-91B simulated waste medium was investigated in two ways. The first method utilized the measurement of the change in the head space gas volume as a function of time at various temperatures. In the second method the composition of the gas phase was determined as a function of

time at various temperatures. Data from both methods were utilized to determine activation energies.

Table 1.2. Rate Constants for the Thermal Degradation of Glycolate under Air in the presence of Glass.

EXPERIMENT	k' (hr^{-1})	$k/[OH^-]^q$ ($hr^{-1}M^{-2}$)
0.21 M Glycolate 1.54 M Aluminate 2.24 M Nitrite 0.42 M Carbonate 2.59 M Nitrate 2.00 M Hydroxide	$6.5 \pm 1.3 \times 10^{-4}$	$1.9 \pm .4 \times 10^{-4}$
0.21 M Glycolate **1.00 M Aluminate** 2.24 M Nitrite 0.42 M Carbonate 2.59 M Nitrate 2.00 M Hydroxide	$4.5 \pm 1.0 \times 10^{-4}$	$2.0 \pm .4 \times 10^{-4}$
0.10 M Glycolate 1.54 M Aluminate 2.24 M Nitrite 0.42 M Carbonate 2.59 M Nitrate 2.00 M Hydroxide	$7.0 \pm 1.5 \times 10^{-4}$	$2.0 \pm .4 \times 10^{-4}$
0.21 M Glycolate 1.54 M Aluminate **1.12 M Nitrite** 0.42 M Carbonate 2.59 M Nitrate 2.00 M Hydroxide	$3.7 \pm 1.0 \times 10^{-4}$	$2.1 \pm .4 \times 10^{-4}$

1.C.3.a Activation energy for total gas formation. The rate of total gas formation from sodium glycolate was investigated at 60° C, 90° C and 120° C under air atmosphere as outlined in the Experimental Section. The temporal production of gas as a function of time at these temperatures is shown in Figure 1.8. After equilibration of the system at 60° C the changes in gas volume up to 6250 h were negative (Figure 1.8a) suggesting that gas was consumed rather than produced. It is postulated that this negative change in gas volume is a result of consumption of oxygen. At 90° C and 120° C the changes in gas volume after equilibration of the system are positive (Figure 1.8b and 1.8c), indicating a greater rate of production of gas than consumption of oxygen.

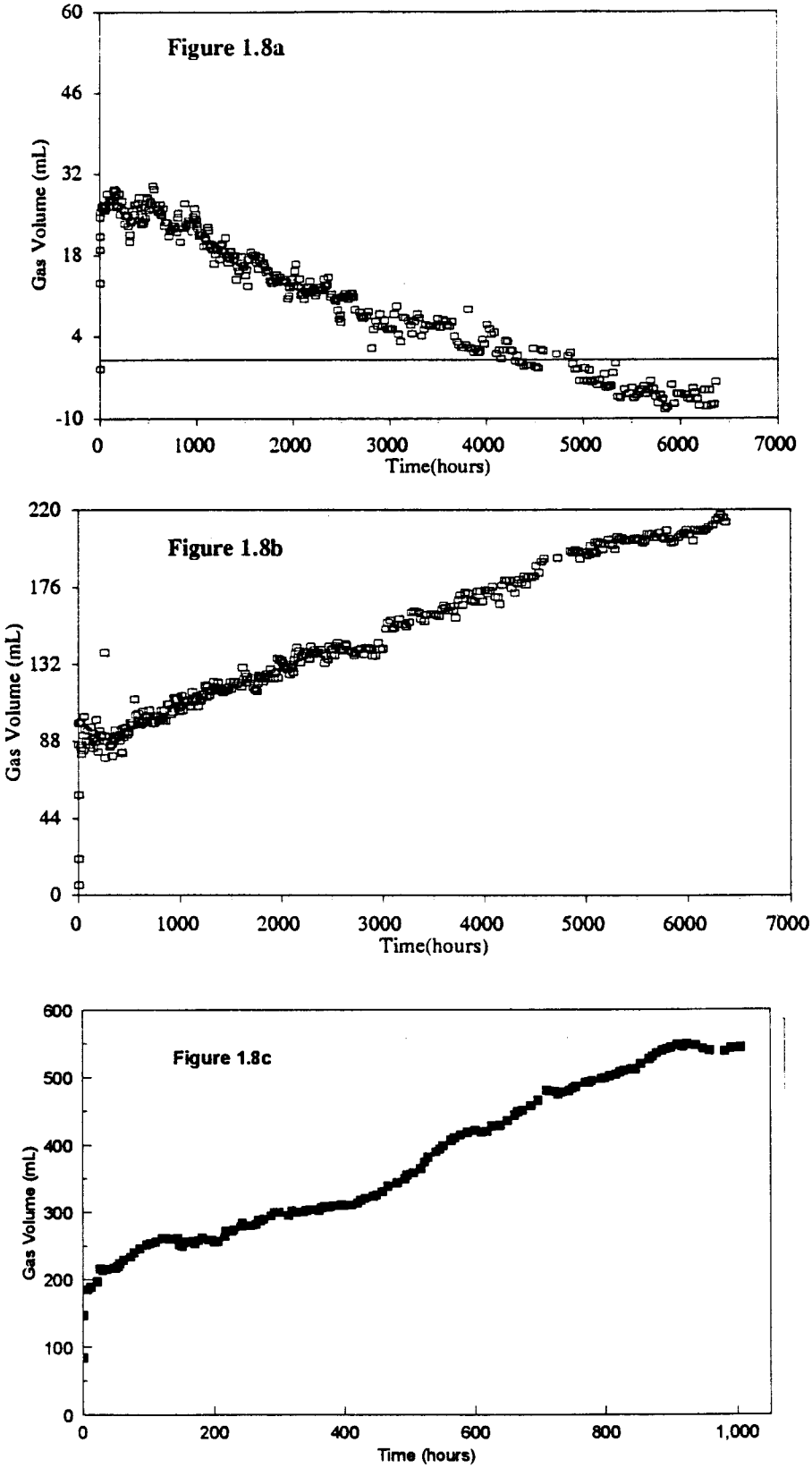

Figure 1.8. Total Gas Evolution for the Reaction of Glycolate in Simulated Waste at (a) 60 ° C; (b) 90° C; and (c) 120° C.

At 90° C the rate of gas formation is ca. 0.021 mL/h, whereas the rate of formation at 120° C is ca. 0.34 mL/h. Using the data obtained at 90° C and 120° C and the Arrhenius equation, a value for the activation energy, E_a, for total gas formation of 26 kcal/mol was calculated.

Table 1.3. Rate Constants for Thermal Degradation of Glycolate under Argon in the Absence of Glass at 120° C.

EXPERIMENT	$k^{/}$ (hr^{-1})	$k/[OH^-]^q$ ($hr^{-1}M^{-2}$)
0.21 M Glycolate 1.54 M Aluminate 2.24 M Nitrite 0.42 M Carbonate 2.59 M Nitrate 2.00 M Hydroxide	$11.4 \pm .6 \times 10^{-3}$	$3.3 \pm .2 \times 10^{-3}$
0.21 M Glycolate **1.00 M Aluminate** 2.24 M Nitrite 0.42 M Carbonate 2.59 M Nitrate 2.00 M Hydroxide	$6.27 \pm .5 \times 10^{-3}$	$2.8 \pm .2 \times 10^{-3}$
0.21 M Glycolate 1.54 M Aluminate **1.12 M Nitrite** 0.42 M Carbonate 2.59 M Nitrate 2.00 M Hydroxide	$6.34 \pm .5 \times 10^{-3}$	$3.7 \pm .3 \times 10^{-3}$

1.C.3.b Activation energies for formation of hydrogen and nitrous oxide. The reactivity of sodium glycolate was investigated at 90° C and 120° C under both argon and oxygen/argon atmospheres. The temporal behavior of gas evolution at 90° C is shown in Figures 1.9 and 1.10 and that at 120° C in Figures 1.11 and 1.12. (The values at 1200 hours corresponding to hydrogen and nitrogen in Figure 1.12 are probably too high due to an experimental error). The overall behavior is similar to that of HEDTA. The formation of nitrous oxide is inhibited by the presence of oxygen, whereas the amount of hydrogen produced is slightly greater (ca. 20%) under the oxygen-containing atmosphere. Using the initial rates of hydrogen evolution at 90° C and 120° C and the Arrhenius equation, activation energies of 30 kcal/mol and 27 kcal/mol were calculated for argon and oxygen-argon atmospheres, respectively. An activation energy for the evolution of nitrous oxide can be determined in a similar fashion using the data from the experiment done under an argon atmosphere (26 kcal/mol). Because nitrous oxide was not observed as a product at 90° C under the oxygen-containing atmosphere a value for the activation energy cannot be calculated. These values agree quite well with the value determined from the rate of total gas formation (section 1.C.3).

Although glycolate was not determined in these experiments, other experiments indicate that all glycolate should have been consumed after 1200 h. Inspection of Figures 9-12 indicates that the product distribution is not consistent with the stoichiometry suggested by the mechanism proposed in equations 1.1-1.13. According to this mechanism, 1 mol of H_2 and 0.5 mol of N_2O, but no N_2 should be formed per mole of glycolate reacting. Less than 1 mol of hydrogen was observed and the sum of the nitrous oxide and nitrogen is greater than 0.5 mol. There is the possibility of the existence of a systematic error in these measurements and therefore the absolute values could be incorrect. However, N_2 is clearly formed. At 120° C some of the N_2 undoubtedly arises from decomposition of N_2O (see Task 5, section 5.B). A possible explanation for the early formation of N_2 and NH_2OH is given in Section 1.D. Since the known pathways for formation of nitrogen involve the disproportionation of hydroxylamine and the concomitant formation of ammonia, the current efforts at Georgia Tech to quantify the amount of formation of ammonia may be enlightening.

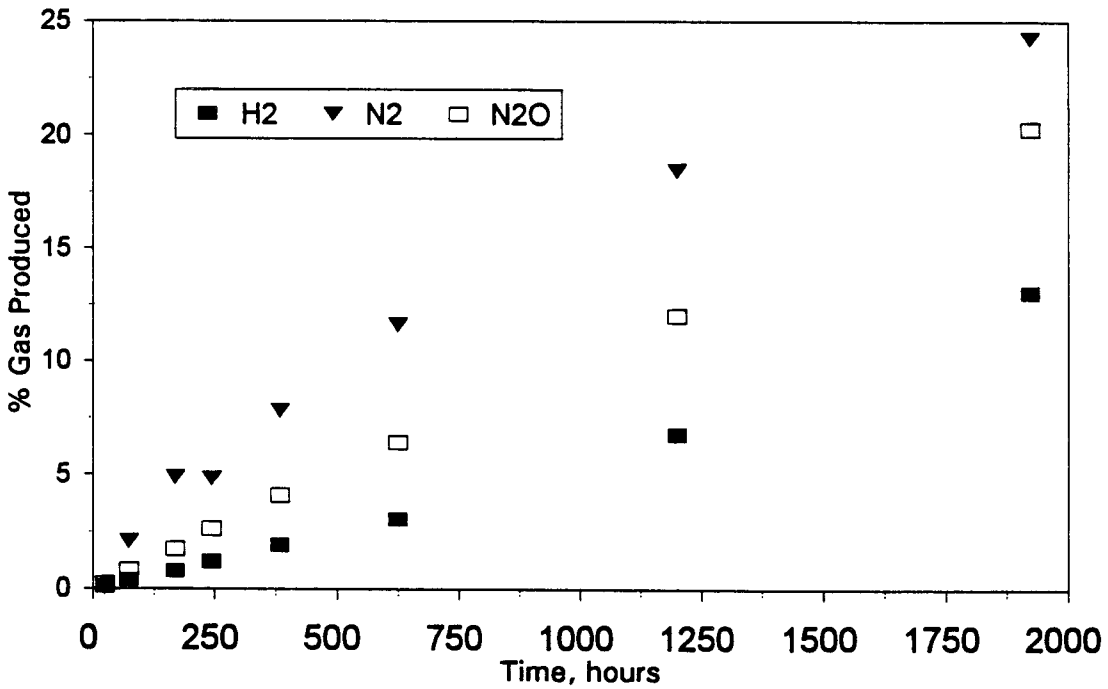

Figure 1.9. Gas Evolution for the Reaction of Glycolate in Simulated Waste (90° C , Ar).

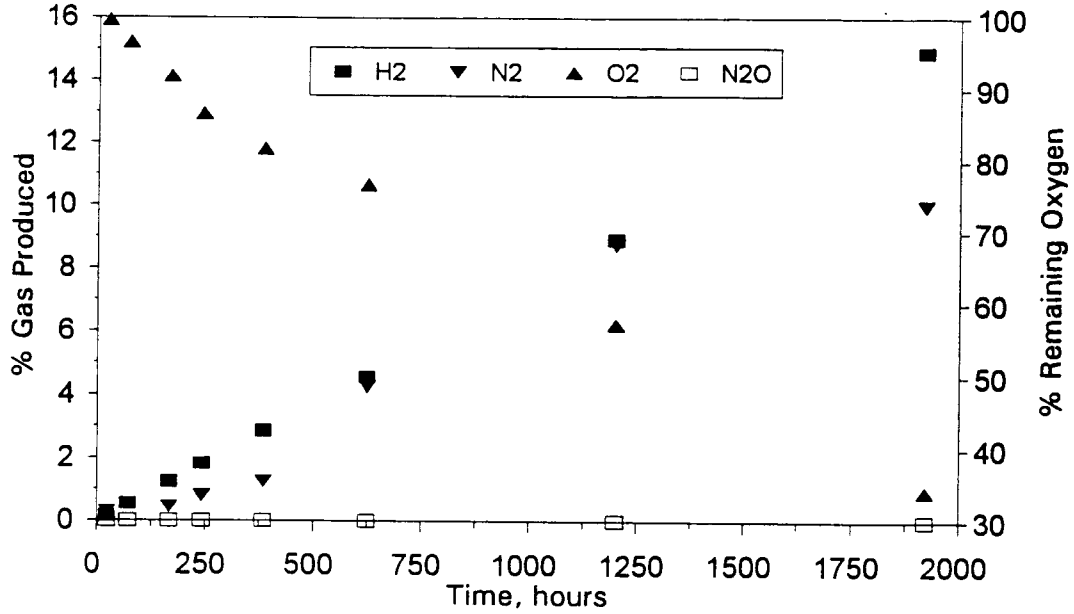

Figure 1.10. Gas Evolution for the Reaction of Glycolate in Simulated Waste (90° C , Ar\O_2).

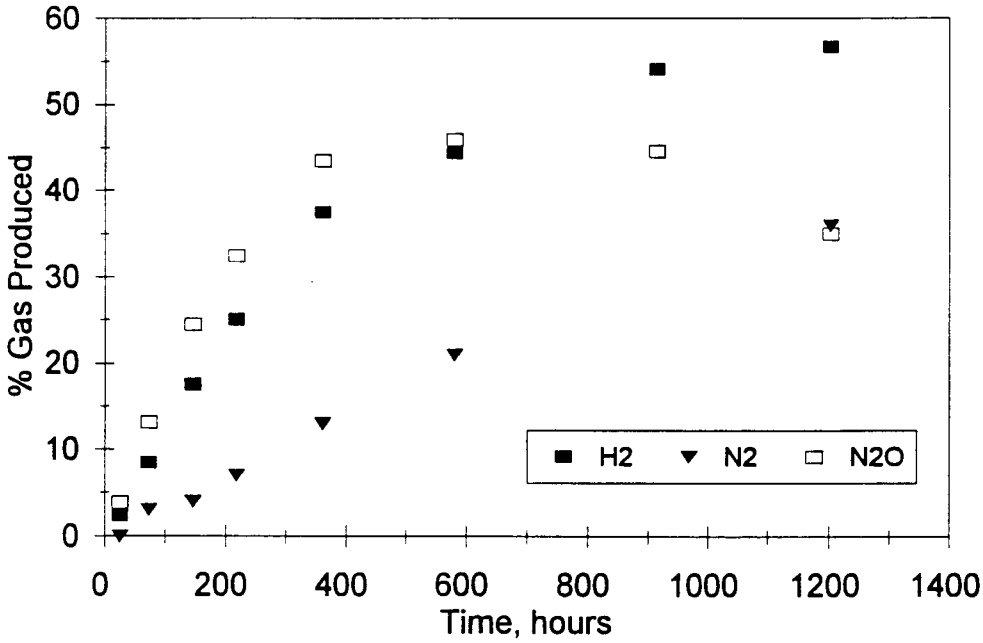

Figure 1.11. Gas Evolution for the Reaction of Glycolate in Simulated Waste (120° C, Ar).

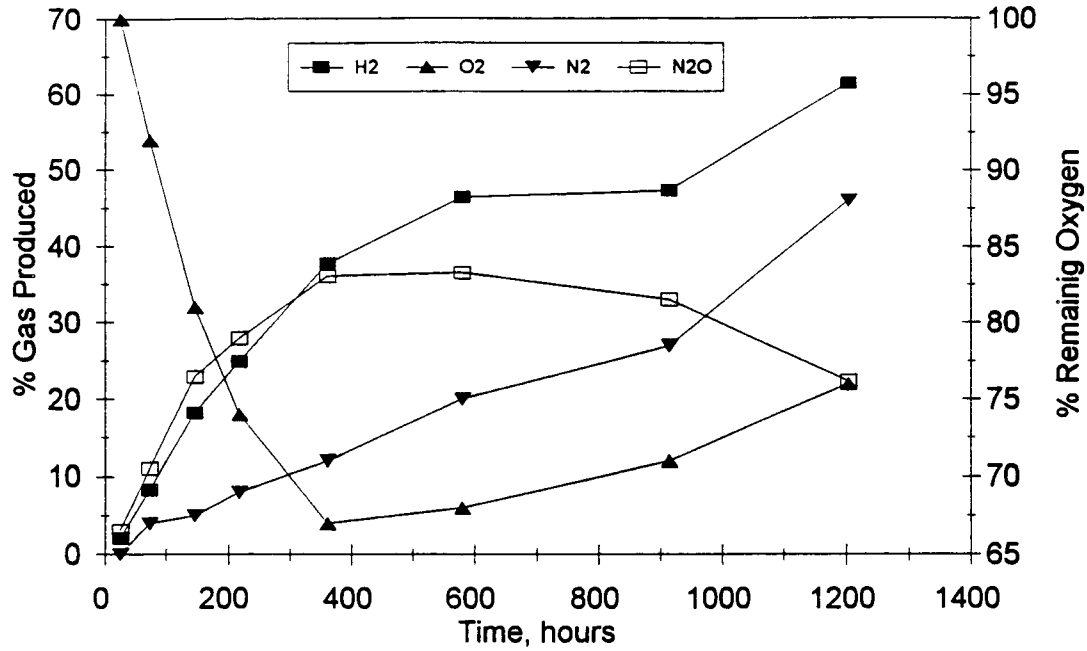

Figure 1.12. Gas Evolution for the Reaction of Glycolate in Simulated Waste (120° C, Ar/O_2).

1.D A possible explanation for the temperature dependence of gaseous product ratios for reactions of HEDTA and glycolate

A striking feature in the temporal appearance of products from both HEDTA and glycolate is the difference in the behaviors at 90° C and 120° C. The difference is seen in the relative amounts of N_2, N_2O, and H_2 as they appear with time in these experiments. For both reactants N_2 is the major product at 90° C, even at the earliest times, while N_2O is the major product at 120° C. That N_2 should be the major product at earliest times in the reaction might appear to be inconsistent with the sequence of reactions presented in Section 5.C, Task 5, which indicate N_2 as a product late in the sequence. However, the same reactions can be used to explain the temporal appearance of the products at 90° C if early formation of hydroxylamine can be accounted for. A promising explanation, which will be tested by further experiments, is based on the fact that these reactions are occurring in a medium of very high viscosity.

In both of the mechanisms for the decomposition of the nitrite ester of glycolate and the nitrite ester of HEDTA (the path leading to ED3A), NO^- and H_2CO are formed adjacent to each other. In a very viscous medium the NO^- and H_2CO formed from a single decomposition will be trapped in the so-called "solvent cage" and may combine with each other before they can diffuse away into the bulk of the solution; this is akin to the "geminate recombination" of photochemistry. The reaction of NO^- and H_2CO gives the known formohydroxamate ion, which then decomposes to formate ion and hydroxylamine. If there is extensive formation of the hydroxamate ion in the "solvent cage", formate and hydroxylamine will be early products, with the gases N_2 and NH_3 appearing later from the disproportionation of H_2NOH. All of these reactions are expected, on the basis of extrapolation of known rate data, to be fast relative to the time scale of the experiments. The behavior at 90° C appears to be consistent with this description. The relative amounts

of N_2 and H_2 formed in these reactions indicate that more than 90% of the NO^- and H_2CO react rapidly within the solvent cage.

At 120° C the viscosity is less than that at 90° C, and the percent of NO^- and H_2CO escaping the solvent cage would be expected to be greater than that at 90° C. The early yields of H_2 and N_2O would be increased, and that of N_2 decreased, as compared to the behavior at 90° C. The data for glycolate indicate that about 60% of the NO^- and H_2CO escape from the solvent cage.

The other difference in the behavior at the two temperatures is the appearance of maxima in the temporal yields of N_2O at 120° C. This effect is attributed to the thermal decomposition of N_2O (See Section 5.B in Task 5). There is nothing in the 90° C data to suggest this reaction need to be considered at this temperature.

1.E Stoichiometry and kinetics of decomposition of nitrosamines

The formation of certain of the lower molecular weight fragmentation products of HEDTA requires the cleavage of the C-N bond in a secondary amine. For example, the mechanistic pathway for formation of U-EDDA or glycine from ED3A involves the nitrosation of the secondary amine followed by base promoted elimination of HNO from the nitrosamine as shown below.

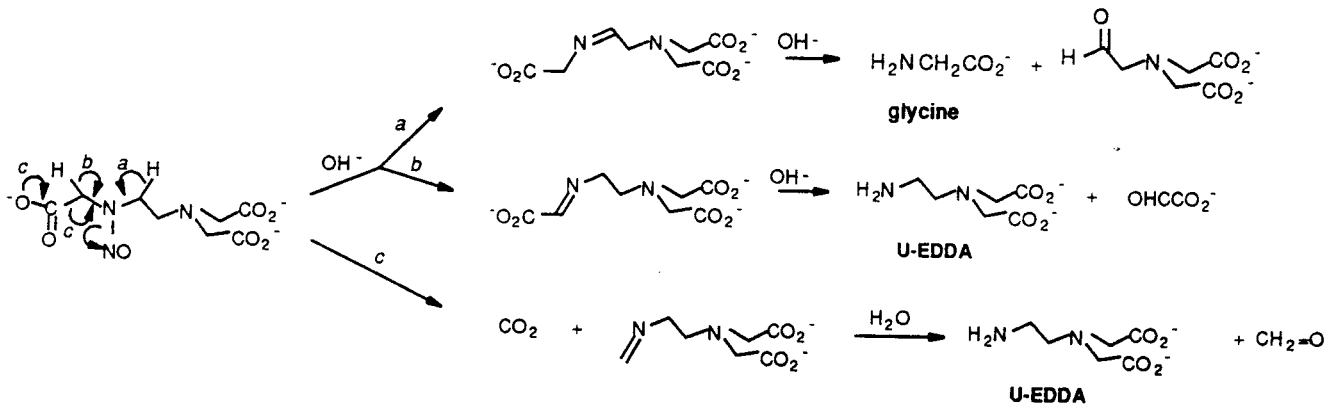

The tentative detection of N-nitrosoiminodiacetate in samples taken from tank 101-SY[2] raises an important issue about the stability of nitrosamines in nuclear waste media. Two nitrosamine compounds, N-nitrosoiminodiacetic acid, NNIDA, and N-nitroso-N-ethylglycine, NNEG, have been synthesized and their decomposition studied in highly basic medium as outlined below.

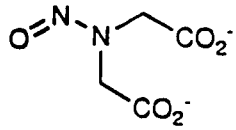

NNIDA (1)

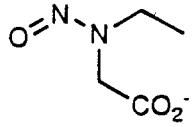

NNEG (2)

1.E.1 Decomposition of N-nitrosoiminodiacetic acid, NNIDA. The reaction of 0.21 M NNIDA, **1**, in 2.0 M NaOH at 120° C under an air atmosphere was monitored by ^1H NMR spectroscopy. Major products detectable by ^1H NMR spectroscopy were formate and glycine (or possibly IDA whose resonance overlaps with that of glycine at 300 MHz) and small amounts of glycolate and acetate. The disappearance of NNIDA was first order with a rate constant of $2.8 \times 10^{-3}\ h^{-1}$, which corresponds to a half-life of 250 h. IC analysis of the reaction mixture after ca. 1200 h indicated that oxalate was also formed and that the ratio of formate to oxalate was about 3:1. A ^{13}C NMR spectrum of the reaction mixture at this time indicated the formation of carbonate. Gas analyses performed on other reactions of NNIDA in 2 M NaOH and in SY1-SIM-91B medium showed the formation of both N_2O and H_2. Equations 1.18-1.23 show a plausible reaction sequence for formation of the major carbon products derived from NNIDA. The formation of N_2O from NO^- and hydrogen from formaldehyde would be according to equations 1.6-1.8 and 1.9-1.11, respectively.

$$ONN(CH_2CO_2^-)_2 \rightarrow CO_2 + CH_2{=}NCH_2CO_2^- + NO^- \quad (1.18)$$

$$CH_2{=}NCH_2CO_2^- + H_2O \rightarrow CH_2{=}O + H_2NCH_2CO_2^- \quad (1.19)$$

$$ONN(CH_2CO_2^-)_2 + OH^- \rightarrow NO^- + H_2O + {}^-O_2CCH_2N{=}CHCO_2^- \quad (1.20)$$

$${}^-O_2CCH_2N{=}CHCO_2^- + H_2O \rightarrow H_2NCH_2CO_2^- + OHCCO_2^- \quad (1.21)$$

$$HC(O)\text{-}CO_2^- + 2\ OH^- \rightleftharpoons ({}^-O)_2\text{-}CH\text{-}CO_2^- + H_2O \quad (1.22)$$

$$({}^-O)_2\text{-}CH\text{-}CO_2^- + H_2O \rightarrow H_2 + {}^-O_2C\text{-}CO_2^- + OH^- \quad (1.23)$$

A reevaluation of the data from the August 31, 1992 report from Georgia Tech indicates that the amount of formate (and oxalate) produced is too large and the amount of glycine formed is too small in view of the low reactivity of glycine expected under these conditions (see section 1.F.6). The system is currently being reinvestigated under conditions where both the condensed and gas phases can be monitored as a function of time to obtain an accurate picture of the complete stoichiometry of the NNIDA decomposition. However, formation of both formate and oxalate points to dual pathways for decomposition of the NNIDA.

1.E.2 Decomposition of N-nitroso-N-ethylglycine, NNEG. The reaction of NNEG, **2**, was conducted in the same fashion as for NNIDA, except that the reaction temperature was 100° C. The lower temperature was chosen because of the greater reactivity of NNEG compared to that of NNIDA. Monitoring of the reaction by ^1H NMR showed the disappearance of NNEG and the appearance of formate, acetate and glycine. The disappearance of NNEG was first order with a rate constant of $1.78 \times 10^{-2}\ h^{-1}$ which gives a half-life of 40 h. This value was determined using the original data from the September 1992 Georgia Tech status report and more recent data obtained in a reinvestigation of this system. In separate experiments the gas phase was analyzed at the completion of the reaction. Both hydrogen and nitrous oxide were detected. Nitrous oxide obtained from NNEG that was prepared using ^{15}N-labelled nitrite (equation 1.23) contained two ^{15}N atoms, indicating that the two nitrogen atoms came

from different NNEG molecules, presumably via NO^- as described in equations 1.6-1.9. $Ni(CN)_4^{2-}$, which absorbs at 498 nm, has been reported to react with NO^- to produce $NiNO(CN)_3^{2-}$ [3] When $Ni(CN)_4^{2-}$ was included in reaction mixtures of NNEG, an absorption at 498 nm was observed after 100 h consistent with the presence of the nitrosonickel complex and presumably NO^-. A plausible reaction sequence for formation of the observed carbon products is given by equations 1.24-1.29. Formaldehyde would react further to produce formate and hydrogen as shown in equations 1.9-1.11.

$$ONN(CH_2CH_3)CH_2CO_2^- \rightarrow CO_2 + CH_2{=}NCH_2CH_3 + NO^- \quad (1.24)$$

$$CH_2{=}NCH_2CH_3 + H_2O \rightarrow CH_2{=}O + H_2NCH_2CH_3 \quad (1.25)$$

$$ONN(CH_2CH_3)CH_2CO_2^- + OH^- \rightarrow CH_3CH{=}NCH_2CO_2^- + NO^- \quad (1.26)$$

$$CH_3CH{=}NCH_2CO_2^- + H_2O \rightarrow CH_3CHO + H_2NCH_2CO_2^- \quad (1.27)$$

$$CH_3CHO + 2\ OH^- \rightarrow CH_3CH(O)_2^{2-} + H_2O \quad (1.28)$$

$$CH_3CH(O)_2^{2-} + H_2O \rightarrow H_2 + CH_3CO_2^{2-} \quad (1.29)$$

The total carbon balance of the identified products from the decomposition of NNEG is not in agreement with the stoichiometry predicted by these reactions. However, acetaldehyde can react under these conditions to produce products other than acetate, and the failure to detect ethylamine, shown as a product in equation 1.25, by ^1H NMR is not unexpected because of its high volatility and the small amount that would be produced.

The observations made on NNIDA and NNEG support the notion that nitrosation of a secondary amine such as ED3A, IDA, etc. would lead to a reactive species that produces the same gaseous products formed in tank 101-SY and in reactions in simulated waste. The organic fragments produced suggest reactivity patterns for ED3A, IDA, etc. that would lead to the same types of products that have been observed for degradation reactions conducted in simulated waste. Also, the higher reactivity of NNIDA compared to HEDTA suggests that the concentration of NNIDA can never be higher than that of HEDTA.

1.F Factors affecting the reactions of HEDTA, EDTA and related compounds in simulated waste

A variety of observations made by investigators at Westinghouse, PNL, Argonne and Georgia Tech have suggested that a variety of materials and conditions can affect the rate at which HEDTA and other complexants decompose in simulated waste media. This section describes studies that attempt to determine the effects of some additives and conditions on the rates and products of decomposition of several complexants. Most of the experiments reported here are of a survey nature and in general were not done in duplicate. Some inconsistencies with other similar experiments are noted in a few instances.

1.F.1 Effect of glass. The effect of the addition of glass on HEDTA decomposition in freshly prepared simulated waste solution is illustrated by the data given in Table 1.4. These data indicate that glass accelerates the rate of decomposition in either an oxygen or argon atmosphere, and that ED3A is a major nitrogen-functionalized product. In all cases the amount of formate observed is approximately twice the amount of ED3A formed. The amount of H_2 produced is higher under oxygen atmosphere compared to Ar atmosphere.

The material balance for the organic molecules, given by the amount (%HEDTA + %ED3A + %EDTA + %S-EDDA) is reasonably good in all cases (80 to 90%). Glycine and U-EDDA were also observed as products, but could not be quantified because their ^{1}H-NMR resonances were coincident with those of other compounds present in the reaction mixture.

The effect of glass was studied in the absence of sodium aluminate, in order to determine if glass, or its constituents, can function as a substitute for aluminate. Table 1.5 shows that practically no reaction is observed in the absence of sodium aluminate, either in the absence or presence of glass. Therefore, it can be concluded that silicate does not play the same role as aluminate in these reactions.

The increase in rate that results from the addition of glass (in the presence of sodium nitrite) could be due to a decrease in $[OH^-]$, i.e., $SiO_2 + 2\ OH^- \rightarrow SiO_2(OH)_2^{2-}$. This conclusion is based upon Delegard's observation[1] that the maximum reactivity for thermal decomposition of HEDTA occurs at $[OH^-]$=1.4 M.

No nitrous oxide was observed when simulated waste solutions, prepared with heating in glass vessels, were heated at 120° C. When the simulated waste solutions were prepared in polypropylene containers or glass containers without heating, the amount of N_2O produced at 120° C increased dramatically. Although the yield of N_2O was strongly affected, the yields of the products in solution (ED3A, formate, etc.) were not affected.

1.F.2 Effect of sodium silicate. In order to determine if the catalytic effect of added glass is due to dissolved silicates from the glass, a solution of sodium silicate ("liquid glass") was added to the simulated waste solution. The data in Table 1.6 indicate that no acceleration resulted, and that there might even be an inhibiting effect due to the added sodium silicate. This suggests that the catalytic effect of added glass is not due to dissolved silicates and is consistent with the earlier suggestion (section 1.F.1) that the effect may be due to a decrease in $[OH^-]$.

Table 1.4. Effect of Glass on the Reaction of HEDTA in Simulated Waste (500 h, 120° C).[1]

TRIAL NAME	HEDTA-16A	HEDTA-18A	HEDTA-15A	HEDTA-17A
Atmosphere	O_2	O_2	Ar	Ar
Material added	-	glass[2]	-	glass[2]
HEDTA	65.2	38.1	51.0	10.5
$HCOO^-$	41.4	71.4	51.0	129
$(COO^-)_2$	12.4	20.2	5.8	18.1
ED3A	22	32	24	60
EDTA	<2	13	<2	~4
s-EDDA	5	6	~4	10
AcO^-	<2	<2	<2	3
H_2	3.3	21.5	1.5	11.9
O_2[3]	12	26	-	-
N_2	12	~4	19	27
CH_4	<0.1	0.4	<0.1	0.4
N_2O	4.6	1.2	5.7	9.0

[1]Unless otherwise stated, all products are indicated as moles per 100 moles of organic starting material. [2]250 mg of borosilicate glass in small pieces were added to 3 mL of solution, just before the heating started. [3]Moles of O_2 *consumed* per 100 moles of organic starting material.

1.F.3 Effect of sodium chloride. Added sodium chloride appeared to accelerate the reaction of HEDTA in simulated waste as indicated by the data in Table 1.7. In the presence of oxygen the ratio of formate to oxalate increased relative to the reaction in the absence of NaCl; the same was true for the ratio of H_2 to N_2O. When argon was used as the cover gas, no appreciable differences in product ratios were observed.

Table 1.5. Effect of Glass on the Reaction of HEDTA in Simulated Waste in the Absence of Sodium Aluminate (500 h, Ar, 120° C).[1]

TRIAL NAME	HEDTA-23A	HEDTA-24A
Material added	glass[2]	-
HEDTA	99.0	97.6
$HCOO^-$	<1	3.8
$(COO^-)_2$	<2	<2
H_2	<0.1	0.2
N_2	<1	~3
CH_4	<0.1	<0.1
N_2O	<0.1	0.2

[1]Unless otherwise stated, all products are indicated as moles of product per 100 moles of organic starting material. [2]250 mg of borosilicate glass were added to 3 mL of solution just before the heating was started.

Table 1.6. Effect of Sodium Silicate on the Reaction of HEDTA in Simulated Waste (500 h, Ar, 120° C).

TRIAL NAME	HEDTA-15A	HEDTA-5B
Material Added	-	SiO_2[2]
HEDTA	51.0	65.7
$HCOO^-$	51.0	41.5
$(COO^-)_2$	5.8	~4
ED3A	24	24
s-EDDA	~2	~4
H_2	1.5	0.5
N_2	19	8
CH_4	<0.1	0.1
N_2O	5.7	4.9

[1]Unless otherwise stated, all products are indicated as moles of product per 100 moles of organic starting material. [2]860 mg of a solution containing 27% SiO_2 and 14% NaOH were added to 5 ml of SY1-SIM-91B solution just before the heating started.

Table 1.7. Effect of Added NaCl on the Reaction of HEDTA in Simulated Waste (500 h, 120° C).[1]

TRIAL NAME	HEDTA-16A	HEDTA-18A	HEDTA-15A	HEDTA-17A
Atmosphere	O_2	O_2	Ar	Ar
Material added	-	NaCl[2]	-	NaCl[2]
HEDTA	65.2	30.0	51.0	29.3
$HCOO^-$	41.4	77.1	51.0	98.1
$(COO^-)_2$	12.4	8.3	5.8	11.9
ED3A	22	37	24	54
EDTA	<2	~2	<2	~2
s-EDDA	5	7	~4	9
AcO^-	<2	<2	<2	~2
H_2	3.3	9.5	1.5	3.2
O_2[3]	12	13	-	-
N_2	12	24	19	27
CH_4	<0.1	0.1	<0.1	0.3
N_2O	4.6	4.8	5.7	7.3

[1]Unless otherwise stated, all products are indicated as moles of product per 100 moles of organic starting material. [2]38 mg of sodium chloride were added to 3 ml of solution, just before the heating started. [3]Moles of oxygen *consumed* per 100 moles of organic starting material.

1.F.4 Effect of aging. Table 1.8 shows the results observed when simulated waste containing HEDTA was aged for 1000 h prior to heating. The reactions carried out with freshly prepared solutions are included for comparison. The reactivity of HEDTA and the amount of H_2 produced are considerably increased by aging, especially for the reactions carried out under oxygen atmosphere. The amount of nitrous oxide produced decreased and the amount of oxygen absorbed increased substantially for the aged solution. These results may indicate that the concentration of an intermediate, which favors oxygen absorption and hydrogen production build up during the aging period.

1.F.5 Effect of light. In general, no attempt has been made to exclude light in most of the work done on thermal decomposition experiments done at Georgia Tech. However, some reaction vessels were opaque, whereas most were glass with Teflon liners that allowed light in from the top. In order to determine if photochemical reactions could play a significant role several experiments were carried out with HEDTA and HEG (an HEDTA model) under continuous irradiation by a 250 watt sun lamp.

Table 1.8. Effect of Solution Aging on the Reaction of HEDTA in Simulated Waste (500 h, 120° C).[1]

TRIAL NAME	HEDTA-15A	HEDTA-16A	HEDTA-31A	HEDTA-30A
	fresh solution	fresh solution	aged solution[2]	aged solution[2]
Atmosphere	O_2	Ar	O_2	Ar
HEDTA	65.2	51.0	17.6	39.5
$HCOO^-$	41.4	51.0	113	88.6
$(COO^-)_2$	12.4	5.8	28.2	7.0
ED3A	22	24	49	42
EDTA	<2	<2	9	4
s-EDDA	5	~4	10	6
AcO^-	<2	<2	~2	~2
H_2	3.3	1.5	14.6	3.8
O_2[3]	12	-	25	-
N_2	12	19	19	11
CH_4	<0.1	<0.1	<0.1	<0.1
N_2O	4.6	5.7	1.2	1.4

[1]Unless otherwise stated, all products are indicated as moles per 100 moles of HEDTA. [2]The solution was aged 1000 h in a polypropylene container at r. t. [3]Moles of O_2 *consumed* per 100 moles of HEDTA.

Control experiments in the absence of light were conducted by wrapping aluminum foil around the reaction vessels. The results (Table 1.9) do not suggest a major effect of light although the reactivity may be slightly enhanced by photolysis. The effect, if it exists, is small and does not argue for a major photochemical pathway.

Table 1.9. Effect of Light on the Reactions of HEDTA and HEG in Simulated Waste (120° C, Ar, 200 h).[1]

Trial Name	Light	Starting Mat.	$HCOO^-$	H_2	N_2	CH_4	N_2O
HEDTA-15A	NO	80	30	0.4	~3	<0.1	2.4
HEDTA-16A	YES	68	33	0.4	~3	<0.1	1.9
HEG-11A	NO	70	7	0.2	<2	<0.1	0.2
HEG-12A	YES	63	11	0.1	~4	<0.1	2.1

[1]Unless otherwise stated, all products are indicated as moles per 100 moles of organic starting material.

1.F.6 Effect of oxygen on the reactivity of metal complexants. Many observations have suggested that the presence of oxygen has a significant effect on the rate of reaction of certain metal complexants and on the amount of some of the gaseous products. To further explore these phenomena a series of survey experiments were undertaken to determine the relative reactivities of a series of compounds under argon or oxygen atmospheres. Table 1.10 presents data for EDTA, glycolate, and for HEDTA and some of its fragments. The data in Table 1.10 suggest the following:

- A reactivity order of glycolate > HEDTA > > U-EDDA, S-EDDA > EDTA, glycine, IDA, NTA in either an oxygen or argon atmosphere.
- The amount of hydrogen produced is substantially greater under an oxygen containing atmosphere.

The latter observation is an important one that should be considered whenever new mitigation procedures are considered for waste storage tanks. Procedures that introduce O_2 into the waste mixture could have the deleterious effect of increasing the amount of H_2 generated.

The mechanistic role of oxygen on the decomposition of HEDTA and other metal complexants is unknown but it is well established that most alkanes can be oxidized by molecular oxygen (autoxidation) at 100-150° C without added initiators.[4] The accepted mechanism of the reaction involves the formation of a radical, followed by a radical chain process (equations 1.30-1.33).

(X· = any radical)

$$X\cdot + RH \rightarrow R\cdot + HX \tag{1.30}$$

$$R\cdot + O_2 \rightarrow RO_2\cdot \tag{1.31}$$

$$RO_2\cdot + RH \rightarrow RO_2H + R\cdot \tag{1.32}$$

$$2\,RO_2\cdot \rightarrow RO_2R + O_2 \tag{1.33}$$

The first step can be catalyzed by the presence of light and photosensitizers, but also by metals (Co, Mn, Cu, Fe) and bases. The mechanism of autoxidation in the presence of bases has been proposed by Russell and Bemis to be that shown by equations 1.34-1.37.[5]

$$R_3CH + Base \rightarrow R_3C^- + BaseH^+ \tag{1.34}$$

$$R_3C^- + O_2 \rightarrow R_3C\cdot + O_2\cdot^- \tag{1.35}$$

$$R_3C\cdot + O_2 \rightarrow R_3CO_2\cdot \tag{1.36}$$

$$R_3CO_2\cdot + R_3C^- \rightarrow R_3CO_2^- + R_3C\cdot \tag{1.37}$$

Table 1.10. Effect of Oxygen on the Reaction of Metal Complexants in Simulated Waste Solution (120° C, 1000 h)[1].

Experiment	Atm	Starting Material	$HCOO^-$	$C_2O_4^=$	H_2	O_2[2]	N_2[3]	CH_4	N_2O
EDTA-5A	Ar	102	<1	<2	1.3	-	~4	<0.1	<0.1
Glycolate-14A	Ar	27.4	29.8	43.5	21.2	-	~7	0.3	14.6
HEDTA-22A	Ar	34.8	73.4	10.0	2.7	-	20	0.1	5.9
Glycine-1A	Ar	97	1.4	6.2	1.5	-	~4	<0.1	0.4
U-EDDA-1A	Ar	90[4]	7.0	<2	0.5	-	~7	0.1	0.5
S-EDDA-2A	Ar	86	1.9	<2	2.0	-	~10	0.8	0.5
IDA-1A	Ar	100	<1	<2	0.9	-	~3	<0.1	<0.1
NTA-2A	Ar	95	1.9	5.0	2.5	-	~11	0.2	<0.1
EDTA-6A	O_2	93	3.0	9.7	6.7	17	~3	0.1	<0.1
Glycolate-12A	O_2	7.8	34.4	48.3	26.8	25	~5	0.3	9.5
HEDTA-21A	O_2	30.4	79.9	10.5	2.6	24	~11	0.3	8.6
Glycine-1A	O_2	81	2.0	16.5	8.5	15	~3	<0.1	0.1
U-EDDA-2A	O_2	80[4]	17.8	4.8	2.2	23	13	<0.1	0.1
S-EDDA-1A	O_2	79	7	15.3	9.3	25	~6	0.1	0.3
IDA-2A	O_2	93	2.3	4.9	4.1	15	~8	<0.1	0.1
NTA-1A	O_2	92	3.3	11.6	6.7	22	~2	0.1	<0.1

[1]Unless otherwise stated, all percentages represent moles of product per 100 moles of organic starting material. [2]Amount of oxygen *consumed* per 100 moles of starting organic material. [3]A considerable deviation (~ 40% when $\%N_2$ is < 10) can be expected for these values, due to air contamination. [4]Estimated values.

Based on the above equations, autoxidation of the organic substrates could be expected when reactions are carried out in simulated waste solution at 120°C under oxygen (or air) atmosphere. Some further investigation of possible autooxidation reactions of several compounds were undertaken. The results are described in the subsequent sections.

1.F.6.a Sodium glycolate. Significant reaction was observed when sodium glycolate was allowed to react under an oxygen atmosphere in simulated waste solution that did not contain $NaNO_2$ (Table 1.11, GLY-3). Furthermore, the reaction proceeded under oxygen atmosphere even when only NaOH and glycolate were present in the solution (GLY-IT). Oxygen absorption was observed in the first case (it was not

determined in the second case), although less than for unmodified simulated waste solutions. The oxalate to formate ratio appeared to be greater in each case than for the unmodified reaction. The following reactions are known to occur:[4]

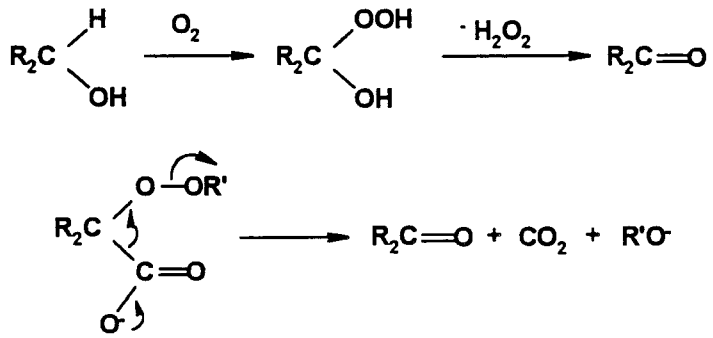

Table 1.11. Reaction of Sodium Glycolate in Modified Simulated Waste Solutions (120° C, 500 h).[1]

Trial	Compound(s) Deleted	Atm.	Starting Material	$HCOO^-$	$C_2O_4^{2-}$	H_2	N_2O	O_2[2]
GLY-3A	-	O_2	33.0	24.1	34.4	27.5	4.4	23
GLY-3	$NaNO_2$	O_2	82.9	3.4	14.7	8.3	0.3	12
GLY-IT[3]	$NaNO_2$\$NaNO_3$\ $NaAlO_2$\$Na_2CO_3$	O_2[4]	89.5	3.8	7.9	-	-	-

[1]Unless otherwise stated, all percentages represent moles of product per 100 moles of organic starting material. [2]Moles of oxygen *consumed* per 100 moles of organic starting material. [3]This reaction was carried out in the brass/teflon apparatus described in Figure 7. Due to the design of the reaction vessel, no data for gas analysis could be recorded. [4]The pressure of the gas over the solution was ~760 mm.

Extending these reactions to the case of glycolate, the following mechanism could be proposed:

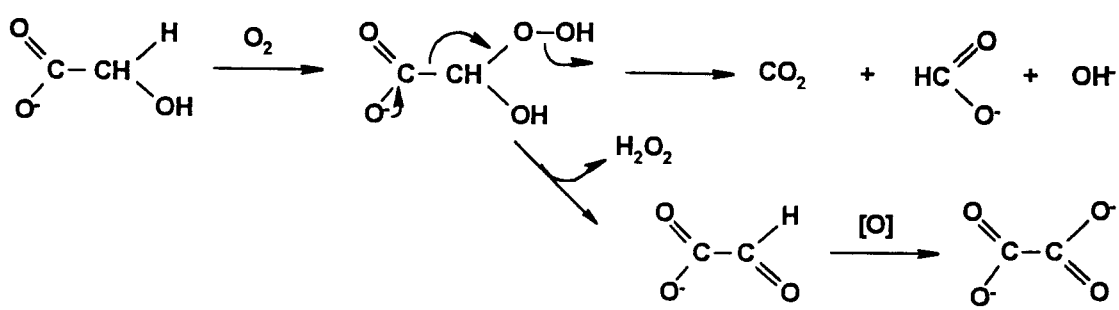

Scheme 1.1. Proposed Mechanism for the Autoxidation of Sodium Glycolate.

1.F.6.b HEDTA. The observations for HEDTA are similar to those for sodium glycolate. Little reaction was observed for any case where $NaNO_2$ was eliminated and oxygen was not present (Table 1.12).

Table 1.12. Effect of Oxygen on Reactions of HEDTA in Modified Simulated Waste (120° C, 500 h).[1]

Trial	Compound Deleted	Atm.	HEDTA	$HCOO^-$	$C_2O_4^{2-}$	H_2	N_2O	O_2[2]
10A	$NaNO_2$	Ar	97.1	<1	<1	1.0	<0.1	-
1A	$NaNO_2$\$NaNO_3$	O_2	92.8	12.3	4.7	5.2	<0.1	32
2A	$NaNO_2$\$NaNO_2$	Ar	100	<1	<1	0.3	<0.1	-

[1]Unless otherwise stated, all percentages represent moles of product per 100 moles of organic starting material. [2]Amount of oxygen *consumed* per 100 moles of organic starting material. [3]Other products found (^{1}H-NMR): ED3A (≈14%), AcO^- (5.9%). [4]This reaction was carried out in the brass/teflon apparatus described in Figure 7. Due to the design of the reaction vessel, no data for gas analysis could be recorded. [5]The gas pressure over the solution was ~760 mm.

The formation of hydroperoxides by autoxidation in the case of tertiary amines is known to occur at the carbon adjacent to the nitrogen function:[6]

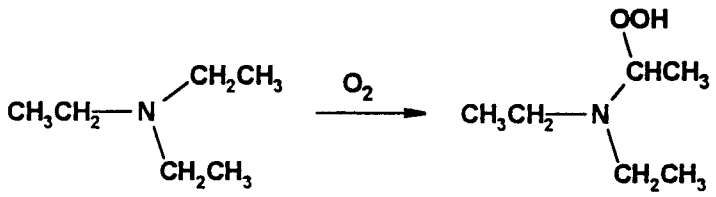

It is also known[7] that when the nitrogen function is γ to the peroxide linkage, the following reaction occurs:

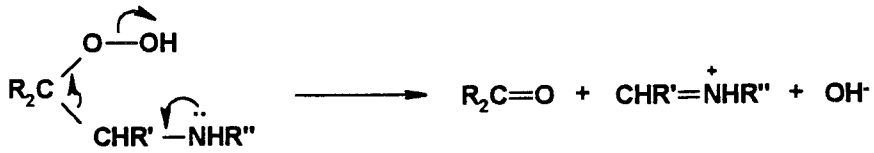

This, together with the reactions suggested for glycolate, allows us to propose the following mechanism for the autoxidation of HEDTA:

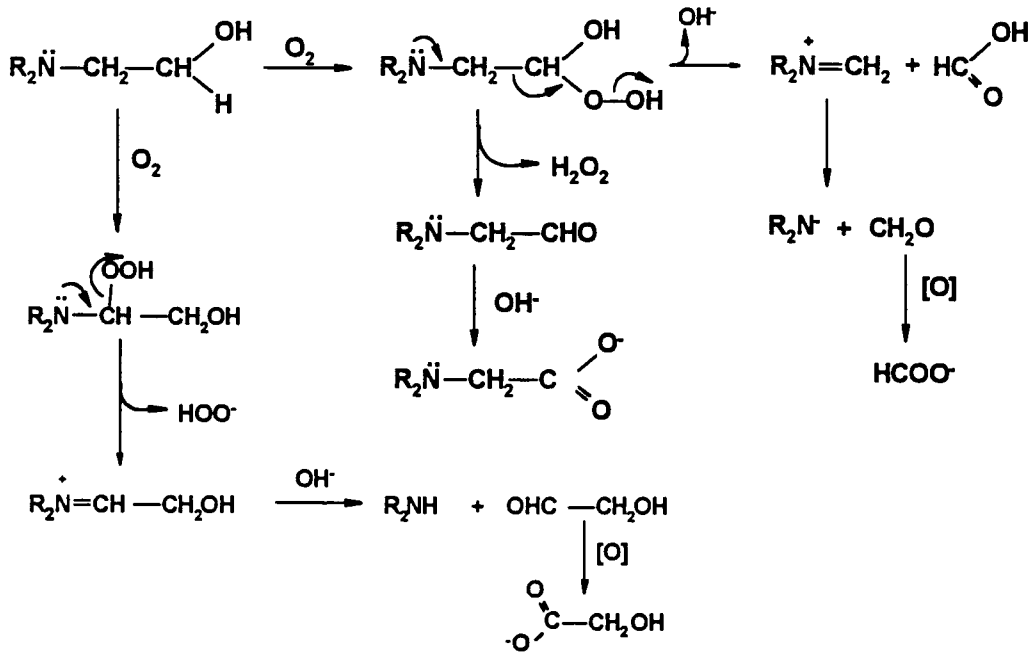

Scheme 1.2. Proposed Mechanism for the Autoxidation of HEDTA.

1.F.6.c EDTA and dimethylglycine (DMG). In this case, where no hydroxyethyl group is present in the molecules, no reaction was observed under Ar atmosphere, but reaction proceeded to a limited extent with evolution of H_2 when O_2 was present (Table 1.13).

Table 1.13. Effect of Oxygen on the Reaction of EDTA and DMG in Simulated Waste (120° C, 1000 h).[1]

Trial	Atm.	Starting Mat.	$HCOO^-$	$(COO^-)_2$	H_2	N_2O	O_2[2]
EDTA-5A	Ar	102	<1	<2	1.3	<0.1	-
EDTA-6A	O_2	93	3.0	9.7	6.7	<0.1	17
DMG-1A	Ar	95	<1	3.5	1.0	0.2	-
DMG-2A	O_2	79	13.2	18.4	14.7	<0.1	25

[1]Unless otherwise stated, all amounts represent moles of product per 100 moles of organic starting material. [2]Amount of O_2 *consumed* per 100 moles of organic starting material.

Taking into consideration the reactions mentioned before, the following mechanism could be proposed for the autoxidation of EDTA, and related compounds:

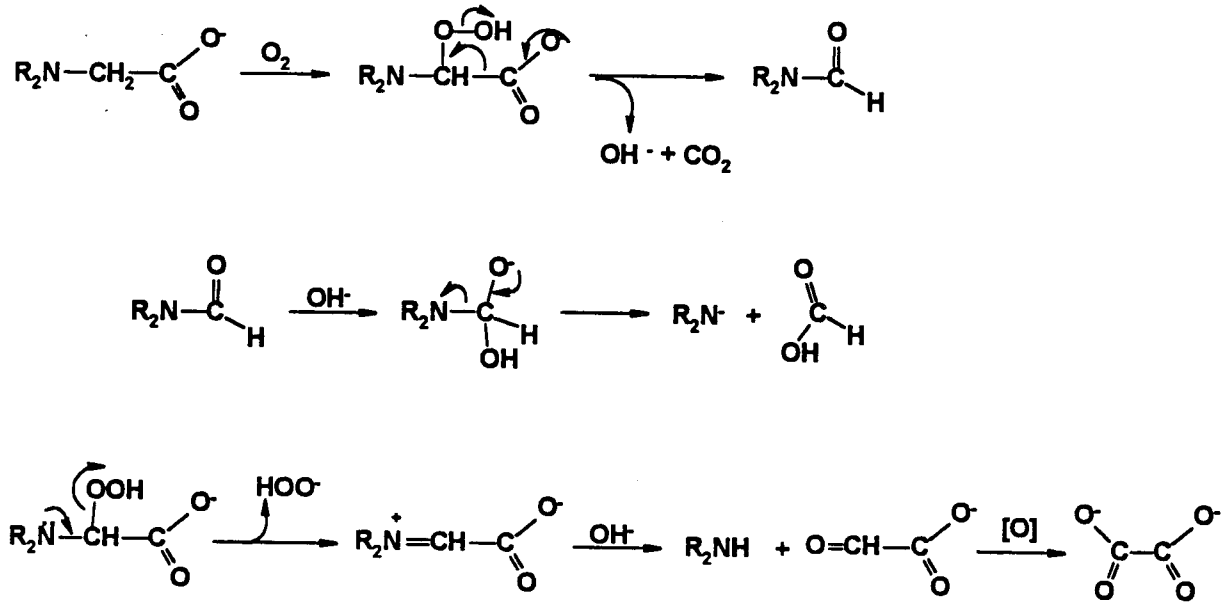

Scheme 1.3. Proposed Mechanism for the Autoxidation of EDTA and Related Compounds.

The extent to which autoxidation contributes to the processes occurring in tank 101-SY cannot be estimated at this time. The temperature in the tank is significantly lower than in the above experiments, and lower than the temperature range in which autoxidation processes are known to be significant. However, because radiolytic processes occurring in the tank will produce radicals that are potential initiators for autoxidation it must be considered as a possible contributor. The availability of oxygen could be an important factor. Since autoxidation appears to produce hydrogen but no nitrous oxide the N_2O/H_2 ratio will depend, at least in part, on the contribution of autoxidation relative to the "nitrite induced" thermal pathway.

1.G References

(1) Delegard, C. *RHO-LD-125*, Dec. **1980**; Avail. INIS, NTIS.
(2) Campbell, J.A.; Pool, K.H.; Melethill P.K. *PNL-8041* March **1992**;Avail. INIS, NTIS.
(3) Bonner, F.T.; Akhtar, M.J. *Inorg. Chem.* **1981**, *20*, 3155, and references therein.
(4) Swern, D. *Organic Peroxides*, **1972** Wiley-Interscience, NY, *I, II, III.*
(5) Russel, G.; Bemis A.G. *J. Am. Chem. Soc.* **1966**, *88*, 5491 and references therein.
(6) Cullis, C.F.; Waddington, D.J. *Proc. Roy. Soc. (London)* **1958**, *A244*, 110; *A246*, 91; *A248*, 136.
(7) Schmitz, E; Habisch, D.; Ohine, R. *J. Prakt. Chem.* **1968**, *37*, 252.

TASK 2: PRODUCT IDENTIFICATION

2.A Identification of HEDTA degradation products using ^{13}C NMR spectroscopy

A major objective of the effort at Georgia Tech has been to utilize the earlier studies done at Hanford and Pacific Northwest Laboratories as the basis for further development of an understanding of both the stoichiometry and the temporal formation of individual degradation products of organic complexants in waste tank 101-SY. One approach has been the use of ^{13}C NMR to monitor the products produced from ^{13}C-enriched HEDTA (two forms HEDTA-A and HEDTA-B, shown below) and glycolic acid. The use of compounds that are highly enriched with ^{13}C in specific positions allows for the detection and identification of products produced early in the reaction from the chemical shifts. In addition, the spin-spin coupling patterns arising from 1,2-labeled derivatives are very useful in assigning structures to the absorptions produced by the products.

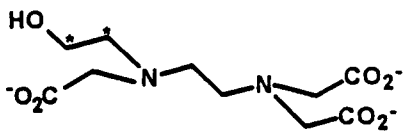

HEDTA-A

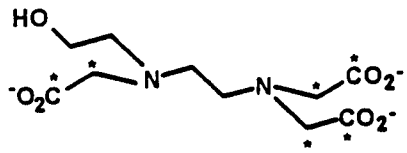

HEDTA-B

To identify the products of complexant degradation it was necessary to establish a data base of ^{13}C NMR spectra of authentic samples of HEDTA, EDTA, glycolate, and known, or probable, degradation products. Commercial samples were used when available, others were synthesized as outlined in the Experimental Section. Spectral data (^{13}C chemical shifts) for all compounds are given in Table 2.1.

Experimentally, the thermal reaction of ^{13}C-labeled HEDTA-A in simulated waste solution was carried out at 120° C for a total of 1452 h (60.5 days). The reaction mixture was transferred at regular intervals to an NMR tube using a pipette, and ^{13}C NMR spectra were recorded. Then, the solution was returned to the reaction vessel and heating was continued. Intensities of all peaks were measured relative to C_6D_6, which was in an external cell. The solution was diluted to 1 mL (starting amount) after 60.5 days of heating at 120° C and the NMR measured again to estimate the amount of remaining HEDTA (50%). It should be noted that the reaction was done under an air atmosphere that was replaced each time a sample was taken. Also the sample was exposed to the glass NMR tube for about one h each time that a spectrum was taken.

After 1.5 days the ^{13}C spectrum of the HEDTA-A reaction mixture contained a new resonance attributed to formate and a more intense resonance for carbonate, which is believed to arise from the formation of CO_2 with subsequent reaction with OH^-. Oxalate was detectable after 18.5 days and labeled glycine after 34.5 days.

Table 2.1 ^{13}C Chemical Shifts (ppm) in Simulated Waste Solution.[a]

EDTA 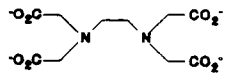	51.95	59.16	180.81					
HEDTA 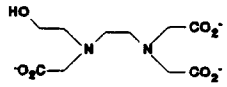	51.47	52.09	56.75	58.45	59.11	59.39	180.71	180.99
ED3A[b] 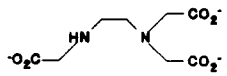	45.71	52.50	54.99	59.92	180.62	180.99		
ED3A LACTAM 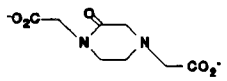	47.18	48.57	50.86	55.66	60.50	169.88	176.53	178.15
NTA 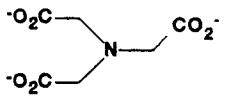	59.37	180.48						
IDA 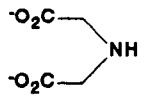	52.19	180.61						
S-EDDA[b] 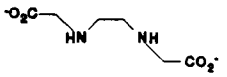	47.63	52.43	180.62					
U-EDDA 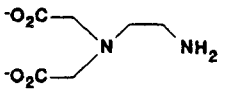	37.81	58.20	59.92	180.60				
N-ME S-EDDA[b] 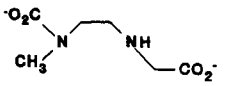	42.31	45.63	52.57	56.31	61.89	179.56	180.56	

Table 2.1 continued

N-ME ED3A[b] 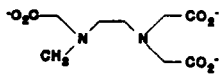	42.60	52.65	54.43	59.88	62.15	180.53	180.80	
HIDA 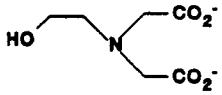	57.49	58.89	59.89	180.64				
DMG[b] 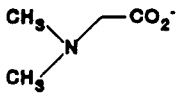	44.73	63.31	179.48					
GLYCINE[b] 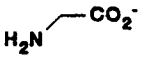	45.05	182.68						
GLYCOLATE 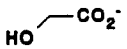	61.86	183.07						
N-ME GLYCINE[b] 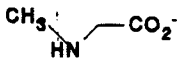	34.83	54.29	180.65					
MIDA[b] 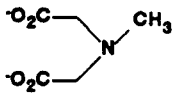	42.86	61.79	180.23					
ED 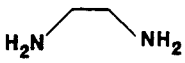	43.49							
N-ME ED 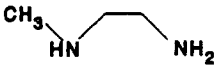	34.90	39.93	53.03					

Table 2.1 continued

HED 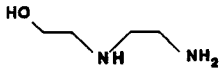	40.28	50.79	50.96	60.23				
EDMA[b] 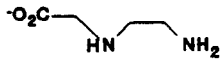	40.06	50.73	52.30	180.56				
N-ME U-EDDA[c] 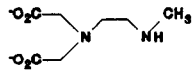	34.99	40.18	44.34	53.03	175.50			
EA 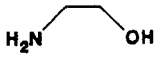	43.25	63.29						
EAMA 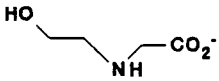	50.68	52.41	60.36	180.74				

[a]Chemical shifts were measured relative to an external C_6D_6 standard unless otherwise indicated. [b]Chemical shifts for these compounds were measured with respect to sodium carbonate in simulated waste solution and converted to the C_6D_6 external standard scale. [c]Spectrum recorded in 2M NaOH due to the sensitivity of N-ME U-EDDA to simulated waste solution.

The spectrum recorded after 60.5 days also contained a singlet due to unlabeled glycine, indicating that its formation occurs from the carboxymethyl groups as well as from the hydroxyethyl group. The relative amounts of glycine formed from $-N^{13}CH_2{}^{13}CH_2OH$ and unlabeled $-NCH_2CO_2H$ after 60.5 days was approximately 1:6. Two pairs of doublets centered at δ 50.51 and 60.28 (J=38 Hz) and δ 43.03 and 63.33 (J=38 Hz) were detected after 13.5 days and 34.5 days, respectively, and have been assigned as ethanolamine-N-monoacetic acid (EAMA) and ethanolamine (EA), respectively, based on a comparison of their chemical shifts with those of authentic material. A summary of the appearance of products versus time data is given below and the ^{13}C NMR spectrum, obtained after 60.5 days of reaction, is given in Figure 2.1.

After	36h	HCO_2^-, CO_3^{-2}
	60h	HCO_2^-, CO_3^{-2}
	108h	HCO_2^-, CO_3^{-2}
	156h	HCO_2^-, CO_3^{-2}
	204h	HCO_2^-, CO_3^{-2}, EAMA (traces)
	444h	HCO_2^-, CO_3^{-2}, EAMA, $C_2O_4^{-2}$
	564h	HCO_2^-, CO_3^{-2}, EAMA, $C_2O_4^{-2}$
	828h	HCO_2^-, CO_3^{-2}, EAMA, $C_2O_4^{-2}$, EA, Glycine (labeled)
	1452h	HCO_2^-, CO_3^{-2}, EAMA, $C_2O_4^{-2}$, EA, Glycine (labeled and unlabeled)

It should be emphasized that because only the hydroxyethyl group is ^{13}C-enriched, only those species derived from the hydroxyethyl group will be detectable in the NMR spectrum, at least in the early stages of the reaction. In addition, resonances from such species may mask resonances from unlabeled products when their chemical shifts are similar. Given the intensity of the peak due to unlabeled glycine that is detectable in Figure 2.1, there should be a proportionate amount of ED3A and S-EDDA, necessarily unlabeled. Resonances for these species will be masked by others, such as those for EAMA, in the spectrum (see the following discussion of the ^{13}C data for HEDTA-B). The presence of significant quantities of S-EDDA may, in fact, be indicated by the unassigned resonance at ca. δ 47.6 in Figure 2.1.

The ^{13}C NMR studies involving the thermal decomposition of HEDTA-B in simulated waste at 120°C were carried out in a similar fashion to those for HEDTA-A. Resonances in the ^{13}C NMR spectrum obtained after 1808 h (Figure 2.2) have been assigned to ED3A, U-EDDA, S-EDDA, IDA, glycine, formate, oxalate and carbonate. The assignment of resonances to ED3A is not straightforward as they overlap with resonances due to U-EDDA and S-EDDA. However, the spectrum also contained five doublets of low intensity at δ 50.86, 55.67, 169.93, 176.62, and 178.25 that are most likely due to ED3A lactam (δ=50.86, 55.66, 60.50, 169.99, 176.53 and 178.15, for authentic material). The doublet at δ 60.50, observed for the authentic lactam, could not be seen as it lies under more intense resonances of HEDTA and U-EDDA. ED3A has been reported to cyclize to give the lactam under acidic conditions and to revert back to ED3A in basic media.[1] Because of the strongly basic nature of the simulated waste solution, ED3A, if present, should be largely in the uncyclized form; therefore the presence of minor amounts of lactam indicates the presence of substantial amounts of the uncyclized material. We therefore believe that the intense doublets at δ 59.96 and 52.46 must be partially due to ED3A, as well as U-

EDDA, and S-EDDA. Further support for the assignment of these resonances is provided by the lowest field carboxylate resonance, observed at δ 181.08 (J=52.6 Hz) in the 1808 h spectrum. Only two compounds, HEDTA (δ=180.71 and 180.99) and ED3A (δ=180.62 and 180.99) have carboxylate resonances with chemical shifts >δ 180.90. The larger coupling constant of HEDTA (55.2 Hz) suggests that this doublet is primarily due to ED3A. It is worth noting that the intensity of the doublet at δ 52.43 that is assigned to S-EDDA increased relative to the doublet at 52.50 assigned to ED3A during the course of the reaction (see Figure 2.3). It should be noted that these assignments differ from those originally reported in the Georgia Tech May and June 1992 monthly reports. (The resonance at δ 52.43 was originally assigned to EAMA and the resonance at δ 52.50 to ED3A and/or S-EDDA.) A summary of the temporal appearance of the products formed from HEDTA as determined from ^{13}C spectra taken at the times indicated is given below.

After	14h	little reaction
	37h	little reaction
	135h	HCO_2^-, CO_3^{-2}, $C_2O_4^{-2}$, ED3A &/or U-EDDA, S-EDDA
	232h	HCO_2^-, CO_3^{-2}, $C_2O_4^{-2}$, ED3A &/or U-EDDA, S-EDDA
	399h	HCO_2^-, CO_3^{-2}, $C_2O_4^{-2}$, ED3A &/or U-EDDA, S-EDDA
	562h	HCO_2^-, CO_3^{-2}, $C_2O_4^{-2}$, ED3A &/or U-EDDA, S-EDDA
	732h	HCO_2^-, CO_3^{-2}, $C_2O_4^{-2}$, ED3A &/or U-EDDA, S-EDDA IDA, ^{13}C-Glycine, ED3A Lactam
	1232h	HCO_2^-, CO_3^{-2}, $C_2O_4^{-2}$, ED3A &/or U-EDDA, S-EDDA IDA, ^{13}C-Glycine, ED3A Lactam
	1808h	HCO_2^-, CO_3^{-2}, $C_2O_4^{-2}$, ED3A &/or U-EDDA, S-EDDA IDA, ^{13}C-Glycine, ED3A Lactam

2.B Identification of irradiated HEDTA degradation products using ^{13}C NMR spectroscopy.

Samples of HEDTA-A and HEDTA-B were irradiated in simulated waste solution (50-60 mg in 5 mL solution contained in steel tubes) at doses of 19.6 Mrad and 20.8 Mrad, respectively at Argonne National Laboratory (D. Meisel) and were returned to Georgia Tech for ^{13}C NMR spectral analysis. As reported previously, HEDTA reacts significantly upon irradiation, as indicated by the low intensity of the resonances for HEDTA in these samples (Figures 2.4 and 2.5). Tentative assignments of resonances are shown in the spectra of the irradiated samples.

Because time dependent irradiation studies are not available it is not possible to draw definitive conclusions concerning differences in products or their distributions between the thermal and irradiative degradation pathways. One obvious difference is that a substantial amount of IDA is formed as one of the products derived from irradiation of HEDTA-B, whereas IDA has not been observed as a significant product from thermal reactions. However, it must be noted that much more HEDTA has been consumed in the irradiation of HEDTA-B than in the corresponding thermal reaction. Large amounts of IDA were detected by Lokken in Tank-107AN;[2] thus it could be conjectured that radiolytic decomposition of HEDTA could be a major pathway for the generation of IDA in the waste storage tank.

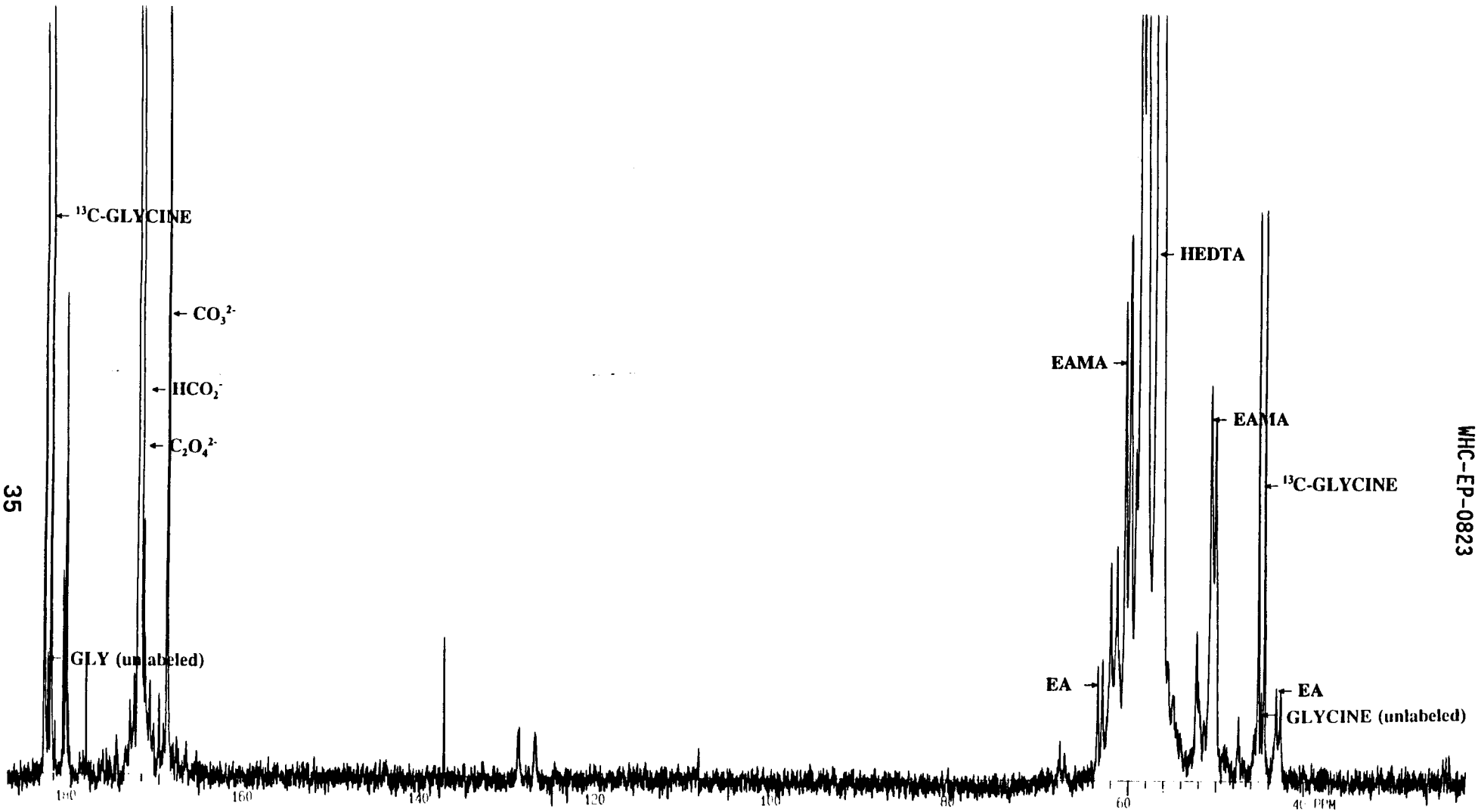

Figure 2.1. ^{13}C NMR spectrum of HEDTA-A in simulated waste mixture after heating at 120° C for 1452 h.

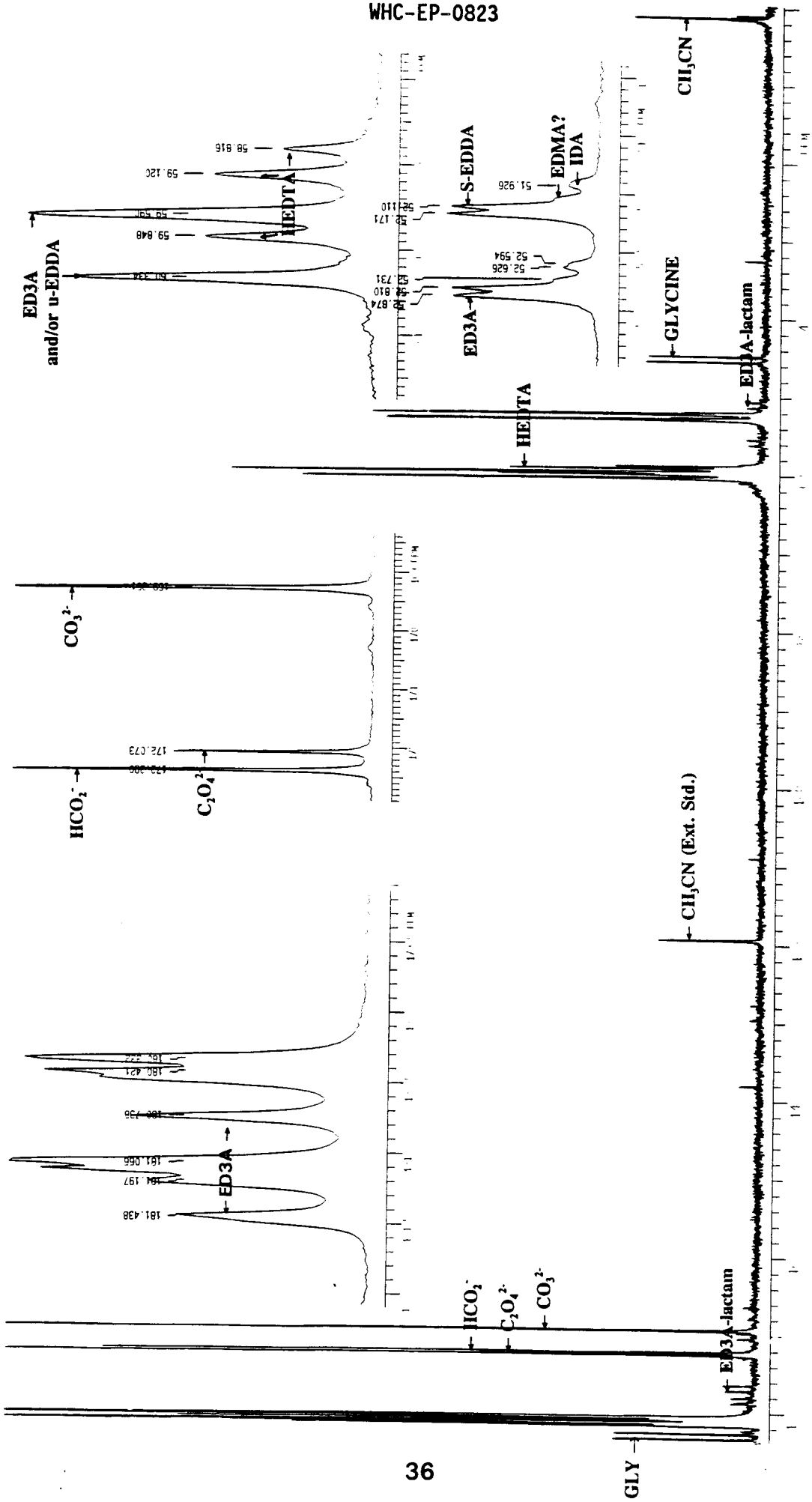

Figure 2.2. ^{13}C NMR spectrum of HEDTA-B in simulated waste mixture after heating at 120° C for 1808 h.

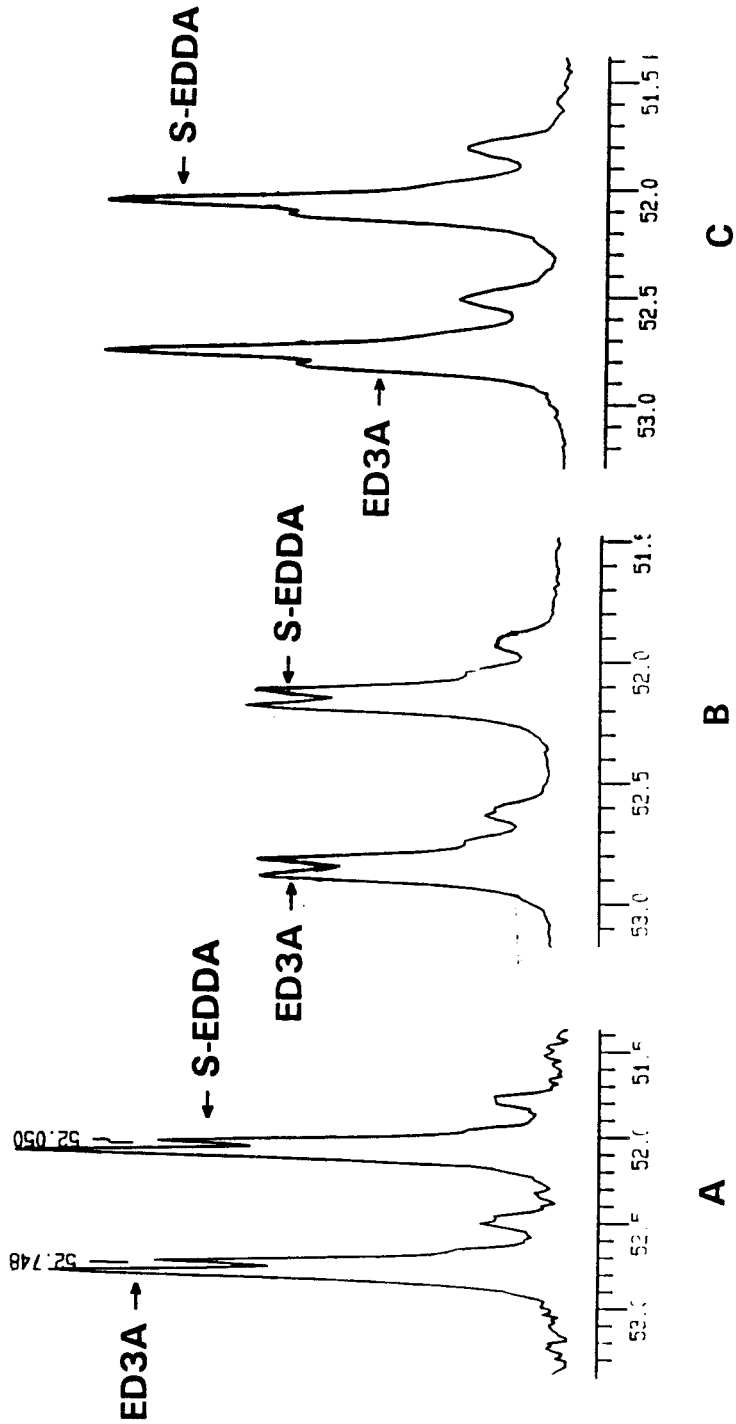

Figure 2.3. ^{13}C NMR Spectrum of HEDTA-B in Simulated Waste (120° C): Signals due to ED3A and s-EDDA. A: 905 h; B: 1808 h; C: 2492 h.

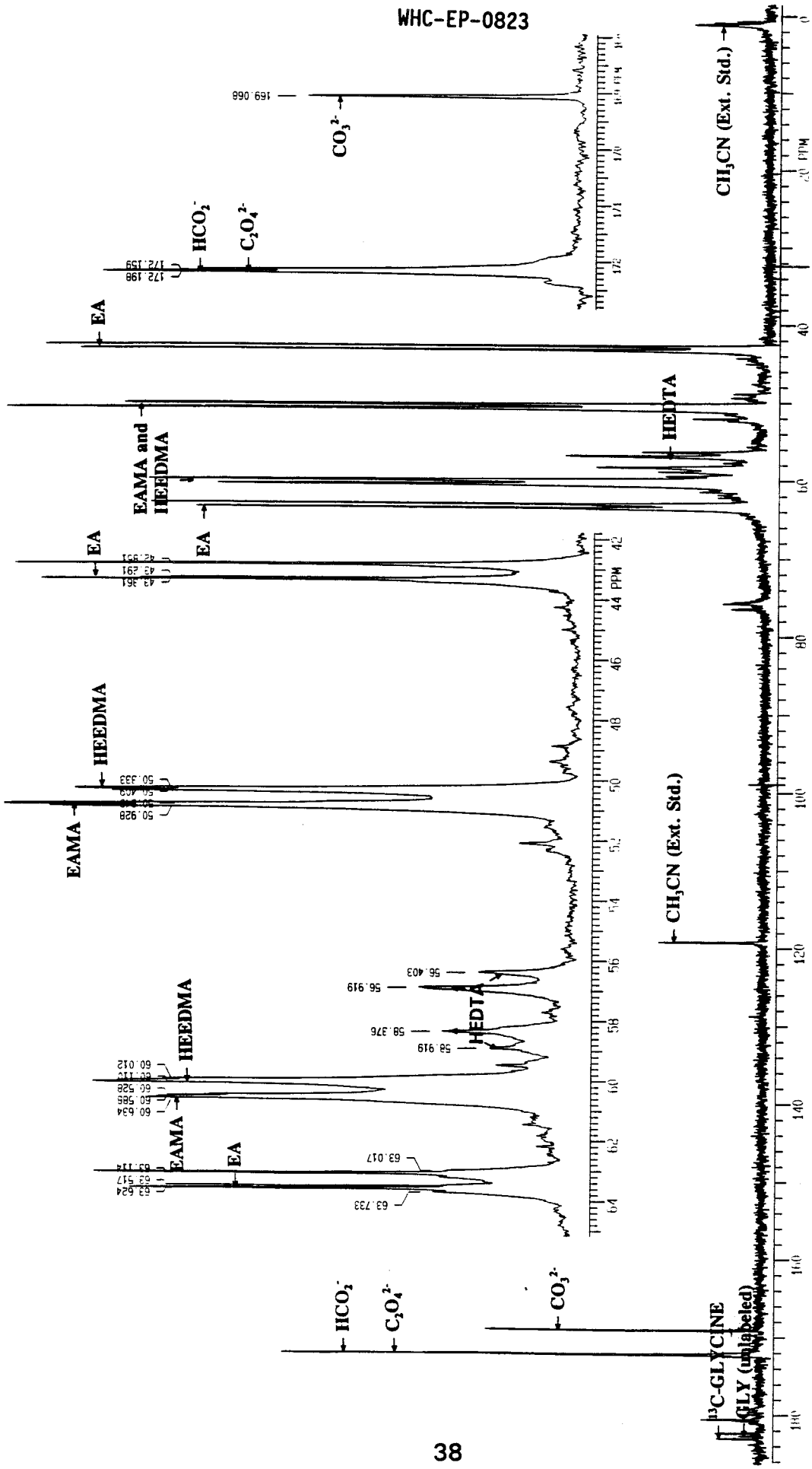

Figure 2.4. ^{13}C NMR spectrum of HEDTA-A in simulated waste mixture after irradiation (19.6 Mrad dose).

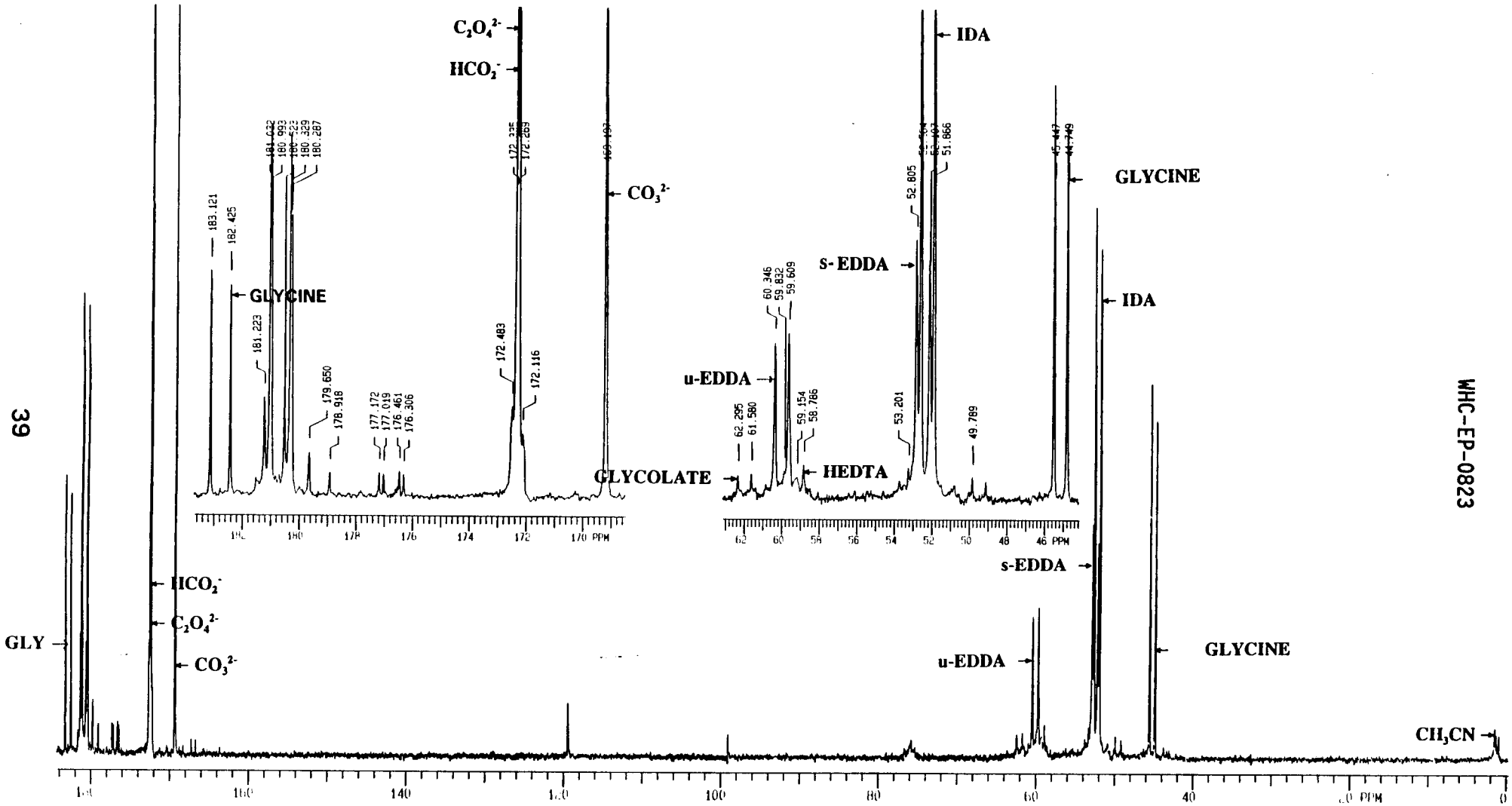

Figure 2.5. ^{13}C NMR spectrum of HEDTA-B in simulated waste mixture after irradiation (20.8 Mrad dose).

Glycine is formed in substantial amounts in radiolytic degradation as it is from the thermal reaction. The ^{13}C spectrum of HEDTA-A contained a significant carboxylate resonance for unlabeled glycine which indicates that a substantial amount of glycine is produced from the carboxymethyl groups (Figure 2.4). This observation is confirmed by the detection of intense doublets at δ 45.09 and 182.77 (J=52.6 Hz) in the spectrum of the carboxymethyl labeled compound that are due to glycine. The low intensity of the ^{13}C-glycine signals in the spectrum of the hydroxyethyl labeled compound indicates that only a small amount of glycine is produced from the hydroxyethyl part of the molecule. Similar observations were made in the thermal decomposition of these labeled materials.

Doublets are present in the spectrum of HEDTA-B at δ 52.45 (J=52.7 Hz) and δ 59.97 (J=55.6 Hz) that are most likely due to S-EDDA and U-EDDA, respectively. ED3A has resonances at comparable chemical shifts but the absence of a low field doublet at ca. δ 180.99 or resonances for the lactam suggests that there is little of this compound present.

The spectrum of HEDTA-B also contains a low intensity doublet at δ 61.94 which may be due to glycolate. The intensity of resonances for carbonate, formate and oxalate in the spectrum of HEDTA-B were very intense compared to those for HEDTA-A. This indicates that the carboxymethyl groups are also major sources of these products. Ion chromatographic analyses of the HEDTA-B product mixture also indicated the presence of formate (111%), oxalate (22%) and glycolate (27%). The preceding percentages are defined as moles of product per 100 moles of starting material. Workers at PNL earlier reported[2] the formation of formate and glycolate in an irradiated sample containing sodium citrate, sodium EDTA, sodium HEDTA and inorganics.

2.C Degradation of model systems in simulated waste

The complexity of the molecular structures of HEDTA and EDTA and the fragmentation products produced by each of these during the early stages of reaction makes the determination of the detailed mechanistic sequence of reactions very difficult. An attractive alternative approach would be to examine smaller model systems that contain the essential functional groups of HEDTA and EDTA but whose simpler molecular structures allow for more facile identification of intermediates and final products. Preliminary studies of the five model compounds shown below have been undertaken. HEG and HIDA were chosen as models for HEDTA, MIDA and DMG as models for EDTA, and MG as a model for ED3A.

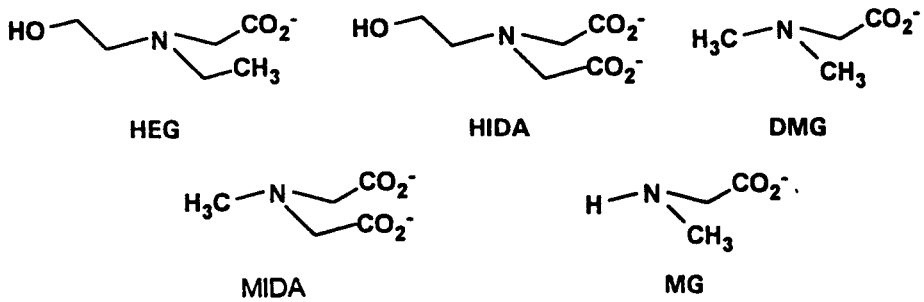

2.C.1 Decomposition of HEG in simulated waste. HEG is considered to be an excellent model for HEDTA since it contains both the N-hydroxyethyl and the N-carboxymethyl functionalities. These portions of the HEDTA molecules have been demonstrated to be the sites of initial reaction. Analyses of condensed and gas phase products derived from HEG after heating in the SY1-SIM-91B simulated waste mixture for 1000 h and 2000 h under argon and oxygen atmospheres are given in Table 2.2 and in equation 2.1. As predicted from results obtained with HEDTA, N-ethylglycine, which corresponds to ED3A, and formate are the main products derived from HEG in both oxygen and argon atmospheres. Glycine, oxalate, and acetate are minor products. The data at 2000 h indicate the high stability of N-ethylglycine toward further reaction. Correspondingly, ED3A also showed high stability.

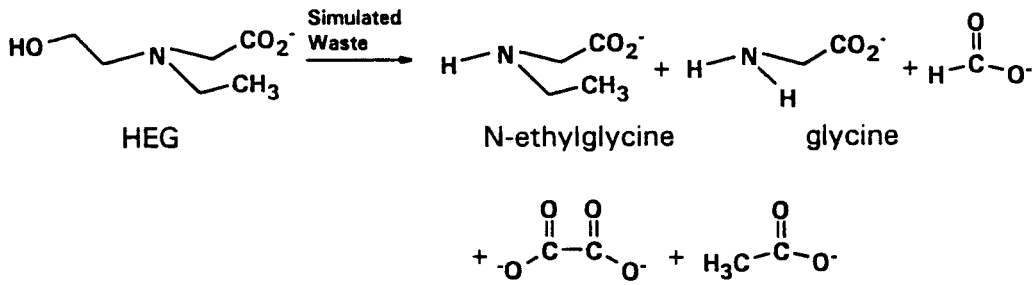

(2.1)

N-ethylglycine is obviously produced from HEG by loss of the hydroxyethyl group. This may be lost as two one-carbon fragments (which ultimately produce formate) or one two-carbon fragment (which ultimately produces oxalate). Accordingly, in the early stages of the reaction one half the amount of formate produced plus the amount of oxalate produced should be approximately equal to the amount of N-ethylglycine detected. Using the data from the first column of Table 2.2.

$$\%HCOO^-/2 + \%C_2O_4^{2-} = 55 + 7 = 62$$

$$\%\ \text{N-ethylglycine} = 63$$

The formation of both oxalate and formate can be accounted for by initial formation of the O- and/or N-nitroso intermediates followed by fragmentation processes. This suggestion is consistent with studies dealing with N,N-diethyl-2-aminoethanol in which both the O- and N-nitroso derivatives were observed. The primary products of such fragmentation reactions would be formaldehyde and glycolaldehyde, which are expected to be further oxidized to formate and oxalate. A reasonable reaction pathway for formation of these products is shown in Scheme 2.1 (page 43).

There are at least two distinct pathways by which nitrite esters may react. The first involves a fragmentation reaction (discussed earlier) in which NO^- is produced. The second involves a homolytic cleavage of the O-N bond to produce nitric oxide. No evidence was obtained for the formation of nitric oxide in the decomposition of HEG (or in decomposition of HEDTA). This contrasts with similar studies conducted

Table 2.2. Reaction of HEG in Simulated Waste at 120° C.[1]

TRIAL NAME	HEG-9A	HEG-16A	HEG-18A	HEG-15A
Atmosphere	Ar	O_2	Ar	O_2
Reaction Time(h)	1000	1000	2000	2000
HEG	17	20	7	<2
$HCOO^-$	85	96.2	117	124
$C_2O_4^{2-}$	6.6	13.7	12.0	24.0
EG	60	60	72	63
Glycine	6	5	7	9
EIDA	<2	~3	<2	4
$CH_3CO_2^-$	7	7	5	9
H_2	1.6	9.5	4.1	7.0
O_2[2]	-	30	-	30
N_2	21	12	22	23
CH_4	0.2	0.1	0.2	0.1
N_2O	7.8	6.5	8.6	14.5

[1]Unless otherwise stated, all products are in moles per 100 moles of organic starting material. [2]Moles of O_2 *consumed* per 100 moles of HEG.

on N,N-diethyl-2-aminoethanol and other ß-hydroxyethylamines in acetonitrile. Nitric oxide presumably arises by homolytic cleavage of the O-NO bond in nitrite esters, which is likely to be favored in the less polar acetonitrile whereas heterolytic cleavage may be favored in the more polar simulated waste medium. Evidence for NO^- has been obtained by trapping experiments with $Ni(CN)_4^{2-}$, which forms $Ni(CN)_3NO^{2-}$ by reaction with NO^-.

Oxidation of formaldehyde and glycolaldehyde must occur by secondary processes similar to those described under Tasks 1 and 5 to produce hydrogen and ammonia, respectively. Mechanistically, the oxidation of formaldehyde and glycolaldehyde to formate and oxalate, respectively, is believed to involve the formation of Cannizzaro intermediates. These processes have been discussed extensively (see Task 1). In order to determine whether or not the N-ethylglycine produced by the reaction of HEG can produce glycine by further decomposition in the presence of simulated waste, N-methylglycine (which is commercially available) was allowed to react in the above mentioned mixture. After 1000 h at 120° C, 90 % of the starting material remained (by NMR analysis); no glycine was detected. Assuming that N - methylglycine should show the same reactivity as the N - ethyl

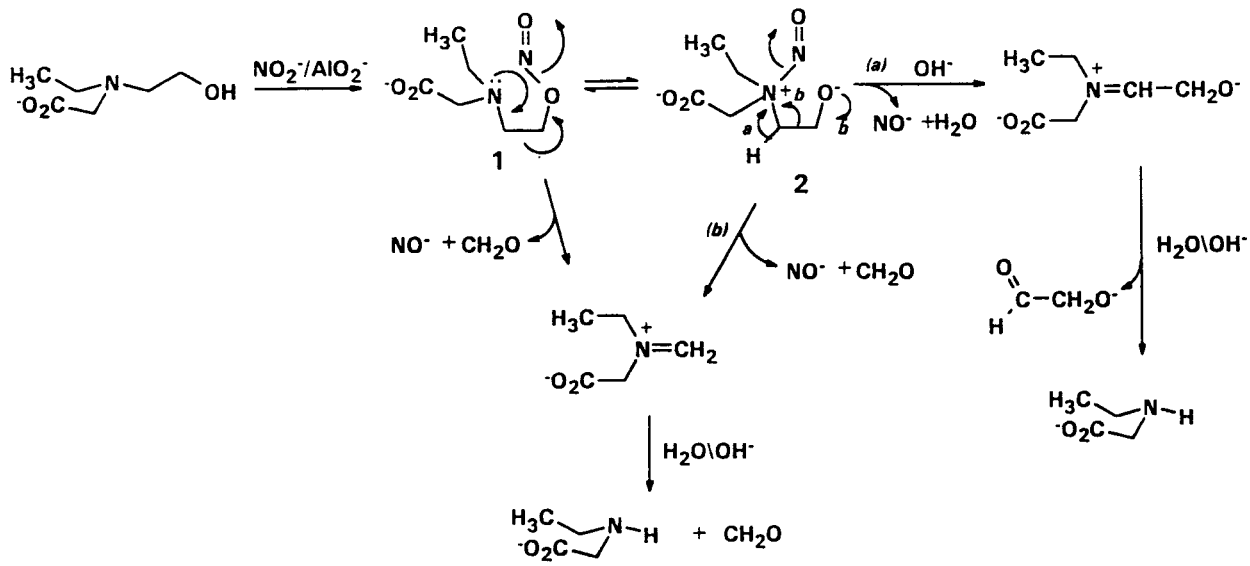

Scheme 2.1. Thermal Degradation of HEG in Simulated Waste.

analog, the origin of glycine is not clear. Nitrosation by the $NO_2^-/Al(OH)_4^-$ mixture is apparently very slow, but it may be that nitrosation occurs by reaction of N-ethylglycine with the nitrite ester of HEG (**1**) to produce N-nitroso-N-ethylglycine that decomposes in the presence of base to produce glycine and acetaldehyde (equation 2.2). Nitrite esters have been used for the nitrosation of amines[3] and evidence for the base promoted decomposition of N-nitroso-N-ethylglycine has been established independently (see Task 1, section 1.E.2). Acetaldehyde could be oxidized in the same way(s) as formaldehyde and glycolaldehyde to acetate. Note that the amounts of glycine and acetate obtained from the decomposition of HEG are nearly equal (Table 2.2), which is in agreement with the proposed mechanism. Nitrosation by the nitrite ester of HEG could be tested by incorporating labeled N-methyl- or N-ethylglycine in HEG decomposition reaction mixtures and looking for the label in the glycine product.

(2.2)

N-ethylglycine N-nitroso-N-ethylglycine glycine

2.C.2 Effect of oxygen on HEG decomposition. Examination of the data in Table 2.2 indicates that there are differences in the reaction of HEG carried out in the presence and in the absence of O_2. In oxygen atmosphere oxalate and hydrogen are produced in greater quantities than in argon atmosphere. In contrast, in oxygen atmosphere nitrogen and nitrous oxide are produced in smaller quantities than in argon atmosphere. O_2 is consumed in the reaction. The significance of an O_2 atmosphere for increased hydrogen

production from HEDTA has already been discussed (section 1.A). The reaction of HEG in simulated waste in the presence of O_2 is likely to proceed according to the same initial pathway (formation of the nitrite ester) as in its absence; little reaction was found to occur when nitrite and aluminate were excluded from the mixture even though O_2 was present. But, O_2 may react with reaction intermediates to produce peroxides, which are known to thermally decompose with evolution of H_2.[5]

2.C.3 Other model systems; HIDA. Because of its commercial availability, HIDA was initially chosen as a model for HEDTA although HEG is even more similar. Not unexpectedly, the primary product derived from decomposition of HIDA in simulated waste medium was IDA, which results from loss of the hydroxyethyl group. Product analyses are given in Table 2.3 for reactions conducted in the presence and absence of O_2. Again the amounts of N_2 and N_2O produced are reduced in the presence of O_2, while H_2 is enhanced.

Table 2.3. Reaction of Model Systems in SY1-SIM-91B Solution (120°C, 1000 h).[1]

TRIAL	HIDA-1A	HIDA-2A	MIDA-1A	MIDA-2A	DMG-1A	DMG-2A
Atm.	Ar	O_2	Ar	O_2	Ar	O_2
Substrate	64	73	91	86	95	79
$HCOO^-$	42.2	23.1	<1	4.7	<1	13.2
$C_2O_4^{2-}$	5.2	5.8	5.0	17.3	3.5	18.4
IDA	34.8[2]	22.4[2]	<2	<2	-	-
glycine	f'note 2	f'note 2	<2	<2	<2	<2
$CH_3CO_2^-$	<1	<1	<2	<2	<2	<2
H_2	0.4	5.0	1.1	10.4	1.0	14.7
O_2[3]	-	24	-	22	-	25
N_2	12	~2	~4	11	~4	~3
CH_4	<0.1	<0.1	0.1	0.1	0.1	0.2
N_2O	4.5	1.5	<0.1	<0.1	0.2	<0.1

[1]Unless otherwise stated, all products are in moles per 100 moles of organic starting material. [2]The chemical shifts of the methylene protons in glycine and IDA are identical so that it is not possible to determine whether glycine is formed. [3]Moles of O_2 *consumed* per 100 moles of starting material.

DMG and MIDA. These compounds are models for EDTA and, as might be predicted based on the low reactivity of EDTA, they do not react at a noticeable rate under Ar atmosphere (Table 2.3). These observations only serve to reinforce the postulate that the ß-hydroxyethyl functionality is necessary for facile reactivity, resulting in the production

of gaseous products. The data in Table 2.3 also suggest that MEIDA and DMG react slowly under an oxygen atmosphere, probably through an autoxidation mechanism similar to that proposed for EDTA (Task 1, Scheme 1.3).

2.D Role of aluminum in degradation of organic complexants: does aluminum(III) promote the reaction of NO_2^- with nucleophiles?

It is well established that thermal decomposition of organic complexants does not occur when aluminum(III) is not present in simulated waste mixtures. The Georgia Tech group has postulated that the function of aluminum(III) is to complex nitrite and thus activate it for reaction with nucleophilic groups in organic complexants. In this scheme, transfer of $[NO]^+$ to the nucleophile initiates a reaction sequence that could produce hydrogen, nitrous oxide, nitrogen, and ammonia. It has not yet been possible to obtain evidence for either the presence of a nitritoaluminum(III) species or of a primary product arising from the reaction of such a species with any tank constituent. This is not unexpected since the concentration of either species under tank conditions is likely to be very low and its reactivity very high. Since aluminum(III) has apparently not previously been demonstrated to activate nitrite for reaction with nucleophiles, a series of survey reactions involving discrete aluminum(III) compounds, nitrite and various nucleophiles were conducted in nonaqueous solvents. The initial studies were done with $N(CH_2CH_2O)_3Al{\cdot}$dioxane, which with three alkoxy ligands, closely mimics the hydroxy aluminate species that are present in the highly basic waste media. However, the poor solubility characteristics of this reagent and the fact that it contains a potentially reactive tertiary amine center resulted in the use of $[(CH_3CH_2)_4N]AlCl_4$ for most trials. Only the reactions involving the latter are reported here. Three types of substrates that are representative of those functional groups that are present in HEDTA and its fragments were considered: secondary amines, ß-hydroxy alcohols, and tertiary amines. Most of this work, and in some cases more detailed results, are given in the October and November 1992, and January and February 1993 Georgia Tech monthly reports. Two related studies dealing with the ^1H NMR characterization of nitroso compounds formed from ß-hydroxyamines by reaction with $NOBF_4$ and base promoted decomposition of nitroso amines are described in following sections.

2.D.1 Nitrosation of secondary amines by sodium nitrite in the presence of $[Et_4N]AlCl_4$. Reactions were conducted with diethylamine, pyrrolidine and piperidine in acetonitrile under a variety of conditions. Control reactions were done to determine that the presence of the aluminum(III) reagent was necessary for reaction and that it, rather than any acid that might be generated during the reaction, was responsible for the nitrosation. The results of these studies are summarized in Tables 2.4 and 2.5.

Table 2.4. Nitrosation of Diethylamine in Acetonitrile Under Various Conditions.[1]

Trial	Amounts of reagents/mmol				Rxn. T/Time	Yield Et_2NNO
	$Et_2NH{\cdot}HCl$	Et_2NH	$[Et_4N][AlCl_4]$	$NaNO_2$		
1	1			10	reflux/1 h	12
2	1			10	reflux/3h	46
3	1			10	reflux/8 h	57
4	1			10	r.t./24 h	12
5	1		7	10	r.t./24 h	88
6		1	7	10	r.t./24 h	86
7		1	7	10	reflux/1 h	99
8		1		10	r.t./24 h	<1

[1]The yield of Et_2NNO was by determined from the ^1H NMR spectrum by integration versus toluene as an internal standard.

Table 2.5. Nitrosation of Piperidine Under Various Conditions.[1]

Trial	Quantities of Reagents (mmol)			Conditions		Yield R_2NNO
	Piperidine	$[Et_4N][AlCl_4]$	$NaNO_2$	Solvent[2]	Rxn T/time	
1	1	7	10	CH_3CN	reflux/1 h	99
2	1		10	CH_3CN	reflux/2 h	0
3	1		10	CH_3CN/H_2O	reflux/15 h	0

[1]The yield of nitrosamine was determined from the ^1H NMR spectrum by integration vs. toluene as internal standard. [2]The quantity of solvent was 75 mL in each experiment. CH_3CN/H_2O mixtures contained 1 mL of H_2O.

As the results in Tables 2.4 and 2.5 indicate, diethylamine and piperidine are converted in high yields to the nitrosamine after 1 h at reflux or 24 h at room temperature. No reaction is observed in the absence of the aluminum reagent as indicated by trial 8, Table 2.4 and trial 3, Table 2.5. These results can be accounted for by a process in which a nitrito-aluminum species serves as a source of $[NO]^+$ (equations 2.3-2.4).

$$AlCl_4^- + NO_2^- \rightarrow AlCl_3ONO^- + Cl^- \quad (2.3)$$

$$AlCl_3ONO^- + Et_2NH \rightarrow AlCl_3OH^- + Et_2N\text{-}NO \quad (2.4)$$

Since the reaction of an Al-ONO species with an hydroxyl or secondary amino group will produce Al-OH and two of these species can react to produce Al-O-Al + H_2O such

reaction mixtures cannot be considered to be totally anhydrous. The possibility that water will hydrolyze Al-Cl bonds to give HCl, which might be at least partially responsible for the production of $[NO]^+$ cannot be ignored. We have attempted to determine the possible importance of protonic acids generated by such processes by a series of experiments utilizing $[Et_2NH_2]Cl$. The results of trials 1-4, Table 2.4 indicate that HCl added via $Et_2NH{\cdot}HCl$ does result in nitrosation but at a reaction rate that is much slower than that observed with diethylamine and the aluminum reagent. The conclusion of this series of experiments is that, at least in acetonitrile, aluminum(III) is very effective in promoting the reaction of nitrite with secondary amines.

2.D.2 Reaction of triethylamine with $[Et_4N]AlCl_4/NaNO_2$ in acetonitrile. In experiments similar to those described in the previous section, refluxing 1 mmol triethylamine, 7 mmol of $[Et_4N]AlCl_4$ and 10 mmol of $NaNO_2$ in acetonitrile produced a 99% yield of nitrosodiethylamine after a 15 h reaction time. A 22% conversion was found after 72 h at room temperature.

2.D.3 Cleavage of ß-hydroxyethylamines by $[Et_4N]AlCl_4/NaNO_2$ in acetonitrile. Two ß-hydroxyethyl amines were subjected to the same reaction conditions described in the previous sections. Both 2-(N,N-diethylamino)ethanol, **I**, and 2-piperidinoethanol, **II**, were cleaved to give the corresponding nitrosamines. A summary of the results of several individual experiments are given in Table 2.6.

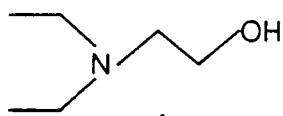

I

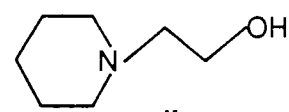

II

A possible reaction sequence to account for these cleavage reactions is given by equations 2.5-2.8 in Scheme 2.2. Alternatively, the initial nitrosation reaction could occur at nitrogen, with subsequent fragmentation as indicated by reactions 2.9 and 2.10.

$$AlCl_4^- + NO_2^- \rightleftharpoons AlCl_3ONO^- + Cl^- \quad (2.5)$$

$$R_2NCH_2CH_2OH + AlCl_3ONO^- \rightarrow R_2NCH_2CH_2ONO + AlCl_3OH^- \quad (2.6)$$

$$R_2NCH_2CH_2ONO \rightarrow R_2N{=}CH_2^+ + CH_2{=}O + NO^- \quad (2.7)$$

$$R_2N{=}CH_2^+ + NO_2^- \rightarrow R_2N\text{-}NO + CH_2{=}O \quad (2.8)$$

$$AlCl_3ONO^- + R_2NCH_2CH_2OH \rightarrow [R_2N(NO)CH_2CH_2OH]^+ + \text{"}AlCl_3O^{2-}\text{"} \quad (2.9)$$

$$[R_2N(NO)CH_2CH_2OH]^+ + Base \rightarrow BaseH^+ + R_2N{=}CH_2^+ + CH_2{=}O + NO^- \quad (2.10)$$

Scheme 2.2

Table 2.6. Cleavage and Nitrosation of 2-(N,N-Diethylamino)ethanol (I) and 2-Piperidinoethanol (II) with $[Et_4N]AlCl_4/NaNO_2$ in Acetonitrile.[1]

Trial	Amounts of reagents/mmol			Rxn. T/Time	Yield R_2NNO
	amine	$[Et_4N][AlCl_4]$	$NaNO_2$		
1	I 1	7	10	reflux/2 h	13
2	I 1	7	10	reflux/24 h	39
3	I 0.1	0.2	1	reflux/27 h	30
4	II 1	7	10	r.t./3 h	trace
5	II 1	7	10	reflux/24 h	34
6	II 1	7	10	reflux/68 h	77

[1]In all but experiment 3, the standard procedure was followed. In experiment 3 the reaction was run in CD_3CN and the conversion to nitrosamine determined by integration versus the resonances of the Et_4N^+ ion.

By either pathway, NO^-, a known precursor to N_2O, is produced along with formaldehyde and an iminium cation. In aqueous base, the iminium ion should rapidly hydrolyze to formaldehyde and a secondary amine, although in the presence of nitrite the iminium ion might react to produce nitrosamine and formaldehyde. This possibility is supported by a literature report[5] that nitrosamines are formed in aqueous solution from mixtures of secondary amine, formaldehyde and nitrite in aqueous solution. Formation of the nitrosamine by reaction of an iminium ion intermediate with nitrite ion was proposed.[5] An interesting question raised by this hypothesis is exactly how the iminium ion reacts with nitrite to produce the nitrosamine. Is hydrolysis to free Et_2NH required, or might the iminium cation react directly with nitrite to generate Et_2N-NO and formaldehyde in an intramolecular, 4-centered transition state as shown by **III**?

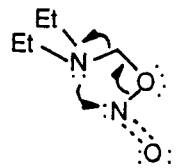

III

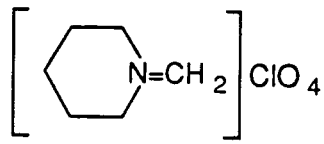

IV

In a separate experiment, the preformed iminium salt N-methylenepiperidinium perchlorate **IV** was treated with sodium nitrite in acetonitrile under a variety of conditions as shown in Table 2.7. (Note that **IV** and piperidine were incorrectly referred to as cyclohexyl methylene iminium perchlorate and cyclohexylamine, respectively, in the January status report from Georgia Tech. Pyrrolidine was also incorrectly referred to as cyclopentylamine in the same report.) The experiments with piperidine given in Table 2.5 served as control experiments to demonstrate the difference in reactivity of the iminium salt and its hydrolysis product.

Table 2.7. Reactivity of N-Methylenepiperidinium Ion Under Various Conditions.

Trial	Amounts of reagents (mmol)			Conditions		Yield R_2NNO[1]
	IV	$[Et_4N][AlCl_4]$	$NaNO_2$	Solvent[2]	Rxn T / time	
1	1	7	10	CH_3CN	reflux/1 h	15
2	1	7	10	CH_3CN	reflux/15 h	97
3	1	7	10	CH_3CN	r.t./72 h	96
4	1	7	10	CH_3CN/H_2O	reflux/20 h	86
5	1	7	10	H_2O	reflux/15 h	88

[1]The yield of $C_5H_{10}NNO$ was by determined from the ^1H NMR spectrum by integration versus toluene as an internal standard. [2]The quantity of solvent was 75 mL in all cases. The acetonitrile/water mixture contained 1 mL of water.

The data in Table 2.7 clearly indicate that the iminium ion reacts with nitrite to produce the nitrosamine without participation of aluminum in either acetonitrile or water. Since piperidine does not react with nitrite in acetonitrile or in acetonitrile-water mixtures (Table 2.5, trials 2 and 3) hydrolysis of the iminium ion is not required for formation of the nitrosamine. Both results are consistent with the reaction sequence proposed in Scheme 2.2. The formation of the nitrosamine via an intramolecular process is consistent with these results although an intermolecular process is not ruled out.

According to Scheme 2.2 formaldehyde should be produced in acetonitrile. We have examined the ^1H NMR spectrum of the reaction mixture carefully and find that there are resonances about 4 ppm downfield of TMS that are probably due to oligomers of formaldehyde but no confirmatory evidence is available yet. In an effort to obtain further evidence for the reaction sequence shown in Scheme 2.2, phenyl substituted ß-hydroxyethylamines **V** and **VI** were subjected to the same types of reactions previously described for **I** and **II**.

Treatment of **V**[6] and **VI**[7] with $AlCl_4^-/NO_2^-$ using the same protocol employed for the other ß-hydroxyethylamines generated the expected nitrosamine and modest quantities of benzaldehyde (Table 2.8) as predicted by the reaction sequence given in Scheme 2.2 (equations 2.5 and 2.6). The amount of benzaldehyde formed should be equal to the

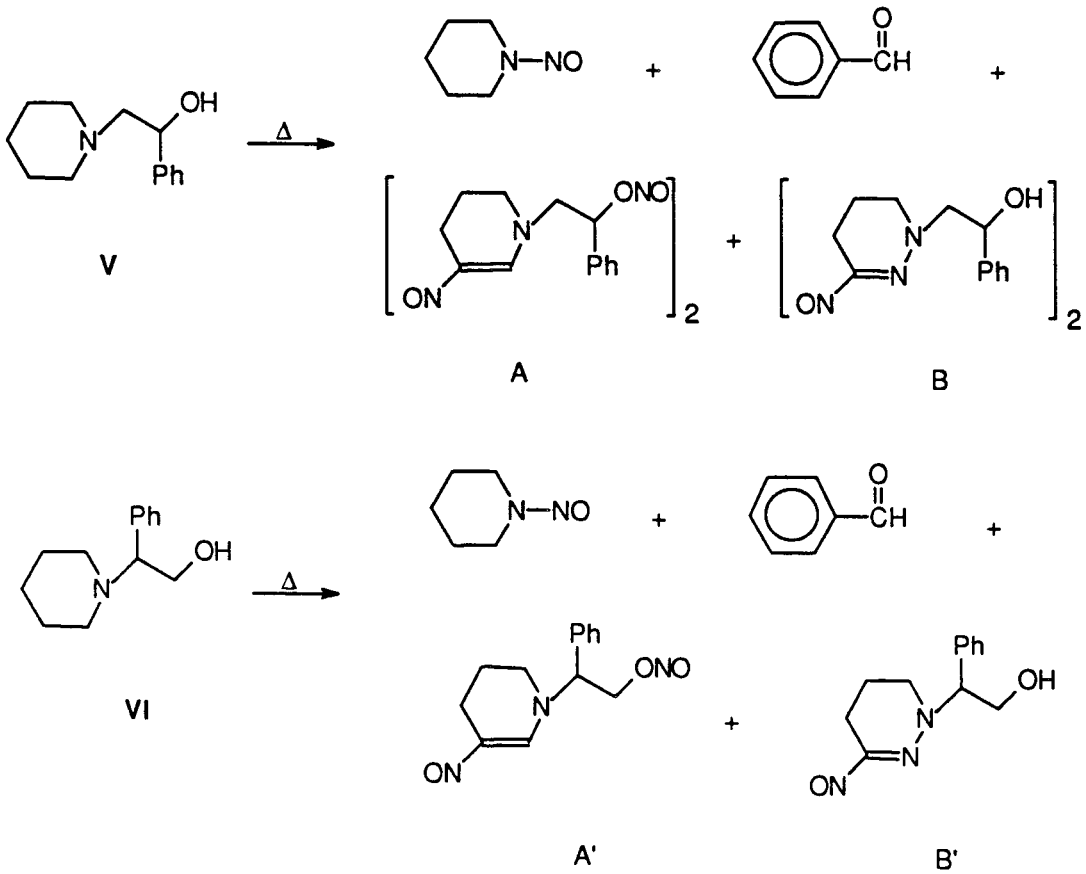

Table 2.8. Cleavage and Nitrosation of N-(2-hydroxy-1-phenylethyl)-piperidine (V) and N-(2-hydroxy-2-phenylethyl)-piperidine (VI) with $[Et_4N][AlCl_4]/NaNO_2$.

Amount of Reagents (mmol)			Solvent	Rxn.T/ Time	Product Yields			
Amine	$[AlCl_4^-]$	$NaNO_2$			A/A'	B/B'	R_2NNO	PhCHO
V 1	7	10	CH_3CN	24 h/reflux	trace	~2	66	27
V 1	7	10	CH_3CN	90 h/reflux	trace	<5%	67	30
V 2	7	10	DMSO	4 h/80° C	23	trace	63	5
V 4	14	20	DMSO	24 h/80° C	40	<5%	57	trace
VI 1	7	10	CH_3CN	24 h/reflux	31	~2%	47	<5%

amount of nitrosamine formed but significantly less is recovered than predicted for both **V** and **VI**. The possibility that the benzaldehyde was oxidized to benzoic acid was considered for **V**. However, none could be extracted from acidified solutions of the crude reaction mixture. Formation of benzaldehyde from **VI** according to the reaction sequence given in Scheme 2.2 would involve the formation of the iminium ion $C_5H_{10}N{=}C(H)Ph^+$ and its subsequent reaction with nitrite to produce the nitrosamine and benzaldehyde. The fluoroborate salt of this iminium ion has been prepared and shown to react rapidly and quantitatively at room temperature to produce N-nitrosopiperidine and benzaldehyde. In

the reactions of **V** and **VI** with the aluminum(III) reagent and nitrite, two additional products A and B and A' and B' were identified for both **V** and **VI**, respectively, which indicate that reaction has occurred in the six-membered piperidine ring. Reaction rates for **V** appear to be greater in DMSO, where sodium nitrite is more soluble. Larger amounts of A and B were also formed in this medium. The observation of these products provides strong evidence for equations 2.9 and 2.10 (Scheme 2.2), which involve nitrosation of the tertiary nitrogen since formation of these products must involve reaction of the piperidine ring. This is, of course, consistent with the observed cleavage of triethylamine, which also must proceed by nitrosation of the tertiary nitrogen. No mechanistic information is available concerning the formation of products A(A') and B(B'). However, it should be noted that formation of the latter compounds must involve opening of the piperidine ring with subsequent ring closure. It is quite possible that related products were formed in the cleavage reactions of **I** and **II** although they were not characterized. Formation of these products does serve to reduce the yield of nitrosamine that can be obtained.

Fragmentation of the nitrite ester of the ß-hydroxyethylamine according to equation 2.7 of Scheme 2.2 would generate NO^-, which is the most likely precursor to the nitrogen gases. Demonstration that this species is actually formed would provide strong evidence for this mechanism. Generation of NO^- in this fashion requires that it be present initially in the singlet form. Singlet NO^- is reported to dimerize to give hyponitrite, which decomposes in aqueous solution to give N_2O. We expect to conduct reactions under conditions where gaseous products can be identified. One could argue, however, that the concentration of NO^- present at any time should be very small and that dimerization should not play a significant role. Intersystem crossing to the expected ground-state triplet form (rate unknown) would allow for reaction with oxygen to generate peroxynitrite, which would isomerize to nitrate.[8] Thus, it might be possible to obtain evidence for generation of NO^- if NO_3^- could be detected as a product in the cleavage reaction products. In preparation for attempting such an experiment, a mixture of $[Et_4N][AlCl_4]$ and $NaNO_2$ in acetonitrile was heated at reflux for 3 h and the resulting mixture analyzed by ion chromatography after dilution with water. Substantial amounts of nitrate were observed. This unexpected result needs further consideration but it clearly means that evidence for formation of NO^- in cleavage reactions such as these cannot be based on the formation of nitrate.

2.E Preparation and degradation of nitroso derivatives of ethanolamines

As described in an earlier section, there is mounting evidence to suggest that initial degradation of HEDTA in media designed to simulate those present in tank 101-SY occurs through nitrosation by a nitritoaluminum species. The product of this reaction is predicted to be a nitrite ester derived from the ß-hydroxyethyl group, or a nitrosammonium ion generated by nitrosation of one of the tertiary nitrogen atoms. No direct evidence for either species has been obtained from reactions conducted in simulated waste or from cleavage studies of ethanolamines by $AlCl_4^-/NO_2^-$ described earlier. Failure to detect such species could be a result of their low concentration and/or their short lifetime. This section describes the preparation and characterization of nitroso derivatives of N,N-diethyl-2-aminoethanol (DEEA), which is a model system for HEDTA, and their thermal degradation. Similar reactions of 1-phenyl-2-piperidinoethanol are also briefly discussed.

Initially, preparation of a nitrite ester of DEEA in aqueous solution was attempted by a standard procedure that utilizes sodium nitrite in aqueous acid. Starting material was recovered in each of several attempts; this strongly suggests that under these conditions the nitrite ester is in equilibrium with free alcohol, and that the equilibrium favors the alcohol (equation 2.11).

$$RONO + H_2O \rightleftharpoons ROH + HNO_2 \qquad (2.11)$$

It is interesting to note that although ethanolamines have been used to catalyze the nitrosation of amines,[3] there are no reports of the synthesis of nitrite esters of ethanolamines. After trying several potential methods, a nitrite ester of DEEA was prepared by the reaction of the alkoxide of DEEA with $NOBF_4$ in acetonitrile (equation 2.12), although the reaction was complicated by the simultaneous formation of the nitrosammonium cation as described below. $NOBF_4$ has been used previously for the preparation of both alkyl nitrites and nitrosamines.[4]

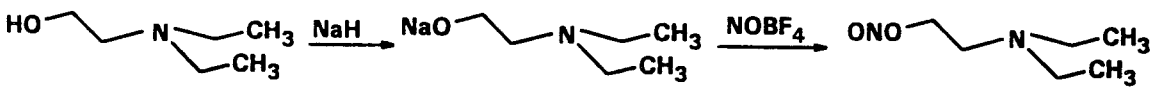

(2.12)

DEEA

DEEA-nitrite ester, 1

The reaction of DEEA alkoxide (prepared by reaction of DEEA with NaH) with $NOBF_4$ was monitored by ^1H NMR and infrared spectroscopies. When a 1:1 ratio of reagents was used, the ^1H-NMR spectrum obtained immediately after mixing the reagents indicated that all of the DEEA alkoxide had disappeared and that two products had formed in a 1:1 ratio. Two nitrosyl stretching absorptions were observed in the infrared spectrum of the reaction mixture. After 15 min the ^1H NMR spectrum indicated that the ratio of the two products had changed to 3:1 (Figure 2.6). The less intense resonances are assigned to the nitrite ester, **1**. This conclusion is based on the large downfield chemical shift of the triplet at δ 4.85, which is assigned to the protons of the methylene group adjacent to the oxygen. The chemical shift of the corresponding triplet for the other product is similar to that for DEEA (Figure 2.7). That the other product is the nitrosammonium species is indicated by the large downfield shift of the methylene protons of the N-ethyl groups. After three days only **2** was present. Addition of less than one equivalent of additional $NOBF_4$ generates a mixture of **2** and a third compound that is most likely the dinitroso compound **3**, based on its ^1H NMR spectrum (Figure 2.8). Complete conversion to **3** can be achieved with additional $NOBF_4$. The conversion of **1** to **2** most likely occurs via the five-membered intermediate shown in equation 2.13, although an intermolecular process is also possible.

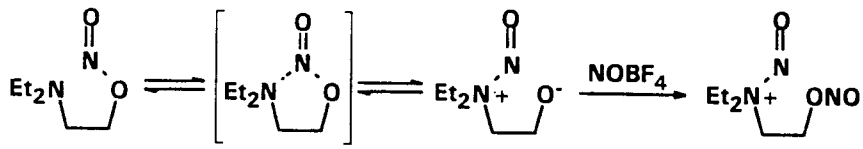

(2.13)

1 2 3

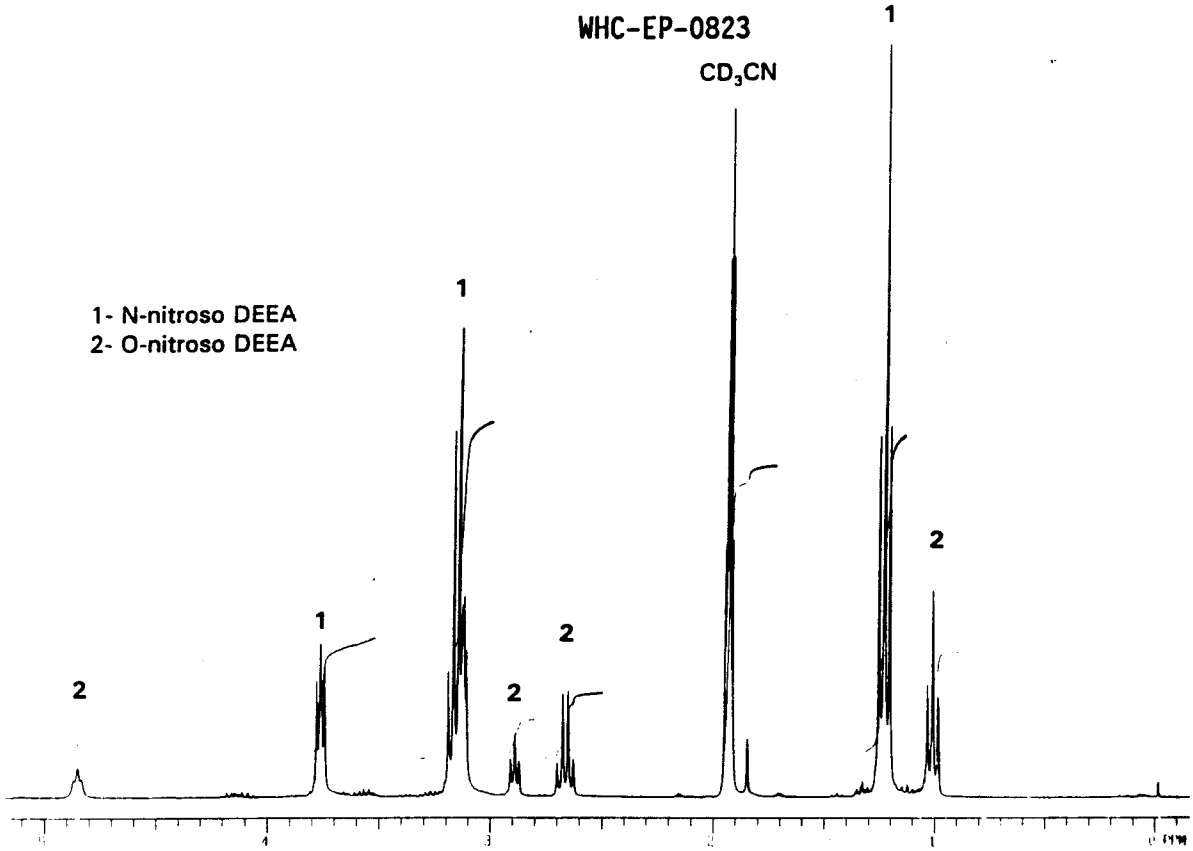

Figure 2.6. ^{1}H NMR of the reaction of DEEA-alkoxide with NOBF4 (DEEA:$NOBF_4$ ~ 1).

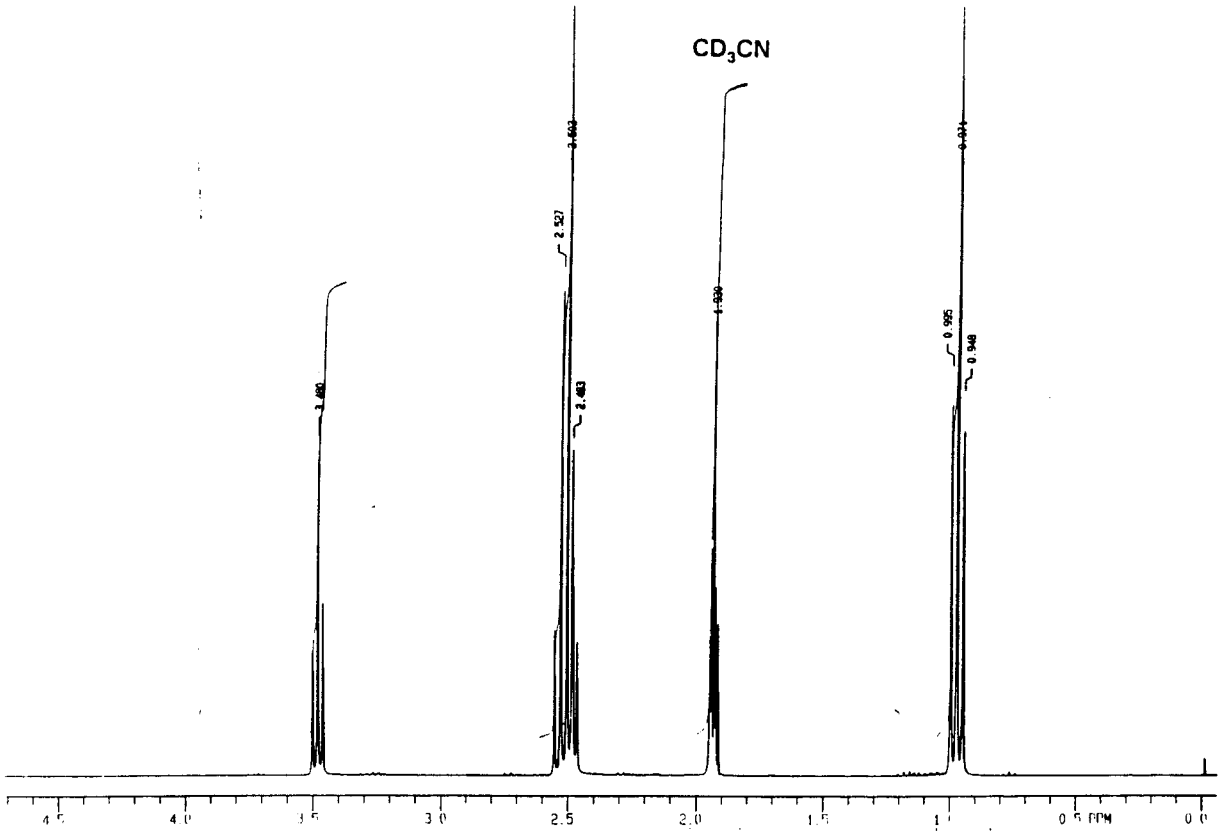

Figure 2.7. ^{1}H NMR of DEEA-alkoxide.

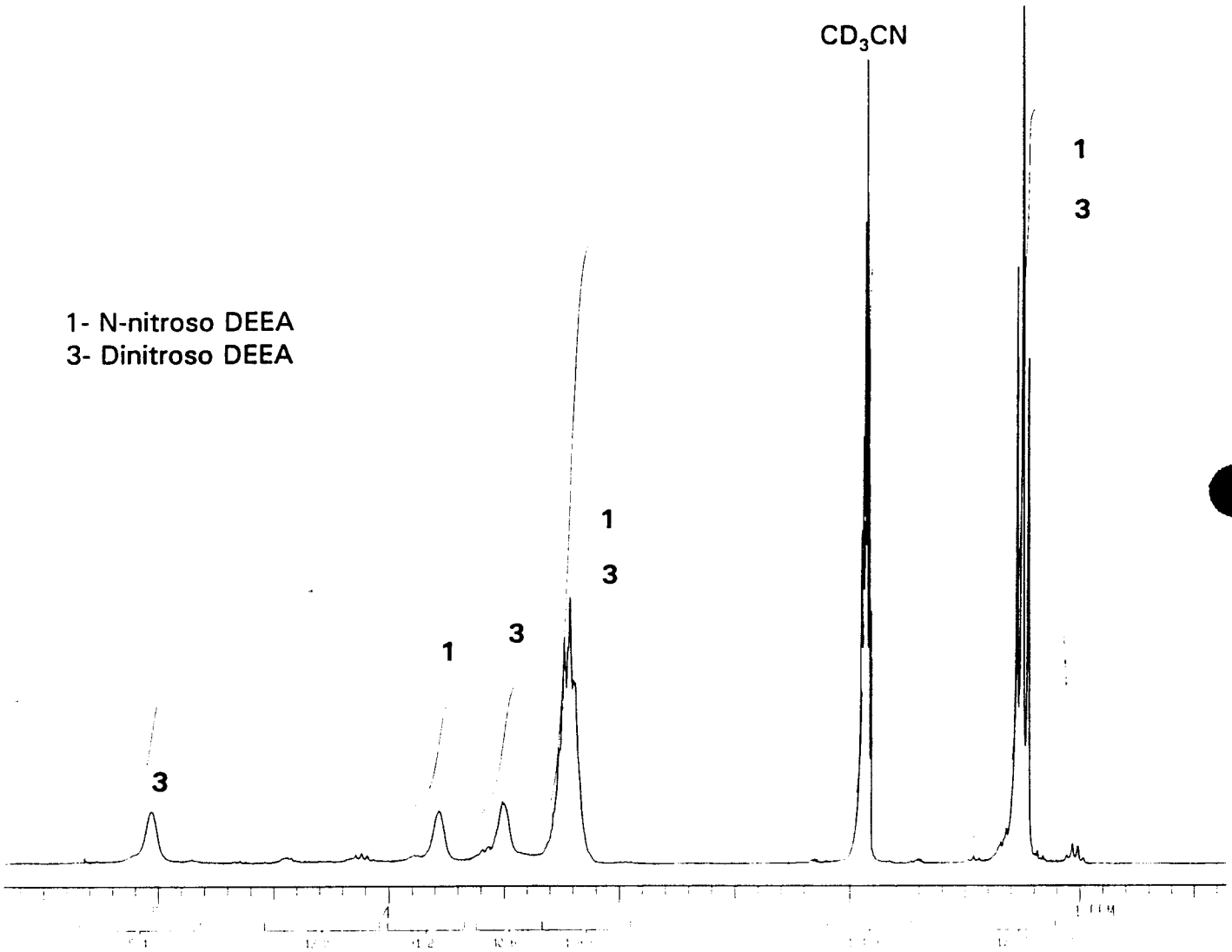

Figure 2.8. ^{1}H NMR of the reaction of DEEA-alkoxide with excess NOBF4.

When a mixture of **1** and **2** was treated with aqueous base DEEA was recovered unchanged in agreement with the equilibrium previously discussed (equation 2.11). When the mixture was heated overnight at 60° C and then hydrolyzed with aqueous base, diethylamine (29%) was formed in addition to DEEA (59%) (equation 2.14). Analysis of the gas phase showed the presence of NO, N_2 and N_2O. Monitoring of the gas phase above such a reaction as a function of time after hydrolysis showed that the amount of NO decreased while the amounts of both N_2 and N_2O increased (Table 2.9).

Table 2.9. Composition of the Gas Phase After Hydrolysis of Nitroso-DEEA Derivative as a Function of Time.[1]

Time,[2] h	N_2	N_2O	NO
0	16	1.4	30
0.2	21	2.9	19
3	27	7.4	8
6	28	8.3	3
70	32	10.1	<1

[1]All amounts are in moles of product per 100 moles of DEEA. [2]Time=0 indicates the time at which D_2O/OD^- was added to the reaction mixture.

There are some troublesome inconsistencies in these data since the amount of nitrogen gained at each stage does not correlate with the amount of nitric oxide lost. However, the apparent conversion of nitric oxide to nitrogen and nitrous oxide is known[9] to occur by reaction with hydroxylamine under basic conditions. As described below, a plausible mechanism can be written for the formation of hydroxylamine in this reaction.

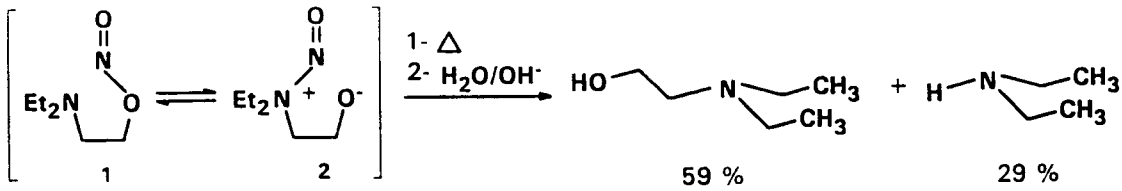

(2.14)

Considering that the pyrolysis of nitrite esters is known to produce an alkoxy radical and nitric oxide[10] formation of nitric oxide in the above reaction most likely results from a similar homolytic cleavage of the ON-O bond in 1. Once the alkoxy radical is formed it could abstract hydrogen from solvent or other compounds to produce DEEA, or the alkoxy radical could fragment to produce formaldehyde and a stabilized α-aminomethyl radical[11] as shown in Scheme 2.3. The α-aminomethyl radical can then react according to the Barton reaction,[12] also shown in Scheme 2.3 and ultimately produce hydroxylamine and diethylamine. Reaction of the nitroso intermediates by a heterolytic pathway could also be possible. This pathway would result in the formation of diethylamine and formaldehyde.

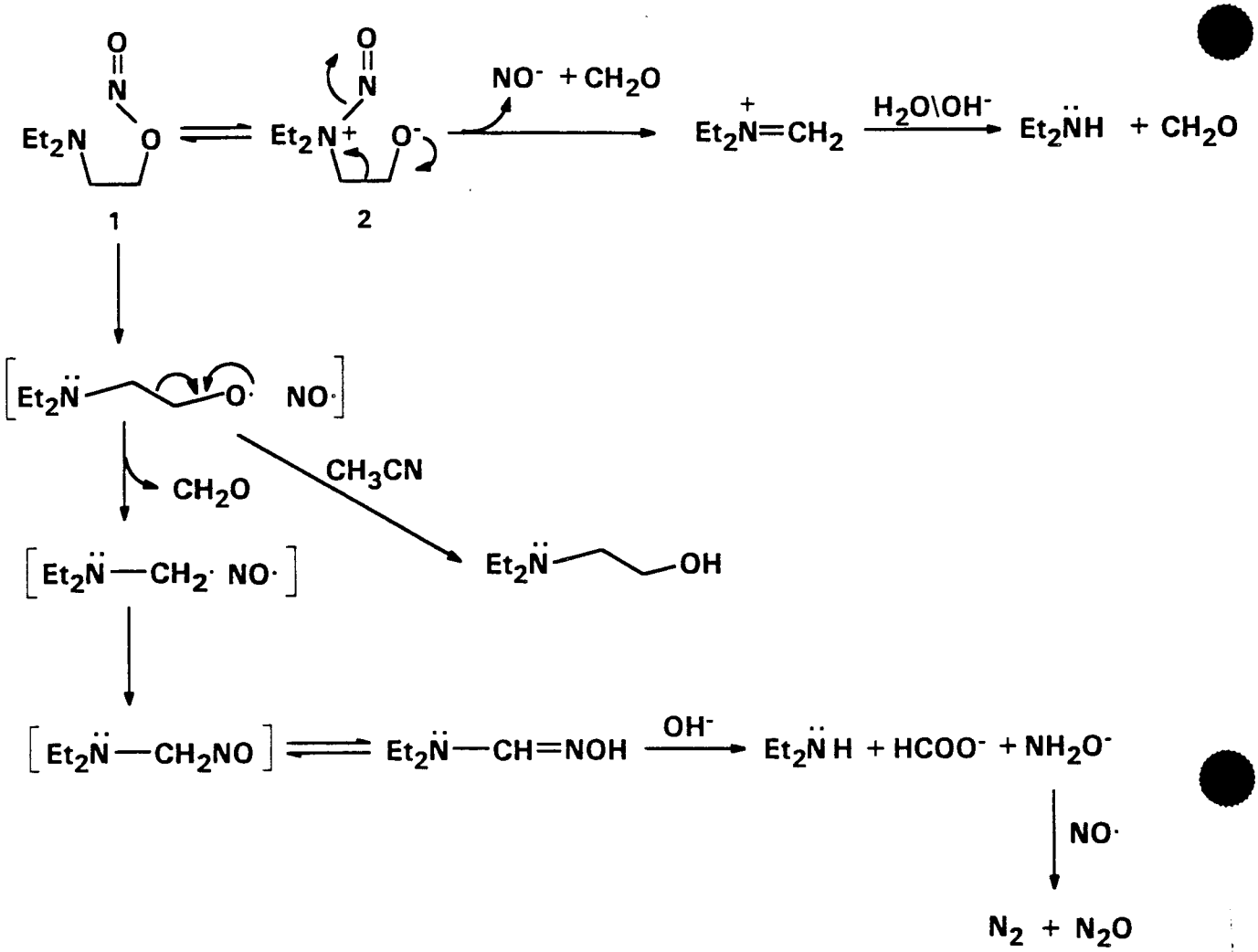

Scheme 2.3. Thermal Degradation of DEEA-Nitrite Ester.

When triethylamine was treated in the same fashion as DEEA (reaction with $NOBF_4$ followed by thermolysis and hydrolysis), no NO was observed (equation 2.15); N-nitrosodiethylamine was produced as well as diethylamine. Earlier studies of the nitrosative cleavage of tertiary amines have concluded that heterolytic elimination to produce secondary amines is the probable mechanism of the reaction.[13] The fact that NO is not formed from triethylamine whereas it is from DEEA supports the notion of the interconversion of nitroso derivatives shown in equation 2.13 and homolytic cleavage of the O-NO bond. It is interesting to note that N-nitrosodiethylamine was formed as a product from triethylamine (equation 2.15), whereas it was not from DEEA (equation 2.14). This could result from a reaction between N-nitrosodiethylamine and DEEA (equation 2.16) that produces the nitrite ester of DEEA and diethylamine; the nitrite ester would then react as shown in Scheme 2.3. As mentioned above, ethanolamines have been used as catalysts for the nitrosation of secondary amines.[3] The mechanism proposed involves the formation of a nitrite ester which reacts with the amine to produce an N-nitroso compound. If this is an equilibrium process as seems likely, the equilibrium may be shifted toward

diethylamine in the case of DEEA due to decomposition of the nitrite ester.

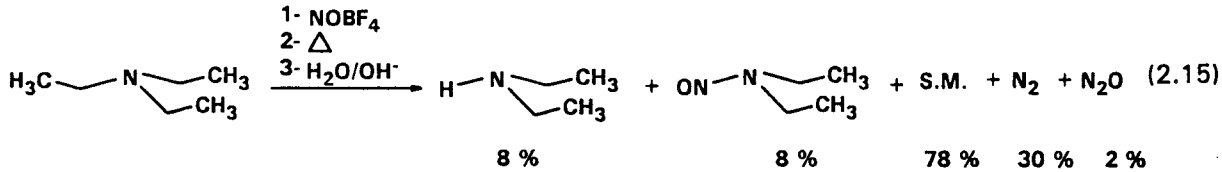

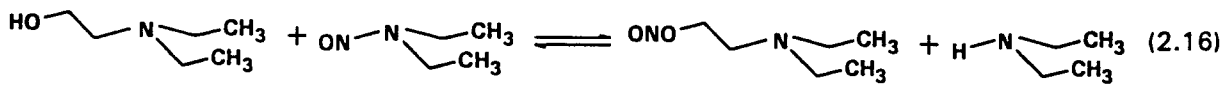

The fate of formaldehyde that should have been formed in the decomposition of DEEA as outlined in Scheme 2.3 is unclear. Only a small amount of formate was recovered, presumably produced by oxidation of formaldehyde. Because of the possibility that most of the formaldehyde that should have been formed was lost due to its volatility, an analogous reaction was conducted using 1-phenyl-2-piperidinoethanol. Fragmentation of the alkoxy radical should produce benzaldehyde instead of formaldehyde as shown in equation 2.17. In fact, benzaldehyde was observed as a product of the reaction, along with N-nitrosopiperidine and small amounts of other unidentified products. As with DEEA, NO was observed as a product of the reaction (17%), which disappeared after hydrolysis with aqueous base, to produce nitrogen and nitrous oxide. The formation of N-nitrosopiperidine is in contrast to what was observed for DEEA. The reason for this difference is not known, but it could result from differences in equilibrium constants and/or rates of reactions analogous to those in Scheme 2.3 and equation 2.16.

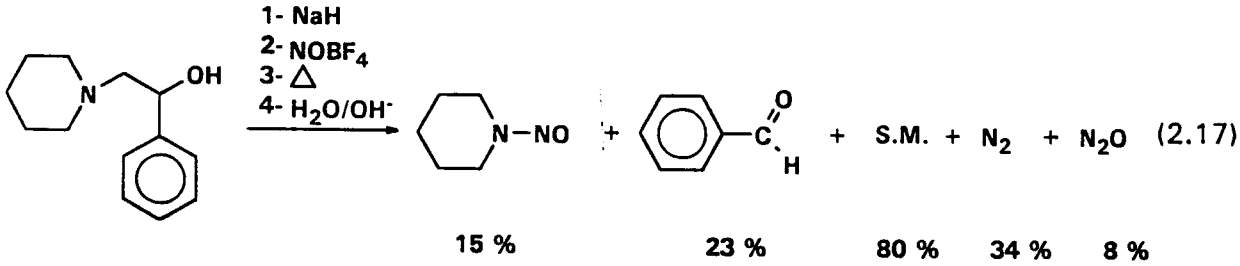

2.F Mechanism of the thermal degradation of HEDTA in simulated waste

A "global" mechanism that accounts for most of the known products formed in the thermal degradation of HEDTA is given in Schemes 2.4 and 2.5. Scheme 2.4 depicts reactions leading to smaller carbon fragments. Reactions leading to gaseous products are shown in Scheme 2.5. These mechanisms, which are derived from the mechanism described earlier,[14] are based upon the accumulated evidence of earlier studies by scientists at Westinghouse Hanford Corporation and Battelle Pacific Northwest Laboratory, and the more recent studies at Georgia Tech. Much of the evidence upon which this mechanism is based has been presented in Task 1 and in the preceding sections of Task 2. Evidence for formaldehyde as an intermediate was previously reported[15] and certain other aspects of the work has appeared in earlier reports from Georgia Tech. The formation of nitrogen gases is discussed under Task 5.

$Al(OH)_4^- + NO_2^- \rightleftharpoons Al(OH)_3ONO^- + OH^-$

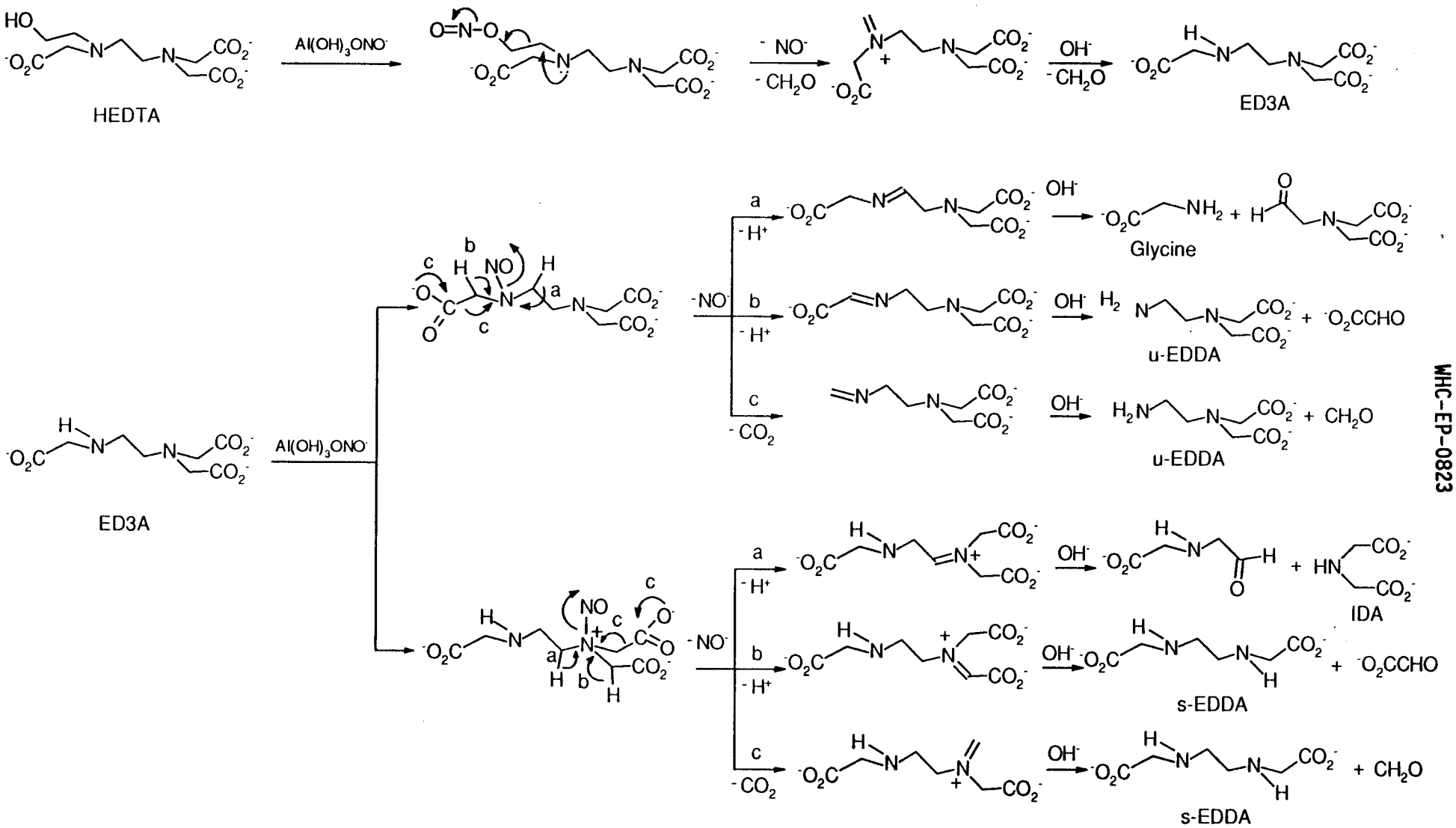

Scheme 2.4. Mechanism of Thermal Degradation of HEDTA to Carbon Products

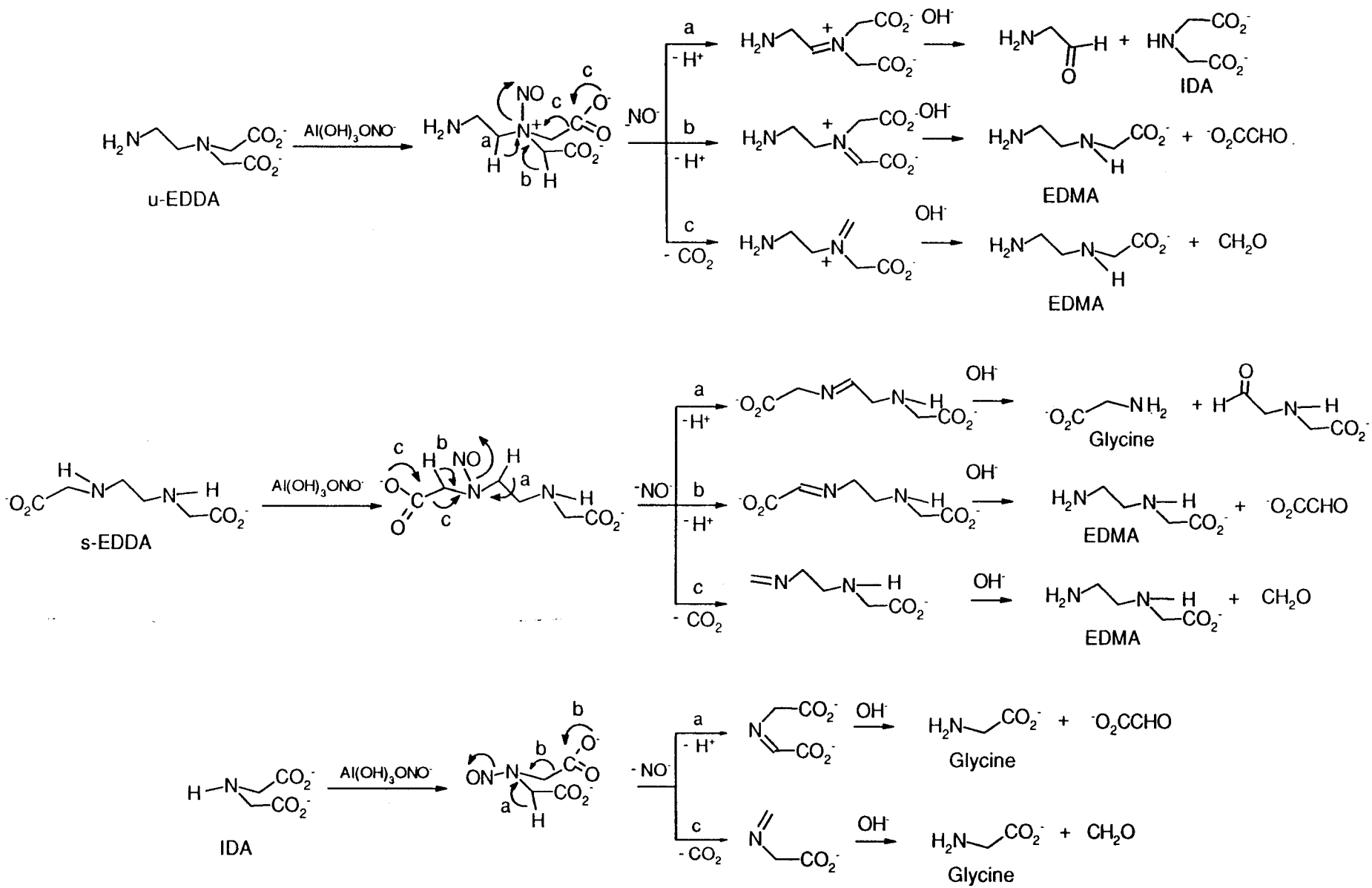

Scheme 2.4. (continued)

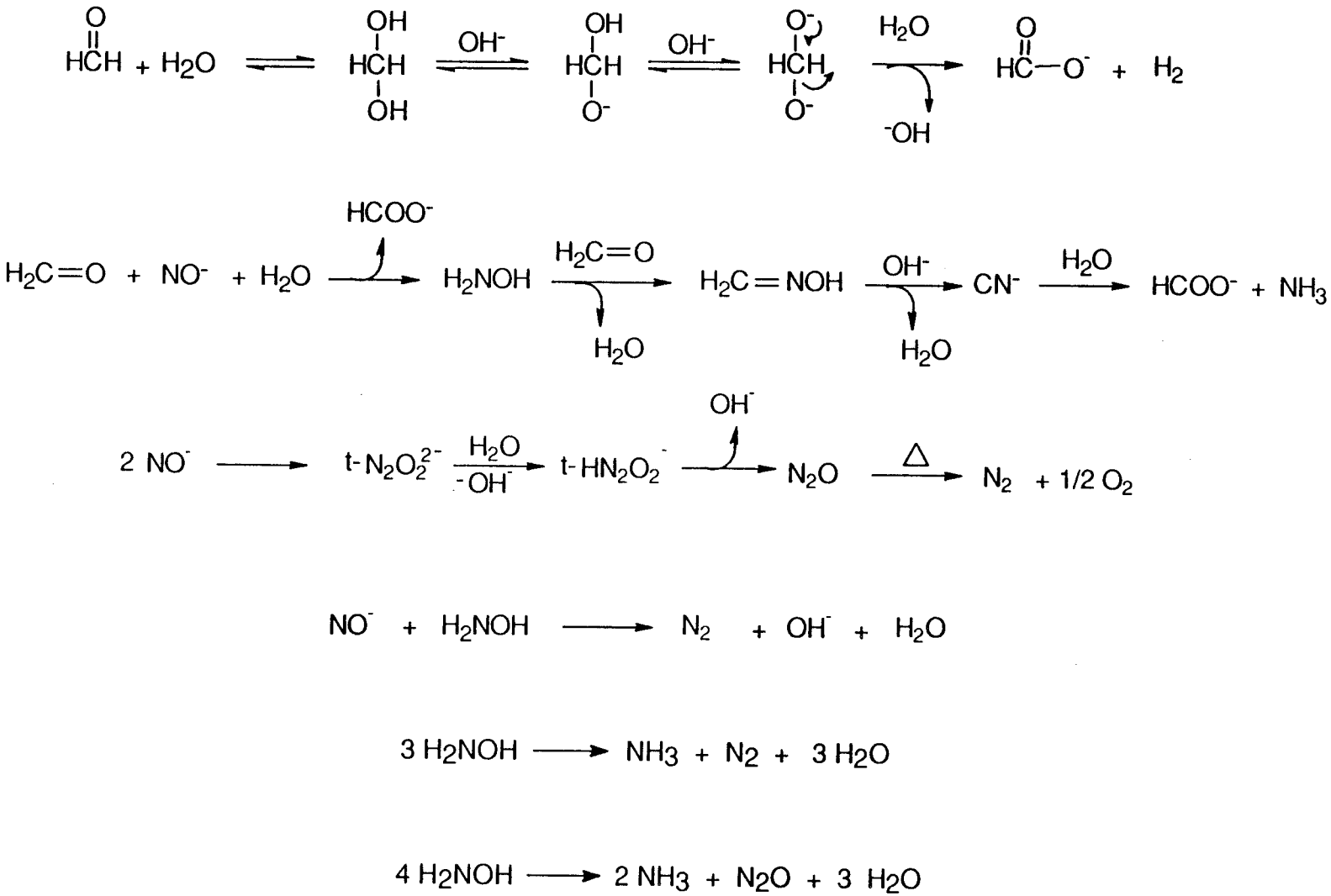

Scheme 2.5. Mechanism of Formation of Gaseous Products

The first two reactions of Scheme 2.4 are key to the understanding of how the decomposition of HEDTA is initiated. In the first reaction nitrite ion (NO_2^-) reacts with aluminate ion ($Al(OH)_4^-$) to substitute one of the hydroxide ligands; the coordinated nitrito ligand is expected to be much more electrophilic then free nitrite ion and thus more reactive toward HEDTA. In the second reaction the nitritoaluminate species acts as a NO^+ donor to HEDTA, which has several nucleophilic sites. The accumulated evidence indicates that it is the nitrite ester, which is formed by nitrosation of the hydroxyl group, that is most reactive. Other species involving nitrosation of tertiary nitrogen must be formed in smaller amounts, or are less reactive, and have not been shown in the Scheme. Note however, that formation of ethanolamine monoacetic acid (EAMA), and the slow degradation of EDTA, most likely arises from an N-nitroso species. Formaldehyde, NO^-, and ED3A are the products of this initial reaction. As shown in Scheme 2.5, formaldehyde reacts competitively with NO^- to give hydroxyl amine (and ultimately nitrogen or ammonia), or with water to give hydrogen. NO^- reacts competitively with formaldehyde or with itself to give hyponitrite ion $(N_2O_2)^{-2}$, which is the source of nitrous oxide.

Further reaction of ED3A by nitrosation at either the secondary or tertiary nitrogen can result directly in several known products, including glycine, u-EDDA, s-EDDA, and IDA. Subsequent oxidation of aldehydic products would also lead to oxalate, IDA and NTA. That ED3A is less reactive than HEDTA is consistent with the above conclusion that nitrosammonium intermediates are either not favored thermodynamically or have low reactivities. The fact that any s-EDDA is formed from ED3A requires cleavage of a carboxymethyl substituent from the tertiary nitrogen, yet such a process occurs even more slowly in EDTA. The answer to this apparent inconsistency may be that ED3A can form a lactam that is expected to result in a substantial increase in the acidity of the methylene protons of the cyclized carboxymethyl group. This would make the following process feasible.

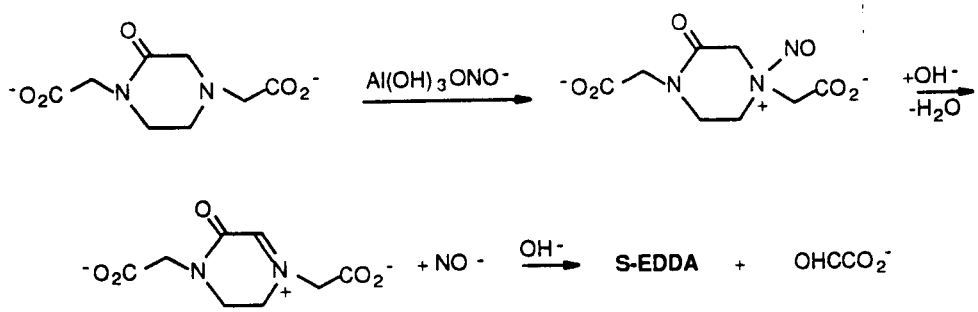

Alternatively, nitrosation of the secondary amine followed by *intramolecular* transfer to the tertiary nitrogen atom to give the intermediate shown in Scheme 2.4 might also be possible. For the sake of simplicity, neither of these modifications have been incorporated into Scheme 2.4.

Scheme 2.5 represents a preliminary view of the formation of the gaseous products. Formaldehyde is the only aldehyde that has been incorporated into this Scheme; however, all of the reactions might be applicable to aldehydes $OHCCO_2^-$, $OHCCH_2N(H)CH_2CO_2^-$ and

H_2NCH_2CHO, which are shown as products in several of the reactions in Scheme 2.4. Such aldehydes would be oxidized to the corresponding carboxylate. As outlined in section 1.D (Task 1), product analyses on degradation reactions of HEDTA and glycolate in simulated waste at different temperatures suggest that there is a substantial difference in the relative amounts of N_2, N_2O and H_2 that may be a result of cage effects. We are continuing to pursue the details of these reactions.

2.G Stability of carboxylic acid salts in simulated waste solution

Thermal decomposition of metal complexants ultimately produces carbonate, formate or oxalate according to the mechanisms previously outlined. Since formate and oxalate have not yet been determined to be present in tank 101-SY in the amounts expected based on the amount of organics that are believed to have reacted, the question of the stability of these anions in the waste medium must be addressed. Sodium oxalate, sodium formate and sodium acetate that were heated at 120° C for 1000 h under air in simulated waste solution (concentration = 0.2 M) were unchanged in concentration within the limits of the analytical method (ion chromatography).

The possibility that hydrogen might be generated by a thermal reaction of sodium formate in simulated waste medium was also examined. Table 2.10 shows the results of experiments performed under inert and oxygen atmospheres. The amount of hydrogen or other gas detected was approximately the same in the presence or absence of sodium formate. It can be concluded that sodium formate does not react to form gaseous products under these conditions. The small amount of H_2 produced is probably due to trace impurities present in the reactants.

Although the possibility that formate or oxalate might react with intermediates produced in thermal reactions cannot be excluded, it would seem that there should be

Table 2.10. Gas Generation in the Reaction of Sodium Formate in Simulated Waste.[1]

TRIAL NAME	FORM-1A	FORM-2A	FORM-3A	FORM-4A
Organic Material	HCOONa	HCOONa	No Organics	No Organics
Atmosphere	Ar	O_2	Ar	O_2
H_2	0.6	1.3	0.8	1.5
O_2[2]	-	10	-	7
N_2	<2	<2	<2	~2
CH_4	<0.1	<0.1	<0.1	0.1
N_2O	0.1	<0.1	0.1	<0.1

[1] Unless otherwise stated, all products are indicated in moles per 100 moles of organic starting material. [2]Moles of O_2 *consumed* per 100 moles of sodium formate.

significant amounts present in tank 101-SY, unless they are rapidly decomposed by radiolytic processes, since they are final products from the thermal decomposition of HEDTA, EDTA, and glycolate.

2.H Reaction of sodium citrate and isocitrate in simulated waste

Citrate ion was one of the complexing agents present in the "complex concentrate" added to Tank 101-SY. The concentrations of various complexants in Tank 107-AN were measured in 1986, and it has been generally assumed that the concentrations in 101-SY are similar to these. Citrate ion was present at a concentration of 0.064M, compared to HEDTA (0.038M) and EDTA (0.031M). The reactivity of citrate ion in simulated waste, and its ability to produce gaseous products was investigated. Parallel studies were conducted with isocitrate; both isomers have structural similarities to glycolate in the sense that all three ions possess the unit $HOCR_2CO_2^-$, which is believed to be responsible for the reactivity of glycolate. Although citrate and isocitrate are highly reactive in simulated waste medium (Table 2.11) the amounts of hydrogen and nitrous oxide produced in the decomposition were negligible compared to those produced in the decomposition of glycolate. Carbon containing products were primarily acetate and oxalate, in approximately a 2:1 ratio, in the case of citrate and a mixture of acetate, oxalate and succinate in the case of isocitrate. Only very small amounts of formate were produced from either compound. That nitrous oxide is not formed suggests that the decomposition does not involve nitrosation and that neither nitrite or aluminate would be required for reaction. That hydrogen is not formed suggests that an aldehyde is most likely not formed in the decomposition pathway. As shown by the data in Table 2.12 reaction proceeds in the absence of either nitrite or aluminate, and the rate and products are very similar to those obtained in simulated waste.

The above results suggest that both citrate and isocitrate decompose thermally in basic solution. A possible mechanism that accounts for the production of acetate and oxalate in a 2:1 ratio from citrate is shown in the first part of Scheme 2.6.

The presence of the extra carboxylate group in the citrate ion allows for a decomposition pathway that is not available in glycolate. The case of isocitrate is more complex. If a similar pathway to that suggested for citrate was followed, then no acetate would be formed and the ratio of oxalate to succinate would be 1:1. However, the observation of acetate and an oxalate to succinate ratio >1 suggests the participation of an alternative pathway(s). Since citrate was formed by thermolysis of isocitrate (Table 2.11) products are expected from both pathways, although this does not account for the large amount of oxalate produced.

It can be concluded from these results that neither citrate or isocitrate can contribute significantly to the production of flammable gases in tank 101-SY, at least from thermal processes.

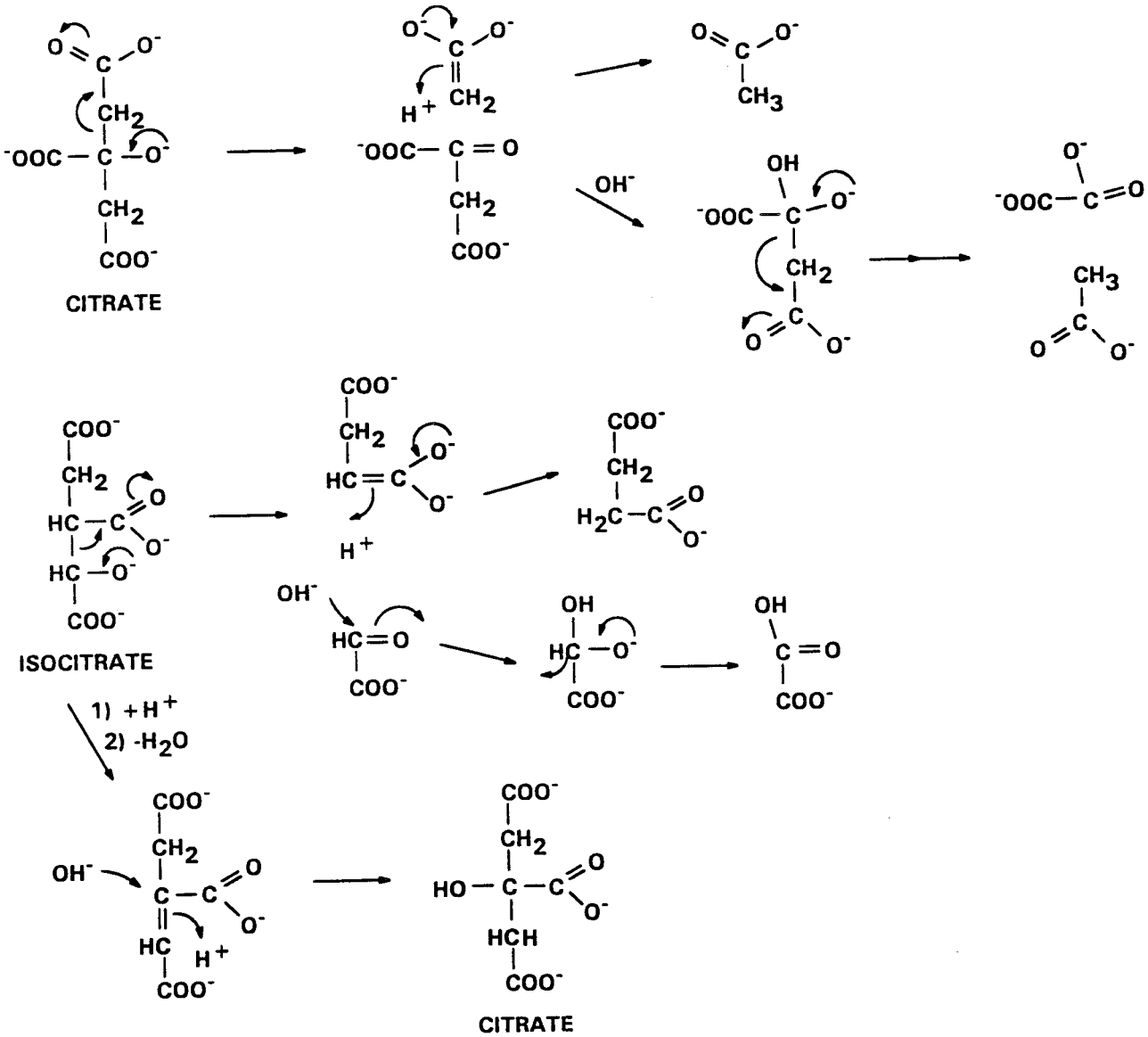

Scheme 2.6. Thermal Degradation of Sodium Citrate.

Table 2.11. Reaction of Citric Acid and Isocitric Acid in SY1-SIM-91B Solution. (1000 h, 120° C). Comparison with Sodium Glycolate.[1]

Trial	CITR-1A	CITR-2A	ICITR-1A	ICITR-2A	GLY-14A	GLY-12A
Atm.	Ar	O_2	Ar	O_2	Ar	O_2
citrate	31	25	8	8	-	-
isocitrate	<2	<2	<2	<2	-	
H_2	0.4	2.9	1.0	1.8	21.2	26.8
O_2[2]	-	17	-	20	-	25
N_2	~2	~2	~3	~7	~7	~5
CH_4	0.1	0.1	0.1	<0.1	0.3	0.3
N_2O	0.1	<0.1	0.2	<0.1	14.6	9.5
$HCOO^-$	2.2	3.5	4.8	4.7	29.8	34.4
$C_2O_4^{-2}$	53	70	24	32	43	48
AcO^-	108	131	32	33	-	-
$(CH_2COO^-)_2$	<2	<2	9	12	-	-

[1]All products are indicated in moles per 100 moles of organic starting material, unless otherwise stated. [2]Moles of oxygen *absorbed* per 100 moles of starting material.

Table 2.12. Reaction of Sodium Citrate in 2 M NaOH (120°C, 1000 h). Comparison with the Reaction in Simulated Waste.[1]

TRIAL NAME	CITR-4A	CITR-1A
Solution	NaOH (2 M)	SY1-SIM-91B
Atmosphere	Ar	Ar
Citrate	47	31
$HCOO^-$	<1	2
$C_2O_4^{2-}$	53	53
AcO^-	108	108
H_2	<0.1	0.4
N_2O	<0.1	0.1

[1]All products are indicated in moles per 100 moles of organic starting material.

2.I Analysis of solids from thermal reactions

In most thermal reactions a solid was formed. In the recovery process the solid first obtained was contacted several times with water, so that the recovered solid consisted mostly of compounds that would normally be considered "water insoluble". The amount of such "water insoluble" solids was greater for reactions in which Teflon covers were not placed on the Teflon liners. The observation of aluminosilicates in these precipitates, *vide infra*, lead to the conclusion that the reactions were being contaminated by glass. This resulted in the design of covered reaction vessels such as those described in the Experimental Section, which were used for all of the experiments described in this report except the present ones and those in section 1.C.1.

The complete procedure for recovery is given in the Experimental Section, but briefly: the solid was dissolved in acid, and the resulting solution was analyzed by ion chromatography. Because of the treatment with acid, any CO_3^{2-} or NO_2^- present in the solid would be lost before analysis. It is possible that some ions (or salts) of normally "water soluble" compounds were occluded in the solid in such a way that they were not dissolved in the recovery process, but we have no positive evidence for such an effect. Although the analysis of the solid was carried out primarily as part of the measurements to obtain mass balance in the reaction, the amount and nature of the solid was of interest on its own.

Data in Table 2.13 and 2.14 show the weight % of oxalate and nitrate in the solids from several experiments. Table 2.13 shows the results when glycolate is the organic component and Table 2.14 shows the results for other organic components. Nitrate appeared in almost all solids to the extent of 4-14%. Formate was not found.

In Table 2.13 the seven reactions in the series Gly-300, through Gly-1000, show that oxalate forms in solution early in the reaction, with some time delay before it appears in the solid. The amount of oxalate in solution levels off with time, so that in the longer reactions more oxalate is in the solid than in the solution.

The data for reactants other than glycolate are given in Table 2.14. Whether or not oxalate is found seems to depend more on the time allowed for reaction, rather than on the nature of the reactant. Oxalate clearly appears at a later time with these reactants than with glycolate.

Analyses for aluminum, by EDTA titration, were performed on some solids. The data are given in Table 2.15.

Examination of the solids by X-ray powder diffraction has provided important information. Diffraction data was taken from the solids from reaction A-97 (rich in oxalate) and A-113 (deficient in oxalate). An automatic search program, available through the School of Materials Engineering at Georgia Tech, compared the patterns observed to the 11,600 patterns in its data base. In this way the compound $Na_2C_2O_4$ was identified as an important constituent in the solid from A-97. No evidence was found for the presence of $Al_3(OH)_7C_2O_4{\cdot}3H_2O$, $NaAl(OH)_2C_2O_4{\cdot}3H_2O$, or $Na_4Al_2(OH)_2(C_2O_4)_2{\cdot}10H_2O$, for which powder

diffraction data have been reported in the literature[16]. The conclusion is that the solid phase containing oxalate is $Na_2C_2O_4$.

Table 2.13. Analysis of Solids Produced by the Reaction of Glycolate in Simulated Waste

Kinetic Run		Weight	Oxalate (%)	Oxalate mmoles (solid)	Oxalate mmoles (solution)	Nitrate (%)
B - 26 Gly/Air	726.5 h	0.496	54	3.04	4.38	trace
B - 11 Gly/He/Cr	1540 h	2.6	34	10.0	3.47	5
B - 4 Gly/Air/Cr	1434 h	0.54	1	0.06	2.62	2
A - 126 Gly/Air	1060 h	0.88	52	5.2	8.71	4
Gly - 300 Gly/Air	310 h	0.051	-	-	0.49	14
Gly - 400 Gly/Air	406 h	0.083	39	0.37	0.51	4
Gly - 500 Gly/Air	514 h	0.081	42	0.39	0.66	6
Gly - 600 Gly/Air	672 h	0.17	42	0.81	0.73	5
Gly - 800 Gly/Air	981 h	0.36	27	1.10	1.11	8
Gly - 900 Gly/Air	1250 h	0.43	30	1.47	1.18	4
Gly - 1000 Gly/Air	1474 h	0.50	30	1.70	1.07	6
App - 7 Gly/Air	1248 h	0.086	-	-	1.13	9
B - 140 Gly/Air	820 h	1.45	61.6	10.2	2.29	4

The low solubility of sodium oxalate in these solutions is not unexpected. The following statement appears in the report "Assessment of Concentration Mechanisms for Organic Wastes in Underground Storage Tanks at Hanford": "In summary, precipitation of sodium oxalate in waste tanks containing more than a few thousandths molar total oxalate concentration is expected in the absence of aluminum".[17] Our results suggest that the estimate is valid even when aluminum is present.

Table 2.14. Analysis of Solids Produced by the Reaction of HEDTA and Related Compounds in Simulated Waste.

Kinetic Run		Weight (grams)	Oxalate (%)	Oxalate mmoles (solid)	Oxalate mmoles (solution)	Nitrate (%)
A - 50 HEDTA/Air	1770 h	0.86	2	0.20	0.15	26
A - 55 HEDTA/He	540 h	0.24	-	-	-	10
B - 19 U-EDDA/Air	403 h	0.104	-	-		
B - 33 U-EDDA/Air	203 h	0.446	-	-	-	5
B - 60 IDA/He	281 h	0.171	-	-	-	8
B - 95 DMG/Air	304 h	0.102	-	-	-	10
B - 73 NTA/Air	357.5 h	0.091	-	-	-	9
B - 77 Sarcosine/Air	908 h	0.935	-	-	-	14
B - 69 IDA/Air	1139 h	0.33	1	0.038	0.31	10
B - 85 MIDA/Air	1060 h	1.24	1.2	0.17	2.94	7
H - 1 HEDTA/Air	200 h	0.11	-	-	-	11
H - 3 HEDTA/Air	300 h	0.05	-	-	-	13
H - 4 HEDTA/Air	400 h	0.10	-	-	-	9
H - 5 HEDTA/Air	500 h	0.15	-	-	-	8
B - 81 SEDDA/Air	1800 h	2.01	62.5	14.3	2.11	9
B - 89 Glycine/Air	1600 h	0.348	2.2	0.087	-	8
A - 113 HEDTA/He	1400 h	5.97	-	-	-	8
A - 97 HEDTA/Air (sonication)	3000 h	3.11	58	20.5	2.95	7

Table 2.15. Aluminum Analysis of Solids Produced by the Reactions of Glycolate and MIDA in Simulated Waste

Kinetic run	Weight (grams)	Aluminum (%)
A - 119 Glycolate/He	1.79	5.5
A - 126 Glycolate/Air	0.882	7.2
B - 85 MIDA/Air	1.24	12.4

The additional lines in the pattern from the A-97 sample and the prominent lines from the A-113 sample were attributed by the search program to $Na_3Al_3(SiO_4)\cdot Na_2CO_3$. This compound belongs to the class of alumino-silicates known as cancrinites. In the cancrinites various anions and cations and water can occupy channels in the alumino-silicate structure. The presence of large percentages of nitrate and small percentages of carbonate in the solids from our reactions suggest that the cancrinite formed is not the one of the formula given above but is instead the cancrinite of formula $Na_3Al_3(SiO_4)_3\cdot NaNO_3\cdot 2H_2O$, which is reported[18] to be formed when alumino-silicates are formed from solutions rich in $NaNO_3$. The retention of NO_3^- in our insoluble solids is thus explained. Another compound considered as a possible insoluble solid to be formed was $NaAl(OH)_2CO_3$. We found no lines in our patterns corresponding to those reported[19] for this compound.

2.J References

(1) Genik-Sas Berezowsky, R.M.; Spinner, I.H. *Can. J. Chem.* **1970**, *48*, 163.
(2) Campbell, J.A.; Pool, K.H.; Melethil, P.K. *PNL-8041*, March **1992**.
(3) Challis, B.C.; Shuker, D.E.G. *J. C. S. Chem. Comm.* **1979**, 315.
(4) Olàh, G.; Noszkó, L.; Kuhn, I.; Szelke, M. *Chem. Ber.* **1956**, *89*, 2374; *Chem. Abs.* **1957**, *51*, 8000.
(5) Keefer, L.K.; Roller, P.P. *Science* **1973**, *181*.
(6) Emerson, W.S. *J. Am. Chem. Soc.*, **1945**, *67*, 516.
(7) Brancaccio, G.; Larizza, A. *Gazz. Chim. Ital.* **1964**, *94*, 37. *Chem. Abst.* **1964**, *61*, 4255f.
(8) Donald, C.E.; Hughes, M.N.; Thompson; J.M.; Bonner, F.T. *Inorg. Chem.*, **1986**, *25*, 2676.
(9) Cooper, J.N.; Chilton, J.E.; Powell, R.E. *Inorg. Chem.* **1970**, *9*, 2303.
(10) Kornblum, N.; Oliveto, E.P. *J. Am. Chem. Soc.* **1949**, *71*, 226; Gray, P.; Rathbone, P.; Williams, A. *J. Chem. Soc.* **1960**, 3932.
(11) Heusler, K.; Kalvoda, J. *Angew. Chem. Int. Ed.* **1964**, *3*, 525.
(12) Barton, D.H.R.; Beaton, J.M.; Geller, L.E.; Pechet, M.M. *J. Am. Chem. Soc.* **1961**, *83*, 4076.
(13) Smith, P.A.S.; Loeppky, R. N. *J. Am. Chem. Soc.* **1967**, 89, 1147.
(14) Ashby, E. C.; Barefield, E. K.; Liotta, C. L.; Neumann, H. M.; Doctorovich, F.; Konda, A.; Zhang, K.; Hurley, J.; Boatright, D.; Annis, A.; Pansino, G.; Dawson, M.;

Juliao, M. *ACS Sym., Emerging Technologies in Hazardous Waste Management IV*, **254**, 249 (1994).

(15) Ashby, E. C.; Doctorovich, F.; Liotta, C. L.; Neumann, H. M.; Barefield, E. K.; Konda, A.; Zhang, K.; Hurley, J. *J. Am. Chem. Soc.* **1993**, *115*, 1171.

(16) Bilinski, H.; Horvath, L.; Ingri, N.; Sjoberg, S. *Geochim. Cosmochim. Acta* **1986**, *50*, 1911.

(17) Gerber, M.A.; Burger,f.L.; Nelson, D.A.; Ryan, J.L.; Zollars, R.L. PNL-8339/AD-940, Sept. 1992.

(18) Barrer, M; Cole, J.F.; Villiger, H. *J. Chem. Soc. (A)* **1970**, 1522. Hund, F.Z. *Anorg. Allg. Chem.* **1984**, *509*, 153.

(19) Frueh, A.J.; Golightly, J.P. *Can. Mineral.* **1967**, *9*, 51. Keenan, F.J. Ph.D. Thesis, University of Wyoming, **1981**.

TASK 5: SOURCE OF NITROUS OXIDE, NITROGEN AND AMMONIA

A number of studies were undertaken to attempt to determine the possible origin(s) and mechanism of formation of the title gases using simulated waste mixtures. At the outset it was necessary to determine the source of nitrogen for each of these gases. This was accomplished using N-15 labeled reagents as outlined in the first section below. In the course of other studies that were concerned with the stoichiometry of HEDTA decomposition, the amount of nitrous oxide was found to go through a maximum. It was determined that nitrous oxide decomposed to nitrogen and oxygen, possibly catalyzed by the hot glass of the reaction vessel. This is a significant observation that will affect any future studies that are done in glass vessels and a summary of results in this area is presented in the second section. The results of preliminary studies on possible mechanistic pathways for nitrogen gas formation from nitrite are then described. These studies are incomplete and much remains to be done to understand the chemical pathways by which the gases are formed. The recent discovery by Westinghouse scientists that ammonia is a major gaseous product from tank 101-SY raises several questions that cannot be addressed by most of the studies on simulated waste since no quantitative assays of ammonia production have been made. However, existing data from some studies of HEDTA decomposition in simulated waste can be utilized to provide an estimate of how much ammonia might be produced. This analysis is given in the final section.

5.A Reactions in SY1-SIM-91B mixtures utilizing N-15 labeled reagents

5.A.1 Source of N_2O and N_2. Several reactions of unlabeled HEDTA in SY1-SIM-91B media prepared with ^{15}N-labeled nitrate and/or nitrite reagents were conducted at 120° C for 49 days under atmospheres of air and helium. Mass spectrometric analyses of the head space gases clearly established that the N_2O and N_2 produced in these reactions originated only from the nitrite and not from nitrate or HEDTA. When the simulated waste mixture contained both $^{15}NO_2^-$ and $^{15}NO_3^-$, and the reaction was conducted under either an air or a helium atmosphere, only doubly labeled N_2O and N_2 were formed. On the other hand, when HEDTA was allowed to react at 120° C in the simulated waste mixture containing $^{15}NO_3^-$ as the only ^{15}N label, only unlabeled N_2O and N_2 were formed. This result indicates that both N_2O and N_2 originate from NO_2^-. In order to verify this conclusion, HEDTA was allowed to react at 120° C in the simulated waste mixture containing $^{15}NO_2^-$ as the only nitrogen labeled compound. In this case both doubly-labeled $^{15}N_2O$ and $^{15}N_2$ were produced. This result shows conclusively that both N_2O and N_2 originate exclusively from NO_2^-.

It would be difficult to prepare ^{15}N-HEDTA in order to check the above results that show that N_2O and N_2 do not originate from the organic portion of the simulated waste; however, it is not necessary to do this since, if any N_2O and N_2 did originate from HEDTA, then some ^{14}N - N_2O and /or N_2 would have been produced in the reaction with $^{15}NO_2^-$. This was not observed.

There are, of course, many organic degradation products produced in the thermal decomposition of HEDTA in simulated waste at 120° C; glycine is one of these. Since ^{15}N-

glycine was available, the decomposition of this compound was studied in simulated waste at 120° C and a trace of $^{15}N_2$ in the ^{14}N-N_2O, N_2 mixture was found. Great significance is not attached to detection of a trace amount of $^{15}N_2$ in this experiment and therefore NO_2^- is still considered the major source of N_2O and N_2 produced in simulated waste.

5.A.2 Source of NH_3. Formation of ammonia in these thermal degradation studies arises after a series of reactions. When HEDTA was allowed to react at 120° C for 49 days in simulated waste, NH_3 was formed in 17% yield (based on HEDTA). The NH_3 was passed into an aqueous solution of HCl and the ammonia determined as NH_4Cl. When HEDTA was allowed to react at 120°C in simulated waste containing $^{15}NO_2^-$ and $^{15}NO_3^-$, both $^{15}NH_3$ (90%) and $^{14}NH_3$ (10%) were formed, as indicated from ^{14}N and ^{15}N NMR spectra of the NH_4Cl solution. When a similar reaction was carried out containing only $^{15}NO_3^-$ as the labeled compound, only unlabeled NH_3 was formed; however, when only $^{15}NO_2^-$ was present, $^{15}NH_3$ (88%) and $^{14}NH_3$ (12%) were formed. All of these results clearly indicate that approximately 90% of the NH_3 produced in the thermal decomposition of HEDTA in simulated waste at 120° C over a period of 49 days originates from $NaNO_2$ and 10% originates from HEDTA and its decomposition products.

5.B Decomposition of nitrous oxide.

In tests of the reliability of the apparatus and procedures being used for studies lasting for hundreds of hours at 120°C it was observed that the concentration of N_2O in the gaseous phase decreased with time. The rate of decrease was about the same whether simulated waste solution was present or not. It was initially thought that the observation could be due to an analytical artifact, but this was shown not to be the case when a similar experiment carried out at room temperature showed that the amount of N_2O remained constant. Since nitrous oxide is thermodynamically unstable, its decrease could be due to its decomposition according to equation 5.1.

$$N_2O \rightarrow N_2 + 1/2\ O_2 \qquad (5.1)$$

An experiment in which N_2O in an argon atmosphere was heated at 120°C for 1000 hours, supports this interpretation as shown by the results in Table 5.1.

Table 5.1. Gas Composition After Heating N_2O at 120° C.

N_2O_i, mmols	N_2O_f, mmols	N_2, mmols	O_2, mmols
0.36 ± 0.05	0.24 ± 0.04	0.10 ± 0.02	0.060 ± 0.012

The decomposition of nitrous oxide to nitrogen and oxygen is well established, and its rate has been the subject of numerous investigations under both homogeneous and heterogeneous conditions. The homogeneous gas phase reaction[1] is one of the most extensively studied unimolecular decompositions in the literature. These studies were generally in the temperature range 800-1100 K. Linders and Hinshelwood[2] found surface effects on the rate in their reactions at 720° C using a silica vessel, but reported this effect

could be eliminated by proper "conditioning" of the vessels. In an early study, Hibben[3] reported unimolecular rate constants for the reaction in a quartz vessel in the temperature range 550-625 K. Since these rates were "approximately 1000 times faster" than rates obtained by extrapolating the known high temperature homogeneous data, he attributed the increased rate to heterogeneous reaction on the surface of the vessel. Although heterogeneous catalysis by metals and by metal oxides has been studied extensively at lower temperatures, there have been no studies of the behavior on glass surfaces. We attribute our results to catalysis produced on the glass walls of the apparatus.

The results of three experiments, all done in the same apparatus at 120°C, are shown in Table 5.2. In one of these experiments, a simulated waste solution (without organics) was present in addition to the gas phase containing N_2O in argon. In the other two experiments only the gas phase was present. The rate of disappearance of N_2O was measured, and a rate constant was calculated assuming that the reaction is first order in N_2O. Table 5.2 shows that the apparent rate constant is practically the same in all three cases, indicating that the presence of simulated waste solution (without organics) does not affect the rate. It must be noted that in all three cases and due to the design of the apparatus, only one third of the gas is being heated, and the rest is at room temperature. The rate constant only has meaning with respect to the particular apparatus used, since it would be expected to depend on the surface area of glass in the system.

Table 5.2. Rate Constant for Nitrous Oxide Decomposition.

Mixture	$[N_2O]_i$, M	k, hrs^{-1}
N_2O in Ar	3.2×10^{-4}	$4.1 \pm 0.2 \times 10^{-4}$
N_2O in Ar + simulated Waste	4.0×10^{-4}	$3.4 \pm 0.2 \times 10^{-4}$
N_2O in Ar	2.6×10^{-3}	$3.5 \pm 0.5 \times 10^{-4}$

These results indicate clearly that in our long-term studies of the decomposition of organics in simulated waste, the measured amounts of N_2O and N_2 at any time are affected by the rate of decomposition of N_2O. In interpreting the measured values of N_2 and N_2O, the sum of the two is more meaningful than the individual values.

5.C Mechanistic pathways for formation of gases containing nitrogen from nitrite.

As described above, use of ^{15}N-labeled inorganic reagents established that nitrogen and nitrous oxide produced from simulated waste reactions are derived exclusively from nitrite and that a major fraction of the ammonia derived from HEDTA decomposition also came from nitrite. If NO^- is generated as an intermediate following aluminum promoted nitrosation then the formation of nitrous oxide is not unexpected since dimerization of NO^- to $N_2O_2^{2-}$ and the decomposition of hyponitrite to N_2O is well established chemistry. Thus, this pathway for formation of nitrous oxide does not involve a "hydride" source or even additional reducing equivalents. Generation of ammonia, on the other hand, requires additional reducing equivalents and/or a "hydride" source. Consideration of known thermal reactions of oxynitrogen species would suggest that formation of ammonia will most likely

arise from further reduction of hydroxylamine (including disproportionation) or by hydrolysis of cyanide. In principle, either of these species could also arise from NO^- by reaction with a suitable reducing agent. The fact that formaldehyde is proposed as a decomposition product of HEDTA and its fragments, suggests that it might serve as the reducing agent for other species besides water (equations 5.2 and 5.3)

$$3H_2O + N_2O_3^{2-} + 2e^- \rightarrow H_2NOH + NO_2^- + 3OH^- \quad (5.2)$$

$$H_2O + H_2NOH + 2e^- \rightarrow NH_3 + 2OH^- \quad (5.3)$$

In each case the formaldehyde would be oxidized to formate. The reduction potential for the reduction of H_2NOH is favorable. Although the potential for $N_2O_3^{2-}$ is unknown, the potential for reduction of NO^- is favorable. Standard potentials and general features of the chemistry of $N_2O_3^{2-}$ and H_2NOH are reviewed in the October 15, 1991 report from Georgia Tech. A series of survey reactions designed to determine whether formaldehyde might be a suitable reducing agent for $N_2O_3^{2-}$ and H_2NOH were undertaken.

5.C.1 The reaction of H_2NOH with organic compounds in basic solution. The reactivity of hydroxylamine toward certain organic compounds was studied in modified SY1-SIM-91B mixtures. The results of some experiments are shown in Table 5.3.

On the basis of literature reports, disproportionation of H_2NOH is expected to occur in basic solutions such as SY1-SIM-91B to give the oxidation products N_2 and N_2O and the reduction product NH_3. The ratio of products is highly sensitive to conditions; a characteristic feature of the disproportionation in our systems is greater formation of N_2 than N_2O (N_2/N_2O ratio between 8:1 and 16:1). Smaller yields of N_2 and N_2O in the experiments when H_2CO is present indicate that a reaction of H_2NOH with H_2CO has occurred. The formation of formate cannot be due to the Cannizzaro reaction, both because of its high yield, and because CH_3OH is not formed. The reaction $H_2NOH + H_2CO + OH^- \rightarrow HCO_2^- + NH_3 + H_2O$ is strongly indicated.

^{14}N NMR spectroscopy provided important information about nitrogen-containing products and intermediates in the above reactions. Interpretation of these experiments utilizes chemical shift data contained in Table 5.4, which was obtained from the literature and from our own measurements as indicated.

The thermal reaction of H_2NOH with H_2CO in basic solution was carried out in a 10 mm NMR tube. A solution of paraformaldehyde (62.5 mg, 2.08 mmol of H_2CO) and hydroxylamine (70 mg, 2.1 mmol) in 4 ml of 2 M $NaOD/D_2O$ (KHA-14) was combined in a 10 mm NMR tube that contained a capillary with an the external standard (CH_3NO_2) and sealed under vacuum. Spectra obtained on this sample as a function of time and temperature are shown in Figures 5.1 to 5.4.

Table 5.3. Results of reactions of H_2NOH in modified SY1-SIM-91B mixtures.[1]

component	KHA-1 520 h		KHA-2 520 h		KHA-3 520 h		KHA-4 170 h		KHA-5 170 h	
	mmol		mmol		mmol		mmol		mmol	
	initial	final	initial	final	initial	final	initial	after	initial	final
OH^-	8.0	-	8.0	-	8.0	-	8.0	-	8.0	-
H_2NOH	1.66	-	1.84	-	1.54	-	1.48	-	1.46	
CH_3OH	0	0	0	0	1.6	1.05	0	0	0	0
H_2CO	0	0	1.6	0	0	0	1.65	0	1.64	0
HCO_2^-	1.59	1.49	0	1.54	0	0.02	0	1.29	0	1.37
NO_2^-	0	0	0	0	0	0	8.96	8.93	0	0
AlO_2^-	0	0	0	0	0	0	6.16	-	0	0
N_2	0	0.32	0	0.026	0	0.26	0	0.045	0	0.025
N_2O	0	0.04	0	0.004	0	0.021	0	0.023	0	0.002
H_2	0	0.023	0	trace	0	0.013	0	trace	0	trace

[1]Reaction conditions: Ar atmosphere; KHA-1, KHA-2, and KHA-3 at 120° C; KHA-4 and KHA-5 at 90° C; reaction volume is 4.0 mL. Analytical measurements were by IC, NMR, and GC. In all cases, when the reaction vessel was opened, wet pH paper turned blue in the product gas, and the odor of ammonia was noticed.

Table 5.4. Nitrogen-14 Chemical Shift (ppm) Referred to External CH_3NO_2.

Molecule or ion	^{14}N shift (ppm)	Conditions	Molecule or ion	^{14}N shift (ppm)	Conditions
NH_3	-377	1 M aqueous NH_3	NO_3^-	-1	1 M $NaNO_3$ in D_2O
NH_4^+	-358	1 M NH_4NO_3 in D_2O	CH_3NO_2	0	neat
H_3NOH^+	-297	1 M $H_2NOHHCl$ in D_2O	$H_2C{=}NOH$	2	1 M in Et_2O[b]
H_2NO^-	-284	in 2 M NaOH	$H_2C{=}NO^-$	17	in 2 M NaOH
CH_3CN	-132	neat	$N_2O_2^{2-}$	78	in 1 M NaOH[c]
CN^-	-102	0.5 M KCN in 2 M NaOH	$H_2N_2O_2$	81	in 1 M $HClO_4$[c]
$N_2O_3^{2-}$	-37 N(1) -21 N(2)	^{15}N measurement at pH 13[a]	NO_2^-	232	1 M $NaNO_2$ in D_2O

a) F. T. Bonner, H. Degani and M. J. Akhtar, *J. Am. Chem. Soc.* **103,** 3739, (1981). b) M. Witanowski, L. Stefaniak, H. Januszevski and S. Szymanski, *Tetrahedron*, **29,** 2833, (1973). c) J. Mason and W. van Bronsewijk, *J. Chem. Soc. (A)*, 791, (1971).

At room temperature, only one peak centered at 17 ppm was observed (Figure 5.1). This indicated that H_2NOH reacts with H_2CO to form $H_2C{=}NOH$ very fast, even in basic solution at low temperature. After heating up to 60° C for 2 h, the second NMR spectra was taken (Figure 5.2). This spectrum indicates that $H_2C{=}NOH$ is relatively stable (the sharper peak results from the measurement of the spectrum at higher temperature). After heating at 90° C for 2.5 h, the CN^- and NH_3 peaks appeared and the $H_2C{=}NOH$ peak disappeared completely (Figure 5.3). The hydrolysis of CN^- is relatively slow. After heating at 90° C for 90 h, a small amount of CN^- remained in solution, while the NH_3 peak increased dramatically (Figure 5.4). Based on the ^{14}N NMR study, the reaction sequence shown by equations 5.4 to 5.6 is proposed.

$$H_2NOH + H_2CO \xrightarrow{\text{fast}} H_2C{=}NOH + H_2O \tag{5.4}$$

$$H_2C{=}NOH + OH^- \xrightarrow{\text{slow}} CN^- + 2H_2O \tag{5.5}$$

$$CN^- + 2H_2O \xrightarrow[OH^-]{\text{slow}} NH_3 + HCO_2^- \tag{5.6}$$

IC analysis showed that 1.8 mmol of HCO_2^- was found (90% based on H_2CO). This indicates that, given sufficient time, H_2NOH reacts with H_2CO in basic solution to quantitatively produce NH_3 and HCO_2^-.

5.C.2 The reaction of $N_2O_3^{2-}$ with H_2CO in basic solution. A series of experiments was undertaken in which $N_2O_3^{2-}$ was combined with various modified SY1-SIM-91B mixtures. In all cases 4 mL of each reaction mixture was heated at 90° C under Ar for 170 hours. When the reaction vessel was opened, the presence of basic gas was indicated by test with wet pH paper. The results of some of these experiments are shown in Table 5.5.

Experiment KON-1 shows how $N_2O_3^{2-}$ reacts when alone in base. The stoichiometry expected on the basis of literature reports is shown in equation 5.7.

$$H_2O + 2\,N_2O_3^{2-} - N_2O + 2NO_2^- + 2OH^- \tag{5.7}$$

Figure 5.1. KHA-14. ^{14}N NMR of Reaction H_2NOH with H_2CO in Basic Solution at Room Temperature for 20 minutes.

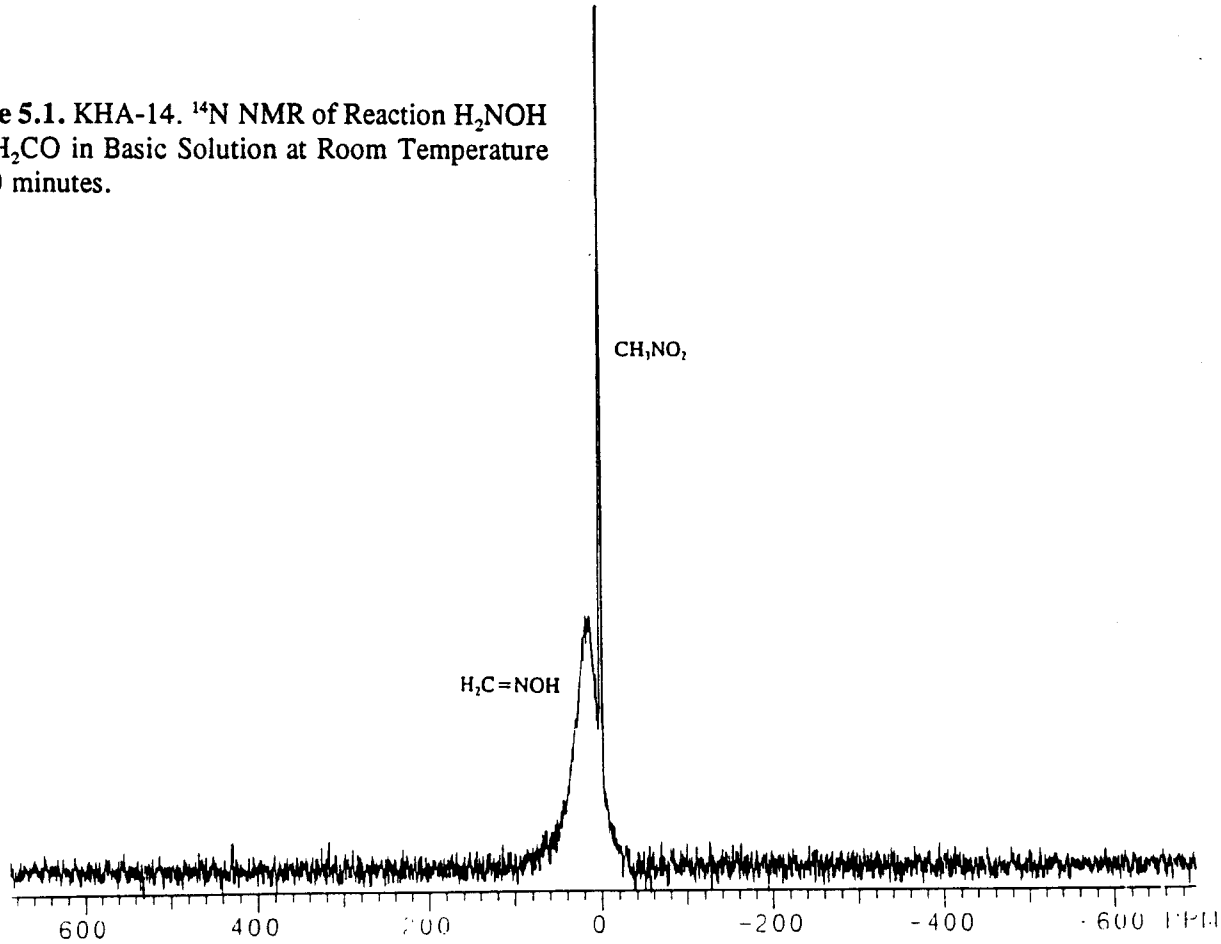

Figure 5.2. KHA-14. ^{14}N NMR of Reaction H_2NOH with H_2CO in Basic Solution at 60° C for 2 hours.

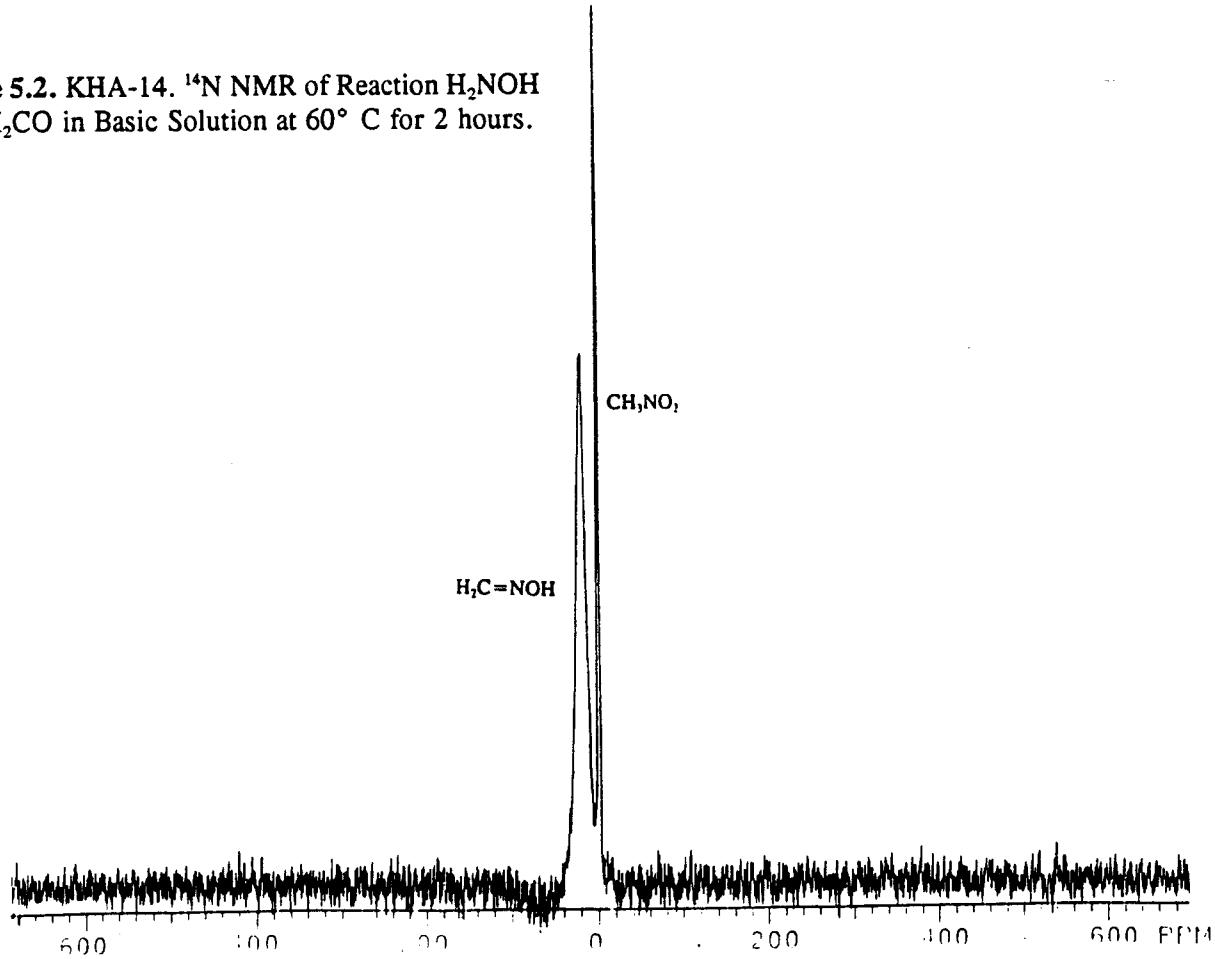

Figure 5.3. KHA-14. ^{14}N NMR of Reaction H_2NOH with H_2CO in Basic Solution at 90° C for 2.5 hours.

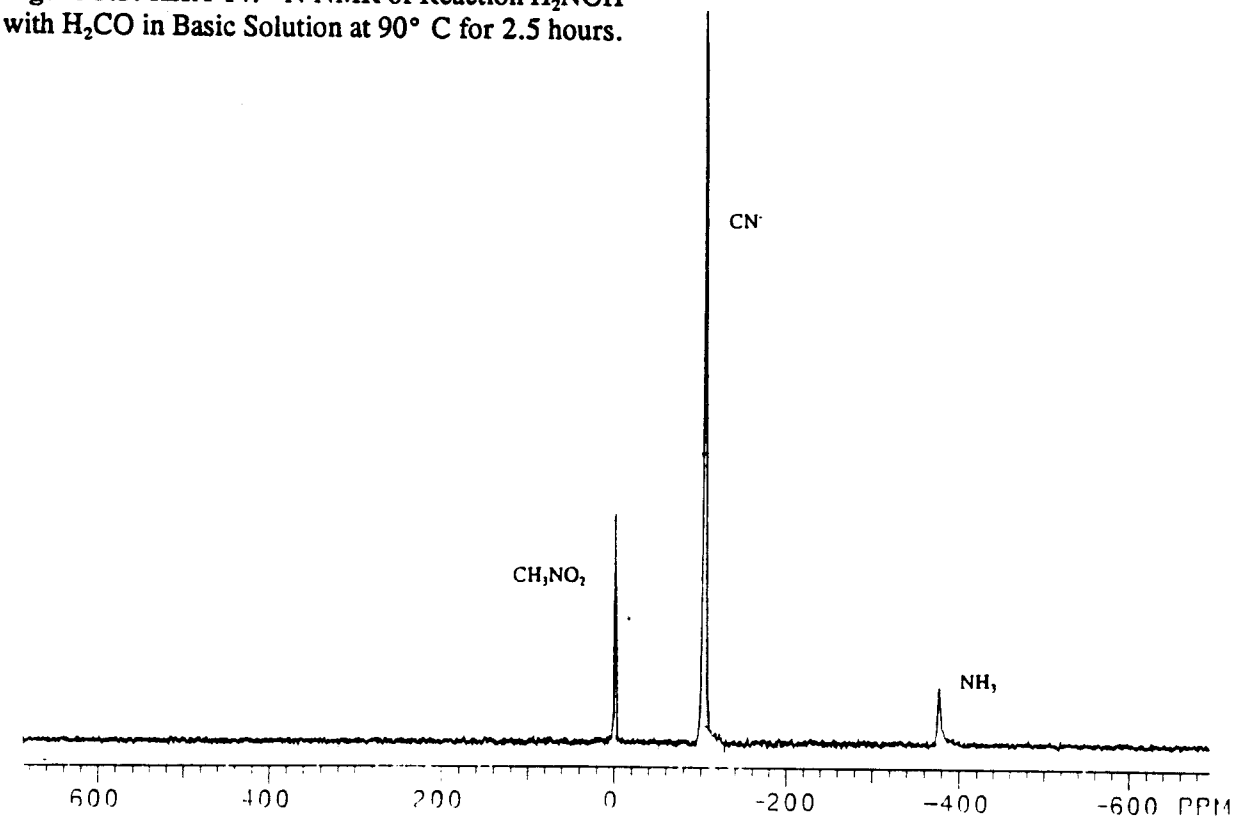

Figure 5.4. KHA-14. ^{14}N NMR of Reaction H_2NOH with H_2CO in Basic Solution at 90° C for 90 hours.

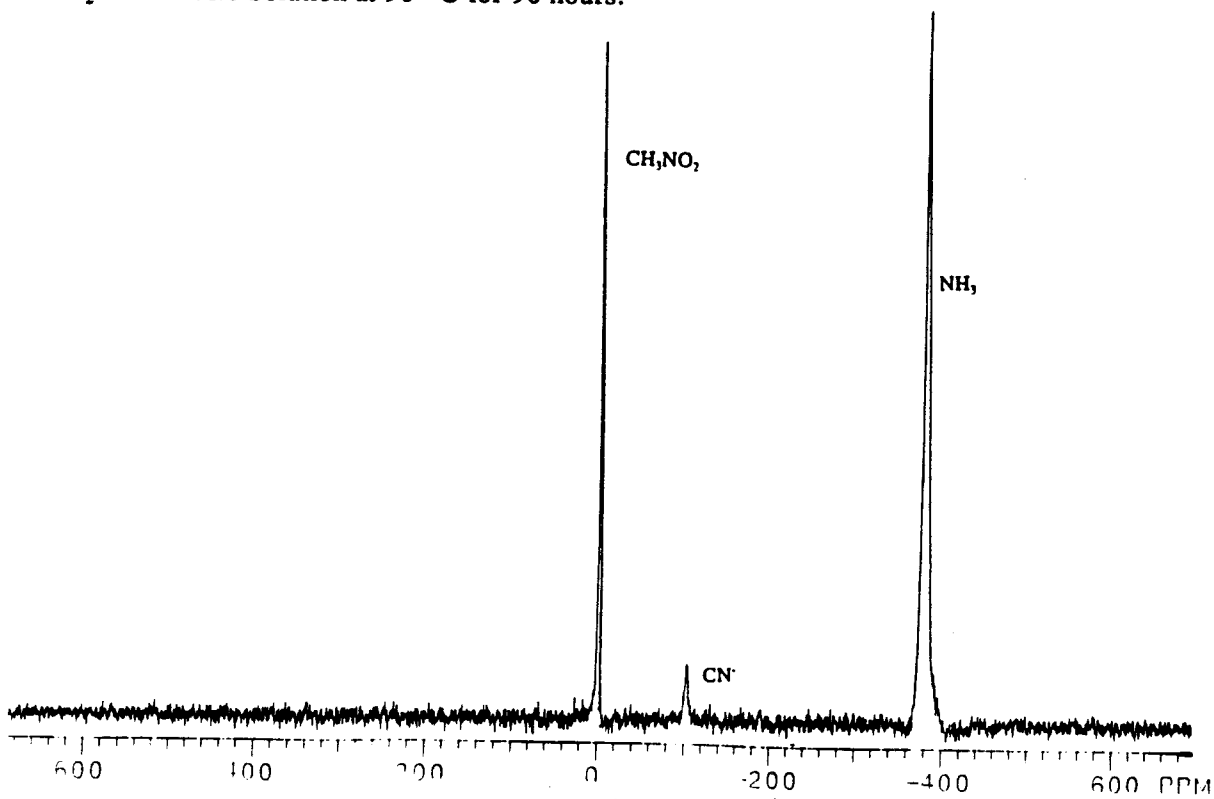

Table 5.5. Results of Reactions of $N_2O_3^{2-}$ in Modified SY1-SIM-91B Mixtures.

component mmol	KON-1		KON-2		KON-6		KON-3	
	initial	final	initial	final	initial	final	initial	final
OH^-	8.0	-	8.0	-	8.0	-	8.0	-
AlO_2^-	0	0	6.16	-	0	0	0	0
$N_2O_3^{2-}$	0.376	<0.01	0.334	<0.01	0.408	<0.01	0.388	<0.01
H_2CO	0	0	0.40	0	0.45	0	0.41	-
HCO_2^-	0	0	0	0.388	0	0.346	0	0.308
NO_2^-	0	0.366	0	0.321	0	0.376	8.96	9.33
N_2	0	trace	0	0.061	0	0.056	0	0.11
N_2O	0	0.065	0	0.012	0	0.052	0	0.043
H_2	0	trace	0	trace	0	trace	0	0.003

It is important to note that no reductant is required to generate nitrous oxide and nitrite from $N_2O_3^{2-}$. However, when formaldehyde was included in the reaction mixture it was largely converted to formate. Although the mass balances for these reactions were not satisfactory, and neither H_2NOH and NH_3 were determined, some conclusions can be drawn. In all cases, regardless of the reaction occurring, half of the nitrogen in $N_2O_3^{2-}$ appeared as NO_2^-. The appearance of formate cannot be attributed solely to the Cannizzaro reaction of formaldehyde since the yield is greater than 50%. The formation of nitrogen in the presence of formaldehyde indicates that reduction has occurred and argues for the reaction of $N_2O_3^{2-}$ (or NO^-) by some process other than equation 5.7.

NMR spectral measurements of reactions of $N_2O_3^{2-}$ were also undertaken. Although complicated, some very interesting conclusions are suggested. At room temperature for 50 h, ^{14}N (Figure 5.5) and ^1H NMR showed that there was no reaction between $N_2O_3^{2-}$ and H_2CO; H_2CO underwent the Cannizzaro reaction (formation of HCO_2^- and CH_3OH in 1:1 ratio as shown by ^1H NMR) and $N_2O_3^{2-}$ underwent self decomposition. At higher temperature, the reaction of $N_2O_3^{2-}$ (144 mg, 1.2 mmol) and H_2CO (59.4 mg, 2 mmol) in 4 ml of 2 M $NaOD/D_2O$ was monitored by ^{14}N NMR (Figures 5.6-5.8).

$N_2O_3^{2-}$, which contains two nonequivalent nitrogen atoms, exhibited only a single broad resonance at room temperature (Figure 5.6) but displayed two resonances at higher temperature. After 2 h at 65° C a resonance due to an unknown intermediate appeared at about -160 ppm (Figure 5.7). After 18 h at 90° C, $N_2O_3^{2-}$ had disappeared completely and NH_3(-377 ppm), and CN^- (-103 ppm) had formed (Figure 5.8).

Figure 5.5. KON-17. ^{14}N NMR of Reaction $N_2O_3^{2-}$ with H_2CO in Basic Solution at Room Temperature for 50 hours.

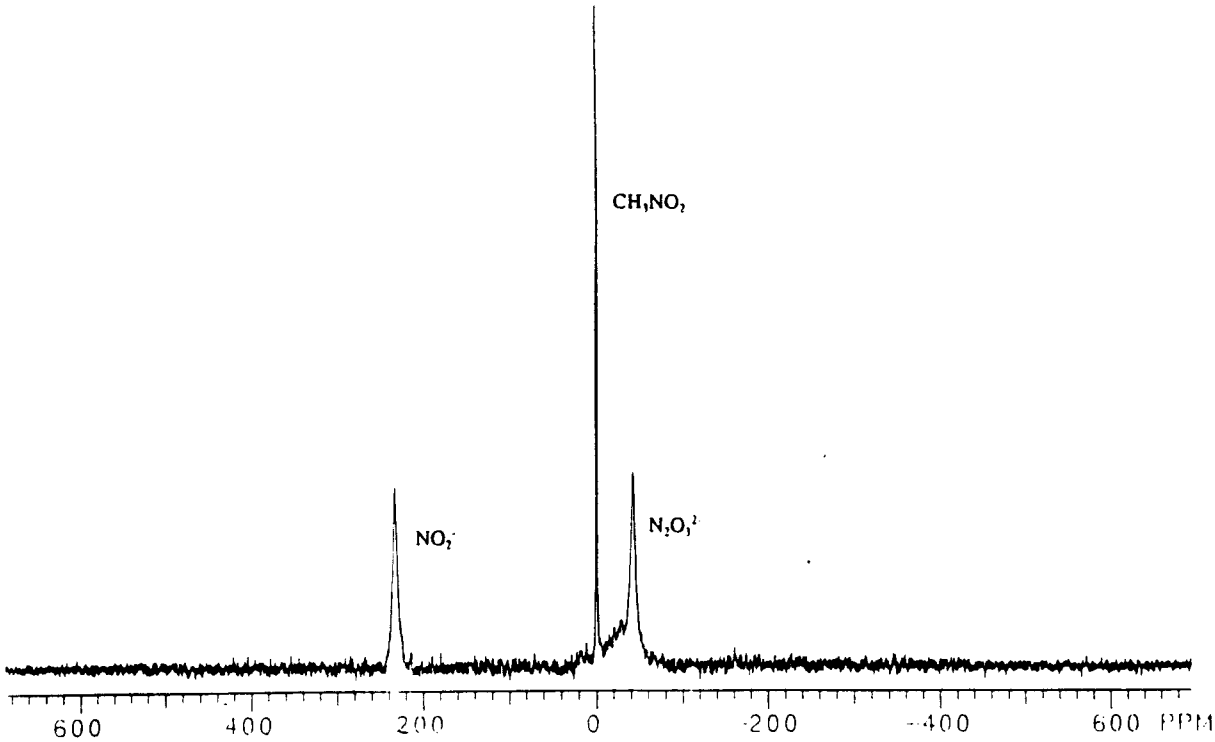

Figure 5.6. KON-19. ^{14}N NMR of Reaction $N_2O_3^{2-}$ with H_2CO in Basic Solution at Room Temperature for 0.5 hours.

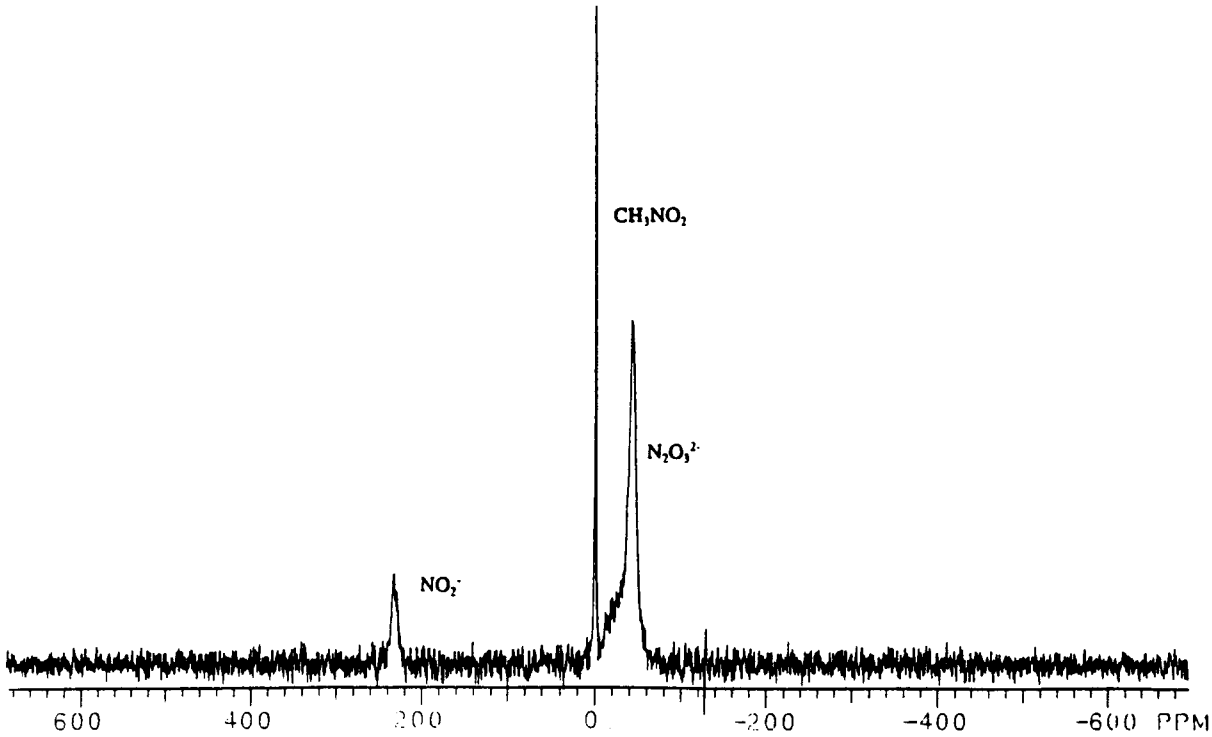

Figure 5.7. KON-19. ^{14}N NMR of Reaction $N_2O_3^{2-}$ with H_2CO in Basic Solution at 65° C for 2 hours.

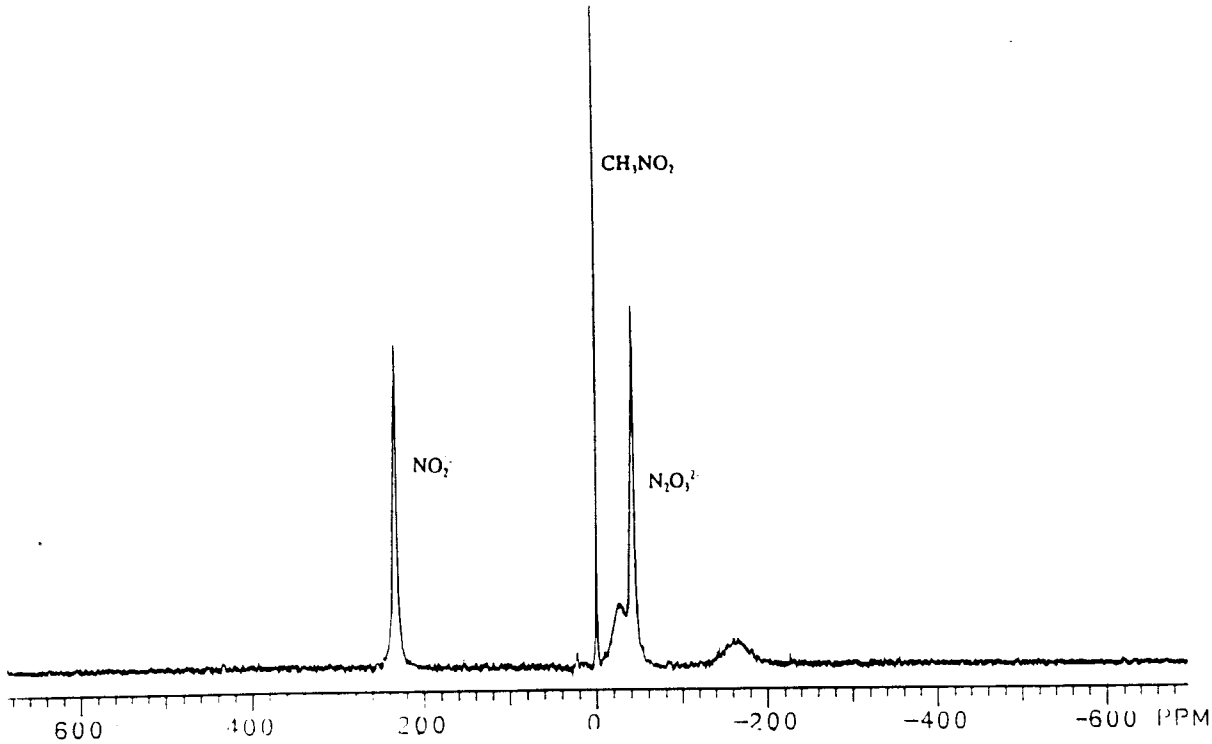

Figure 5.8. KON-19. ^{14}N NMR of Reaction $N_2O_3^{2-}$ with H_2CO in Basic Solution at 90° C for 18 hours.

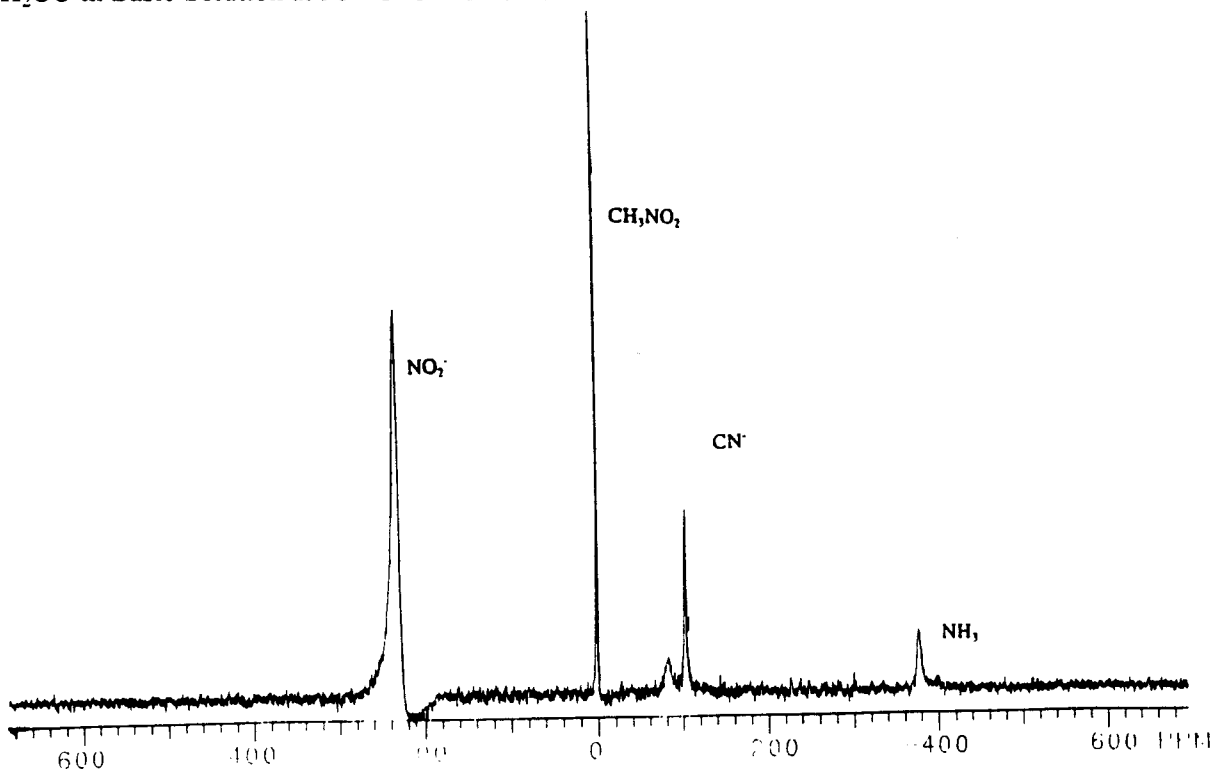

The formation of CN^- suggests that H_2NOH was an intermediate in this reaction, but that the concentration of the latter was too low for it to be detected in the NMR spectrum. Since it hydrolyses slowly, CN^- can accumulate in solution. These results in combination with the results in the previous section suggest the overall reaction: $OH^- + N_2O_3^{2-} + 2H_2CO \rightarrow NH_3 + 2HCO_2^- + NO_2^-$. The results from a second set of experiments, in which only gaseous products were monitored, are shown in Table 5.6. The experiments were conducted in the same way as those in Table 5.5, except that the time and solution components were varied. Experiment KON-25 provides strong evidence for equation 5.8 where the NO^- required results from decomposition of $N_2O_3^{2-}$ (or its conjugate acid).

$$NO^- + NH_2OH \rightarrow N_2 + OH^- + H_2O \qquad (5.8)$$

The relatively high yield of N_2 in experiment KON-22 is probably due to the same reaction; $N_2O_3^{2-}$ is in excess with respect to its reaction with H_2CO, and hence available for reaction with NH_2OH as the latter is formed. In a study[4] of the reaction between $N_2O_3^{2-}$ and NH_2OH at pH 6-8, both N_2 and N_2O were observed as products. Equation 5.8 has also been suggested[5,6] as a step in the mechanism of the reaction of nitric oxide with hydroxylamine. In reaction KON-24, NH_2OH and H_2CO were combined in 1:1 ratio in 2 M NaOH and allowed to stand at room temperature for oxime to form, then $N_2O_3^{2-}$ was added. Since only a trace of N_2 was detected, it can be concluded that oxime and $N_2O_3^{2-}$ do not react to give N_2.

Table 5.6. Survey of Reactions of $N_2O_3^{2-}$ with Formaldehyde and Hydroxylamine.

Component/mmol		KON-21 70 h	KON-22 165 h	KON-23 190 h	KON-24 70 h	KON-25 70 h
Reactants	OH^-	8	8	8	8	8
	H_2CO	0	0.95	1.93	1.14	0
	$N_2O_3^{2-}$	1.1	1.96	0.98	1.12	1.12
	NH_2OH	0	0	0	1.17	1.22
Products	N_2	0	0.33	0.16	trace	0.66
	N_2O	0.39	0.19	0.06	0.18	0.23
	NH_3[1]	yes	yes	yes	yes	no

[1]Ammonia was detected in the product gases by moist pH paper and by its odor.

5.C.3 Conclusions. On the basis of the above observations and information in the literature, the following sequences of reactions can account for formation of N_2O, NH_3, and N_2 in a system that contains formaldehyde and some source of HNO (or its conjugate base NO^-). Hydroxylamine is a necessary intermediate in the formation of NH_3 and N_2 but not of N_2O.

1) Formation of N_2O

$$2\ NO^- + H_2O \rightarrow N_2O + 2\ OH^- \quad (5.9)$$

$$2\ NO^- \rightarrow trans\text{-}N_2O_2^{2-} \quad (5.10)$$

$$trans\text{-}N_2O_2^{2-} + H_2O \rightarrow trans\text{-}HN_2O_2^- + OH^- \quad (5.11)$$

$$trans\text{-}HN_2O_2^- \rightarrow N_2O + OH^- \quad (5.12)$$

2) Formation of NH_3

$$NO^- + H_2CO \rightarrow HC(O)NHO^- \quad (5.13)$$

$$HC(O)NHO^- + H_2O \rightarrow HCO_2^- + NH_2OH \quad (5.14)$$

$$H_2NOH + H_2CO \rightarrow H_2C{=}NOH + H_2O \quad (5.15)$$

$$H_2C{=}NOH + OH^- \rightarrow CN^- + 2\ H_2O \quad (5.16)$$

$$CN^- + 2H_2O \rightarrow NH_3 + HCO_2^- \quad (5.17)$$

Reactions 5.13 and 5.14 appear on the basis of literature information. Formaldehyde is one of the aldehydes that gives the Angeli-Rimini test for aldehydes,[7] which is based on the reaction of $N_2O_3^{2-}$ (or other source of NO^-) with the aldehyde to give the corresponding hydroxamate ion, $RC(O)NHO^-$.

3) Formation of N_2

$$NO^- + NH_2OH \rightarrow N_2 + OH^- + H_2O \quad (5.18)$$

In addition, the disproportionation of hydroxylamine via a combination of equations 5.19 and 5.20 could contribute to the formation of ammonia, nitrogen and nitrous oxide.

$$3\ NH_2OH \rightarrow NH_3 + N_2 + 3\ H_2O \quad (5.19)$$

$$4\ NH_2OH \rightarrow 2\ NH_3 + N_2O + 3\ H_2O \quad (5.20)$$

Our results indicate that the first of these reactions is more important in our solutions, but we have no results that provide information about the mechanism of either reaction.

The fact[8,9] that at pH ~5 the presence of NO_2^- causes kinetic stabilization of $N_2O_3^{2-}$ has been explained as being due to the existence of the equilibrium $HN_2O_3^- \rightleftharpoons NO^- + HNO_2$. Although there is no information on the effect of NO_2^- in more basic solutions, it is reasonable to assume that $N_2O_3^{2-}$ (or its conjugate acid) can be formed by combination of NO^- and NO_2^- (or their conjugate acids), thus providing a steady-state concentration of $N_2O_3^{2-}$, which acts as a reservoir for NO^- in organic degradations in simulated waste, and also in tank 101-SY.

5.D A redox analysis of HEDTA decomposition: how much NH_3 might be formed?

The recent discovery by Westinghouse scientists that ammonia is a major gaseous product from tank 101-SY raises several questions that cannot be addressed by most of the studies on simulated waste since no quantitative assays of ammonia production have been

made. However, existing data from some studies of HEDTA decomposition can be utilized to provide an estimate of how much ammonia might be produced. To make such an analysis requires data from an experiment in which a good carbon mass balance and analyses of other known reduction products (H_2, N_2 N_2O) was achieved. Experiment 11B in Table 1.1 (Task 1) meets these requirements and the data obtained have been used to calculate the moles of electrons available for reduction that are not accounted for by other reduction products.

In experiment 11B decomposition of HEDTA at 90° C under argon consumed 64% of the starting HEDTA (assumed to be 1 mol in the analysis) after 4942 h; the amounts (in moles) of oxidation and reduction products that were identified are listed below.

Oxidation: 1.07 HCO_2^-, 0.12 $C_2O_4^{2-}$, 0.55 ED3A, 0.06 s-EDDA, < 0.02 EDTA, ~ 0.02 $CH_3CO_2^-$

Note that 0.55 mol of ED3A plus 0.06 mol of s-EDDA accounts for 0.61 mol of the HEDTA consumed. Also note that one-half of the formate produced (0.54 mol) plus the amount of oxalate (0.06 mol) accounts for 0.60 mol of the HEDTA consumed.

Reduction: 0.04 H_2, 0.30 N_2, 0.245 N_2O, trace CH_4

The stoichiometry suggested by these data can be interpreted using the following half-reactions and certain assumptions as described below.

Reductions:

$$6\ e^- + 2\ NO_2^- + 4\ H_2O \rightarrow N_2 + 8\ OH^-$$
$$4\ e^- + 2\ NO_2^- + 3\ H_2O \rightarrow N_2O + 6\ OH^-$$
$$2\ e^- + 2\ H_2O \rightarrow H_2 + 2\ OH^-$$
$$6\ e^- + NO_2^- + 5\ H_2O \rightarrow NH_3 + 7\ OH^-$$

Oxidations:

$$HEDTA + 8\ OH^- \rightarrow 2\ HCO_2^- + ED3A + 5\ H_2O + 6\ e^-$$
$$HEDTA + 10\ OH^- \rightarrow C_2O_4^{2-} + ED3A + 7\ H_2O + 8\ e^-$$
$$ED3A + 5\ OH^- \rightarrow C_2O_4^{2-} + S\text{-}EDDA + 3\ H_2O + 4\ e^-$$

- Assuming that ED3A is converted to s-EDDA with production of oxalate: 0.06 mol oxalate x 4 e^-/mol = 0.24 mol e^-
- Assuming that the remaining oxalate (0.06 mol) was derived from conversion of HEDTA to ED3A: 0.06 mol oxalate x 8 e^-/mol = 0.48 mol e^-
- Assuming that all of the formate is derived from conversion of HEDTA to ED3A: 1.07 mol formate x 3 e^-/mol = 3.21 mol e^-

<u>With these assumptions the total mol of e^- available for reduction is 3.93.</u>

A similar analysis for the reduction products leads to the following:

- Formation of N_2: 0.30 mol N_2 x 6 mol e^-/mol = 1.8 mol e^-
- Formation of N_2O: 0.245 mol N_2O x 4 mol e^-/mol = 0.98 mol e^-
- Formation of H_2: 0.04 mol H_2 x 2 mol e^-/mol = 0.08 mol e^-

The total mol e^- consumed by the known reduction products is 2.86.

From this analysis, 1.07 moles of electrons are unaccounted for. If these go to ammonia then 1.07 mol e^- x 1 mol NH_3/6 mol e^- = 0.17 mol of ammonia should have been formed by reduction of nitrite. The amount of ammonia produced would be still greater if some of the nitrogen was produced by thermal decomposition of nitrous oxide. Note that no ammonia can arise from HEDTA at this point because all of the nitrogen is still contained in the fragmentation products. More complete analyses of HEDTA product formation planned for FY 1994 should demonstrate the validity of the above analysis.

5.E References

(1) Preston, K.F.; Cvetanovic, R.J.; *Comprehensive Chemical Kinetics*; Banford, C.H. and Tipper, C.F.H. eds.; Elsevier Publishing Co., **1972**, *4*, 65-70.

(2) Linders, F.J.; Hinshelwood, C. *Proc. Roy. Soc.* (London), Ser. A, **1955**, *231*, 162.

(3) Hibben, J.H. *J. Am. Chem. Soc.* **1928**, *50*, 940.

(4) Bonner, F.T.; Dzelzkalns, L.S.; Bonucci, J.A. *Inorg. Chem.* **1978**, *14*, 2487.

(5) Cooper, J.N.; Chilton, J.E.; Powell, R.E. *Inorg. Chem.* **1970**, *9*, 2303.

(6) Bonner, F.T.; Wang, N.-Y. *Inorg. Chem.* **1986**, *25*, 1858.

(7) Rodd's Chemistry of Carbon Compounds, 2nd Edition, S. Coffey, Ed., Elsevier Publishing Co., 1965; Vol. I, Part C, p. 10.

(8) Hughes, M.N.; Wimbledon, P.E. *J. Chem. Soc., Dalton*, **1977**, 1650.

(9) Akhtar, M.J.; Lutz, C.A.; Bonner, F.T. *Inorg. Chem.* **1979**, *18*, 2369.

EXPERIMENTAL SECTION

TASK 1: KINETIC STUDIES

Materials

All organic reagents were purchased from Aldrich Chemical Company and were used with out further purification. Inorganic reagents were obtained from several sources; all were ACS reagent grade or better.

Product identification and quantitation.

Instrumentation. Gas samples were taken with a CR-700-50 Hamilton gas-tight syringe. Gas mixing was performed with 1 mL or 5 mL SGE gas-tight syringes. Measurements of gas composition were made on Hewlett-Packard 5890 gas chromatographs equipped with thermal conductivity detectors. N_2O was analyzed by using an HP Chromopack Poraplot Q capillary column, while H_2, O_2 and N_2 were analyzed with a Molecular Sieves 6 Å (60/80 mesh) packed column.

NMR analyses were conducted on a Gemini 300 MHz Fourier transform NMR spectrometer.

Ion chromatographic analyses were performed using a Dionex DX-300 ion chromatograph equipped with a Ionpac AS10 4 mm column and an electrical conductivity detector.

Gas analysis. All gases were identified by comparing retention times with those of authentic samples. Knowing the pressure, temperature, amount of headspace over the reaction mixture and comparing the observed responses with those of known amounts of authentic samples, the amounts of gases produced could be calculated according to the expression n=PV/RT, where n represents the amount (in moles) of gas produced, P is the value for atmospheric pressure (all measurements were performed at atmospheric pressure), V is the headspace volume (calculated as the difference between the total volume, which was measured, and the initial volume of solution used in the experiment)., R is a constant, and T is the temperature in the reaction vessel. In the case of the "A" experiments, T was equal to room temperature. In the case of the "B" experiments, two different temperatures were used: for the gases in the region above the reaction mixture and below the condenser (see Figure 2) T was supposed to be equal to the temperature inside the oil bath, while T = room temperature was used for the remaining part of the vessel. To that effect, the volumes of both regions were previously determined.

Solution analysis. Nonvolatile products were identified by ^{1}H-NMR or ion chromatography by comparison with authentic samples. Concentrations were determined by NMR by integration of peak intensities versus an external standard contained in a separate capillary that was inserted into the 5 mm tube. Data were acquired to insure that nuclear spin relaxation was complete prior to acquisition of the next FID.

Concentrations of ions were determined by ion chromatography by establishing the instrument response with authentic samples of salts of the ions to be determined. Experimental uncertainties associated with measurements of ion concentrations have not been included in all tables; however, the reproducibility of IC measurements has been examined. The following data indicate the reproducibility and accuracy of the determinations of several ions. These experiments were done on samples that were used as control experiments in thermal decompositions of glycolate in SY1-SIM-91B medium. In each case, a 100 mL aliquot of SY1-SIM-91B solution was heated at 120° C for h, the contents recovered and diluted to 250 mL.

Table E.1. Reproducibility of ion chromatographic analyses of nitrite and nitrate ion.

Sample	$NaNO_2$ moles/250 mL	$NaNO_3$ moles/250 mL
SY1-SIM-91B, no organics	0.227 0.226 0.218	0.252 0.252 0.248
SY1-SIM-91B, no organics	0.224 0.222 0.229	0.254 0.252 0.258
SY1-SIM-91B, no organics	0.220 0.226	0.250 0.257
SY1-SIM-91B no aluminate	0.227 0.222 0.229	0.257 0.258 0.250
	avg 0.225; sd 0.0036	avg 0.254; sd 0.0036

A similar analysis of data was performed for nitrate in series of thermal reactions of glycolate in SY1-SIM-91B solution that were heated for different periods of time. In this case the concentration of NO_2^- decreased with time as expected. There was no obvious trend in the concentration of NO_3^-, which is assumed to mean that the concentration did not change during the period of the reaction and the deviation in the results is taken as indicative of the reliability of our procedures.

Methods

Preparation of simulated waste solutions (SY1-SIM-91B). To prepare 100 mL of simulated solution, 50 mL of distilled water was placed in a polypropylene Erlenmeyer flask along with a Teflon coated magnetic stirring bar. The following reagents were added sequentially with vigorous magnetic stirring at room temperature: sodium carbonate (4.5 g), sodium hydroxide (8.0 g), sodium aluminate (14.6 g), sodium nitrate (22.0 g), sodium nitrite (15.5 g) and organics (21 mmoles). The addition of each component was done only after the previous component had dissolved completely. Approximately 10 mL of water was added after the additions of sodium aluminate, while 5 mL was added after the additions of sodium nitrite and nitrate. After all components were added and the solution

Table E.2. Reproducibility of ion chromatographic analyses of nitrate ion.

Reaction Time/h	$NaNO_3$, mol/ mL
0	0.0638 0.0643
100	0.0620 0.0630
200	0.0655 0.0643
300	0.0633 0.0638
400	0.0645 0.0665
500	0.0638 0.0645
600	0.0673 0.0638
800	0.0663 0.0668 0.0633
	avg 0.0645; sd 0.0015

became clear, the mixture was vacuum filtered through a Büchner funnel provided with filter paper (generally only trace amounts of solid were collected). The solution was transferred to a volumetric flask and water was added to bring the total volume to 100 mL. Where carboxylic acids were used as organic starting materials, sufficient additional sodium hydroxide was added to neutralize the acid. Except for those instances where solutions were deliberately aged prior to use, all solutions were used immediately after preparation.

Standard procedure for recovery of reactants and non-gaseous products after reaction in simulated waste. After completion of a reaction the reaction vessel was removed from the gas collection system (see descriptions below). The vessel cap was removed, and the edge of the vessel cleaned of any grease. The Teflon beaker was then removed carefully, and the outside wall of the beaker rinsed three times with deionized water, with the rinsings collected in a volumetric flask. For reactions run on a 100 mL scale a 250 mL volumetric flask was utilized; proportionately smaller volumetric flasks were used for smaller scale reactions. The remainder of the description is given for the 100 mL scale reaction. A 20-40 mL portion of deionized water was added to the Teflon beaker, and the mixture stirred with a glass rod. The mixture was filtered using a filter funnel, with the

filtrate being added to the 250 mL volumetric flask. The Teflon beaker and the inner wall of the reaction vessel were each rinsed three times, and the rinsings passed through the filter into the volumetric flask. The filter was then washed three times with deionized water, the washings added to the volumetric flask. Finally, deionized water was added to the flask to the mark. The solution was transferred to a dry, clean plastic bottle for storage.

After analyses of portions of this solution, the number of moles of each component in the 250 mL volume is calculated. In tabulations of results of kinetic runs in earlier monthly reports this number appears as "Dissolved Final Moles". In the final report these values and those determined for the undissolved solids were generally combined.

Any solid remaining in the filter funnel was removed, allowed to dry in air, and weighed. A sample (about 10 mg) of the solid was separated out and weighed, and treated with 3 or 4 drops of 20% HCl and 1 mL of water. After agitation and waiting about 10 min, the solution was transferred to a 100 mL volumetric flask, and deionized water was added to the mark. The solution was then filtered although the amount of undissolved solid was generally very small. After analyses of this solution the number of moles of each component in the total solid was calculated. In earlier monthly reports tabulations of results of kinetic runs included this number as "Undissolved Final Moles". In this report the values were generally combined with those of the "Dissolved Final Moles". X-ray powder diffraction analyses described under Task 2 were done on solids isolated and treated in the same manner as described here.

Reactions in simulated waste. The degradations of simulated waste were performed in two different types of apparatuses (see Figures E.1 and E.2). The trial names indicate which apparatus was used in each case: those names followed by an "A" were done in the apparatus of Figure E.1, while those followed by a "B" were done in the apparatus shown in Figure E.2. In both cases, the Teflon liner and Teflon cap shown in Figure E.3 were placed inside the glass container.

Procedure for "A" runs. A 5 mL portion of SY1-SIM-91B mixture was placed in the Teflon-lined glass vessel provided with a valve and side arm for gas sampling (Figure 1). The vessel was closed and the gas in the headspace removed under vacuum. The vessel was refilled with around 1/3 of the headspace volume with Ar or O_2, depending the case, and placed in an oil bath at 120° C. The temperature was monitored by means of a thermometer placed inside the oil bath, and the variation was generally smaller than ±2° C. After a period of 500, 1000 or 2000 h, the solution was allowed to cool down to room temperature. The valve was opened and Ar was injected through the side arm until atmospheric pressure was reached inside the vessel. The gases inside the vessel were mixed with a 5 mL gas-tight syringe, by pulling and pushing the plunger 4 or 5 times (the total volume of the vessel was around 25 mL). Samples (50 μL) were taken and analyzed by GC. After that the vessel was opened and samples for ^{1}H-NMR and IC analysis were taken.

Procedure for "B" runs. A 5 mL portion of SY1-SIM-91B mixture was placed in the Teflon-lined glass vessel provided with a condenser, as shown in Figure 2. The headspace

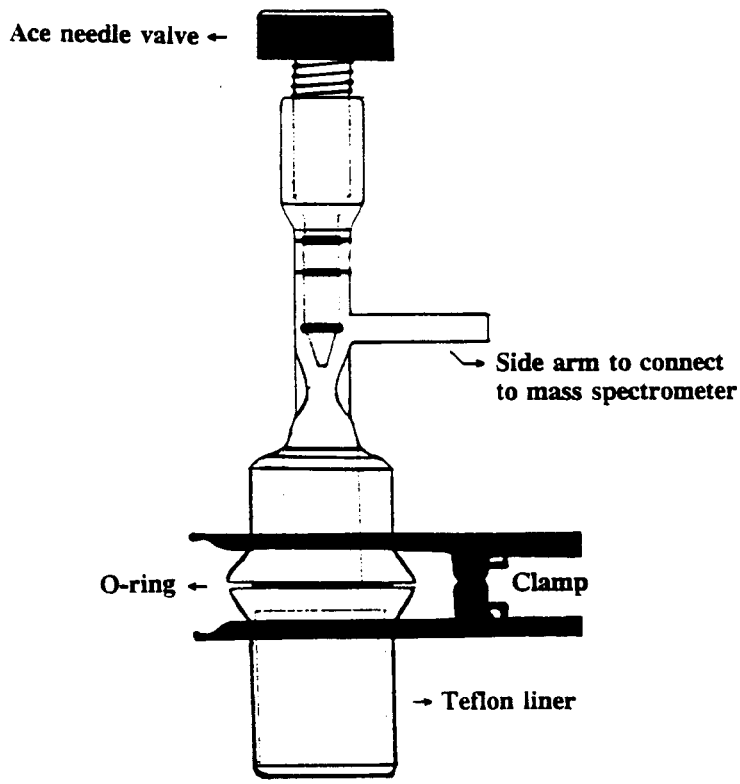

Figure E.1. Apparatus used for Reactions in Simulated Waste ("A" Runs).

over the reaction mixture was purged during a period of 30 minutes with an Ar stream. In the cases where Ar/O_2 atmosphere was used, a known amount of pure oxygen was injected by means of a gas tight syringe. The total headspace before oxygen was added was around 64 mL; therefore, 16 mL of oxygen were added in order to achieve an $Ar:O_2$ ratio equal to 80:20. Also, 1 mL of helium and 1 mL of ethane were added. These gases were used as standards: as they were not produced nor consumed, the areas of all other gases obtained by GC at different reaction times were normalized against the average areas of helium and ethane (helium was used as a standard when the molecular sieves column was used, while ethane was the standard in the case of the Poraplot Q capillary column).

The vessel was immersed in an oil bath stabilized at the desired temperature. The temperature was monitored by means of a thermometer placed inside the oil bath, and the variation was generally smaller than ±2° C. The pressure inside the apparatus was maintained close to atmospheric pressure all throughout the experiment, by adjusting the

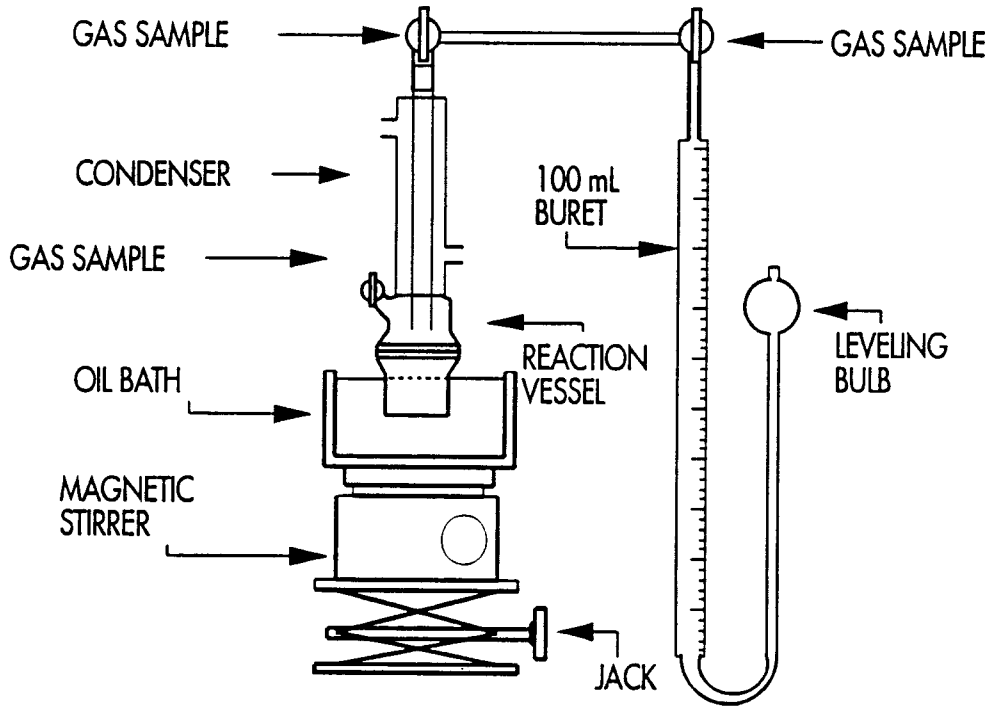

Figure E.2. Apparatus used for Reactions in Simulated Waste ("B" Runs).

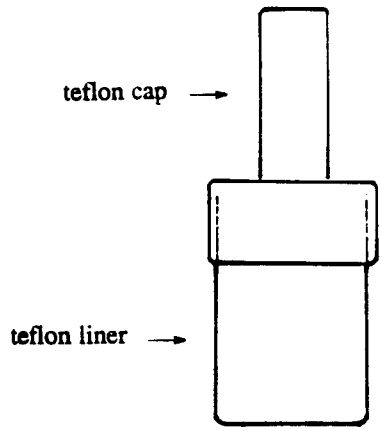

Figure E.3. Teflon Liner with Cap.

height of the mercury bulb shown in Figure E.2. Duplicate samples for GC analysis (50 μL each) were taken from all three stopcocks at different reaction times (see Figure 2), by means of a gas tight syringe. After a variable lapse of 500, 1000 or more hours, depending the case, the reaction mixture was allowed to cool down. The vessel was opened and samples for ^{1}H-NMR and IC analysis were taken.

Time dependent analytical results used to plot Figures 1.1 to 1.7 and 1.9- 1.12, which were obtained by the above procedures, are give in Tables E.3 to E.113. All gases (except oxygen) were calculated as moles of gas produced per 100 moles of organic starting material. Oxygen was calculated as remaining percentage of gas relative to the initial amount present in the headspace, which was defined as 100%.

Table E.3. Data for Figure 1.1 (Trial: HEDTA-10B).

Time (h)	H_2	N_2O	CH_4
45	< 0.05	< 0.1	< 0.1
265	< 0.05	< 0.1	< 0.1
598	<0.05	< 0.1	< 0.1
958	0.06	< 0.1	< 0.1
1555	0.09	< 0.1	< 0.1
2302	0.15	< 0.1	< 0.1
3046	0.23	< 0.1	< 0.1
3862	0.34	< 0.1	< 0.1
4532	0.46	< 0.1	< 0.1
5036	0.58	< 0.1	< 0.1

Table E.4. Data for Figure 1.2 (Trial: HEDTA-11B).

Time (h)	H_2	N_2	N_2O	CH_4
46	< 0.1	< 1	< 0.1	< 0.1
189	0.2	1	< 0.1	< 0.1
430	0.3	2	< 0.1	< 0.1
795	0.6	4	0.1	< 0.1
1294	0.8	6	0.8	< 0.1
2014	1.2	10	5.4	< 0.1
2618	1.5	15	10.8	< 0.1
3309	2.3	22	16.3	< 0.1
4030	2.5	25	19.9	0.3
4942	3.9	30	24.5	0.5

Table E.5. Data for Figure 1.3 (Trial: HEDTA-12B).

Time (h)	H_2	N_2	N_2O	CH_4
20	0.1	< 1	0.4	< 0.1
46	0.1	< 1	1.0	< 0.1
101	0.3	1	2.9	< 0.1
140	0.5	2	4.1	< 0.1
265	0.9	5	8.3	< 0.1
430	1.5	8	13.3	0.4
794	2.4	19	21.9	0.9
1293	4.1	24	29.1	1.9
2017	6.4	31	31.9	3.5
2833	8.2	37	30.5	5.0
3553	10.1	42	29.3	6.1
4273	11.1	50	27.9	6.9
4921	11.3	53	27.1	7.5

Table E.6. Data for Figure 1.4 (Trial: HEDTA-19B).

Time (h)	H_2	N_2	CH_4	N_2O
119	0.9	1	0	5.9
263	1.7	5	0	12
574	2.7	14	0	21.3
792	3.3	18	0.4	25.3
1105	4.4	22	0.6	30.5
1471	5.3	30	1.4	33.2
2038	6.3	33	1.8	36.1

Table E.7. Data for Figure 1.5 (Trial: HEDTA-12B).

Time (h)	N_2+N_2O
20.0	0.5
46.0	1.5
101.0	4.2
140.0	6.1
265.0	13.1
430.0	21.1
794.0	40.8
1293.0	53.0
2017.0	62.5
2833.0	67.9
3553.0	71.5
4273.0	78.3
4921.0	80.5

Table E.8. Data for Figure 1.6 (Trial: HEDTA-17B).

Time (h)	H_2	N_2	N_2O	CH_4	O_2
120	0.3	< 1	< 1	< 1	86
480	1.2	5	< 1	< 1	74
961	2.4	4	< 1	< 1	63
1703	4.7	7	< 1	< 1	47
2279	6.6	10	0.2	< 1	38
2951	8.9	13	0.6	< 1	31
3695	11.7	16	1.1	< 1	23

Table E.9. Data for Figure 1.7.

Trial Name	1/T (1/K)	ln k
HEDTA-10B	0.00299	-9.6
HEDTA-11B	0.00274	-7.5
HEDTA-12B	0.0254	-5.8

Table E.10. Data for Figure 1.9 (Trial: GLY-3B).

Time (h)	H_2	N_2	N_2O
24	0.1	11	0.2
73	0.4	13	0.8
168	0.8	16	1.8
243	1.2	16	2.6
384	1.9	19	4.1
625	3.0	23	6.4
1200	6.8	30	12.0
1922	13.1	35	20.3

Table E.11. Data for Figure 1.10 (Trial: GLY-4B).

Time (h)	H_2	N_2	N_2O	O_2
25	0.1	< 1	0	100
73	0.5	-	0	97
168	1.2	< 1	0	92
243	1.8	< 1	0	87
384	2.9	1	0	82
625	4.5	4	0	77
1200	8.9	9	0	57
1922	14.9	10	0	34

Table E.12 . Data for Figure 1.11.

Time (h)	N_2O	H_2	N_2
25	3.9	2.4	0
73	13.2	8.5	3
146	24.5	17.6	4
217	32.5	25.1	7
361	43.5	37.5	13
580	45.9	44.4	21
915	44.6	54.1	-
1203	35.1	56.7	36

Table E.13. Data for Figure 1.12.

Time (h)	N_2O	H_2	O_2	N_2
25	3.1	2.1	100	0
73	11.1	8.3	92	4
146	22.9	18.2	81	5
217	28	24.9	74	8
361	36.1	37.8	67	12
580	36.6	46.5	68	20
915	33.1	47.4	71	27
1203	22.4	61.5	76	46

Kinetics of the thermal decomposition of glycolate at 120° C. Series 1. Four sets of experiments were done to test the dependence of the reaction rate on the concentration of glycolate, aluminate and nitrite. For each set, fifteen portions of a stock solution were pipetted into individual Teflon-lined reaction vessels of the type shown in Figure 4. The reaction vessels were immersed in an oil bath maintained at 120° C until reaction was terminated by removing vessels from the bath and cooling to room temperature. Five reactions were removed from the bath at after 100 h, 200 h, and 300 h intervals and their contents were analyzed for glycolate, formate, nitrite and oxalate by ion chromatography. Nitrate was assumed to be constant and was used as an internal

standard for these measurements. These analytical results, which were used to determine the rate constants given in Table 1.2, are given in Tables E.14-E.17.

Series 2. In these experiments reactions for each set of conditions were run in triplicate in the vessels shown in Figure 2, which were heated at 120° C in an oil bath. Samples were withdrawn by syringe from each vessel at 25 h, 50 h, 75 h, 100 h, 150 h, and 200 h and analyzed for glycolate and nitrite; nitrate was again used as an internal standard. The raw data from these analyses, which were used to determine the rate constants given in Table 1.3 are contained in Tables E.18-20.

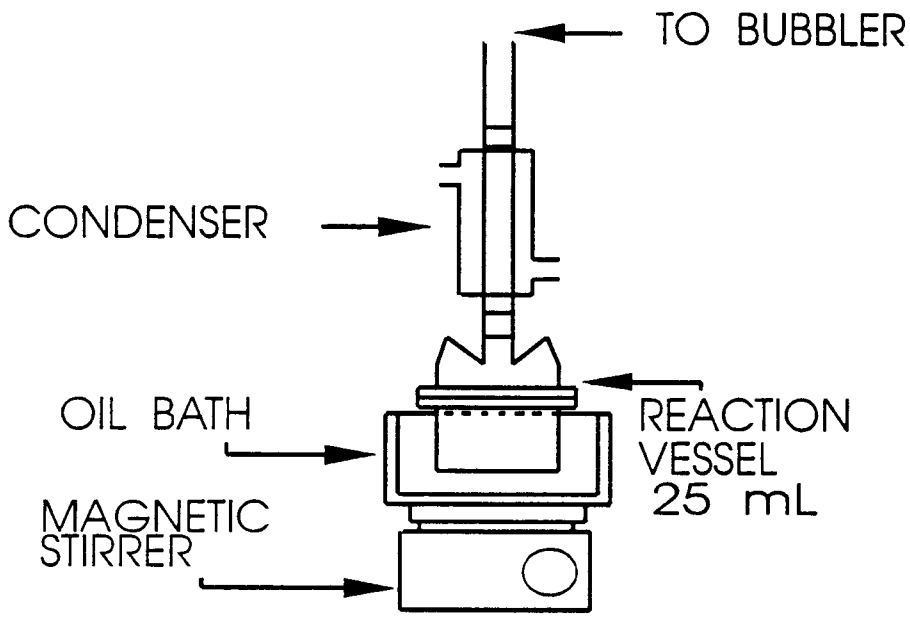

Figure E.4. Reaction Vessel for Series 2 Glycolate Kinetics.

Table E.14. Analysis of Nonvolatile Reaction Components of the Reaction of SY1-SIM-91B Containing 0.21 M Glycolate; 1.54 M Aluminate; 2.24 M Nitrite; 0.42 M Carbonate; 2.59 M Nitrate; 2.00 M Hydroxide in Air.

TIME (hours)	NITRITE (mmoles)	NITRATE (mmoles)	OXALATE (mmoles)	FORMATE (mmoles)	GLYCOLATE (mmoles)
0	56.0±1.68	64.8±1.94	0	0	5.25±.21
100	55.5±1.67	64.9±1.95	.311±.016	.230±.012	4.67±.19
100	56.1±1.68	65.1±1.95	.185±.009	.148±.007	4.91±.20
100	55.9±1.68	65.0±1.95	<0.1	.127±.006	4.92±.20
100	55.7±1.67	64.8±1.94	.269±.013	.173±.009	4.75±.19
100	55.8±1.67	64.6±1.94	.269±.013	.181±.009	4.80±.19
199	55.6±1.67	64.9±1.95	.359±.018	.221±.011	4.51±.18
202	56.1±1.68	65.1±1.95	.326±.016	.251±.013	4.68±.19
202	55.7±1.67	65.0±1.95	.419±.021	.349±.017	4.41±.18
300	55.6±1.67	65.0±1.95	.487±.024	.392±.020	4.18±.17
307	55.7±1.67	65.0±1.95	.441±.022	.421±.021	4.30±.17
307	55.8±1.67	64.9±1.95	.339±.017	.314±.016	4.34±.17
307	55.9±1.68	64.7±1.94	.661±.033	.421±.021	4.12±.16

Table E.15. Analysis of Nonvolatile Reaction Components of the Reaction of SY1-SIM-91B Containing 0.10 M Glycolate; 1.54 M Aluminate; 2.24 M Nitrite; 0.42 M Carbonate; 2.59 M Nitrate; 2.00 M Hydroxide in Air.

TIME (hours)	NITRITE (mmoles)	NITRATE (mmoles)	OXALATE (mmoles)	FORMATE (mmoles)	GLYCOLATE (mmoles)
0	56.0±1.7	64.8±1.9	0	0	2.50±.08
98	56.0±1.7	64.2±1.9	<0.05	<0.05	2.28±.07
98	55.3±1.7	64.8±1.9	<.02	trace	2.41±.07
98	55.9±1.7	64.9±2.0	<.07	0.03±.003	2.40±.07
99	55.5±1.7	64.8±1.9	.095±.009	.050±.005	2.34±.07
99	55.9±1.7	64.9±2.0	.086±.009	<.02	2.40±.07
200	56.4±1.7	65.1±2.0	0.15±.02	0.073±.01	2.20±.06
200	55.1±1.7	64.8±1.9	0.11±.003	0.07±.007	2.30±.07
200	54.9±1.7	65.0±2.0	.221±.007	.076±.008	2.21±.07
200	55.5±1.7	65.0±2.0	.196±.006	.084±.008	2.01±.06
200	55.7±1.7	64.3±1.9	.118±.004	.052±.005	2.36±.07
297	55.0±1.7	64.9±2.0	0.22±.006	0.12±.004	2.12±.06
297	55.7±1.7	64.4±1.9	.301±.009	.136±.004	2.07±.06
300	56.2±1.7	65.7±2.0	0.15±.02	0.092±.01	2.18±.07
331	55.0±1.7	64.8±1.9	.448±.013	.144±.004	1.78±.05
331	55.9±1.7	64.7±1.9	.280±.008	.102±.003	2.05±.06

Table E.16. Analysis of Nonvolatile Reaction Components of the Reaction of SY1-SIM-91B Containing 0.21 M Glycolate; 1.00 M Aluminate; 2.24 M Nitrite; 0.42 M Carbonate; 2.59 M Nitrate; 2.00 M Hydroxide in Air.

TIME (hours)	NITRITE (mmoles)	NITRATE (mmoles)	OXALATE (mmoles)	FORMATE (mmoles)	GLYCOLATE (mmoles)
0	56.0±1.7	64.8±1.9	0	0	5.25±.16
98	55.7±1.7	63.4±1.9	<0.05	<0.05	5.07± .15
98	54.9±1.7	64.0±1.9	0.171±.02	0.145±.01	4.89±0.15
98	55.4±1.7	64.9±2.0	0.19±.02	0.10±.01	4.94±.15
99	55.5±1.7	65.0±2.0	.134±.004	<.05	5.07±.15
99	55.1±1.7	65.3±2.0	.127±.004	.110±.003	5.01±.15
200	55.5±1.7	64.9±2.0	0.275±.01	0.15±.012	4.64±0.14
200	55.5±1.7	64.9±2.0	0.24±.01	0.13±.01	4.78±.14
200	55.8±1.7	64.7±1.9	<.1	.154±.005	4.89±.15
200	55.1±1.7	64.8±1.9	.321±.010	.264±.008	4.75±.14
297	56.0±1.7	65.1±2.0	.401±.012	.165±.005	4.29±.13
297	54.6±1.6	65.0±2.0	.268±.008	.169±.005	4.66±.14
300	54.6±1.6	63.8±1.9	0.41± .01	0.21±.006	4.65±.14
331	54.3±1.6	65.0±2.0	.215±.006	.267±.008	4.69±.14
331	54.3±1.6	64.7±1.9	.522±.016	.301±.009	4.34±.13

Table E.17. Analysis of Nonvolatile Reaction Components of the Reaction of SY1-SIM-91B Containing 0.21 M Glycolate; 1.54 M Aluminate; 1.12 M Nitrite; 0.42 M Carbonate; 2.59 M Nitrate; 2.00 M Hydroxide in Air.

TIME (hours)	NITRITE (mmoles)	NITRATE (mmoles)	OXALATE (mmoles)	FORMATE (mmoles)	GLYCOLATE (mmoles)
0	28.0±.8	64.8±1.9	0	0	5.25±.16
100	28.5±.8	65.3±2.0	trace	trace	4.99±.15
100	27.9±.8	64.4±1.9	trace	trace	5.00±.15
100	27.9±.8	64.8±1.9	.166±.005	.021±.002	5.05±.15
100	27.5±.8	64.7±1.9	.128±.004	.084±.008	5.01±.15
200	27.8±.8	64.4±1.9	.140±.004	.081±.008	4.90±.15
200	28.2±.8	64.6±1.9	.135±.004	.115±.003	4.97±.15
300	28.4±.8	66.0±2.0	.346±.010	.225±.006	4.64±.14
300	28.0±.8	64.8±1.9	.168±.005	.223±.007	4.66±.14

Table E.18. Analysis of Nonvolatile Reaction Components of the Reaction of SY1-SIM-91B Containing 0.21 M Glycolate; 1.54 M Aluminate; 2.24 M Nitrite; 0.42 M Carbonate; 2.59 M Nitrate; 2.00 M Hydroxide under an Argon Atmosphere.

TIME (hours)	GLYCOLATE (mmoles)	NITRITE (mmoles)
0	1.68	17.92
25	1.38	17.84
50	1.11	17.67
75	.84	17.34
100	.65	16.96
150	.28	16.78
200	.21	16.65

Table E.19. Analysis of Nonvolatile Reaction Components of the Reaction of SY1-SIM-91B Containing 0.21 M Glycolate; 1.00 M Aluminate; 2.24 M Nitrite; 0.42 M Carbonate; 2.59 M Nitrate; 2.00 M Hydroxide under an Argon Atmosphere.

TIME (hours)	GLYCOLATE (mmoles)	NITRITE (mmoles)
0	1.68	17.92
25	1.66	17.75
50	1.57	17.76
75	1.40	17.63
100	1.14	17.41
150	.85	17.06
200	.63	16.83

Table E.20. Analysis of Nonvolatile Reaction Components of the Reaction of SY1-SIM-91B Containing 0.21 M Glycolate; 1.54 M Aluminate; 1.12 M Nitrite; 0.42 M Carbonate; 2.59 M Nitrate; 2.00 M Hydroxide under an Argon Atmosphere.

TIME (hours)	GLYCOLATE (mmoles)	NITRITE (mmoles)
0	1.68	8.96
25	1.42	8.82
50	1.32	8.48
75	1.14	8.26
100	1.03	8.04
150	.63	7.56
200	.52	7.66

Determination of total gas evolution from glycolate as a function of temperature. The temporal formation of gases from glycolate decomposition in SY1-SIM-91B simulated waste prepared as described previously with glycolate at 0.21 M, was determined at 60° C, 90° C and 120° C using the apparatus shown in Figure E.5. A Teflon liner in the reaction vessel was used to prevent contact of the caustic simulated waste solution with glass. The leveling bulbs were filled with mercury. The oil bath, reaction vessel, buret and holding bulbs were all insulated. Barometric pressure and temperature measurements were at the same time as each volume measurement. All barometric pressure readings were corrected for temperature, latitude and height above sea level. Each experiment was begun by placing a 100 mL portion of the reaction mixture in the reaction vessel, sealing the system and raising the preheated oil bath to a point just below the flange. Data used in constructing the plots shown in Figure 1.8 are given in Tables E.21-23.

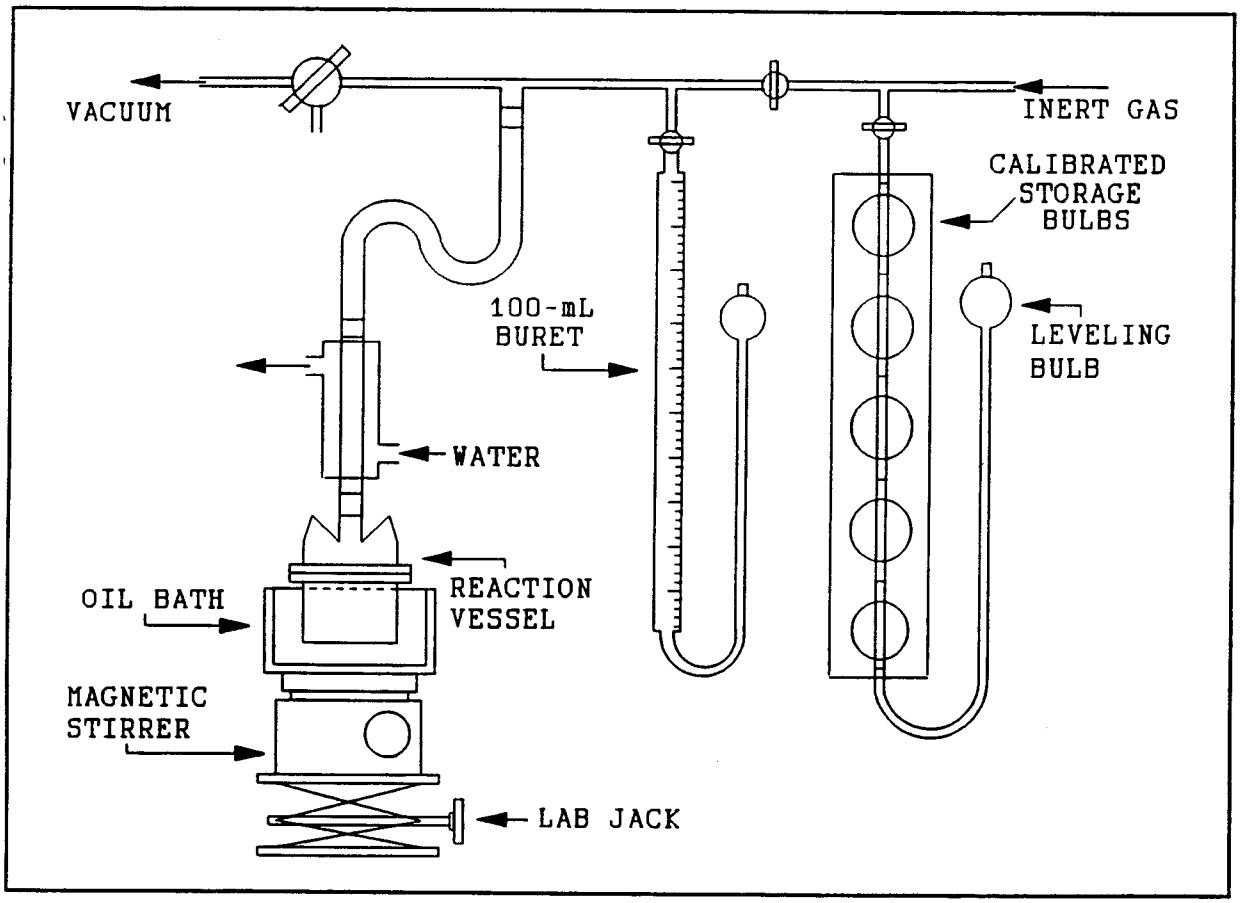

Figure E.5. Long Term Gas Kinetics Apparatus.

Table E.21. Total Gas Measurements for the Reaction of SY1-SIM-91B Containing 0.21 M Glycolate at 60°C in Air.

TIME (hours)	BURET READING (mL)	BAROMETER READING (mm Hg)	OIL BATH TEMPERATURE (°C)	CORRECTED READING (mL)
0	0	730	58	-1.51057402
0.5	12	740	58	13.280967
1	19	740	60	19
2	26	731	63	21.258036
3	30	731	64	24.505935
6	31	731	64	25.482047
18	33	732	66	26.40177
23	30	732	62	26.155224
27	30	732	62	26.155224
43	31	735	64	26.715875
47	28	735	61	25.781437
55	27	736	60	25.772973
68	27	738	60	26.386486
79	32	738	64	28.626706
90	28	740	61	27.317365
95	28	738	60	27.383784
103	26	737	58	26.443807
114	31	736	63	27.7
120	28	734	58	27.517825
124	31	734	62	27.759104
138	31	736	61	29.063473
143	29	735	60	27.452703
146	30	734	60	28.135135
152	32	736	62	29.368358

163	31	736	61	29.063473
168	30	735	60	28.445946
173	26	737	58	26.443807
187	28	738	61	26.702994
190	27	738	60	26.386486
199	28	742	60	28.616216
210	28	737	63	25.048214
219	30	736	64	26.041543
231	30	736	62	27.391045
245	30	735	64	25.734421
256	26	736	62	23.436418
261	26	736	60	24.778378
280	25	739	60	24.695946
285	25	740	60	25
294	0	741	26	23.043478
304	20	741	60	20.297297
310	20	741	58	21.628399
313	24	740	60	24
318	25	740	62	23.656716
328	25	741	62	23.958955
332	25	740	61	24.326347
342	27	740	62	25.644776
352	29	736	64	25.058754
357	29	735	61	26.771707
365	30	734	62	26.773134
378	30	734	63	26.098214
391	30	734	62	26.773134
402	32	735	65	27.023669

405	33	735	65	28.002219
414	26	736	61	24.105389
424	26	738	63	23.376786
429	25	738	61	23.72006
432	27	742	62	26.254627
437	27	737	62	24.73
448	25	737	61	23.416916
453	25	736	60	23.783784
462	30	735	63	26.40625
473	29	734	64	24.447181
477	29	734	62	25.787164
486	33	735	65	28.002219
496	31	734	62	27.759104
501	29	734	62	25.787164
510	29	735	62	26.094776
520	29	735	60	27.452703
525	31	734	63	27.08125
547	35	735	65	29.95932
557	34	734	64	29.347774
573	30	736	63	26.714286
582	30	736	63	26.714286
592	30	736	64	26.041543
597	28	736	62	25.413731
607	29	736	63	25.728571
618	28	736	62	25.413731
622	30	736	63	26.714286
626	28	734	61	25.474251
630	29	736	64	25.058754

640	26	737	60	25.083784
645	26	736	60	24.778378
654	28	738	62	26.026269
664	24	737	60	23.091892
679	25	738	61	23.72006
689	25	740	62	23.656716
701	25	740	62	23.656716
713	24	740	64	21.341246
722	24	740	62	22.662687
727	24	738	62	22.060896
737	24	739	62	22.361791
749	24	736	60	22.789189
760	24	736	60	22.789189
766	24	736	60	22.789189
773	24	737	60	23.091892
784	23	739	60	22.698649
797	22	740	60	22
808	26	742	63	24.5875
813	26	742	62	25.25791
822	24	741	62	22.963582
832	20	741	60	20.297297
846	24	741	62	22.963582
856	24	741	62	22.963582
869	24	740	62	22.662687
880	28	741	62	26.945075
891	26	738	63	23.376786
912	27	739	64	24.002522
917	26	740	63	23.982143

928	26	741	64	23.619288
934	26	740	64	23.317507
941	25	740	62	23.656716
952	25	740	62	23.656716
958	25	739	64	22.028932
966	27	739	63	24.669196
976	28	739	65	24.323669
982	27	737	60	26.07973
989	27	738	62	25.034925
1000	27	739	64	24.002522
1005	27	739	65	23.339793
1013	24	740	62	22.662687
1024	24	741	64	21.640356
1030	22	740	61	21.335329
1039	23	742	63	21.60625
1048	24	742	64	21.939466
1063	24	741	64	21.640356
1076	19	742	60	19.591892
1084	21	745	62	21.164925
1096	22	741	62	20.972836
1102	22	740	62	20.674627
1109	21	740	62	19.680597
1120	24	745	64	22.836795
1125	25	740	64	22.329377
1135	19	740	59	19.659639
1144	19	741	60	19.295946
1149	20	740	60	20
1157	19	741	59	19.956476

1168	19	742	61	18.934431
1174	18	741	59	18.952108
1182	16	742	60	16.583784
1192	16	743	58	18.186103
1200	17	742	59	18.241867
1205	18	742	59	19.24759
1218	18	743	60	18.883784
1228	18	741	59	18.952108
1243	16	740	58	17.305136
1254	20	739	60	19.702703
1264	20	738	59	20.066265
1271	20	736	60	18.810811
1276	19	737	59	18.769127
1288	19	739	60	18.704054
1301	19	738	56	21.063526
1312	18	739	60	17.705405
1319	18	738	59	18.065663
1326	16	738	58	16.717825
1336	18	739	60	17.705405
1342	18	738	58	18.724471
1348	18	738	60	17.410811
1360	19	739	60	18.704054
1372	17	739	58	18.016163
1385	18	740	61	17.347305
1396	18	740	60	18
1410	11	741	56	13.853951
1421	15	739	58	16.006798
1432	13	739	56	15.298328

1446	14	738	57	15.361818
1456	16	738	58	16.717825
1462	17	738	58	17.721148
1469	16	738	58	16.717825
1481	15	739	58	16.006798
1494	15	740	58	16.299094
1504	13	741	58	14.576586
1518	13	742	57	15.517273
1528	9	742	55	12.759451
1534	18	742	62	17.284179
1559	18	742	60	18.589189
1582	18	740	60	18
1600	19	739	62	17.398358
1614	19	739	61	18.049251
1624	18	738	61	16.75988
1641	16	739	60	15.708108
1648	18	739	60	17.705405
1655	18	739	61	17.053593
1661	19	740	62	17.692537
1687	18	739	62	16.405672
1695	17	739	60	16.706757
1709	16	740	60	16
1721	16	739	61	15.062275
1735	17	739	62	15.412985
1746	16	740	61	15.353293
1756	14	739	60	13.710811
1768	14	739	60	13.710811
1774	14	739	60	13.710811

1781	12	740	58	13.280967
1792	12	741	58	13.569184
1805	14	741	60	14.289189
1816	14	740	60	14
1829	14	738	58	14.711178
1839	14	738	60	13.421622
1853	14	739	60	13.710811
1863	14	741	60	14.289189
1869	14	741	60	14.289189
1890	13	742	60	13.575676
1918	13	743	60	13.863514
1925	14	743	62	13.584776
1935	12	745	60	13.432432
1948	9	739	57	10.615
1960	10	744	60	11.135135
1965	10	744	58	12.410876
1969	13	739	60	12.712162
1982	13	741	60	13.287838
1995	13	741	59	13.930271
2006	13	739	60	12.712162
2012	13	737	59	12.775452
2020	19	732	62	15.339104
2030	18	735	60	16.527027
2041	12	736	57	12.770909
2056	12	740	59	12.638554
2068	14	740	60	14
2082	10	742	59	11.201807
2093	10	741	58	11.554381

2104	10	742	59	11.201807
2116	9	741	58	10.546979
2128	10	742	58	11.839879
2141	10	741	58	11.554381
2153	11	741	58	12.561782
2164	13	741	61	12.649251
2175	12	741	58	13.569184
2187	12	742	60	12.572973
2199	10	742	58	11.839879
2213	12	743	61	12.222156
2222	12	743	61	12.222156
2237	10	744	60	11.135135
2247	12	743	62	11.588657
2261	12	744	61	12.507784
2271	12	742	61	11.936527
2282	12	742	60	12.572973
2289	12	742	60	12.572973
2298	12	740	60	12
2308	12	741	60	12.286486
2322	14	740	60	14
2332	13	740	60	13
2345	14	740	62	12.722388
2356	13	740	60	13
2364	13	740	58	14.287009
2390	9	742	58	10.831118
2404	9	744	58	11.399396
2428	8	744	58	10.387915
2441	8	743	58	10.105136

2451	8	745	58	10.670695
2465	5	744	56	8.6139818
2476	5	743	58	7.0747734
2490	6	742	58	7.8048338
2500	6	742	60	6.5567568
2512	11	740	60	11
2524	11	739	60	10.714865
2539	12	738	60	11.427027
2550	12	738	60	11.427027
2560	12	737	60	11.140541
2574	12	737	61	10.508383
2584	12	737	60	11.140541
2598	13	737	61	11.501347
2607	12	736	60	10.854054
2619	13	735	60	11.560811
2632	12	736	60	10.854054
2644	8	738	58	8.6912387
2693	8	741	60	8.2810811
2704	6	741	58	7.5247734
2719	6	740	58	7.244713
2730	6	740	58	7.244713
2740	7	739	59	7.3429217
2762	7	738	58	7.6879154
2787	9	740	61	8.3742515
2815	0	741	57	2.0909091
2835	5	741	60	5.277027
2859	7	739	60	6.7202703
2879	7	736	60	5.8810811

2900	13	731	64	7.9120178
2931	6	739	60	5.7216216
2954	6	743	60	6.8351351
2978	5	741	60	5.277027
3003	6	738	60	5.4432432
3028	5	739	59	5.3396084
3049	11	738	64	7.9320475
3076	13	738	65	9.2819527
3093	6	739	62	4.4934328
3115	2	740	58	3.2205438
3145	8	742	62	7.3170149
3164	8	744	63	7.2571429
3199	8	740	62	6.758209
3223	6	740	60	6
3235	4	742	60	4.5513514
3262	7	743	62	6.5983582
3289	9	745	64	7.9146884
3308	6	749	62	7.260597
3332	2	748	60	4.1837838
3357	4	747	61	5.3131737
3377	7	741	62	6.0422388
3414	8	737	62	5.92
3430	7	738	61	5.8224551
3478	8	737	62	5.92
3502	8	737	60	7.1567568
3526	8	736	62	5.640597
3554	10	738	64	6.9465875
3584	9	736	62	6.6292537

3599	9	734	62	6.0677612
3622	7	738	61	5.8224551
3647	9	736	62	6.6292537
3671	7	734	62	4.0958209
3695	2	740	58	3.2205438
3717	1	746	60	2.6297297
3742	0	748	60	2.1621622
3765	0	748	60	2.1621622
3791	3	743	62	2.6061194
3813	13	734	64	8.7652819
3838	3	741	62	2.0607463
3868	0	745	60	1.3513514
3886	0	747	60	1.8918919
3910	0	745	60	1.3513514
3933	1	744	61	1.4814371
3957	4	743	62	3.6041791
3979	4	740	62	2.7820896
4004	10	735	64	6.1053412
4029	9	736	64	5.4029674
4053	8	734	63	4.4714286
4077	7	741	64	4.8194362
4103	2	737	60	1.1810811
4133	0	742	58	1.7522659
4150	0	741	60	0.2702703
4173	2	739	60	1.727027
4197	6	737	63	3.3330357
4221	3	745	62	3.1514925
4245	3	742	63	1.73125

4266	2	743	62	1.6080597
4297	0	744	62	-0.119403
4318	2	740	62	0.7940299
4341	0	743	62	-0.38806
4365	1	733	59	-0.301657
4388	0	736	60	-1.081081
4410	0	739	61	-0.868263
4437	-2	744	60	-0.92973
4461	0	741	62	-0.925373
4485	5	738	64	2.0192878
4508	-1	744	62	-1.118806
4532	-1	743	62	-1.386119
4560	4	741	64	1.8510386
4584	3	746	65	1.6186391
4725	3	746	66	1.0238938
4846	2	742	63	0.7375
4871	2	744	63	1.2785714
4894	0	742	62	-0.656716
4918	-1	740	61	-1.595808
4941	1	733	61	-1.497455
4964	-3	738	60	-3.532432
5013	-6	745	58	-3.509063
5036	-4	742	60	-3.47027
5061	-2	741	60	-1.732432
5076	-4	742	60	-3.47027
5099	-4	741	60	-3.735135
5021	-1	741	61	-1.327695
5046	-3	740	61	-3.58982

5094	-5	748	61	-3.482036
5118	-6	750	60	-3.378378
5143	-5	743	60	-4.209459
5168	-3	741	61	-3.324401
5222	-2	743	62	-2.384179
5239	-6	745	60	-4.689189
5263	-5	742	60	-4.472973
5287	-4	741	61	-4.322754
5311	-2	744	62	-2.118209
5335	-1	744	61	-0.523353
5360	-8	749	61	-6.246707
5383	-6	743	62	-6.376418
5432	-6	744	60	-4.951351
5479	-7	745	60	-5.695946
5503	-6	745	60	-4.689189
5527	-5	739	62	-6.426119
5551	-4	737	62	-5.96
5575	-4	737	61	-5.379042
5599	-6	744	60	-4.951351
5624	-4	743	62	-4.380299
5647	-4	738	62	-5.696716
5671	-2	733	62	-5.043881
5694	-1	735	62	-3.524627
5720	-4	739	61	-4.850898
5743	-7	743	60	-6.217568
5767	-6	737	61	-7.36497
5791	-7	744	60	-5.956757
5815	-8	743	59	-6.640964

5839	-10	744	59	-8.39759
5863	-8	740	60	-8
5912	-2	734	61	-4.193413
5935	-8	740	59	-7.421687
5960	-7	745	60	-5.695946
5983	-8	744	58	-5.79577
6007	-7	740	58	-5.833837
6054	-7	744	60	-5.956757
6079	-7	742	60	-6.478378
6103	-5	738	62	-6.68806
6127	-2	734	62	-4.77791
6151	-2	731	62	-5.575821
6175	-5	736	61	-6.634731
6199	-7	739	61	-7.837874
6247	-4	738	61	-5.11497
6271	-7	741	62	-7.892985
6295	-2	737	64	-5.143323
6319	-7	742	62	-7.633731
6343	-7	740	61	-7.577844
6365	5	715	63	-3.694196

Table E.22. Total Gas Measurements for the Reaction of SY1-SIM-91B Containing 0.21 M Glycolate at 90°C in Air.

TIME (hours)	BURET READING (mL)	BAROMETER READING (mm Hg)	OIL BATH TEMPERATURE (°C)	CORRECTED READING (mL)
0	0	730	80	5.7729117
0.5	9	740	80	20.586402
1	45	740	80	57.606232
2	104	731	99	85.825022
3	110	731	94	98.306319
6	117	731	99	98.356223
18	110	732	94	98.987996
23	87	732	88	84.404028
27	82	732	87	80.762432
43	103	735	96	91.477752
47	86	735	90	82.716216
55	123	736	103	102.18827
68	107	738	98	94.726663
79	87	738	88	88.374553
90	105	740	98	94.110512
95	86	738	89	86.025399
103	91	737	91	87.666027
114	86	736	88	86.05094
120	103	734	92	96.187805
124	103	734	92	96.187805
138	93	736	91	88.988061
143	82	735	86	84.07743
146	105	734	96	92.760602
152	93	736	90	90.335135

163	94	736	91	89.979923
168	86	735	86	88.09467
173	108	737	94	100.4262
187	84	738	86	88.070075
190	78	738	86	82.019619
199	96	742	94	91.919935
210	96	737	90	93.989189
219	97	736	92	91.604946
231	96	736	92	90.615802
245	94	735	92	87.973602
256	94	736	90	91.32973
261	76	736	86	78.70198
280	94	739	92	90.629241
285	88	740	90	88
304	88	741	93	84.654054
310	88	741	92	85.981873
313	88	740	92	85.326027
318	90	740	93	85.983607
328	79	741	90	79.647297
332	85	740	89	86.339779
342	92	740	92	89.30411
352	96	736	94	87.942146
357	96	735	92	89.949204
365	104	734	94	94.464865
378	96	734	90	91.978378
391	96	734	91	90.626789
402	96	735	91	91.295218
405	93	735	91	88.323675

414	105	736	96	94.103274
424	78	738	86	82.019619
429	76	738	85	81.343591
432	97	742	92	95.612595
437	95	737	92	90.29191
448	95	737	90	92.993243
453	98	736	90	95.308108
462	108	735	96	96.363217
473	96	734	89	93.337435
477	96	734	90	91.978378
486	98	735	91	93.276247
496	98	734	90	93.962162
501	103	734	90	98.921622
510	102	735	91	97.238306
520	102	735	90	98.608108
525	102	734	90	97.92973
547	120	735	93	112.25299
557	110	734	92	103.093
573	99	736	89	97.673705
582	115	736	96	103.8875
592	102	736	90	99.286486
597	103	736	90	100.28108
607	96	736	87	97.42991
618	101	736	90	98.291892
622	100	736	89	98.671047
626	100	734	87	100.07883
630	111	736	92	105.45297
640	101	737	90	98.968919

645	109	736	93	102.09907
654	102	738	89	102.02624
664	107	737	92	102.17777
679	107	738	92	102.85916
689	106	740	90	106
701	106	739	92	102.54736
713	100	740	90	100
722	100	740	90	100
727	100	738	90	98.648649
737	100	739	91	97.952554
749	100	736	89	98.671047
760	105	736	90	102.27027
766	105	736	90	102.27027
773	105	737	90	102.9527
784	99	739	89	99.702266
797	98	740	88	100.759
808	98	742	88	102.11241
813	107	742	92	105.58468
822	98	741	88	101.4357
832	98	741	89	100.05052
846	108	741	92	105.89916
856	99	741	90	99.674324
869	112	740	92	109.19452
880	110	741	91	109.2862
891	115	738	93	109.39821
912	100	739	87	103.48536
917	107	740	90	107
928	107	741	92	104.9033

934	107	740	90	107
941	113	740	90	113
952	107	740	90	107
958	115	739	91	112.89113
966	113	739	90	112.30676
976	111	739	88	113.13666
982	112	737	92	107.13022
989	114	738	93	108.40908
1000	106	739	90	105.31622
1005	109	739	90	108.31216
1013	114	740	90	114
1024	108	741	92	105.89916
1030	109	740	89	110.40608
1039	108	742	89	110.78008
1048	113	742	92	111.56793
1063	111	741	91	110.2848
1076	108	742	89	110.78008
1084	114	745	94	111.83294
1096	107	741	89	109.08758
1102	107	740	89	108.40055
1109	108	740	90	108
1120	110	745	88	116.29052
1125	112	740	90	112
1135	112	740	91	110.59341
1144	112	741	90	112.69189
1149	112	740	90	112
1157	119	741	94	114.03703
1168	114	742	92	112.56514

1174	109	741	87	113.93524
1182	104	742	88	108.16195
1192	106	743	87	112.28511
1200	107	742	88	111.18673
1205	110	742	90	111.37838
1218	109	743	87	115.32238
1228	117	741	92	114.86194
1243	123	740	92	120.13425
1254	126	739	94	119.56397
1264	115	738	90	113.60811
1271	122	736	90	119.17838
1276	122	737	92	117.03511
1288	118	739	92	114.46548
1301	121	738	92	116.74481
1312	121	739	92	117.44501
1319	118	738	89	118.02707
1326	128	738	93	122.2568
1336	120	739	90	119.2973
1342	120	738	91	117.16988
1348	120	738	90	118.59459
1360	119	739	91	116.87475
1372	128	739	94	121.53949
1385	114	740	88	116.84765
1396	118	740	90	118
1410	114	741	88	117.54609
1421	114	739	88	116.1492
1432	115	739	87	118.58992
1446	117	738	89	117.02702

1456	120	738	90	118.59459
1462	120	738	90	118.59459
1469	116	738	88	117.4564
1481	120	739	90	119.2973
1494	125	740	92	122.12329
1504	117	741	90	117.69865
1518	119	742	90	120.4027
1528	118	742	88	122.27756
1534	123	742	92	121.54001
1559	119	742	90	120.4027
1582	120	740	89	121.43646
1600	120	739	90	119.2973
1614	134	739	92	130.35631
1624	128	738	92	123.68764
1641	132	739	93	126.92632
1648	125	739	92	121.41772
1655	126	739	90	125.28919
1661	128	740	93	123.67213
1687	124	739	90	123.29189
1695	124	739	90	123.29189
1709	126	740	91	124.55495
1721	118	739	89	118.72901
1735	115	739	88	117.15338
1746	115	740	88	117.85319
1756	116	739	89	116.72619
1768	116	739	86	121.04424
1774	125	739	89	125.73886
1781	125	740	90	125

1792	122	741	89	124.14934
1805	123	741	90	123.70676
1816	122	740	90	122
1827	128	738	91	125.12634
1839	126	738	90	124.57838
1853	126	739	89	126.74026
1863	126	741	92	123.82472
1869	126	741	90	126.71081
1890	122	742	86	129.24269
1918	122	743	88	127.01991
1925	122	743	90	124.11622
1935	118	745	86	127.31058
1948	133	739	93	127.91678
1960	134	744	91	135.41152
1965	131	744	92	130.94495
1969	128	739	92	124.39725
1982	137	741	92	134.77923
1995	135	741	91	134.25121
2006	135	739	90	134.27703
2012	135	737	90	132.83108
2020	140	732	93	129.78378
2030	133	735	89	130.86108
2041	134	736	90	131.11351
2056	126	740	88	128.91413
2068	130	740	90	130
2082	122	742	88	126.31059
2093	127	741	87	132.10976
2104	123	742	86	130.25656

2116	130	741	92	127.80818
2128	130	742	88	134.37666
2141	139	741	91	138.24561
2153	144	741	92	141.75029
2164	132	741	88	135.67027
2175	145	741	94	139.7884
2187	132	742	90	133.43784
2199	140	742	93	137.02127
2213	135	743	90	137.16892
2222	140	743	92	139.21829
2237	138	744	92	137.94423
2247	138	743	92	137.22118
2261	138	744	91	139.4221
2271	138	742	93	135.0323
2282	134	742	90	135.44324
2289	144	742	92	142.48139
2298	141	740	92	138.03562
2308	138	741	90	138.72703
2322	142	740	91	140.51099
2332	140	740	91	138.51648
2345	139	740	90	139
2356	141	740	92	138.03562
2364	142	740	92	139.03014
2390	139	742	90	140.45676
2404	131	744	87	138.31919
2428	127	744	88	132.7841
2441	132	743	88	137.11607
2451	130	745	89	135.05506

2465	132	744	90	134.87568
2476	137	743	88	142.16416
2490	139	742	90	140.45676
2500	136	742	90	137.44865
2512	141	740	90	141
2524	138	739	90	137.27297
2539	144	738	90	142.52973
2550	146	738	90	144.52432
256	141	737	90	138.80676
2574	144	737	90	141.79459
2584	143	737	90	140.79865
2598	145	737	92	139.81635
2607	145	736	91	140.56489
2619	147	735	92	140.32705
2632	145	736	89	143.55144
2644	144	738	90	142.52973
2693	136	741	88	139.69787
2704	132	741	86	138.65451
2719	137	740	90	137
2730	137	740	89	138.48343
2740	139	739	90	138.27162
2762	145	738	92	140.5488
2787	144	740	92	141.01918
2815	131	741	86	137.642
2835	141	741	90	141.73108
2859	142	739	90	141.26757
2879	142	736	89	140.55941
2900	142	731	89	136.88714

2931	135	739	88	137.23701
2954	145	743	92	144.21105
2978	140	741	90	140.72973
3003	144	738	91	141.03926
3028	153	739	90	152.2527
3049	162	738	93	155.88697
3076	165	738	94	157.33158
3093	147	739	86	152.34728
3115	150	740	88	153.04709
3145	149	742	87	155.07115
3164	158	744	92	157.94215
3199	155	740	90	155
3223	152	740	88	155.05817
3235	152	742	90	153.49189
3262	157	743	92	156.19368
3289	161	745	92	161.6958
3308	159	749	92	162.69838
3332	156	748	90	162.01081
3357	158	747	91	161.73091
3377	157	741	90	157.7527
3414	159	737	90	156.73378
3430	162	738	90	160.48108
3478	163	737	90	160.71757
3502	163	737	90	160.71757
3526	163	736	90	159.95676
3554	161	738	90	159.48378
3584	167	736	90	163.93514
3599	172	734	91	165.80347

3622	166	738	90	164.47027
3647	169	736	92	162.82337
3671	173	734	92	165.23979
3695	166	740	92	162.89863
3717	151	746	88	158.54495
3742	163	748	90	169.08649
3765	167	748	91	171.5552
3791	167	743	92	166.1792
3813	181	734	92	173.13144
3838	175	741	92	172.62208
3868	162	745	88	168.93191
3886	163	747	90	168.32568
3910	164	745	90	167.81081
3933	174	744	92	173.9405
3957	173	743	91	173.74242
3979	168	740	90	168
4004	185	735	94	174.71436
4029	179	736	92	172.71482
4053	182	734	92	174.1179
4077	179	741	92	176.60554
4103	173	737	90	170.67703
4133	164	742	87	170.23703
4150	164	741	89	166.32228
4173	178	739	90	177.21892
4197	184	737	91	180.03454
4221	178	745	91	180.30676
4245	180	742	91	179.96985
4266	167	743	86	175.64181

4297	165	744	87	172.78784
4318	183	740	93	178.22131
4341	178	743	90	180.34324
4365	189	733	93	178.64618
4388	192	736	94	182.38256
4410	175	739	88	177.40426
4437	179	744	90	182.12973
4461	181	741	90	181.78514
4485	187	738	92	182.20577
4508	185	744	90	188.16216
4532	182	743	90	184.35946
4560	193	741	92	190.54765
4584	191	746	92	192.52728
4725	188	746	90	192.76757
4846	200	742	93	196.6903
4871	199	744	94	195.67394
4894	199	742	92	197.32786
4918	200	740	92	196.71233
4941	201	733	92	192.05287
4964	201	738	92	196.09143
5013	190	745	90	193.98649
5036	193	742	90	194.6027
5061	198	741	92	195.52697
5076	198	742	92	196.33065
5099	198	741	92	195.52697
5021	197	741	91	196.16443
5046	203	740	92	199.69589
5094	200	748	93	201.51529

5118	197	750	92	201.75213
5143	198	743	90	200.42432
5168	200	741	92	197.5187
5222	204	743	92	203.12564
5239	200	745	92	200.74417
5263	200	742	91	199.96881
5287	200	741	92	197.5187
5311	205	744	92	204.93728
5335	202	744	91	203.59127
5360	200	749	92	203.96964
5383	200	743	90	202.43243
5432	203	744	92	202.93749
5479	203	745	92	203.74789
5503	203	745	92	203.74789
5527	202	739	89	202.84722
5551	207	737	92	201.22665
5575	208	737	92	202.21713
5599	205	744	91	206.5992
5624	204	743	90	206.44865
5647	208	738	90	206.35676
5671	212	733	91	204.5454
5694	212	735	92	204.5341
5720	208	739	90	207.17838
5743	202	743	90	204.44054
5767	206	737	90	203.54324
5791	205	744	90	208.27027
5815	201	743	90	203.43649
5839	193	744	87	201.17378

5863	200	740	89	201.65746
5912	211	734	91	204.38098
5935	206	740	90	206
5960	203	745	90	207.07432
5983	202	744	88	208.60726
6007	206	740	90	206
6054	196	744	88	202.54141
6079	207	742	90	208.64054
6103	213	738	92	207.99342
6127	217	734	92	208.64389
6151	219	731	92	208.12109
6175	219	736	94	208.94393
6199	213	739	91	210.48983
6247	220	738	94	211.58509
6271	220	741	94	214.07121
6295	223	737	93	215.38847
6319	219	742	92	217.27203
6343	219	740	92	215.60822
6365	238	715	92	213.06816

Table E.23. Total Gas Measurements for the Reaction of SY1-SIM-91B Containing 0.21 M Glycolate at 120°C in Air.

TIME hours	mL GAS EVOLVED	OIL BATH °C	HOOD °C	BAROM PRESS mmHg
0	0	119	27	742
0.5	84	114	28	742
1	147	120	28	742
7	185	127	28	742
11.5	189	128	29	742
21.5	197	130	26	744
26	210	133	27	744
29.5	213	129	28	742
36.5	215	129	28	742
47.5	218	129	28	742
50	214	128	28	741
53	220	130	28	741
55.5	224	129	28	739
61.5	229	129	28	739
71.5	234	130	27	739
77.0	240	130	28	739
85.5	246	130	28	739
96	252	130	28	738
102	254	127	27	738
110	256	125	26	738
120	261	130	28	740
126	261	129	26	739
134	260	127	26	739
144	261	126	24	739
146.5	252	125	26	740

151.0	249	126	26	740
152.5	255	122	26	739
157.5	256	125	27	739
168.0	257	126	26	740
170.5	253	122	26	740
176	258	122	26	740
181.5	262	122	26	740
192.0	259	122	26	740
196	259	120	26	740
199.5	256	119	26	739
205.5	257	118	26	739
216.0	264	118	25	742
217.5	272	118	25	742
226.5	272	120	26	741
229.5	274	120	26	740
240.0	279	122	25	743
242.5	284	122	25	742
247.5	280	118	26	740
255.5	280	118	26	740
263.5	282	118	26	740
267.5	288	118	26	739
271.5	288	120	25	738
275.5	290	124	25	738
286.5	295	124	25	738
291.5	300	124	25	737
299.5	300	129	26	735
314.0	295	120	26	736
318.5	302	122	26	740
325.5	300	120	26	742
337.0	301	119	26	738

341	303	119	26	738
349.5	304	123	26	738
360.5	303	124	24	740
364	307	116	24	740
368.5	309	115	25	739
373.5	308	126	25	740
378.0	309	120	26	740
385.5	310	121	26	740
395.5	312	120	25	741
398.5	310	122	26	742
410.5	311	122	26	742
419.5	314	122	26	742
424.5	318	123	26	742
431.5	321	122	26	742
443.5	324	123	26	743
448.5	326	124	26	743
457.5	331	125	26	743
466	339	127	26	743
480.5	344	126	26	743
492	350	126	26	744
495	356	120	27	744
505	359	120	26	744
516	365	119	26	744
522	375	128	27	743
527.5	382	127	27	743
539.5	390	126	27	743
545.5	394	126	28	740
550.5	399	127	27	740
562.5	407	134	27	740
568	411	124	27	740

577	415	125	27	740
587.5	419	126	26	739
599.5	422	127	26	740
608.5	419	127	26	740
617.5	420	128	27	740
624.5	428	129	27	742
637.5	428	132	26	744
648.5	436	127	25	744
659.5	444	122	24	745
664.5	449	125	24	744
671.5	451	122	24	744
684.5	458	122	24	744
695.5	466	122	26	740
709.5	480	125	25	741
718.5	479	123	26	741
726.5	475	122	26	741
732.5	478	123	26	741
743.5	480	123	26	741
748.5	484	125	26	742
753.5	486	124	26	742
768.5	492	125	25	742
773.5	493	126	25	742
777.5	495	126	24	742
792.5	498	127	24	744
798.5	499	127	24	743
805.5	502	126	24	742
815.5	504	126	24	742
821.5	508	124	24	742
827.5	510	125	24	742
838.5	512	127	25	742

844.5	512	129	25	741
852.5	520	131	25	740
865.5	527	130	25	740
870.5	531	130	25	740
876.5	536	131	25	740
885.5	540	130	25	740
891.5	542	129	25	740
898.5	544	134	25	740
908.5	548	128	25	739
917.5	545	136	26	738
923.5	549	132	26	740
936.5	547	129	26	741
947.5	542	128	26	741
957.5	539	126	27	742
981.0	538	124	27	741
990.5	543	126	28	738
1004.5	544	128	27	740
1010.5	550	129	27	738
1018.5	560	131	27	739
1029.5	571	133	27	740
1034.5	563	129	26	740
1042.0	556	125	25	741
1053	547	118	25	742
1060.5	553	130	25	741

TASK 2: PRODUCT IDENTIFICATION

Materials

All organic reagents (except those mentioned below) were purchased from Aldrich Chemical Company and used without further purification. Inorganic reagents were ACS reagent grade or better. N-(2-hydroxyethyl)-N-ethylglycine (HEG),[1] N-(2-hydroxy-1-phenylethyl)-piperidine,[2] and N-(2-hydroxy-2-phenylethyl)-piperidine[3] were prepared according to literature procedures.

N-$^{13}C_2$-Hydroxyethylethylenediamine triacetic acid (HEDTA-A). The synthesis of this compound begins with C-13 labeled ethylene oxide. In the first step the ethylene oxide is converted to N-hydroxyethylenediamine, which is then converted to the triacetic acid.

N-$^{13}C_2$-Hydroxyethylethylenediamine. Ethylenediamine (3 g, 0.05 mol) was dissolved in water (20 mL) in a 100 mL, 3-necked round-bottomed flask, which was equipped with a dry ice-acetone condenser that was cooled to 0° C with salt-ice mixture. The break-seal flask containing the $^{13}C_2$-ethylene oxide (0.5 g, 0.01 mol) was connected to a T-connector and cooled in a dry ice-acetone bath. One opening of the T-connector was connected to a Pasteur pipette with Tygon tubing and the other end was stoppered with a rubber septum. The rubber septum was pierced with a long needle connected to a nitrogen line. The seal of the flask was broken with the nitrogen inlet needle and the tip of the pipette was positioned below the surface of the ethylenediamine solution. The flask of ethylene oxide was brought to room temperature and bubbling with nitrogen was continued for 3 h to carry ethylene oxide into the reaction vessel, which was kept at 0° C for a total of 5 h and then left at room temperature for overnight. Excess ethylenediamine and water were removed with a rotary evaporator and the residue was distilled using Kugelrohr apparatus at 130° C/0.3 torr. The distillate (0.8 g, 73%) showed only resonances expected for the product and was used without further purification for the next step. ^{1}H NMR spectrum (D_2O): δ 2.57 (poorly resolved triplets, 2H, CH_2NH_2), 2.67 (poorly resolved triplets, 2H, CH_2NH), 2.87 and 2.40 (2 poorly resolved triplets, 1H each, $J_{H,C}$=141 Hz, $^{13}CH_2NH$) and 3.82 and 3.34 (2 poorly resolved triplets, 1H each, $J_{H,C}$=144 Hz, $^{13}CH_2OH$). ^{13}C NMR spectrum (D_2O): (3-tristrimethylsilyl-propionate was used as an internal standard) δ 52.78 (d, $J_{C,C}$=39.1 Hz, $^{13}CH_2NH$) and 63.03 (d, $J_{C,C}$=39.2 Hz, $^{13}CH_2OH$).

Conversion of N-$^{13}C_2$-Hydroxyethylethylenediamine into N-$^{13}C_2$-Hydroxyethylethylenediamine triacetic acid. A solution of N-$^{13}C_2$-hydroxyethylethylenediamine (54 mg, 0.5 mmol), bromoacetic acid (231 mg, 0.55 mmol) and NaOH (120 mg, 3 mmol) in 10 mL water was allowed to stand at room temperature overnight. Hydrobromic acid solution (1 mL of 49% HBr solution in 2 mL of water) was added to the reaction mixture until the pH was 2.5 after which the solvent was removed under vacuum. The residual solid was recrystallized from methanol to give 72 mg (40%) of HEDTA, which was contaminated with 14% Br^- (determined by ion chromatography). The product showed only resonances expected for HEDTA and was used for thermal decomposition experiments in simulated waste media. ^{1}H NMR spectrum (D_2O) at pH=2.5: δ 3.15 (t, 1H, $J_{H,C}$=144 Hz, ^{13}CHN), 3.63 (broad singlet, 6H, 2 CH_2N, ^{13}CHN, ^{13}CHOH), 3.81 (s, 4H, 2

CH_2CO_2H), 3.87 (broad s, 2H, CH_2CO_2H) and 4.14 (t, 1H, $J_{H,C}$=147 Hz, $^{13}CHOH$). ^{13}C NMR spectrum (D_2O): (3-tristrimethylsilylpropionate was used as an internal standard) δ 59.13 (d, $J_{C,C}$=40.3 Hz, $^{13}CH_2N$) and 61.68 (d,$J_{C,C}$=40.4 Hz, $^{13}CH_2OH$).

Preparation of N-Hydroxyethylethylenediamine-$^{13}C_2$-triacetic acid (N-$^{13}CH_2{}^{13}CO_2H$) (HEDTA-B). This compound was prepared in 46% yield from unlabeled hydroxyethylethylenediamine and $Br^{13}CH_2{}^{13}CO_2H$ by the same procedure described above. The product obtained after recrystallization from methanol contained 15% bromide (by IC analysis) but its NMR spectra contained only resonances expected for HEDTA. ^1H NMR spectrum (D_2O) at pH=2.5: δ 3.48 (poorly resolved triplet because of 1,3 and 1,4 coupling, 2H, CH_2N), 3.55 and 3.88 (poorly resolved triplets, 2H each, $^{13}CH_2{}^{13}CO_2H$) 3.62 (broad singlet, 5H, 2 CH_2N and $^{13}CH^{13}CO_2H$), 3.88 (t, 2H, CH_2OH) and 4.11 (d, 1H, $^{13}CH^{13}CO_2H$). ^{13}C NMR spectrum (D_2O): (C_6D_6 was used as an external standard) δ 56.28 (d, $J_{C,C}$=52.0 Hz, $^{13}CH_2{}^{13}CO_2H$), 57.94 (d, $J_{C,C}$=52.8 Hz, 2 $^{13}CH_2{}^{13}CO_2H$), 171.18 (d, $J_{C,C}$=52.4 Hz, 2 $^{13}CO_2H$), and 171.34 (d, $J_{C,C}$=52.7 Hz, $^{13}CO_2H$).

N-Ethylglycine (EG). A 0.40 mL portion of 70% solution of ethylamine in water (5 mmoles) in a round-bottomed flask was treated with a solution of 70 mg (0.5 mmol) of bromoacetic acid and 40 mg (1 mmol) of NaOH in 3 mL of water with stirring. After heating for 30 minutes at 70° C, the water was removed under reduced pressure on a rotary evaporator and the resulting solid was dissolved in 1.6 mL of D_2O and 0.4 mL of SY1-SIM-91B solution for NMR analysis.

N-Ethyliminodiacetic acid (EIDA). A 0.040 mL portion of 70% solution of ethylamine in water (0.5 mmoles) in a round-bottomed flask was treated with a solution of 139 mg (1 mmol) portion of bromoacetic acid and 60 mg (1.5 mmoles) of NaOH in 3 mL of water with stirring. After heating for 30 minutes at 70° C, the water was removed was removed under reduced pressure on a rotary evaporator and the resulting solid was dissolved in 1.6 mL of D_2O and 0.4 mL of SY1-SIM-91B solution for NMR analysis

Product Identification and Quantitation

Gas and ion chromatographic instrumentation and procedures and NMR instrumentation were the same as those described for Task 1. In the case of model systems, the ^1H NMR database given in Table E.24 was established using authentic compounds and used to identify the products. In all cases the products were quantified by means of a calibrated cell with cyclohexane (dissolved in $CDCl_3$) as standard. When ion chromatography was used, the products were quantified by comparison of responses with those of authentic samples.

Methods

Thermal Decomposition of Labeled HEDTA. The thermal decomposition of HEDTA-A and HEDTA-B in simulated waste was conducted in the vessel shown in Figure 6. One mL of solution that was 0.21 M in labeled HEDTA was placed in the Teflon container, the cover placed on top, and then sealed by screwing down the brass cap. The container was placed in an oil bath whose temperature was maintained at 120±3° C. At

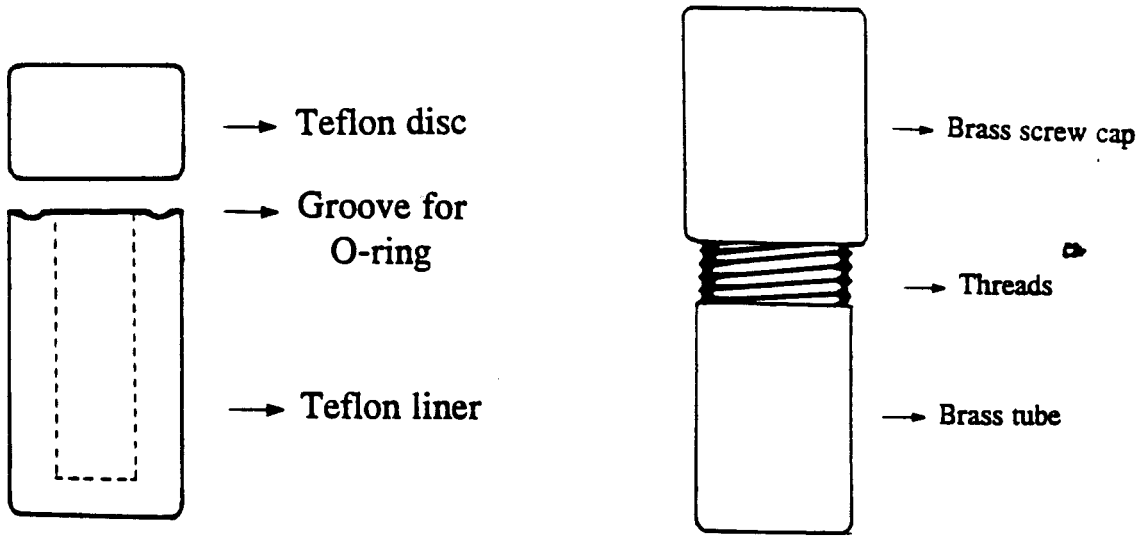

Figure E.6. Reaction Vessel Used for the Thermal Decomposition of ^{13}C-Labeled Compounds.

regular intervals the container was removed from the bath, cooled to room temperature, and opened to allow transfer of the solution to an NMR tube for measurement of the ^{13}C NMR spectrum. Intensities and chemical shifts of the resonances were determined versus an external C_6D_6 standard. After acquisition of the NMR spectrum the solution was returned to the vessel for continued heating. The reaction of HEDTA-A was conducted for 1452 h and that of HEDTA-B for 1808 h. Identification of reaction mixture components was made using a database (Table 2.1) generated with authentic samples of probable products.

Table E.24. ^{1}H-NMR Database for Model Systems.

Compound	^{1}H-NMR Chemical Shifts, ppm[1]				
	$-CH_3$	$-CH_2-$	$-CH_2-$	$-CH_2-COO^-$	$-CH_2-O-$
GLYCINE				3.06	
EG	0.93	2.42		3.02	
EIDA	0.84	2.39		3.00	
HEG	0.91	2.52	2.58	3.03	3.53
IDA				3.06	
MIDA		2.12		2.93	
DMG		2.08		2.85	

[1]Determined respect to the signal due to cyclohexane (external standard). All the compounds were dissolved in a SY1-SIM-91B/D_2O mixture (1:4).

Nitrosation and cleavage reactions employing tetraethylammonium tetrachloroaluminate and sodium nitrite. For each reaction 7 mmol $[Et_4N][AlCl_4]$ and 10 mmol $NaNO_2$ and 75 mL solvent were combined in a 250 mL round bottom flask which was fitted with a condenser. Acetonitrile was used for most reactions because of its relatively low volatility; however, DMSO was used for some reactions because of the greater solubility of $NaNO_2$ in this medium. The mixture was heated at reflux for 2 h after which 1 mmol of substrate (amine or ethanol amine) was added. Reflux was continued for the desired period of time after which the mixture was cooled to room temperature and treated ca. 20 mL of saturated aqueous sodium bicarbonate and the resulting solution extracted with portions of methylene chloride. The combined extracts were dried over sodium sulfate or magnesium sulfate after which the drying agent was removed by filtration and the solvent evaporated on a rotary evaporator. The residue was taken up in deuterochloroform and a known amount of toluene (50 µL) added as an internal standard. The yield of nitrosated product was determined by integration versus the toluene standard. In the case of the two phenyl substituted ethanol amines, N-(2-hydroxy-1-phenylethyl)-piperidine, and N-(2-hydroxy-2-phenylethyl)-piperidine, the NMR spectrum of the extracted

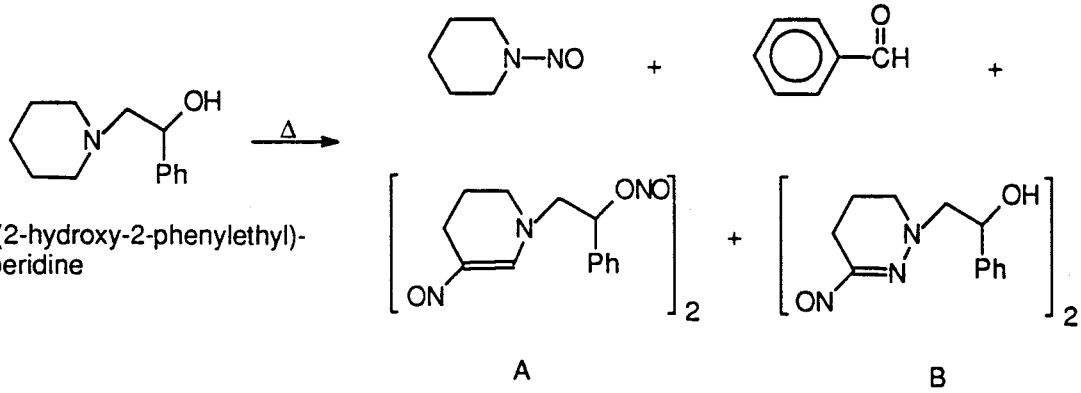

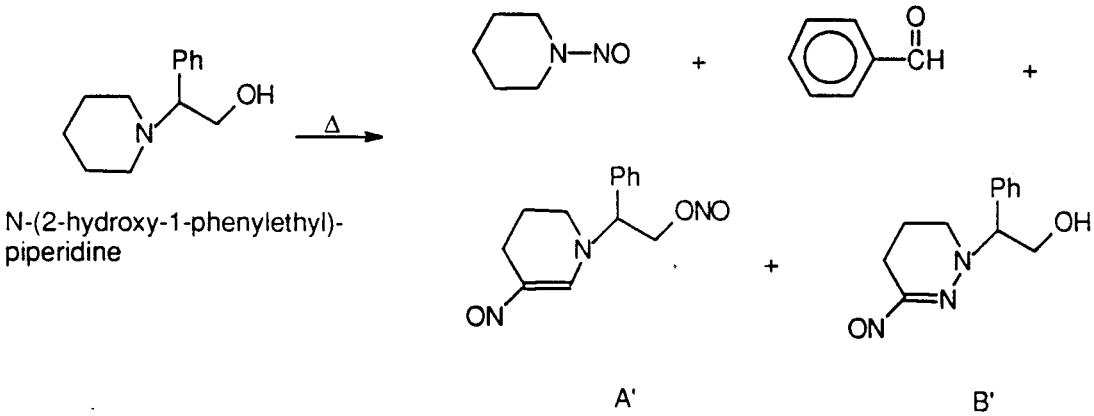

product mixture contained additional resonances besides those due to benzaldehyde and N-nitrosopiperidine. Reactions performed in DMSO produced more of these new compounds. Chromatography of the product mixture on silica gel using ether/hexane as eluent allowed for the separation of N-nitrosopiperidine, benzaldehyde and two additional products from each of these compounds. Although the NMR spectra of these four new compounds suggest that none was completely pure the major resonances in their ^{1}H and ^{13}C NMR spectra coupled with their mass spectra (Table E.25) suggest structures A and B and A' and B' respectively. The ^{13}C NMR spectra and suggested assignments are shown in Figures E.7-E.10.

Table E. 25. High Resolution Mass Spectral Data for New Compounds

Compound	MW, Calcd for M+1	MW, Found for M+1
A	523.2305081	523.235626
B	467.2406788	467.236588
A'	262.1191665	a
B'	234.1242519	234.128754

[a]The high resolution spectrum of this compound was not obtained. The low resolution spectrum exhibited the M+1 peak at 262.

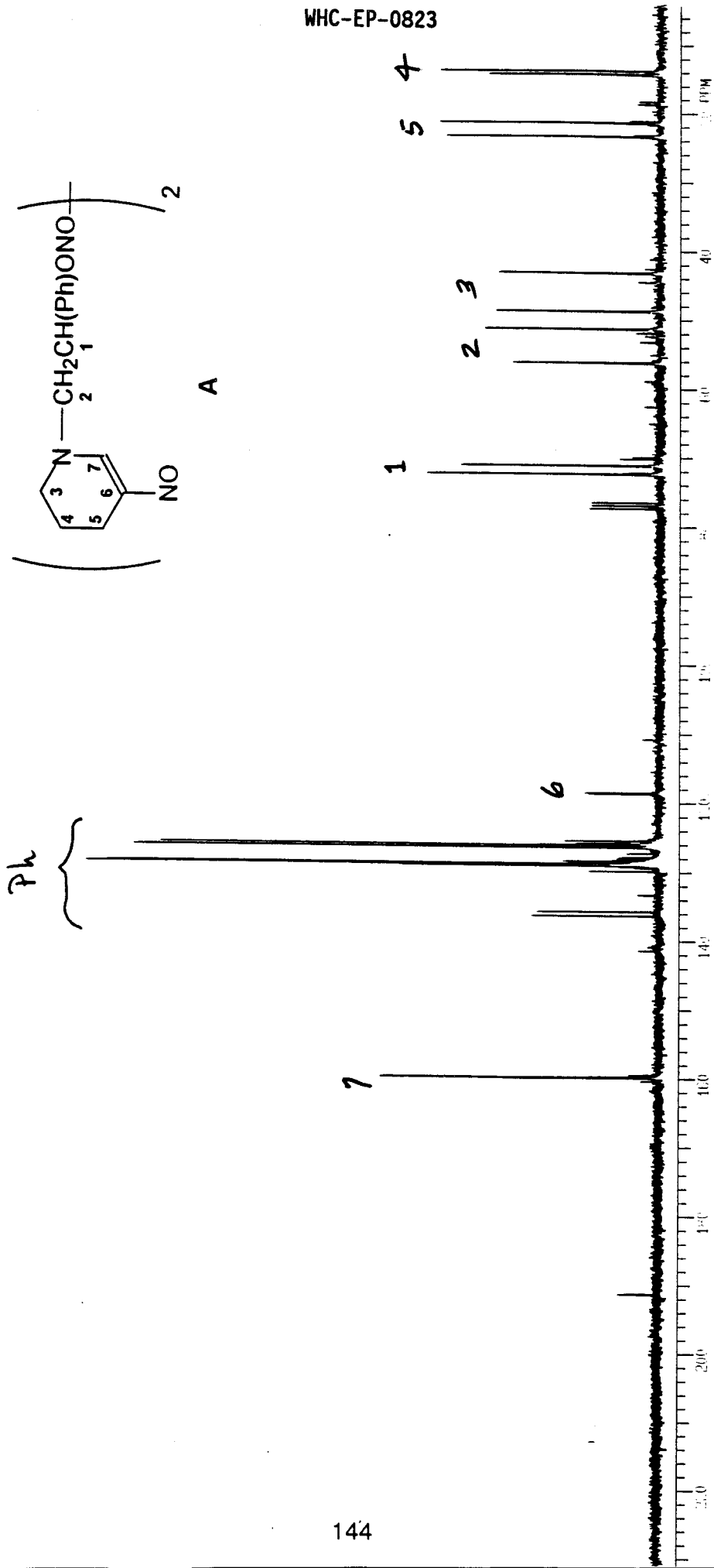

Figure E.7. Decoupled ^{13}C NMR spectrum of A (mixture of diastereoisomers).

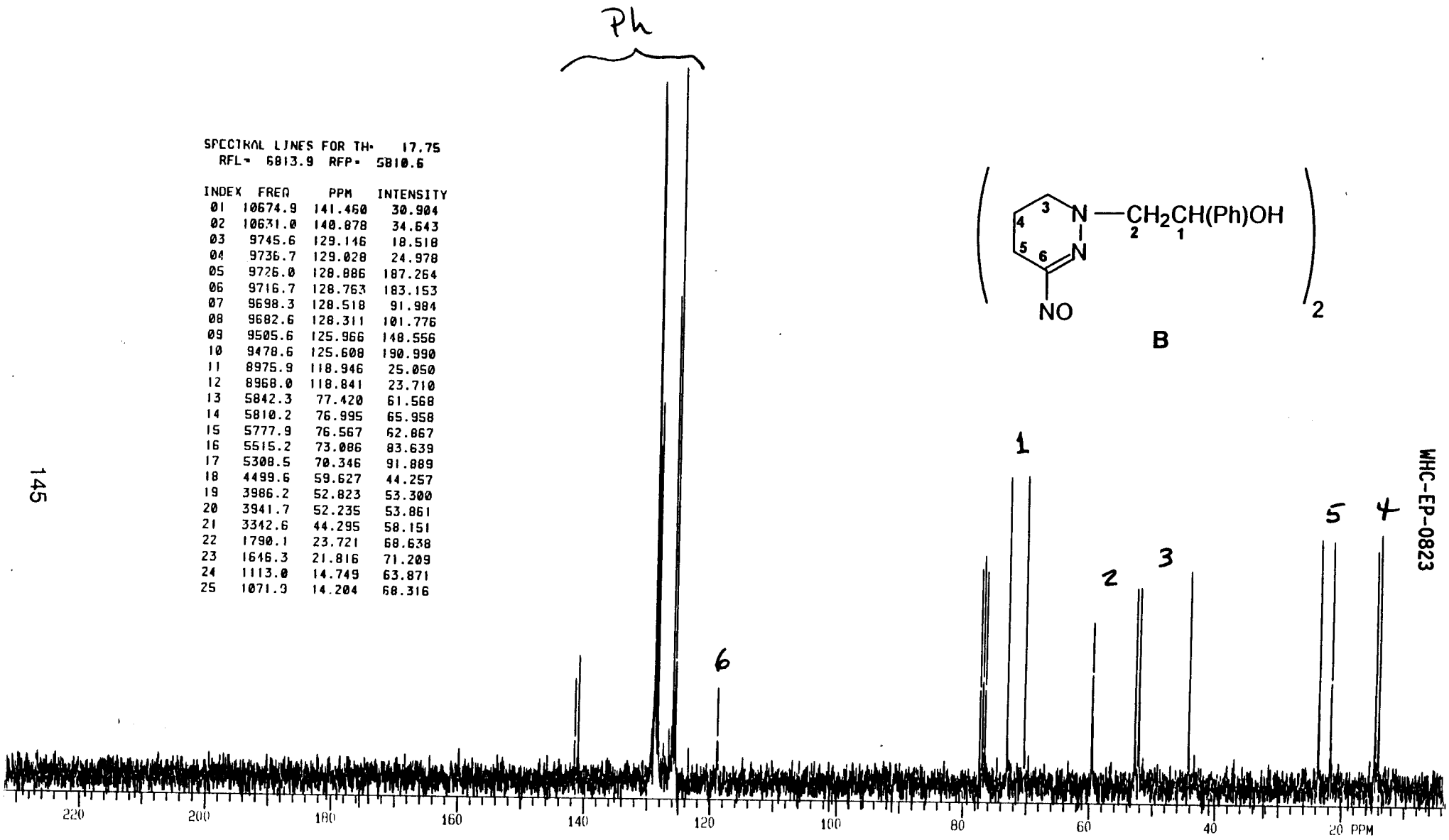

SPECTRAL LINES FOR TH= 17.75
RFL= 6813.9 RFP= 5810.6

INDEX	FREQ	PPM	INTENSITY
01	10674.9	141.460	30.904
02	10631.0	140.878	34.643
03	9745.6	129.146	18.518
04	9736.7	129.028	24.978
05	9726.0	128.886	187.264
06	9716.7	128.763	183.153
07	9698.3	128.518	91.984
08	9682.6	128.311	101.776
09	9505.6	125.966	148.556
10	9478.6	125.608	190.990
11	8975.9	118.946	25.050
12	8968.0	118.841	23.710
13	5842.3	77.420	61.568
14	5810.2	76.995	65.958
15	5777.9	76.567	62.867
16	5515.2	73.086	83.639
17	5308.5	70.346	91.889
18	4499.6	59.627	44.257
19	3986.2	52.823	53.300
20	3941.7	52.235	53.861
21	3342.6	44.295	58.151
22	1790.1	23.721	68.638
23	1646.3	21.816	71.209
24	1113.0	14.749	63.871
25	1071.9	14.204	68.316

B

Figure E.8. Decoupled ^{13}C NMR spectrum of B (mixture of diastereoisomers).

EGK-494/4 16.17
SPECTRAL LINES FOR TH= 21.96
RFL= 6807.0 RFP= 5810.6

INDEX	FREQ	PPM	INTENSITY
01	12106.9	160.436	63.174
02	10146.3	134.456	59.971
03	9793.4	129.780	80.589
04	9783.3	129.645	149.502
05	9769.0	129.456	36.576
06	9760.4	129.341	23.819
07	9626.4	127.566	136.996
08	8949.2	118.592	31.201
09	5843.0	77.430	147.311
10	5811.0	77.005	151.394
11	5778.9	76.580	154.969
12	4946.1	65.544	35.592
13	4940.2	65.466	26.228
14	4748.9	62.930	128.070
15	3239.6	42.930	48.690
16	3232.2	42.833	24.332
17	1673.1	22.172	125.745
18	1117.6	14.810	71.239

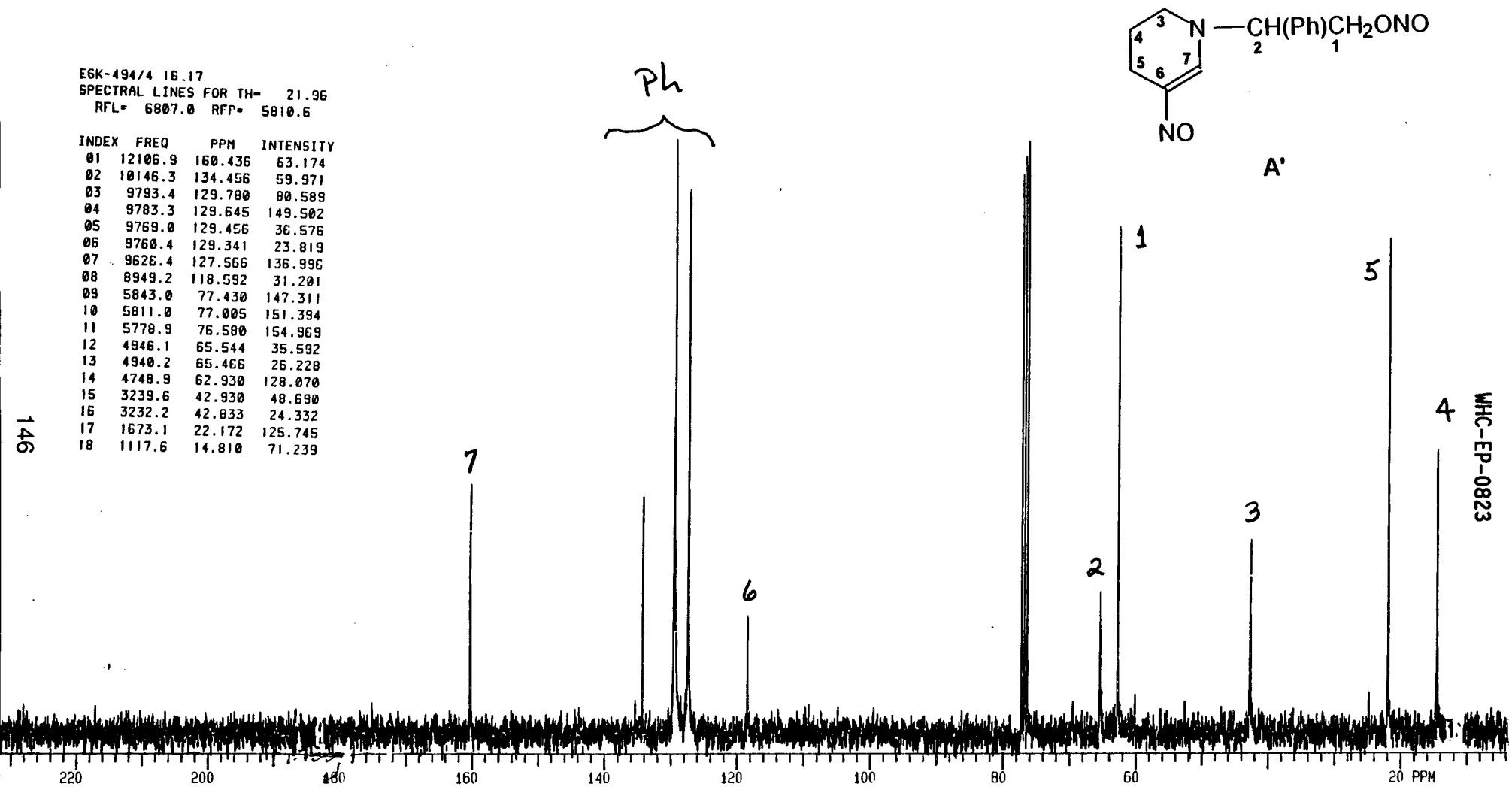

Figure E.9. (a) Decoupled ^{13}C NMR spectrum of A' .

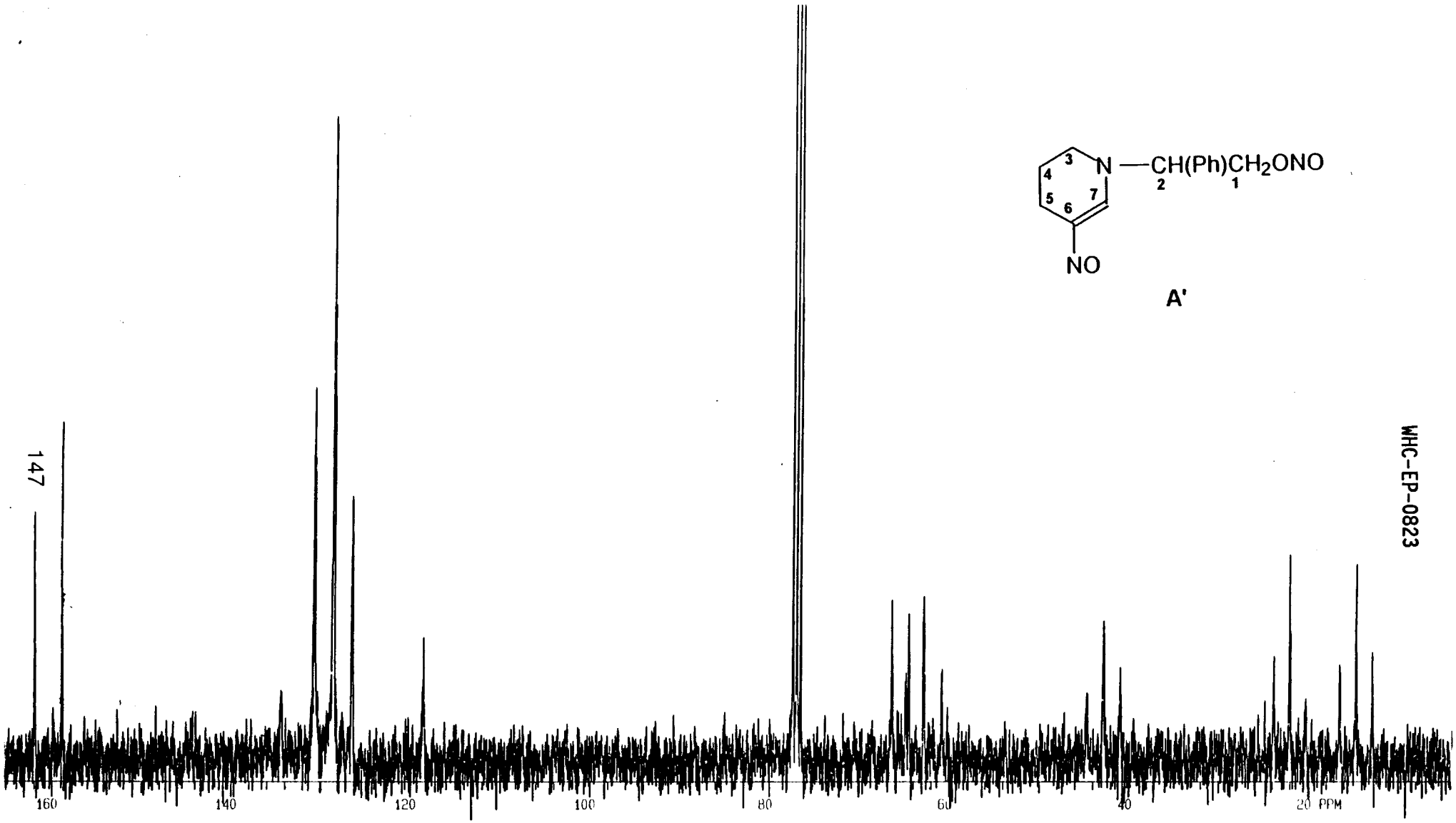

Figure E.9 cont'd. (b) Off-resonance decoupled ^{13}C NMR spectrum of A' .

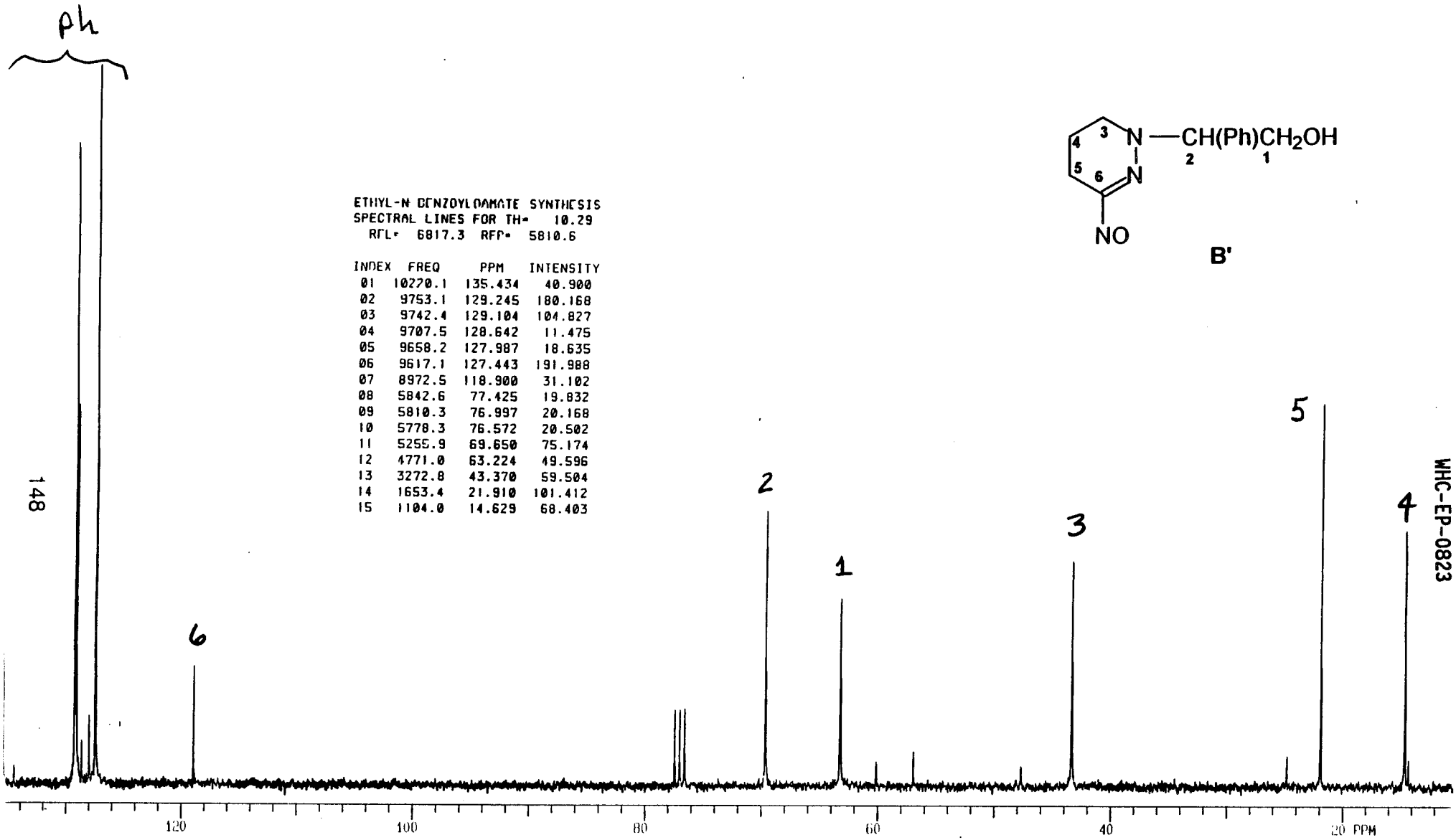

ETHYL-N BENZOYLOAMATE SYNTHESIS
SPECTRAL LINES FOR TH= 10.29
RFL= 6817.3 RFP= 5810.6

INDEX	FREQ	PPM	INTENSITY
01	10270.1	135.434	40.900
02	9753.1	129.245	180.168
03	9742.4	129.104	104.827
04	9707.5	128.642	11.475
05	9658.2	127.987	18.635
06	9617.1	127.443	191.988
07	8972.5	118.900	31.102
08	5842.6	77.425	19.832
09	5810.3	76.997	20.168
10	5778.3	76.572	20.502
11	5255.9	69.650	75.174
12	4771.0	63.224	49.596
13	3272.8	43.370	59.504
14	1653.4	21.910	101.412
15	1104.0	14.629	68.403

B'

Figure E.10. (a) Decoupled ^{13}C NMR spectrum of B'.

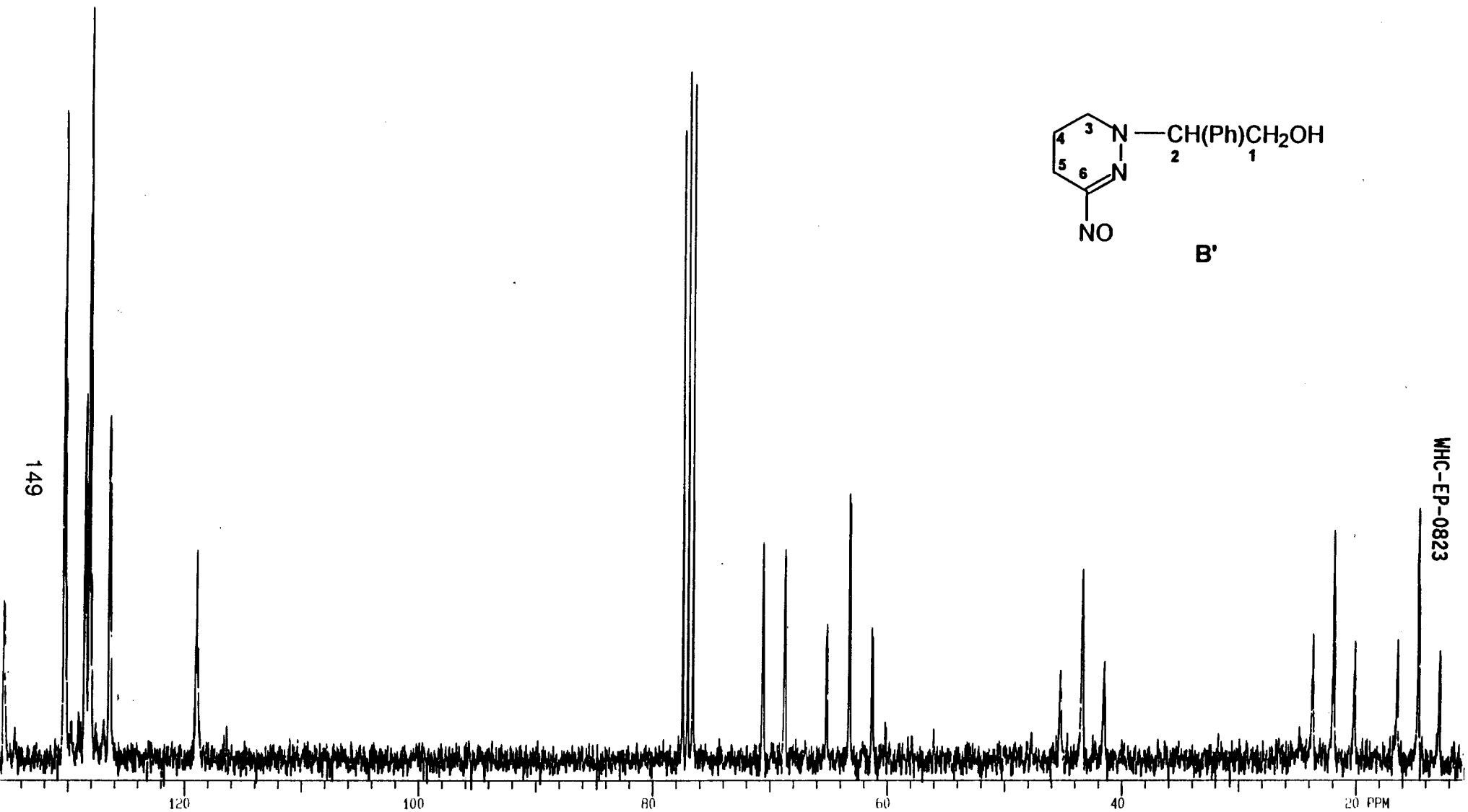

Figure E.10 cont'd. (b) Off-resonance decoupled ^{13}C NMR spectrum of B'.

Reactions of ethanolamines with $NOBF_4$. The corresponding ethanolamine (0.4 mmol) was dissolved in 2 mL of CD_3CN. To this was added at room temperature, with stirring, an excess of NaH. The resulting mixture was allowed to react under an inert atmosphere 30 min with stirring. After that time the mixture was filtered and transferred to a 5 mL round-bottomed flask containing 0.4 mmol of $NOBF_4$. The reaction proceeded almost instantly judging by the prompt dissolution of $NOBF_4$ and by ^{1}H-NMR, which showed a pronounced shift (> 1 ppm) toward lower fields for the signal corresponding to the methylene attached to the alkoxide.

Thermal degradation of nitrosated ethanolamines. The solution obtained from the procedure described above was heated overnight at 60° C under inert atmosphere. After that time, the gas phase was analyzed by GC and the solution hydrolyzed with ~2 ml of 3 M D_2O/OD^-. Part of the resulting solution was removed by means of a syringe and analyzed by ^{1}H-NMR. After that the solution was poured back into the flask and kept at room temperature. The gas phase was monitored by GC. After no more changes were observed in the gas phase, the mixture was diluted and analyzed by IC in order to determine the amount of oxalate produced in the reaction.

TASK 5: SOURCE OF NITROUS OXIDE, NITROGEN AND AMMONIA

Materials

N-15 labeled sodium nitrite and sodium nitrate were obtained from Merck Isotopes and were 99.5% enriched. Other reagents were from sources described under Tasks 1 and 2.

Product Identification and Quantitation

Gas and ion chromatographic instrumentation and procedures and NMR instrumentation were the same as those described for Task 1. Mass spectral analysis of labeled nitrogen gases was done using a VG Model 70SE spectrometer using electron impact ionization at 70 eV.

Quantitation of ammonium chloride by ^{14}N NMR spectral measurements. A standard curve was generated for ammonium chloride versus an external nitromethane standard as follows. A 15.0 mg portion of dry ammonium chloride was dissolved in 1.0 mL of D_2O and four NMR were prepared by diluting 0.020 mL, 0.060 mL, 0.190 mL and 0.380 mL aliquots of the stock solution to 0.5 mL. These samples were transferred to NMR tubes and ^{14}N NMR spectra were measured using nitromethane as an external standard. The plot of relative intensities of the ammonium chloride signal to that of the nitromethane external standard versus the known concentration of ammonium chloride in the solutions was linear.

Methods

Thermal decomposition of HEDTA in SY1-SIM-91B prepared with N-15 labeled reagents. Origin of N_2 and N_2O. Three different reactions were performed with SY1-SIM-91B solutions prepared using N-15 labeled reagents; 4.5 mL of solution was prepared for each reaction. The first reaction employed both N-15 labeled sodium nitrite and sodium nitrate. The second reaction employed N-15 labeled sodium nitrite and unlabeled sodium nitrate and the third reaction employed unlabeled sodium nitrite and N-15 labeled sodium nitrate. These solutions were heated at 120° C for 1000 h in the same vessel used for the HEDTA "A" runs (Figure E.1). Prior to placing the apparatus in the oil bath, the vessel was evacuated to aspirator pressure (ca. 25 torr). For reactions that were done under an inert atmosphere, the Teflon needle was replaced with a septum the solution was bubbled for 10 min with helium or argon using a long needle. The Teflon needle was replaced and aspirator vacuum was applied for a minute. After carrying out the reactions, the vessels were cooled to room temperature and the side arm was connected to a mass spectrometer for head space gas analysis. Representative mass spectra obtained on these samples are shown in Figures E.11-E.12. Labeled nitrogen appears in N_2 and N_2O only from reactions that contain labeled nitrite. Peaks at m/e = 29 and 45, which could be due to $^{15}N^{14}N$ and $^{15}N^{14}NO/^{14}N^{15}NO$, respectively were determined to be artifacts of undetermined origin. There was no difference in the isotopic content of samples heated under oxygen containing and those heated under an inert atmosphere.

With the reaction vessel shown in Figure E.1, there is the possibility that the caustic solution can splash onto the glass condensation tube, which could result in the introduction of silica into the reaction mixture. One reaction employing a simulated waste solution made with N-15 labeled sodium nitrite was repeated in which a Teflon cap was placed over the Teflon liner to prevent splashing of the solution onto the glass walls. Only N-15 labeled nitrous oxide was produced; N-15 labeled nitrogen was also present.

Nitrous Oxide Decomposition. The same procedure was applied for reactions in the presence or absence of simulated waste. A known volume of nitrous oxide was injected by means of a gas-tight syringe into the glass apparatus used for the reactions in simulated waste ("B" runs; Figure 2), which have been previously purged with Argon. The Teflon-lined glass vessel located at the bottom of the apparatus was immersed in an oil bath at 120° C. The amounts of N_2O, N_2 and O_2 at various times were determined by using the GC technique previously described (see "Product Identification and Quantitation").

Origin of NH_3. After completion of headspace gas analyses of the reaction mixtures prepared with N-15 labeled sodium nitrite and/or sodium nitrate, the Teflon needle in the reaction vessel was replaced with a septum and the side arm was connected to a Tygon tube that was fitted with a Pasteur pipette at the other end. The Pasteur pipette was immersed in 90 mL of 0.5 mL HCl solution contained in a 100 mL graduate cylinder, the septum was pierced with a long needle that directed a flow of nitrogen through the sample. The vessel was placed into a 120° C oil bath for several h to drive the ammonia from the solution. After completion of the purge, the HCl solution was evaporated under reduced pressure and the residue that remained was dissolved in D_2O (0.5 mL) and ^{14}N and ^{15}N NMR spectra were obtained. The ^{14}N spectra were measured using the same external

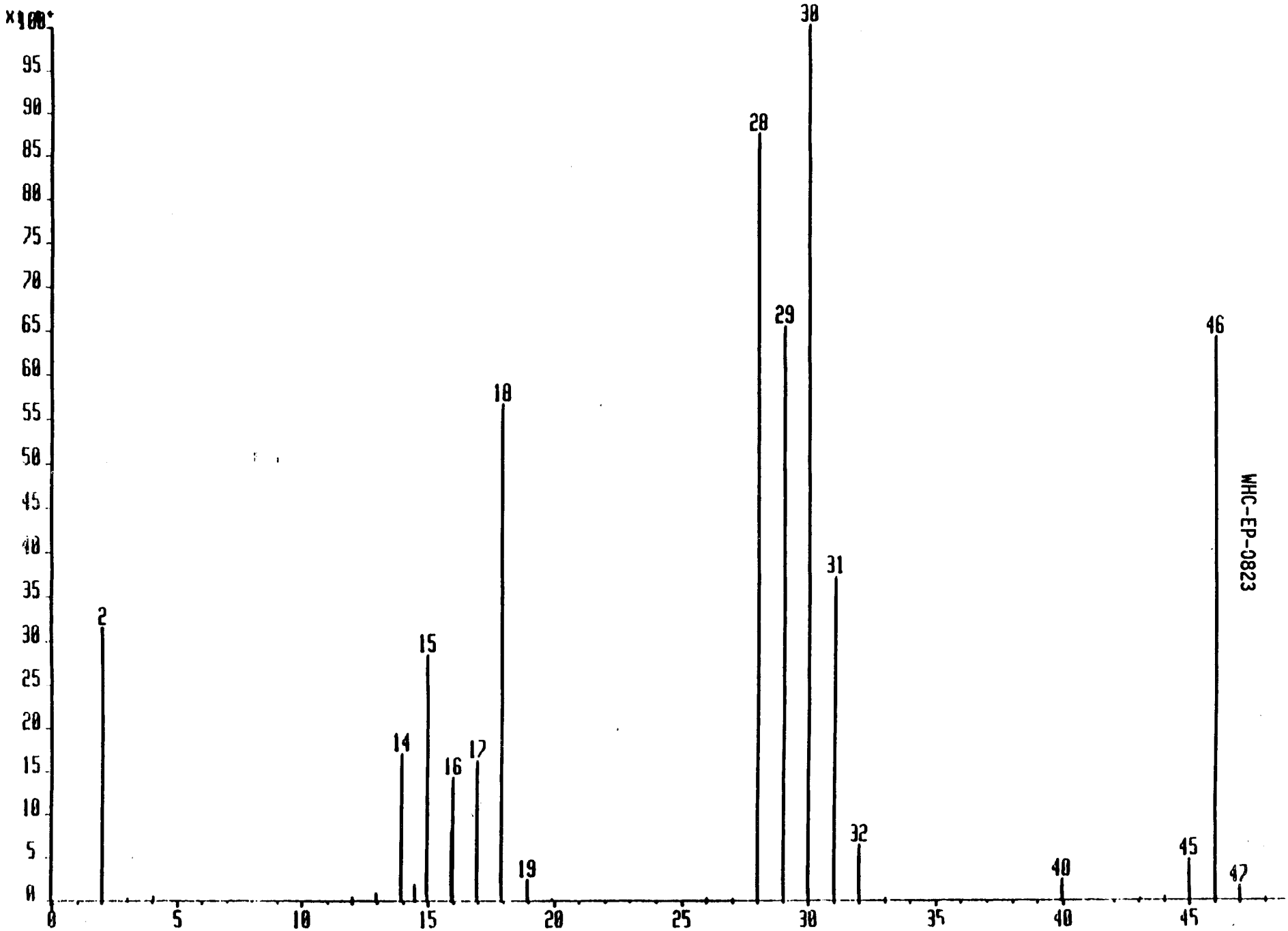

Figure E.11 Mass spectrum of headspace gases for reaction of HEDTA in SY1-SIM-91B made with $Na^{15}NO_2$ (helium atmosphere).

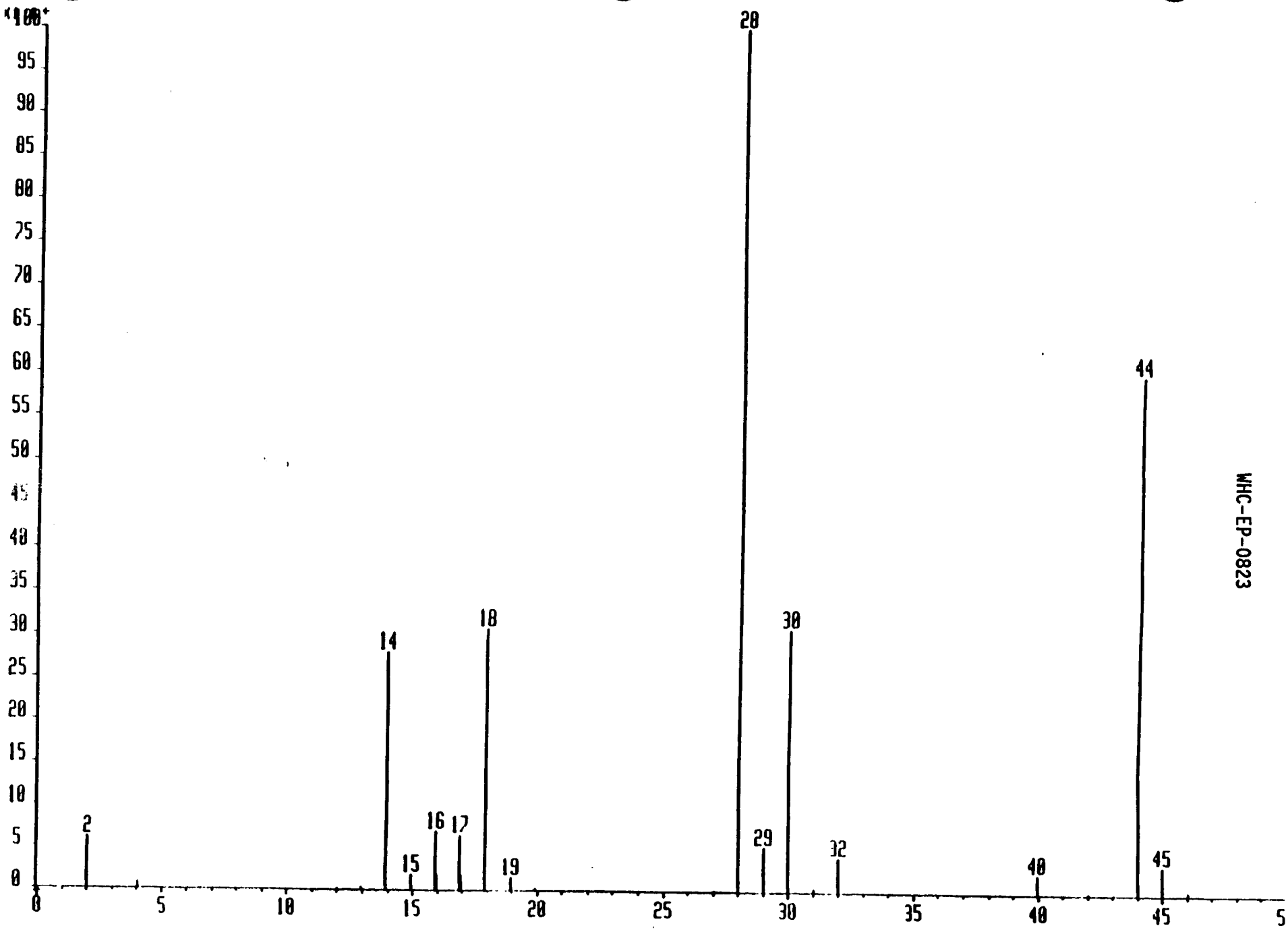

Figure E.12 Mass spectrum of headspace gases for reaction of HEDTA in SY1-SIM-91B made with $Na^{15}NO_3$ (helium atmosphere).

nitromethane standard described above. The ^{15}N spectra were obtained versus an aqueous $Na^{15}NO_2$ solution as an external standard. Because of the long relaxation times of the N-15 nucleus, measurements of concentration were considered problematic, and these spectra were used for qualitative observations only. To estimate the ratio of N-14 to N-15 ammonia produced, control experiments that employed only N-14 reagents were run to established the total yield of ammonia that was produced (more correctly, trapped) in these experiments. Then, the yield of N-14 labeled ammonia produced in experiments involving labeled reagents was determined by integration of the NH_4^+ signal intensity versus the nitromethane standard.

Reactions of hydroxylamine and $N_2O_3^{2-}$ with formaldehyde. ^{14}N NMR spectroscopy was utilized to monitor the fate of nitrogen from hydroxylamine and $N_2O_3^{2-}$ in reactions with formaldehyde. These reactions utilized a capillary of nitromethane as an external standard in the same fashion as described above. Quantitation of condensed phase species was done by ion chromatography (nitrite, formate) and ^1H NMR (methanol, formate) spectroscopy. Determinations of gas phase constituents (hydrogen, nitrogen, nitrous oxide) were done by gas chromatography as previously described. Reaction stoichiometries are given in Section 5.C. Chemical shifts of potential products were measured under the same conditions as the reactions with formaldehyde; these data are contained in Table 5.4.

References and Footnotes

(1) Kiprianov, A.I.; Tisel'skii, A.P., Ushenko, I.K. *Chem. Abs.* **1940**, *34*, 1024.

(2) Brancaccio, G.; Larizza, A. *Gazz. Chim. Ital.* **1964**, *94*, 37. *Chem. Abst.* **1964**, *61*, 4255.

(3) Emerson, W. S. *J. Am. Chem. Soc.* **1945**, *67*, 516; Minato, H.; Shinichi, F.; Okuma, K. and Kobayashi, M. *Chem. Lett.* **1977**, 1091.

DISTRIBUTION

Number of Copies	
OFFSITE	
10	Georgia Institute of Technology School of Chemistry and Biochemistry Atlanta, GA 30332-0440 Dr. E. Kent Barefield
4	Argonne National Laboratory Chemistry Division Argonne, IL 60439 Dr. Dani Meisel
4	Los Alamos National Laboratories MS-K555 Los Alamos, NM 87545 Kemal Passmechmetoglu
3	U. S. Department of Energy Trevion II, Rm 330 19901 Germantown Road Germantown, MD 20874 Dave Pepson
1	Westinghouse Savannah River Company P. O. Box 616 Aiken, SC 29802 D. Douglas Walker
1	David Campbell 102 Windham Road Oak Ridge, TN 37830
1	Pr. Zinfer R. Ismagilov Prospekt Akademika Lavrentieva, 5 Novosibirsk, 630090 Russian Federation
1	J. Louis Kovach P. O. Box 29151 Columbus, OH 43229-0151
1	W. W. Schultz 727 Sweetleaf Drive Wilmingon, DE 19808

DISTRIBUTION (continued)

Number of Copies

ONSITE

76 Westinghouse Hanford Company

D. H. Alexander	S7-51
H. Babad (2)	S7-30
R. M. Bean	P8-08
S. O. Branch	S7-54
J. W. Brothers (2)	K5-22
S. A. Bryan	P7-25
D. M. Camaioni	K2-38
J. A. Campbell	P8-08
M. H. Campbell	S7-73
R. J. Cash	S7-15
R. F. Christensen	S7-54
N. G. Colton	K3-75
T. D. Cooper	T5-12
C. H. Delegard	T6-09
K. A. Gasper	G3-21
R. E. Gerton	S7-54
J. M. Gray	S7-54
D. L. Herting	T6-09
J. D. Hopkins	R2-11
J. L. Huckaby	S7-15
J. R. Jewett	T5-09
R. P. Johnson	H5-09
G. D. Johnson (5)	S7-15
N. W. Krich	R2-11
J. W. Lentsch	S7-15
N. G. McDuffie (10)	S7-15
R. H. Marusich	H4-65
G. B. Mellinger	B1-40
M. A. Payne	S7-14
L. R. Pederson (3)	K2-44
J. C. Person	T6-09
A. K. Postama	H4-62
D. A. Reynolds	R2-11
E. L. Richards	B4-41
G. W. Rosenwald	S7-54
W. D. Samuels	K2-44
D. J. Sherwood	S7-15
D. E. Simpson	B3-55
D. D. Stepnewski	H4-63
D. M. Strachan	K2-44
D. A. Turner	S7-15
R. J. Van Vleet	H4-63

DISTRIBUTION (continued)

Number of Copies

ONSITE

Westinghouse Hanford Company (continued)

K. D. Wiemers (2)	P7-14
D. D. Wodrich	S7-84
Chemistry Sub-TAP	
% Patsy Culver (5)	S7-15
Central Files	L8-04
Document Processing and	
Distribution (2)	L8-15
EDMC	H6-08
OSTI (2)	L8-07
TFIC	R1-20

This page intentionally left blank.

DISTRIBUTION (continued)

Number of Copies

ONSITE

Westinghouse Hanford Company (continued)

K. D. Wiemers (2)	P7-14
D. D. Wodrich	S7-84
Chemistry Sub-TAP	
% Patsy Culver (5)	S7-15
Central Files	L8-04
Document Processing and	
Distribution (2)	L8-15
EDMC	H6-08
OSTI (2)	L8-07
TFIC	R1-20